KINGDOM OF SAUDI ARABIA

KING ABDULAZIZ UNIVERSITY

Abdullah O. Nasseef

President

FACULTY OF EARTH SCIENCES

Ahmed N. BaSahel

Dean

KING KHALID

I. A. G. BULLETIN No. 3

EVOLUTION AND MINERALIZATION OF THE ARABIAN–NUBIAN SHIELD

Volume 4

Published for the

FACULTY OF EARTH SCIENCES, KING ABDULAZIZ UNIVERSITY
JEDDAH, KINGDOM OF SAUDI ARABIA

by

PERGAMON PRESS

OXFORD · NEW YORK · TORONTO · SYDNEY · PARIS · FRANKFURT

U.K.	Pergamon Press Ltd., Headington Hill Hall, Oxford OX3 0BW, England
U.S.A.	Pergamon Press Inc., Maxwell House, Fairview Park, Elmsford, New York 10523, U.S.A.
CANADA	Pergamon of Canada, Suite 104, 150 Consumers Road, Willowdale, Ontario M2J 1P9, Canada
AUSTRALIA	Pergamon Press (Aust.) Pty. Ltd., PO Box 544, Potts Point, NSW 2011, Australia
FRANCE	Pergamon Press SARL, 24 rue des Ecoles, 75240 Paris, Cedex 05, France
FEDERAL REPUBLIC OF GERMANY	Pergamon Press GmbH, 6242 Kronberg-Taunus, Hammerweg 6, Federal Republic of Germany

First edition A.D. 1980–A.H. 1400

British Library Cataloguing in Publication Data

Evolution and mineralization of the Arabian-Nubian Shield. - (King Abdul Aziz University. Institute of Applied Geology. IAG bulletins; no. 3).
Vol. 4
1. Geology - Near East - Congresses
I. Al-Shanti, Ahmed II. Series
555.6 QE319.N4 80-40043

ISBN 0-08-024481 5

Printed in Great Britain by Hillman Printers (Frome) Ltd., Somerset
Bound by A. Wheaton & Co. Ltd., Exeter

SYMPOSIUM PERSONNEL

Convenor: A. M. S. AL-SHANTI

Organizers: M. L. ABDEL-KHALEK, A. B. AL-KHATIB, A. M. S. AL-SHANTI, A. N. BA-SAHEL, P. L. BINDA, O. R. EL-MAHDY, A. A. A. HUSSEIN, N. J. JACKSON, W. J. MACLEAN, J. G. MOLTZER, F. I. OSMAN, C. R. RAMSAY, M. J. ROOBOL, S. A. TAHOUN, and M. A. TOFIQ.

Field Excursion Leaders: A. M. AL-SARI, P. L. BINDA, O. R. EL-MAHDY, N. J. JACKSON, M. E. KUKANDY, C. R. RAMSAY, M. J. ROOBOL, J. H. SCHELLEKENS, M. I. THEKAIR, and M. O. ZUBEIR.

Editorial Board: A. M. S. AL-SHANTI, P. L. BINDA, C. R. RAMSAY, and S. A. TAHOUN.

Referees: M. L. ABDEL-KHALEK, A. A. ABDEL-MONEM, M. A. AL-GAZZAZ, A. N. BA-SAHEL E. Z. BASTA, P. L. BINDA, H. R. BLANK, C. B. DUBOIS, O. R. EL-MAHDY, H. A. HAKIM, A. A. A. HUSSEIN, N. J. JACKSON, M. M. KHUDA, W. J. MACLEAN, J. G. MOLTZER, C. R. RAMSAY, M. J. ROOBOL, J. WAKEFIELD, and A. J. WARDEN

Arabic Abstracts: I. A. M. FARAG

Associate Editors: P. L. BINDA, A. A. A. HUSSEIN, N. J. JACKSON, M. M. KHUDA, C. R. RAMSAY, and M. J. ROOBOL.

Editors of Volume 4: P. G. COORAY and S. A. TAHOUN.

الجرانيتات الفوق قلوية والكلس ـ قلوية بعدالتجبل ومايصاحبها من تمعدن فى الدرع العربية ـ المملكة العربية السعودية

د. ب. ستوسر و ج. ى. أليوت

الخلاصة

إن جرانيتات بعد التجبّل من عمر الحِمَى الافريقى (٦٧٠–٥٥٠ مليون سنة) قد تَموْضعت فى الدرع العربية بعد فترة طويلة من نشاط تجبلى شبه قوس جزرى. ومعظم هذه الصخور تحت ذوْبيّة (تتميز بوجود پوتاسيوم فلسپار وپلاجيوكلاز) طرزية بيوتيت مونزوجرانيت كلس ـ قلوية . وجرانيتات الحِمَى الإفريقى المبكرة تصحبها متدخلات من الجابرو الثولييتىّ صغيرة وواسعة الانتشار، كثير منها طباقىّ. والجرانيتات الكلس ـ قلوية لاتتوزع بانتظام ، ومنطقة ظهورها ـ بالنسبة الى طرز الصخور الأخرى ـ تزداد من الجنوب الغربى الى الشمال والشمال الشرقى . وفى الجزء الشمالى الشرقى من الدرع تصاحب هذه الصخور ريوليتات لها نفس التركيب ، وقِنْديد (دِبْس) جاء من الأرض الجرانيتية .

ولقد تم وصف خمسة وأربعين موقعا من الجرانيتات القلوية المتأخرة ،معظمها فوق قلوى، كما نوقشت كيميائيتها . وجلّ هذه الصخور جرانيتات قليّة فرط ذوْبية (تتميز بغياب البلاجيوكلاز إلا كمكوّن للبِرْثيت) متوسطة الى غليظة التحبب ، ولكن تشيع كذلك الضروب الظاهرة التبلور الدقيقة النسيج. معادن السليكات المافيّة للجرانيتات القليّة هى : أرْفِيدْسونيت ، إيجيرين ، إيجيرين ـأوجيت ، ريبكيّت ، بيوتيت متناثر، إينجماتيت ، باركفيكيت .ولاتقع الجرانيتات القليّة فى الثلث الجنوبى الغربى من الدرع العربية ولا فى الجزء الجنوبى الشرقى من الدرع النوبية الافريقية المجاورة. ولقد تم التعرف على إقليم من سيانيت ـ شوتكينيت فى الجزء الجنوبى الغربى من الدرع العربية.

ولم تعرف آية قراره من معادن اقتصادية تصاحب جرانيتات الحِمَى الإفريقى ولقد وُجِد كثير من مواقع التمعدن والشاذات الكيميائية الأرضية (الجيوكيميائية) تحوى : تنْجِسْتن ، موليبدينوم ، قصدير ، بريليوم ، زركونيوم ، نيوبيوم ، ثوريوم ، يورانيوم ، عناصر أرضية نادرة ، فلوريت . وأهم هذه المواقع قد تمت جدولتها واستبان توزّعها .

POST-OROGENIC PERALKALINE AND CALC-ALKALINE GRANITES AND ASSOCIATED MINERALIZATION OF THE ARABIAN SHIELD, KINGDOM OF SAUDI ARABIA

D. B. STOESER and J. E. ELLIOTT

U.S. Geological Survey, Jeddah, Saudi Arabia

Abstract—Following a long period of island arc-like orogenic activity, post-orogenic granites of Pan-African age (670–550 Ma) were emplaced throughout the Arabian Shield. Most of these rocks are typical subsolvus calc-alkaline biotite monzogranite. The early Pan-African granites are associated with widespread small tholeiitic gabbro intrusions, many of which are layered. The calc-alkaline granites are not evenly distributed and their area of exposure relative to other rock types increases from S.W. to north and N.E. In the north-eastern part of the shield, they are associated spatially with rhyolites of similar composition and with molasse derived from granitic terrane.

The occurrence of 45 late alkali granites, most of which are peralkaline, is described and their chemistry discussed. The bulk of these rocks are medium- to coarse-grained hypersolvus alkali granites, but phenocrystal and micrographic varieties are also common. The mafic silicate minerals of the alkali granites are arfvedsonite, aegirine, aegirine–augite, riebeckite, and sparse biotite, aenigmatite, and barkevikite. The alkali granites do not occur in the south-western third of the Arabian Shield nor in the south-eastern portion of the adjacent Nubian Shield of Africa. A syenite–shonkinite province located in the south-western part of the Arabian Shield is identified.

No economic mineral deposits are known to be associated with the Pan-African granites. Numerous mineral occurrences and geochemical anomalies have been found that contain W, Mo, Sn, Be, Zr, Nb, Th, U, rare earths, and fluorite. The most important of these occurrences are tabulated and their distribution shown.

INTRODUCTION

Among the projects of the Saudi Arabian Directorate General of Mineral Resources (DGMR) five-year plan is a study of the petrogenesis and mineral potential of the granitic rocks of the Arabian Shield. The Acid Plutonic Rock Project involves two DGMR geologists and the two authors, members of the U.S. Geological Survey Saudi Arabian Mission. Stoeser's primary concern is the petrology of the rocks and Elliott's their economic geology. This paper is our first contribution to the geology of the Arabian Shield granites.

The Arabian Shield is the eastern half of the Arabian–Nubian Shield, which was exposed by early to middle Tertiary uplift and ensuing erosion and split into two segments by the Red Sea rift (Coleman *et al.*, 1977). The Arabian portion of the shield occupies an area of approximately 770,000 km^2 and is composed of approximately 40% granitoid plutonic rocks (quartz diorite and tonalite to granite) and most of the remainder is volcanic and sedimentary rocks, many of which have been metamorphosed to the greenschist facies (Brown and Jackson, 1960; Greenwood and Brown, 1973; Greenwood *et al.*, 1976). The rocks of the Arabian Shield appear to be late Proterozoic in age (Fleck *et al.*, 1976, 1979; Baubron *et al.*, 1976). Their history can be divided into two main periods, an early island arc-like orogenic phase (1165–680 Ma) succeeded by a post-orogenic period (Pan-African, 670–550 Ma) during which massive amounts of granite were emplaced throughout most of the shield (Brown and Jackson, 1960; Greenwood *et al.*, 1976; Delfour, 1977). It is the purpose of this paper to briefly describe the general geologic setting, distribution, characteristics, and economic geology of the post-orogenic granites, with emphasis on the peralkaline rocks.

The primary method of plutonic rock classification used is the IUGS system (Streckeisen, 1975). In addition, the following modifying terms for granites are used: alkaline, alkali, peralkaline, and metaluminous. Alkaline (or alkalic) granite is used as a general chemical term for a granite that contains more alkali metals than is considered average for the group of rocks to which it belongs. An alkali granite is one containing soda pyroxene and/or amphibole (Sorensen, 1974). A peralkaline granite is one in which molecular $Al_2O_3 < Na_2O + K_2O$ (Carmichael *et al.*, 1974). A metaluminous granite, however, has $Al_2O_3 < CaO + Na_2O + K_2O$ but $Al_2O_3 > Na_2O + K_2O$ (Carmichael *et al.*, 1974). Common granites are metaluminous. As used in this paper, a shonkinite is a mafic syenite whose essential mineralogy is potassium feldspar plus augite and that is composed of more than half mafic silicates (pyroxene, amphibole, olivine, and biotite).

ANALYTICAL METHODS

Nineteen chemical analyses are presented in this paper, of which ten are new and nine are taken from the literature. The new analyses were performed by Skyline Labs, Inc. of Wheat Ridge, Colorado, USA. The following were determined by atomic absorption: SiO_2, Al_2O_3, MgO, CaO, Na_2O, K_2O, and Li. TiO_2 and P_2O_5 were determined by colorimetry (TiO_2 using Tiron and P_2O_5 by the vanadate-molybdate procedure). P_2O_5 was below the limit of detection (0.2%) for all samples and therefore no values for this oxide appear in Table 2. Sr and Rb were determined by flame emission spectroscopy, and fluorine by the specific ion electrode method using an ammonium citrate solution after fusion in sodium hydroxide. Total volatiles were detected by loss on ignition (L.O.I.) at 1000°C for two hours.

EVOLUTION OF THE SHIELD

The evolution of the southern shield has been documented by Greenwood *et al.* (1976) and by Fleck *et al.* (1976, 1978, 1979) and the northern part of the shield has been described by Baubron *et al.* (1976) and Delfour (1977). The geologic history of the Arabian Shield can be divided into two main periods. The first and longer period (1165–680 Ma) is dominantly orogenic and was characterized by calc-alkaline intermediate volcanic and plutonic rocks and associated clastic sediments. The second period (680–550 Ma) is dominantly non-orogenic and characterized by silicic volcanics, granites, and arkosic molasse deposits. The volcanic, sedimentary, and plutonic rocks of the first period appear to be typical of those found in subduction-related late Phanerozoic island arcs and, therefore, a number of subduction models for the evolution of the Arabian–Nubian Shield were put forth (Jackman, 1972; Greenwood *et al.*, 1976; Bakor *et al.*, 1976; Garson and Shalaby, 1976; Neary *et al.*, 1976; Frisch and Al-Shanti, 1977).

Studies of the southern shield indicate that the oldest known rocks are the Baish meta-basalt greenstones and overlying Bahah meta-graywackes, which are cut by 900 Ma plutons and may be as old as 1165 Ma (Greenwood *et al.*, 1976; Fleck *et al.*, 1979). To the east and intercalated(?) with the Baish–Bahah belt is a broad belt of andesitic and dacitic metavolcanic rocks and lesser amounts of metasedimentary rocks, the Jiddah Group, which is about the same age or somewhat younger (Greenwood *et al.*, 1976).

The layered rocks of the Baish, Bahah, and Jiddah Groups have been intruded by a belt of tonalitic calc-alkaline batholiths that stretches along the western side of the shield from the Yemen border to north of Jiddah. Greenwood *et al.* (1976) report that these rocks were emplaced during two main episodes. Their "first dioritic series" (960 Ma) had an early phase of gabbro, diorite, and quartz diorite that was followed by more voluminous and more leucocratic biotite–hornblende tonalite (Fig. 1). This first episode of tonalitic plutonism was followed by orogeny and a "second episode of tonalitic plutonism" (800–680 Ma) which included tonalite and trondjemite. The tonalites of the second series are similar to those of the first series, but appear to be spread over most of the Arabian Shield (Greenwood *et al.*, 1976; Baubron *et al.*, 1976; Schmidt *et al.*, 1979). During the later part of the second episode, granodiorite was emplaced largely as syn-tectonic gneiss domes throughout at least the southern half of the shield (Nebert, 1970; Fleck *et al.*, 1978; Schmidt *et al.*, 1979; Cooper *et al.*, 1979). In the northern half of the shield during this time massive amounts of intermediate volcanics and associated clastic sediments, the Halaban (Hulayfah) Group were deposited (Greenwood *et al.*, 1976; Baubron *et al.*, 1976; Delfour, 1977).

After the end of the long orogenic episode at about 700–680 Ma, plutonism changed from intermediate composition to acidic so that massive amounts of calc-alkaline monzogranite accompanied by minor gabbroic magma were emplaced throughout the shield (Fleck *et al.*, 1976, 1979; Baubron *et al.*, 1976). These granites were generally emplaced as simple circular or ovoid plutons, although some were ring structured (Dodge, 1979). In the following 80 to 100 Ma there was a general shift from calc-alkaline to alkaline granite. In the northern shield these granitic magmas also appear to be represented by the Murdama and Shammar Group rhyolitic intrusives (Delfour, 1977; Schmidt *et al.*, 1979). The Murdama Group, although containing acidic flows, is dominantly composed of clastic sediments that apparently are a molasse derived from this granitic terrane (Schmidt *et al.*, 1979). In the southern shield the Murdama and Shammar are lacking, possibly due to a greater depth of erosion.

One outstanding question presently being debated is whether the late Proterozoic rocks of the Arabian Shield are underlain by an older evolved crystalline basement. At present there is no good evidence to support this idea. For the southern shield the lack of older dates, low initial $^{87}Sr/^{86}Sr$ ratios of 0.702 to 0.704 (Fleck *et al.*, 1979) and lack of old granites suggest no contamination by, or partial melting of, an underlying older evolved crust, thus indicating that no such basement exists. For the northern part of the shield, however, the question of an older basement is more debatable. Although no dates are available that would provide direct evidence for an older evolved crust, six granites dated by Baubron *et al.* (1976) have initial $^{87}Sr/^{86}Sr$ ratios in the range 0.704 to 0.7122. The higher of these ratios clearly suggests that evolved crustal material was involved in the formation of these granites. Fundamentally, the question awaits more and definitive isotopic studies.

PETROGRAPHY

Calc-alkaline Granites

The bulk of the calc-alkaline granites of the Arabian Shield are pink to gray subsolvus, equigranular to porphyritic, medium-grained monzogranites and granodiorites that contain 1–8% mafic silicates, mostly biotite with or without hornblende. They occur mainly as oval to somewhat irregularly shaped plutons, and more rarely as ring dikes having calc-alkaline granite or country rock cores (Dodge, 1979). No attempt will be made here to synthesize the considerable data already available on this group of rocks; for further information the reader is referred to Greenwood and Brown (1973); Nasseef and Gass (1977); Delfour (1977); and Kanaan (1979).

Less common members of the calc-alkaline group are rapakivi granites, alaskites with or without garnet, and 'big-feldspar' porphyroblastic monzogranites. The garnet-bearing alaskites are volumetrically insignificant but appear to be distributed throughout at least the central and southern

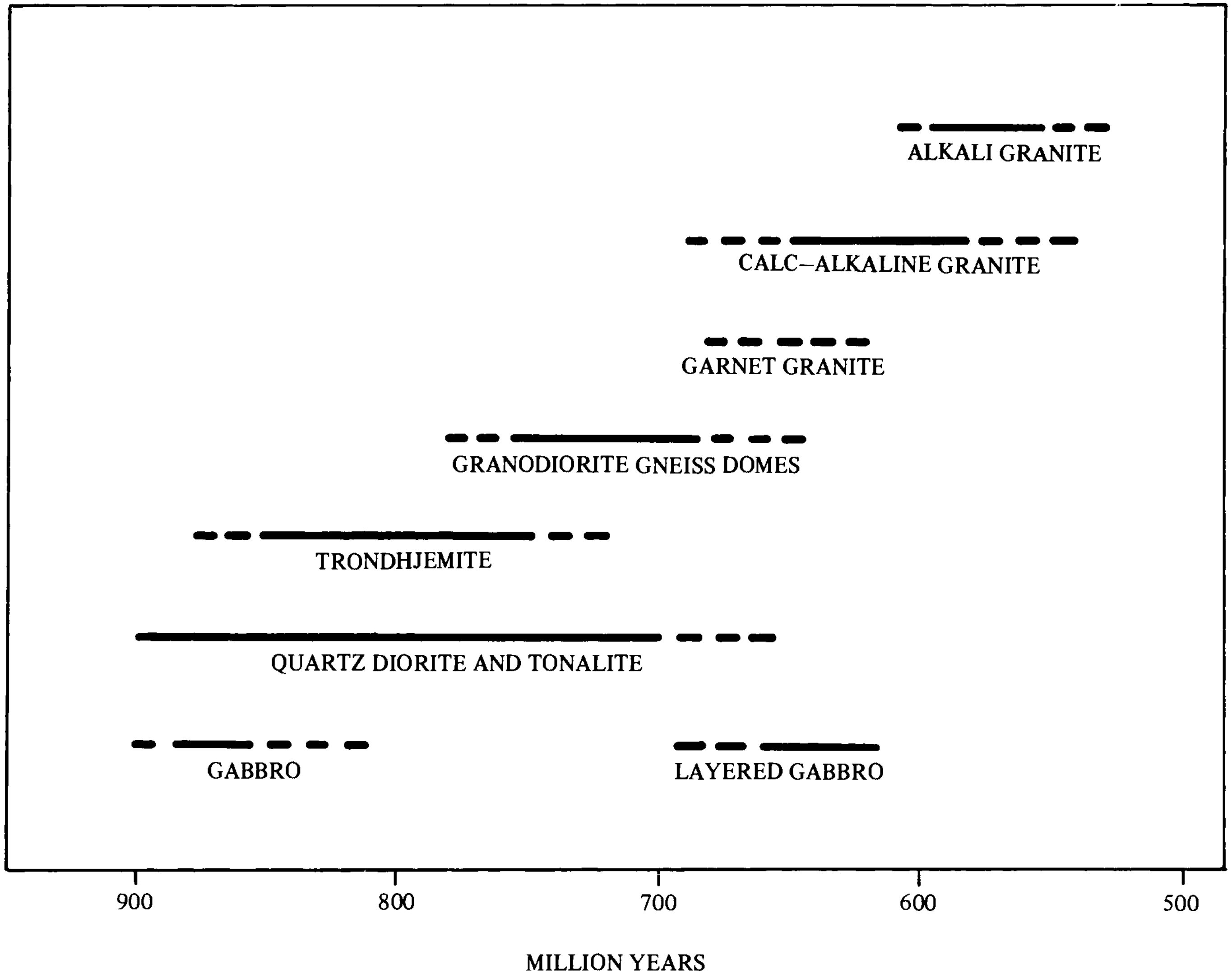

FIG. 1. Plutonic rock geochronology of the Arabian Shield. Data from Coleman *et al.* (1972), Baubron *et al.* (1976), Fleck *et al.* (1976, 1979), and Cooper *et al.* (in press).

shield and are reported from Egypt as well (Schurmann, 1966). They are typically medium-grained, have xenomorphic inequigranular texture, and contain less than 5% total garnet, biotite, and muscovite. What are interpreted to be potassium-metasomatized monzogranites, containing porphyroblasts as large as 5–10 cm, are concentrated mainly in the southern shield. Insufficient data are presently available on the Arabian rapakivi granites to describe them accurately.

In addition to the calc-alkaline granites, post-orogenic gabbros occur throughout most of the Arabian Shield but are distinctly concentrated in the south-central shield (Coleman *et al.*, 1972). The best criterion for field recognition is the presence of olivine and pyroxene, both of which have been destroyed in the older gabbros through metamorphism. Many of these late gabbros are layered, and the layering appears to be due to repeated infusions of magma rather than to crystal settling (Al-Shanti, 1974; Coleman *et al.*, 1977). The composition of the parental magma of these gabbros appears to have been olivine tholeiitic. Coleman *et al.* (1972, 1977) give K–Ar dates on these gabbros that fall in the range 415–769 Ma, many of them around 630 Ma. In the southern shield, we have found these gabbros in intrusive complexes with the older calc-alkaline granites but never with the younger alkaline granites. In general it seems unlikely that these gabbros could be any younger than about 500 Ma since neither they nor the granites have been observed to intrude the basal Cambro-Ordovician cover rocks.

Alkali Granites

The alkali granites of the Arabian Shield are mainly gray, pink, or red, medium- to coarse-grained, hypersolvus alkali granites. In the field, they can often be distinguished by their dark red to almost black weathered surface and their tendency to weather to very large, smooth, rounded blocks. Seen in thin section, they consist of alkali feldspar that has exsolved to a patch perthite, 20–30% quartz and 5–15% late interstitial, sodic mafic silicates, which include aegirine, aegirine-augite, arfvedsonite, and less commonly aenigmatite, and barkevikite. A reddish-brown biotite is also present in some samples. Deep blue, very pleochroic riebeckite (?) is present in many samples, usually as a secondary amphibole replacing the primary sodic pyroxene or amphibole. Most of the peralkaline granites are more mafic than the calc-alkaline granites. Accessory minerals are magnetite, allanite, zircon, fluorite, and in several samples brick-red elpidite ($Na_2ZrSi_6O_{1.5}{\cdot}H_2O$). Plagioclase is usually present only as secondary albite, partially replacing the primary alkali feldspar. The alkali feldspar of the red granites is typically turbid and clouded by very fine, dark inclusions (hematite?).

In the north-eastern part of the shield, the alkali granites are commonly associated with pink to red granophyric granites. These granophyric granites typically consist of 10–50% phenocrysts of alkali feldspar and lesser quartz in a micrographic groundmass. Mafic minerals are usually extensively altered or completely destroyed. The alkali granites and granophyres are often closely associated with rhyolitic volcanics of the Shammar Group, which typically are also porphyritic and have phenocrysts of alkali feldspar and quartz (Delfour, 1977).

DISTRIBUTION OF GRANITES

Arabian Shield

On the basis of the distribution of the calc-alkaline and alkali granites, the Arabian Shield is here divided into three regions (Fig. 2). From the S.W. to the N.E. these are the Asir, Hijaz–Najd, and Hail–ad Dawadimi regions. The post-orogenic granites as a whole are not homogeneously distributed over the shield. They are least abundant in the Asir region and increase in areal extent to the N.E. Small-scale maps and LANDSAT imagery covering the north-eastern portion of the Arabian Shield reveal that granites are the dominant rock type.

The first two are separated by the alkali-granite line which is defined by the distribution of alkali granites in the Arabian Shield. A literature search combined with the authors' own work produced the location of 45 Saudi Arabian alkali granites (Fig. 2). One noticeable aspect of their distribution is that an alkaligranite line can be drawn through the shield, south and west of which no such granites have been reported.

The boundary between the Hijaz–Najd and Hail–ad Dawadimi regions, is based on the relative amounts of granite in the two regions. The increase in area of exposed granite from the central shield to the N.E. is not gradational but is sharply demarcated. This demarcation is the dividing line between our Hijaz–Najd and Hail–ad Dawadimi regions.

Calc-alkaline granites are least abundant in the Asir region, and in south-western Asir they are very sparse. Interestingly, it is here that recent mapping has revealed a linear shonkinite-alkali syenite province (Fig. 2). Coleman (1973b) and Ratte (1974) reported a pluton, a plug, and several dikes of shonkinite in the Abha area in the southern part of the Asir region. Farther to the N.W. is the Lakathah ring complex which consists of a core of layered mafic and ultramafic rocks and

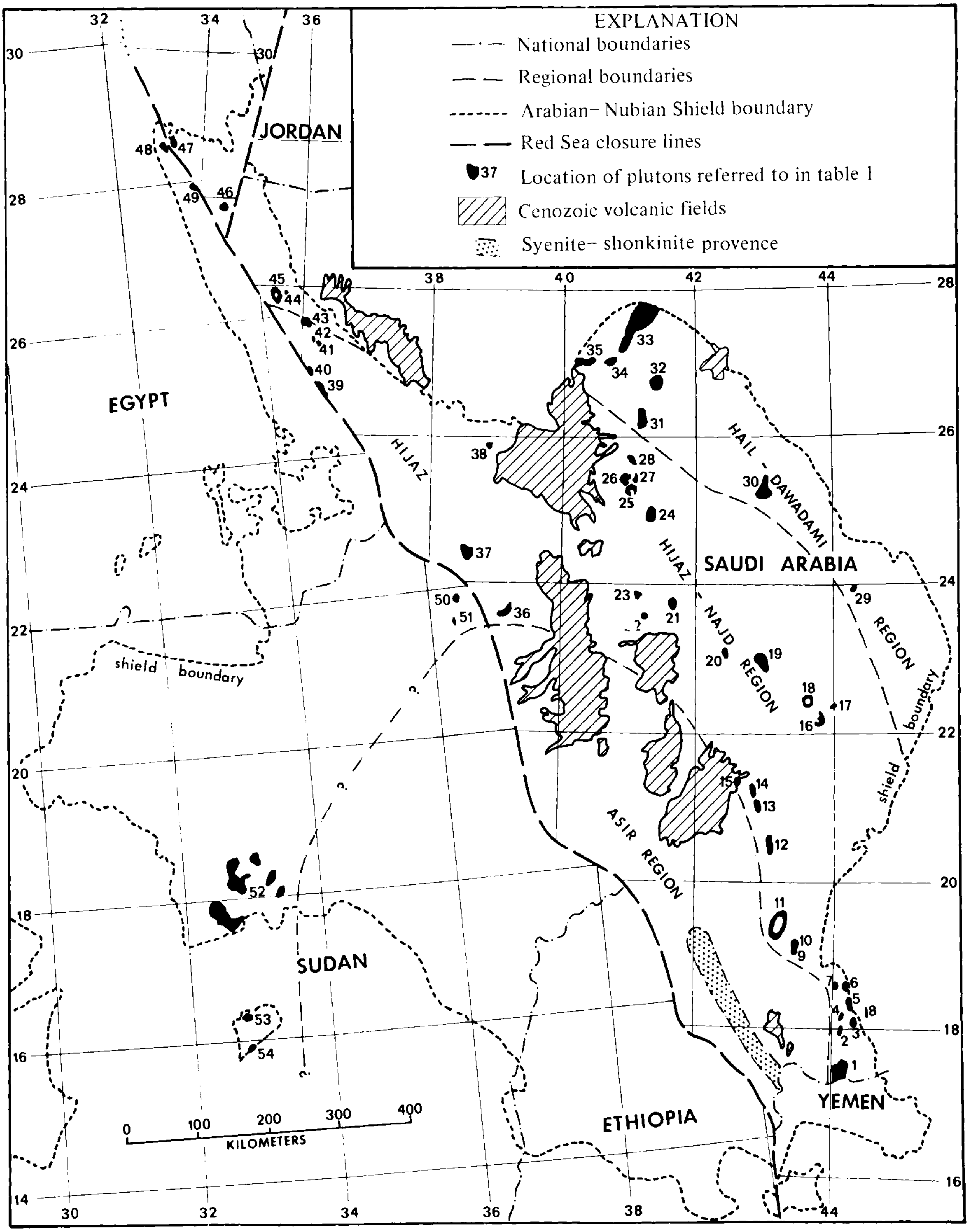

FIG. 2. Pre-Red Sea rift palinspastic map of the Arabian-Nubian Shield showing the location and distribution of alkali granite plutons.

TABLE 1. LOCALITY NAMES, REPORTED ROCK TYPES, AND REFERENCES TO ARABIAN-NUBIAN ALKALI GRANITE PLUTONS

Locality number	Locality name	Rock type	References
1	unnamed	biot.-arf.-rieb. gr.	this paper
2	unnamed	biot.-arf. gr.	Greenwood, in press
3	J. Ashirah ring complex	biot.-arf.-rieb. gr.	-do-
4	unnamed	-do-	-do-
5	unnamed	-do-	-do-
6	Wadi Idimah ring complex	-do-	-do-
7	unnamed	biot.-arf. gr.	-do-
8	unnamed	rieb. granophyre	-do-
9	unnamed	aeg.-rieb. gr.	this paper
10	unnamed	biot.-arf. gr.	-do-
11	J. Al-Hassir ring complex	-do-*	-do-
12	J. Taweel	aen.-rieb.-acmite gr.*	Schmidt, in prep.
13	unnamed	arf.-rieb. gr.	R. C. Greene, personal comm., 1978
14	unnamed	-do-	-do-
15	unnamed	-do-	-do-
16	J. Dahul	bark. gr.	Brosset, 1975
17	J. Salamah	-do-	-do-
18	J. Al-Kursh ring complex	bark. gr.	-do-
19	unnamed	bark.-biot. gr.	Letalenet and Bounny, 1977
20	J. Safwah	aeg.-rieb.-biot. gr.	-do-
21	J. Hasla	biot.-aeg. gr.	Conraux, 1969
22	J. Hadeb ring complex	aeg.-rieb. gr.	Conraux, 1969, Radain, 1978
23	J. Sayid	-do-	-do-
24	J. Bidayah	aeg. gr.*	Delfour, 1977
25	J. Tuwalah	aeg.-rieb. gr.*	-do-
26	Ar Raqab	aeg.-arf. gr.	-do-
27	An Namar	rieb. gr.*	-do-
28	J. Awja	-do-	-do-
29	unnamed	arf. (?) gr.	Bois and Shanti, 1971
30	J. Aban Al-Ahmar	arf. gr.	Aguttes, 1971
31	J. Al-Qunnawat	aeg.-arf. gr.	this paper
32	J. Ar-Rumman	-do-	-do-
33	J. Aja	aeg.-arf.-aen. gr.*	-do-
34	J. Al-Raud	aeg.-arf. gr.	-do-
35	Bayda Nathil	biot.-aeg., arf., rieb. gr.	-do-
36	J. Subh	rieb. gr.	V. Skiba, personal comm., 1978
37	J. Radwah	aeg. gr.	Petot, 1976
38	J. Lyaynat Al-Badan	rieb. gr.	Hadley, 1974
39	unnamed	soda-amphibole gr.	J. Kemp, personal comm., 1978
40	unnamed	-do-	-do-
41	unnamed	-do-	-do-
42	unnamed	-do-	-do-
43	unnamed ring dike	rieb. microgr.	-do-
44	Al-Ghurayyah	rieb.-albite gr.	Lalande, 1977
45	J. Dibbagh	aeg.-arf. gr.*	Harris, 1978
46	unnamed	rieb. gr.	Schurmann, 1966
47	J. Merzeqa	-do-	-do-
48	J. Gharib	-do-	-do-
49	Ras Zeit	-do-	-do-
50	J. Shendib	granophyric hastingsite gr.	Neary *et al.*, 1976
51	Karam Arit	granophyric rieb. gr.	-do-
52	Bayuda Desert complex	aeg.-arf.-rieb. gr.	Almond *et al.*, 1977
53	Sabaloka complex	soda-amphibole microgr.	Almond, 1977
54	Sileitat es Sufr	rieb. gr.	Vail, 1976

The following abbreviations are used: J.—Jabal, aeg.—aegirine or aegirine augite, aen.—aenigmatite, arf.—arfvedsonite, bark.—barkevikite, biot.—biotite, gr.—granite, microgr.—microgranite, rieb.—riebeckite. An asterisk (*) after a rock name indicates that an analysis for that rock is presented in Table 2.

thick outer ring of alkali syenite (Martin *et al.*, 1978). Greenwood (in press) also reports several small syenite plugs just to the east of the Lakathah complex. Current mapping in the southern end of the Asir region in the Jizan area by G. M. Fairer (personal comm., 1978) has revealed several major plutons and dikes of shonkinite, mafic-rich quartz-poor alkali granite and related rocks. No detailed petrography or chemical analysis of these rocks are available as yet.

The Hijaz–Najd and Hail–ad Dawadimi regions are distinguished from the Asir region not only by the occurrence of alkali-granites but also by the presence of the Shammar and Murdama Groups. The Hijaz–Najd region also contains the broad N.W.-trending latest Proterozoic Najd fault zone (Fleck *et al.*, 1976, 1979) which extends throughout most of the region approximately parallel to our regional boundaries. The boundary between the Hijaz–Najd and Hail–ad Dawadimi regions also appears to coincide with the northern limit of the Najd fault zone.

In our work to date, which has been mainly on granites in the southern and north-eastern portions of the shield, we have come to accept as a general rule that the calc-alkaline granites are older and give way temporally to alkaline and peralkaline granites. These later plutons are generally simple ovoid masses which cut all major rock types and are rarely cut by dikes or directly associated with other igneous rock types. A few are more complex and some are ring complexes (Table 1). Two of these complexes, the Jabal Al-Hassir and Jabal Aja granites should provide much information on the evolution of the late post-orogenic granites when they are more thoroughly studied.

The Jabal Al-Hassir ring complex (loc. 11, Fig. 2, Table 1) is a North-trending, nearly perfect oval with axial dimensions of 17 by 35 km. It consists of an outer ring of coarse hypersolvus peralkaline granite (analysis 5, Table 2) more than a kilometer thick, and a complex core of medium-grained leucocratic biotite monzogranite and granodiorite. Separating the two main units is a partial ring dike of quartz porphyry whose phenocrysts are set in a fine-grained groundmass. Large angular xenolithic blocks of unaltered country rock are abundant in both the core and rim granites, and in the southern half of the core unit they are more voluminous than the granitic matrix itself; one block is more than 5 km long. The Al-Hassir complex probably represents a subvolcanic caldera complex in which both calc-alkaline and peralkaline granitic magmas were emplaced. It is presently being studied in detail by Stoeser. The Jabal Al-Kursh, Jabal Hadeb, and Jabal Dibbagh ring complexes (locs. 18, 22 and 45, Table 1) are all similar to the Al-Hassir complex in that they all consist of peralkaline granite rims and metaluminous granite cores.

The Jabal Aja granite complex (loc. 33, Fig. 2, Table 1) is a huge, somewhat dumb-bell shaped pluton about 80 km long. The complex consists of four main units: (1) on the east and north, a thick partial outer ring of coarse, greenish-gray peralkaline granite (analysis 11, Table 2); (2) a complex core of pink to red granophyric granite (analysis 15, Table 2); (3) a xenolithic block or intrusion more than 5 km long of a green, probably comenditic (peralkaline) rhyolite and granite porphyry; and (4) a partial cap of red porphyritic rhyolite (analysis 18, Table 2). In addition, the core and rim contain large xenolithic blocks, as much as several kilometers in diameter, of country rock and pink (cogenetic?) granophyric granite. On one steep wadi face of 150 m of relief, the granophyre decreases in grain size upwards and is capped by three flow (?) units of rhyolite. The Jabal Aja complex apparently comprises a subvolcanic caldera complex. It is presently under detailed study by the authors.

Two basic interpretations of the distribution of granites in the Arabian Shield are that (1) the shield is more deeply eroded in the south so that previously existing high crustal-level granites and effusives still present in the north have been removed, or (2) post-orogenic granites were more voluminous in the north-eastern shield. The distribution of rhyolites of the Shammar Group strongly suggests that depth of erosion is greater to the south. These rocks are voluminous to the N.E. and in a number of places even cap granitic complexes, such as at Jabal Aja, indicating about a kilometer or less of erosion. Moving southwards, the volume of Shammar volcanic rocks gradually decreases, and in the southern third of the shield they are absent altogether even though the same types of granites occur there. Furthermore, in the north-eastern area, contacts of granites often dip outward, whereas in the south they are very steep and typically dip inwards, suggesting a greater depth of erosion in the south.

Even assuming that the above is correct, no great depth of erosion of the post-orogenic (Pan-African) crust in the south is apparent. It seems unlikely that the present level of exposure of the Al-Hassir represents a depth of more than several kilometers. Coleman *et al.* (1977) have estimated a depth of erosion of about 1.2 km for the Jabal Shayi gabbro, which lies about 70 km S.W. of Jabal Al-Hassir; and Dodge (1979) has estimated approximately 3 km of erosion on the calc-alkaline Uyaijah ring structure in the east-central shield.

In the Asir region there is over 2 km of relief on the Red Sea escarpment, so exposures near sea level should represent a minimum depth of erosion of at least 3 to 5 km in the crust. Given this depth of erosion, there is not enough granite exposed in the Asir region to suggest that the eroded portion of the crust contained as much granite as that observed in the north. Thus, the distribution pattern of granites in the Arabian Shield probably reflects that a greater volume of Pan-African granite was emplaced in the northern and north-eastern shield. In addition, the bulk of the layered rocks in the southern shield have only been metamorphosed to the greenschist facies, which would not be true had significant amounts of granite passed through them.

Nubian Shield

We have extended the alkali granite line into the Nubian part of the Arabian–Nubian Shield (Fig. 2). We found no reports of peralkaline granites east of this line either in south-eastern Sudan or in Ethiopia. Although the search of literature on the Nubian Shield was limited, it is clear that a late Proterozoic (Pan-African) peralkaline granite province extends over much of the Arabian–Nubian Shield and is possibly the largest such province in the world.

Several differences between the Arabian versus Nubian shield segments became apparent. The first relates to the distribution of syenites in the two areas. In Sudan, many of the post-orogenic granites are closely associated with minor gabbroic and over- and undersaturated syenitic rocks, and over half of the ring complexes, including those of the coastal region north of Port Sudan, contain syenite (Vail, 1976; Neary *et al.* 1976). Except in the syenite–shonkinite province of the Asir region, syenites are rare in the Arabian Shield, including the coastal area north of Jeddah which would match the area north of Port Sudan. A second difference is that many intrusions of Paleozoic and Mesozoic age are reported from Sudan and Egypt, and even Tertiary granitic intrusions have been recognized in Egypt (Vail, 1976; Neary *et al.*, 1976; El-Ramly *et al.*, 1969a,b). Radiometric age determinations have not revealed, so far, any such young rocks for the Arabian Shield although only a few determinations have been made for rocks in the Hijaz region. Intrusions cutting the basal Cambrian and Ordovician sedimentary rocks east of the Red Sea are known from only two localities, the Ar-Raha dacites just north of Harrat Ar-Raha (Villemur *et al.*, in press) and quartz porphyry dikes of about 560 Ma in Jordan (Lenz *et al.*, 1972).

AGE OF ROCKS

The original definition by Kennedy (1964) of the Pan-African thermotectonic episode was applied to events of about 500 Ma age in central Africa. Since then, common usage has expanded the Pan-African episode to cover the approximate range 500–650 Ma. Using the K–Ar dating method, Fleck *et al.* (1976) show that the Arabian Shield was subjected to a major thermal event between 560 and 610 Ma ago and to a minor one between 510 and 540 Ma ago. Dates for these thermal events are close to that assigned to the Pan-African by Kennedy (1964). The net result of the thermal episodes was that the K–Ar systematics were disturbed throughout the Arabian Shield, thus rendering the method of little use in dating the older rocks.

Considerable Rb–Sr dating has now been done and a clear picture of the emplacement dates of the post-tectonic metaluminous calc-alkaline granites has emerged. For granites of the southern shield, Fleck *et al.* (1979) have obtained ages mainly in the 600–650 Ma range. Zr age determinations on post-tectonic granites and gabbros of the southernmost shield indicate that they were emplaced around 660–670 Ma (Cooper *et al.*, 1979; Stacey and Stoeser, work in progress). For metaluminous granites of the north-central and eastern shield, Baubron *et al.* (1976) have determined somewhat younger Rb–Sr ages, in the 552–638 Ma range and Nasseef and Gass (1977) report 525 Ma and 592 Ma respectively for two metaluminous granites from the At-Ta'if area east of Mecca. It remains to be seen whether the apparent progressive decrease in ages towards the north for the post-tectonic granites is real or is merely an artifact of the data.

Baubron *et al.* (1976) give two Rb–Sr age determinations for peralkaline granites: Jabal Bidayeh 571 ± 8 Ma (initial $^{87}Sr/^{86}Sr = 0.7055 \pm 0.0006$) and Jabal At-Tuwalah, 600 ± 24 Ma (initial $^{87}Sr/^{86}Sr = 0.7041 \pm 0.0006$) (localities 24 and 25, Fig. 2; analyses 7 and 9, Table 2). Given these data plus the field relationships of the late alkaline and peralkaline granites which indicate that they are the last major plutonic phase of the Arabian Shield, we tentatively assume that these granites were largely emplaced during the period 550–620 Ma ago. If this assumption is correct, then emplacement of the peralkaline granites and the major Pan-African thermal event found by Fleck *et al.* (1976) were broadly contemporaneous.

CHEMISTRY

Table 2 presents a number of new analyses as well as selected analyses from the literature for Arabian Shield granites and rhyolites. The bulk of these analyses are of alkaline-granitic rocks of the shield. Chemically, a rock is defined as peralkaline if the agpaitic ratio $[(Na_2O + K_2O)/Al_2O_3]$ is greater than one (Carmichael *et al.*, 1974). For the Arabian rocks a maximum ratio of 1.29 was found (Table 2).

Table 2.--*Major and minor element analyses for*

ANALYSIS NO.	1	2	3	4	5	6	7	8	9
SAMPLE NO.	112765	112361	112326	79G-JCB91[2/]	112522	83248A[3/]	86E-LC442[2/]	86A-LC443[2/]	78H-JCB123[2/]
LATITUDE	19°24.8'	18°54.4'	19°12.2'	25°44'20"	19°37.2'	20°46.8'	25°07'55"	25°26'15"	25°31'40"
LONGITUDE	43°20.6'	43°43.4'	43°11.4'	41°34'40"	43°05.2'	42°55.9'	41°09'40"	41°04'05"	40°58'10"
LOCALITY	NE ¼ Duthur as Salam quad.	Jabal Lahu	Jabal Duthur as Salam	Jabal ar Rahadah	Jabal al Hassir, rim	Jabal Taweel	Jabal Bidayah	Jabal Tuwalah	Jabal Tuwalah
ROCK TYPE	late biotite syenogranite	late biotite monzogranite	leuco. biotite monzogranite	biotite monzogranite	aenig. biotite arfved. peralk. granite	aenigmatite acmite peralk. granite	aegirine alkali granite	aegirine alkali granite	riebeckite alkali granite
Major									
SiO_2	67.6	74.0	75.0	77.00	75.1	74.26	73.60	76.10	75.20
TiO_2	0.48	0.25	0.31	0.10	0.41	0.42	0.43	0.19	.19
Al_2O_3	14.5	13.0	11.9	11.75	11.1	11.20	12.40	10.80	11.20
Fe_2O_3	1.1	0.39	1.0	1.03	0 94	5.28	1.55	2.15	1.40
FeO	2.6	0.64	0.52	0.15	2.0	4/	0.90	1.10	1.15
MnO	----	----	----	0.03	----	0.02	0.10	0.03	0.04
MgO	0.19	0.22	0.18	0.05	0.14	0.10	0.40	0.15	0.10
CaO	1.3	1.1	0.63	0.52	0.74	0.65	0.85	0.45	0.42
Na_2O	5.0	4.3	4.2	4.10	4.0	4.80	4.80	4.40	4.60
K_2O	5.9	4.7	4.4	4.66	4.8	5.15	4.30	4.30	4.24
P_2O_5	----	----	----	0.01	----	----	0.06	0.05	0.02
CO_2	----	----	----	0.04	----	----	0.11	0.05	0.08
SO_3	----	----	----	0.03	----	----	----	----	0.01
F	0.057	0.086	0.057	----	0.092	----	----	----	----
H_2O^+	----	----	----	0.36	----	----	0.30	0.25	0.34
H_2O^-	----	----	----	0.00	----	----	0.15	0.20	0.03
L.O.I.[1/]	0.34	0.41	0.44	----	0.21	----	----	----	----
TOTAL	99.07	99.10	98.64	99.83	99.53	101.88	99.95	100.22	99.02
Minor									
Rb	144	346	182	189[5/]	118	----	104[6/]	179[7/]	----
Sr	42	162	51	20[5/]	51	----	54[6/]	12[7/]	----
Li	20	10	40	----	20	----	----	----	----
CIPW Norms									
Q	13.44	29.18	32.82	34.52	32.29	27.29	27.35	33.75	32.58
C									
OR	35.19	28.03	26.36	27.58	28.50	29.87	25.46	25.41	25.30
AB	42.13	36.72	36.03	34.55	30.52	28.40	39.92	31.61	34.34
AN		2.31	0.63						
TH				0.05					0.02
AC	0.51				3.08	5.40	0.68	3.38	2.69
NS						1.24		0.41	0.43
WO	2.53	1.06	0.87	0.95	1.26	1.32	1.31	0.66	0.67
EN	0.48	0.55	0.45	0.13	0.35	0.24	1.00	0.37	0.25
FS	2.60	0.50	0.83	0.94	2.79	5.45	1.83	3.56	2.78
MT	1.71	0.54	0.81	0.61			0.94		
IL	0.92	0.48	0.60	0.19	0.78	0.78	0.82	0.36	0.36
AP				0.02			0.14	0.12	0.05
FR	0.12	0.19	0.13		0.19				
CC				0.09			0.25	0.11	0.18
TOTAL	99.63	99.56	99.53	99.63	99.76	99.99	99.70	99.74	99.65
SALIC	90.76	96.24	95.84	96.70	91.31	85.56	92.73	90.77	92.24
FEMIC	8.87	3.32	3.69	2.93	8.45	14.43	6.97	8.97	7.41
AGPAITIC RATIO	1.01	0.94	0.98	1.00	1.06	1.20	1.01	1.10	1.09

1/ loss on ignition (L.O.I.) values equal originally reported L.O.I. values minus the fluorine values above

2/ from Delfour, 1977

3/ from Schmidt, in prep.

4/ all Fe reported as Fe_2O_3

5/ average of 9 samples from Baubron and others, 1976 *selected granites of the Arabian Shield*

10 79E-JD3924 2/ 25°35'20" 41°04'20" an Namar riebeckite alkali granite	11 112991 27°20.8' 41°26.1' Jabal Aja rim granite aenigmatite, aegirine arfved. peralk. granite	12 124017 27°54'55" 35°44'38" J. Dibbagh rim granite aeg. arfved. peralk. granite	13 78G-JD3985 2/ 25°43'00" 40°33'20" 2 km SE of Suhur granophyric rhyolite	14 78D-JD3955 2/ 25°48'45" 40°49'25" 6 km SW of Bir al Biday granophyre	15 112981 27°20.9' 41°24.6' Jabal Aja core granite medium-grained biot. alkali granite	16 112914 25°48.4' 41°54.4' Nuqrah quad. Shammar plagioclase porphyritic rhyolite	17 79E-JD3919 2/ 25°39'40" 41°07'10" Jabal al Malhah Shammar porphyritic alkali rhyolite	18 112975 27°22.0' 41°22.3' Jabal Aja cap rhyolite alkali-feld. quartz porphyritic rhyolite	19 128032 27°09.9' 42°14.5' Jabal Selma cap rhyolite feldspar porphyritic rhyolite
73.40	77.2	76.4	66.80	68.60	78.9	71.4	72.20	77.4	77.0
0.25	).42	0.31	0.68	0.45	0.27	0.54	0.26	0.29	0.25
11.30	9.4	11.0	13.80	15.05	10.6	13.4	13.35	10.4	11.7
1.75	2.4	1.6	2.75	1.35	1.3	1.8	1.60	1.2	0.72
1.75	1.4	1.2	2.45	1.85	0.39	0.60	1.00	0.26	0.39
0.09			0.11	0.06		----	0.07	----	----
0.35	0.027	0.032	0.90	0.90	0.080	0.39	0.50	0.051	0.13
0.80	0.35	0.27	2.40	1.30	0.36	1.0	1.00	0.38	0.55
4.50	4.4	4.2	4.15	4.50	3.6	5.5	4.35	3.5	3.8
4.85	4.5	4.6	3.95	4.10	4.5	3.6	4.90	4.4	5.0
0.03	----	----	0.19	0.14	----	----	0 05	----	----
----	----	----	----	----	----	----	----	----	----
0.10	----	----	0.075	0.055	----	----	0.03	----	----
----	0.17	0.12	----	----	0.21	0.11	----	0.18	0.12
0.45	----	----	1.55	1.20	----	----	0.80	----	----
0.10	----	----	0.10	0.05	----	----	0.00	----	----
----	<0.1	<0.1	----	----	0.39	0.59	----	0.42	0.48
99.72	100.27	99.73	99.91	99.61	100.60	98.93	100.11	98.48	100.14
----	200	155	----	----	264	118	----	391	255
----	34	34	----	----	34	114	----	34	42
----	90	60	----	----	30	20	----	20	30
28.31	38.83	34.51	20.99	22.38	39.97	23.58	25.06	40.33	34.84
				1.26					
28.77	26.51	27.24	23.39	24.34	26.43	21.50	28.92	26.40	29.51
31.24	23.22	31.04	34.66	37.85	29.29	47.04	36.57	29.45	32.11
			7.65	5.56		1.26	2.53		0.10
0.18			0.14	0.11			0.05		
3.66	3.95	2.93			0.87			0.55	
0.51	2.19	0.29							
1.58	0.21	0.19	1.27		0.10	1.23	0.88	0.24	0.73
0.87	0.07	0.08	2.25	2.25	0.20	0.98	1.24	0.13	0.32
3.88	3.76	2.78	3.66	2.19	1.28	1.24	1.97	0.96	0.56
			2.72	1.68	0.44	1.26	1.36	0.50	0.58
0.48	0.80	0.59	1.29	0.86	0.51	1.04	0.49	0.56	0.47
0.07			0.45	0.33			0.12		
	0.35	0.25			0.43	0.23		0.38	0.25
99.55	99.89	99.90	98.47	98.81	99.52	99.36	99.19	99.50	99.47
88.50	88.56	92.79	86.83	91.50	95.69	93.38	93.13	96.18	96.56
11.05	11.33	7.11	11.64	7.31	3.83	5.98	6.06	3.32	2.91
1.12	1.29	1.09	0.81	0.79	1.02	0.97	0.93	1.01	1.00

6/ average of 13 samples from Baubron and others, 1976

7/ average of 11 samples from Baubron and others, 1976

The ratio is quite sensitive to errors in the analysis, and the presence of soda-mafic silicates such as aegirine or arfvedsonite in the rock generally confirms their peralkalinity. Rocks with ratios slightly greater than one in Table 2 should not be taken as necessarily peralkaline unless the presence of such minerals is indicated in the table.

The calc-alkaline granites of the Arabian Shield appear to represent the end products of 300 million years of calc-alkaline evolution (Fleck *et al.*, 1979). Figure 3 is a standard AMF triangular diagram which illustrates that the plutonic and volcanic rocks of the western and central parts of the shield have a typical calc-alkaline trend (Carmichael *et al.*, 1974). Several new analyses of alkalic metaluminous granites are given in Table 2 (analyses 1–4). For detailed descriptions of the chemistry of the calc-alakaline granites the reader is referred to Delfour (1977), Nasseef and Gass (1977), Kanaan (1979), and Dodge (1979). Various plots using available major element analyses show that a continuum appears to exist between the calc-alkaline and peralkaline granites (Figs. 4, 5). In the field, it is usually possible to distinguish the two classes of granites with a total count scintillometer (Geometrics C_1R-101A, 43.1 cm^3 NaI crystal), because the calc-alkaline granites typically produce 60 to 150 counts per second, whereas

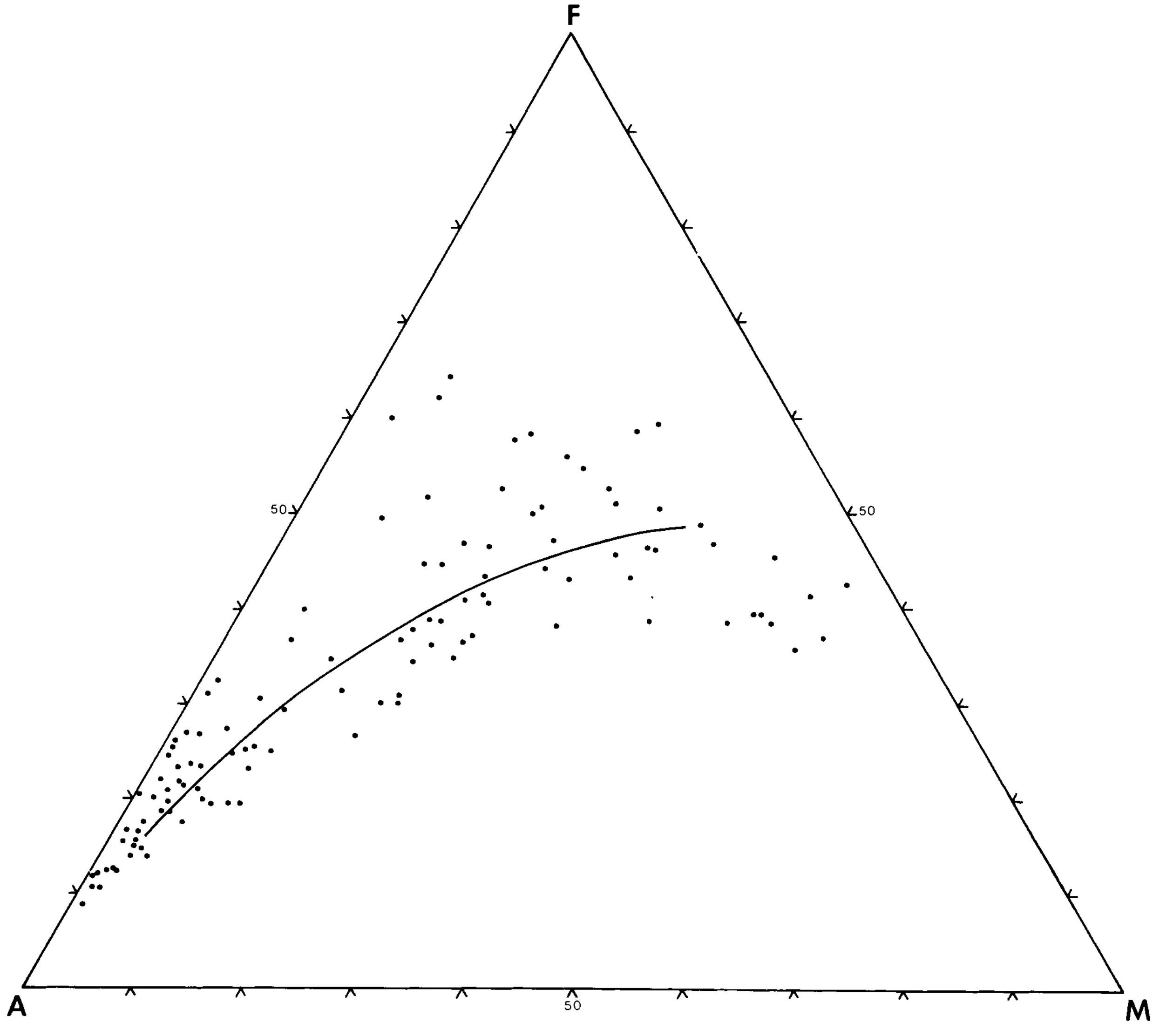

FIG. 3. AMF triangular diagram for plutonic and volcanic rocks of the Arabian Shield. $A = Na_2O + K_2O$, $M = MgO$, and $F = FeO + Fe_2O_3$. Data from R. J. Fleck (unpublished data), F. C 'V. Dodge (unpublished data), Nasseef and Gass (1977), Delfour (1977), and Kanaan (1979). The curve is the average trend line for the Sierra Nevada batholith (Carmichael *et al.*, 1974).

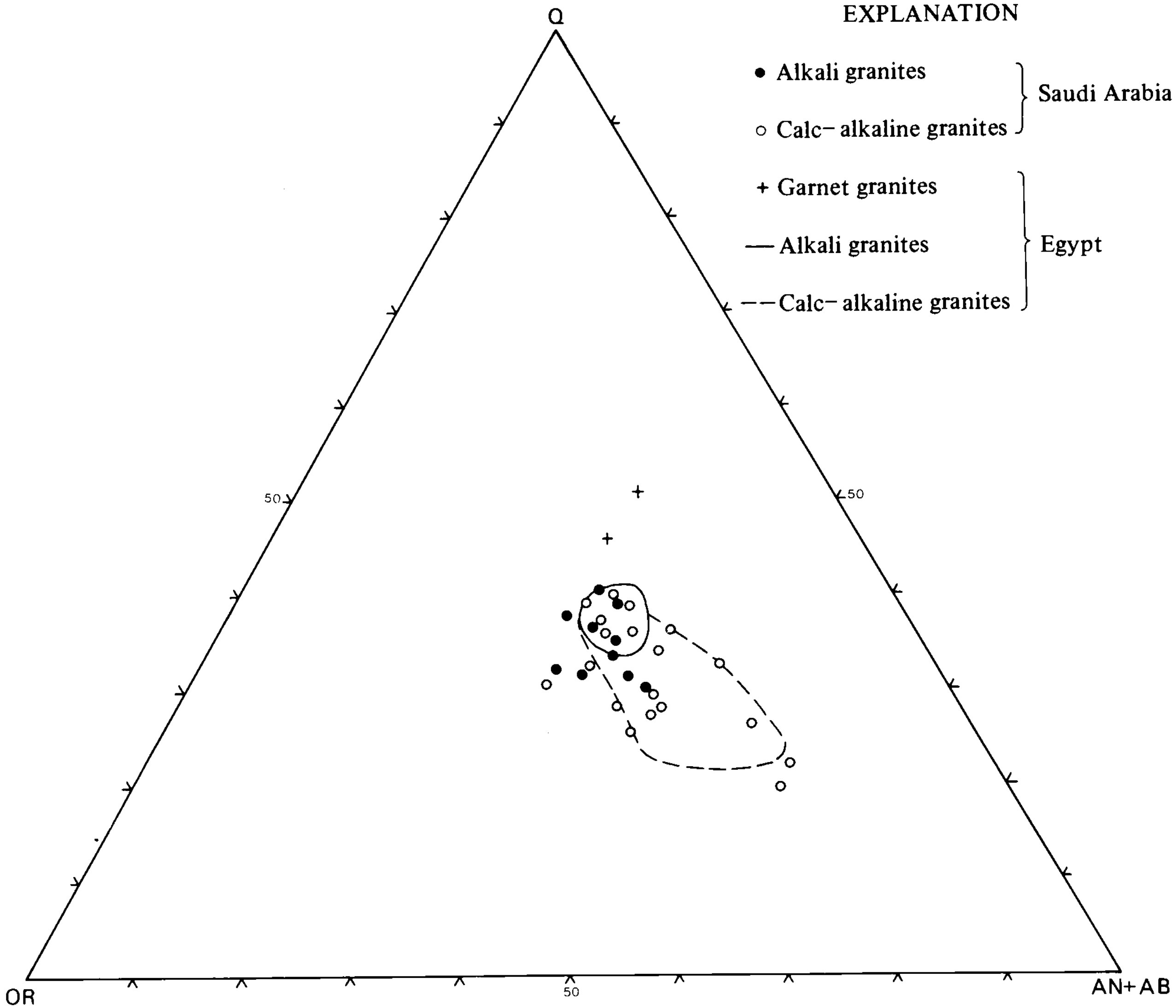

FIG. 4. Normative quartz (Q)–orthoclase (OR)–plagioclase (AN + AB) triangular diagram for Saudi Arabian and Egyptian granites (Schurmann, 1966). Diagram includes data from Delfour (1977), Greenwood and Brown (1973), and Schmidt *et al.* (in press).

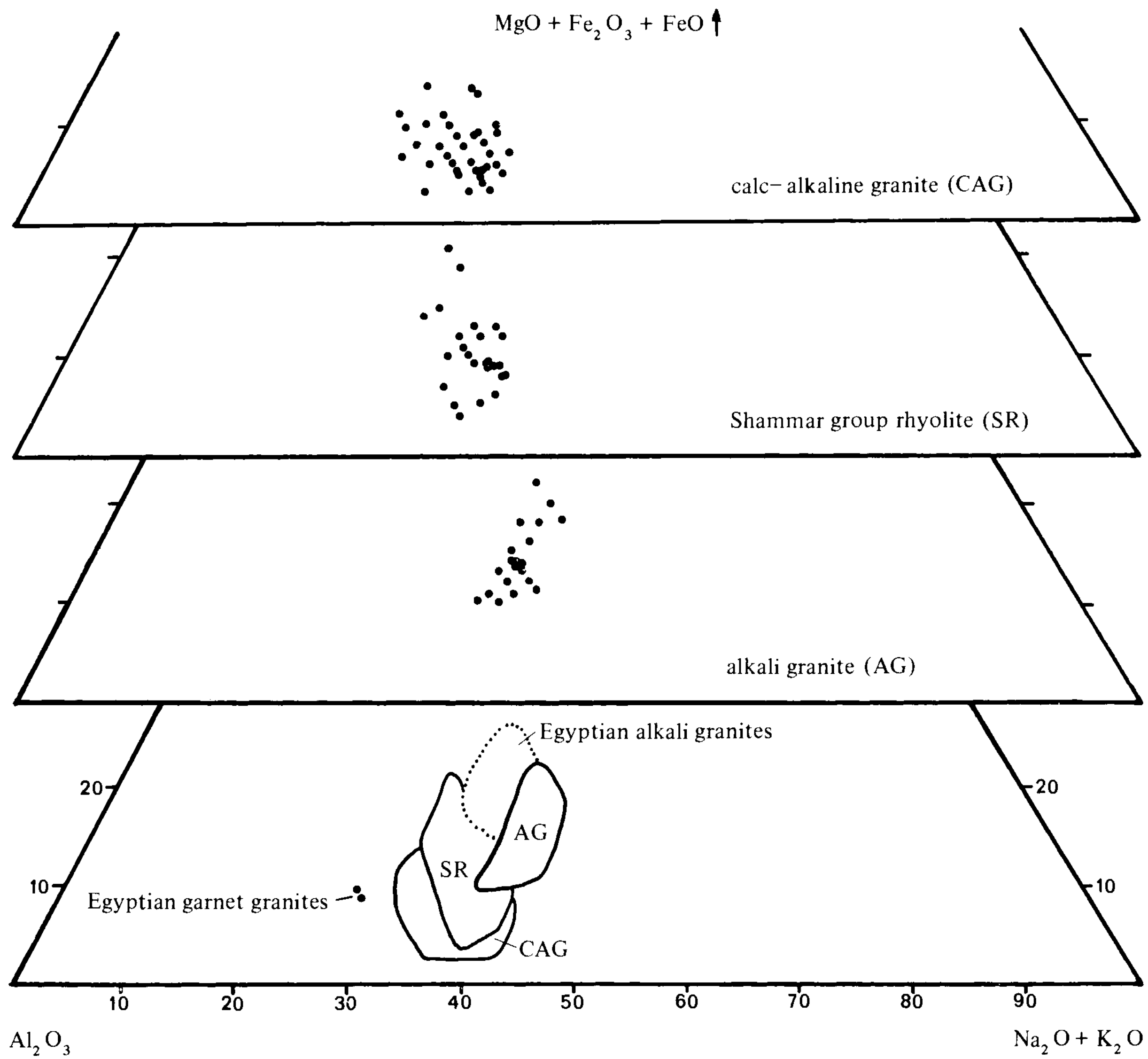

FIG. 5. Total alkali–alumina–total iron oxides and magnesia ternary diagrams (weight percent) for Arabian granites and rhyolites. The four fields shown in the lower diagram are for calc-alkaline granites (CAG) of the Arabian Shield, Shammar rhyolite (SR), Saudi Arabian alkali granites (AG), and Egyptian alkali granites (after Schurmann, 1966); also plotted are two Egyptian garnet granites. Arabian data from R.J. Fleck (unpublished), Greenwood and Brown (1973), Nasseef and Gass (1977), Delfour (1977), and Kanaan (1979).

the peralkaline granites typically give 150 to 350 counts per second.

The peralkaline granites of the Arabian Shield are typical of such granites elsewhere and are very similar to the classic suite of the Jos Plateau of Nigeria (Jacobsen *et al.*, 1958). The Arabian peralkaline granites have total alkali contents similar to the calc-alkaline granites, but are relatively low in Al (thus leading to the peralkalinity) as well as Mg and Sr and are enriched in Fe (Table 2, Figs. 4, 5).

As noted earlier, the alkaline and peralkaline granites are often closely associated with rhyolites of the Shammar Group. Based on their chemistry, the rhyolites do not, however, appear to be effusive equivalents of the peralkaline granites, because although some of them are alkaline, they are generally not peralkaline and appear to be transitional in composition between the calc-alkaline and peralkaline granites (Table 2, Fig. 5). Nevertheless, because of the possibility of post-eruptive changes in the composition of the rhyolites, particularly loss of alkalis which generally occurs for over-saturated peralkaline volcanics during crystallization or glass hydration (Noble, 1968; Macdonald and Bailey, 1973), a firm conclusion on the relationship of the Shammar rhyolites to the late post-tectonic granites must await more field and analytical data. The close spatial relationship of the peralkaline granites, pink and red granophyres, and Shammar rhyolites, however, strongly suggests a genetic link.

One characteristic of many of the late post-tectonic granites is their red, often brick-red, color. Taylor (1978) finds that this color is typical of many granites from Precambrian terranes, and that such rocks also show a strong enrichment in O^{18}. Taylor also has observed that these granites typically have turbid feldspars due to hematitic dust; primary mafic minerals altered to uralitic amphibole, chlorite, Fe–Ti oxides and epidote; and local mariolitic cavities. These features are also characteristic of the late alkali granites of Arabia, particularly the granophyric granites. Taylor (1978) also notes that the Rb–Sr systematics of the red granites are altered, making these rocks difficult or impossible to date by this method. Radiometric work in the Arabian Shield by Fleck (personal comm., 1979) indicates a similar situation for the Arabian red granites. Taylor attributed these changes to a low temperature hydrothermal alteration event of long duration involving meteoric water. Radain (1978) gives a similar interpretation to peralkaline granites of the Jabal Sayid area of Saudi Arabia which have very high O^{18} contents (locs. 22, 23; Fig. 2). Clearly, the interpretation of chemical data for such rocks will be difficult.

PETROGENESIS

The origin of oversaturated magmas is not understood. The study of oversaturated peralkaline rocks has focussed on the glassy phases of peralkaline effusive rocks, the comendites and pantellerites, in order to minimize the problems related to composition changes caused by hydration or crystallization, such as loss of Na and gain or loss of Si, K, halogens and alkaline rare earths (Noble, 1968). These two rock types compositionally grade into one another; the comendites are mildly peralkaline (agpaitic ratio 1.00–1.25) whereas the pantellerites are very peralkaline (agpaitic ratio 1.25) (Bowden, 1974; Macdonald and Bailey, 1973). From Table 2 the Arabian peralkaline granitic rocks are seen to be comenditic in composition.

Theories of origin for the peralkaline effusive rocks differ from those for the plutonic peralkaline granites. Many authors apparently believe that the peralkaline effusive rocks are the products of crystal fractionation which followed the general trend from transitional or mildly alkaline basalt through trachyte and oversaturated alkaline trachyte to comendite or pantellerite, although addition of alkalis by volatile transfer at a late stage may also play a role (Noble, 1968; Noble *et al.*, 1969; Bowden, 1974). These rock types are sometimes found together in volcanic sequences for which a genetic relationship seems likely (Dickinson and Gibson, 1972; Berberi *et al.*, 1975).

For the peralkaline granites a wide range of theories of genesis have been presented, most of which involve partial melting of the crust. These are: (1) metaluminous granitic melts fractionate to leave a peralkaline residual magma (Wright, 1969); (2) basaltic and metaluminous granitic melts form in the mantle and lower crust and upon rising into the upper crust generate peralkaline partial melts (Bowden and Turner, 1974); (3) basaltic melts rise into the crust and through interaction with palingenetic melts generated in the crust form peralkaline granitic melts; and (4) peralkaline melts are the primitive melts of the lower crust, and as they rise are converted by reaction and contamination with sialic crustal material to normal metaluminous granitic melts (Bailey and Schairer, 1966). These ideas are mainly suggestions as none are supported by detailed modelling. In any event, the facts that the Arabian peralkaline granites appear late, after the bulk of the calc-alkaline metaluminous granites, and are closely associated only with these granites, is highly suggestive that the two are related and that the metaluminous granites have an antecedent role. Genesis of the peralkaline granites by partial melting of the calc-alkaline plutonic rocks seems possible. In contrast, the Sudanese peralkaline granites appear to be closely associated with gabbro and syenite which suggests an origin similar to that proposed for the comendites and pantellerites. It will be interesting to see if further work in the Arabian–Nubian Shield substantiates the apparent difference in associations for the peralkaline granites of the two halves of the shield. Many of the ideas above can be tested by determining the initial $^{87}Sr/^{86}Sr$ ratios for carefully selected suites of these rocks.

The correlation of peralkaline magmas with both oceanic and continental anorogenic tensional environments is one of their outstanding characteristics and has been widely recognized (Bailey and Schairer, 1966; Wright, 1969; Bowden, 1974). The general nature of the occurrence of peralkaline granites in the Arabian Shield and their appearance before and during the period of Najd faulting, which was in part tensional, seems consistent. Models relating this period to a time of nearby continental collision have been proposed by Fleck *et al.* (1979) and Schmidt *et al.* (1979).

MINERALIZATION ASSOCIATED WITH YOUNGER GRANITES

Despite the abundance and widespread distribution of granites in the Arabian Shield, very few mineral deposits have been discovered thus far which show evidence of a common origin with the granitic rocks. Some quartz veins bearing precious and/or base metals, which were exploited in ancient times, may have a genetic relationship to younger granites in some areas but in most instances this relationship is difficult to establish. Many fluorite occurrences, some of which have ancient workings, are commonly associated with younger granites (Kemp, 1977).

Even though few deposits are associated with the younger granites in the Arabian Shield, numerous occurrences and geochemical anomalies of W, Mo, Sn, Nb, Be, Zr, Th, U, rare earths and fluorite show a close spatial relationship with these granites. Table 3 is a compilation from all available sources, published and unpublished, of these mineral occurrences and areas of geochemical anomalies. Figure 6 shows that these occurrences and anomalies are widely but irregularly distributed throughout the shield. They appear to be concentrated in the north-eastern shield, north of lat. 24° and east of long. 40°, and in the east-central part of the shield, between lats. 20 and 24° and east of long. 42°. The distribution shown in Fig. 6 may reflect in part the difference in the scope of geologic investigation in various parts of the shield. However, most of these occurrences were found during reconnaissance geologic and geochemical surveys, and practically all of the shield has been covered by these surveys; therefore, Fig. 6 is believed to reflect fairly accurately the distribution of mineralization associated with granitic rocks. Occurrences and anomalies are concentrated where granitic rocks are abundant relative to dioritic rocks; in the north-eastern and central parts of the shield, the ratio of granite to diorite is about 1:2, whereas in the south-western part of shield in which mineral occurrences of these types are few, the ratio is about 1:7 (Mineral Resources Activities, 1976).

Although no deposits are known to have significant past production or reserves of present commercial value, at least three areas where deposits are associated spatially with granites have been investigated in sufficient detail to allow these deposits to be classified as resources. These are the Ablah Hill fluorite deposit, the Uyaijah–Thaaban area and the Ghurayyah radioactive granite (nos. 45, 31, and 1, Table 3 and Fig. 6).

The Ablah Hill fluorite deposit in the southern part of the shield is a pipe in a breccia zone that is probably related to an unexposed granite intrusion. The deposit was worked in ancient times, probably to extract high-grade pockets of metallic ores dispersed through the fluorite. About 20,000 tonnes of fluorite possibly remain in the pipe to a depth of 50 m (Kemp, 1977).

In the east-central part of the shield, occurrences of Mo and W are associated with the Uyaijah ring structure. The location and nature of these occurrences were first indicated by reconnaissance geochemical sampling of sediments, which revealed strong anomalies in W and Mo and weaker anomalies in Sn and other elements (Whitlow, 1966a). Later work by Theobald and Allcott (1973) outlined two areas of about 40 km^2 each in the Uyaijah ring structure, in which heavy mineral concentrates of surficial debris contained anomalous amounts of W, Mo and Bi. More detailed geologic and geochemical investigations were made in both of these areas, the Buhairan–Abu Khurg area (Dodge, 1973) and the Uyaijah–Thaaban area (Dodge and Helaby, 1974).

The Uyaijah ring structure consists of an older batholith of granodiorite that is intruded by a small stock and a ring dike of calc-alkaline granite and cut by numerous late epithermal quartz veins. In the Buhairan–Abu Khurg area, the geochemical anomalies, principally of W, are believed to result from the weathering of small occurrences of powellite and sheelite in high-temperature quartz-rich veinlets and in pods in contact metamorphic rocks. No valuable mineral deposits were found or are thought to be present. The Uyaijah–Thaaban area contains many molybdenite-bearing quartz veins as much as 2 m wide and several hundred

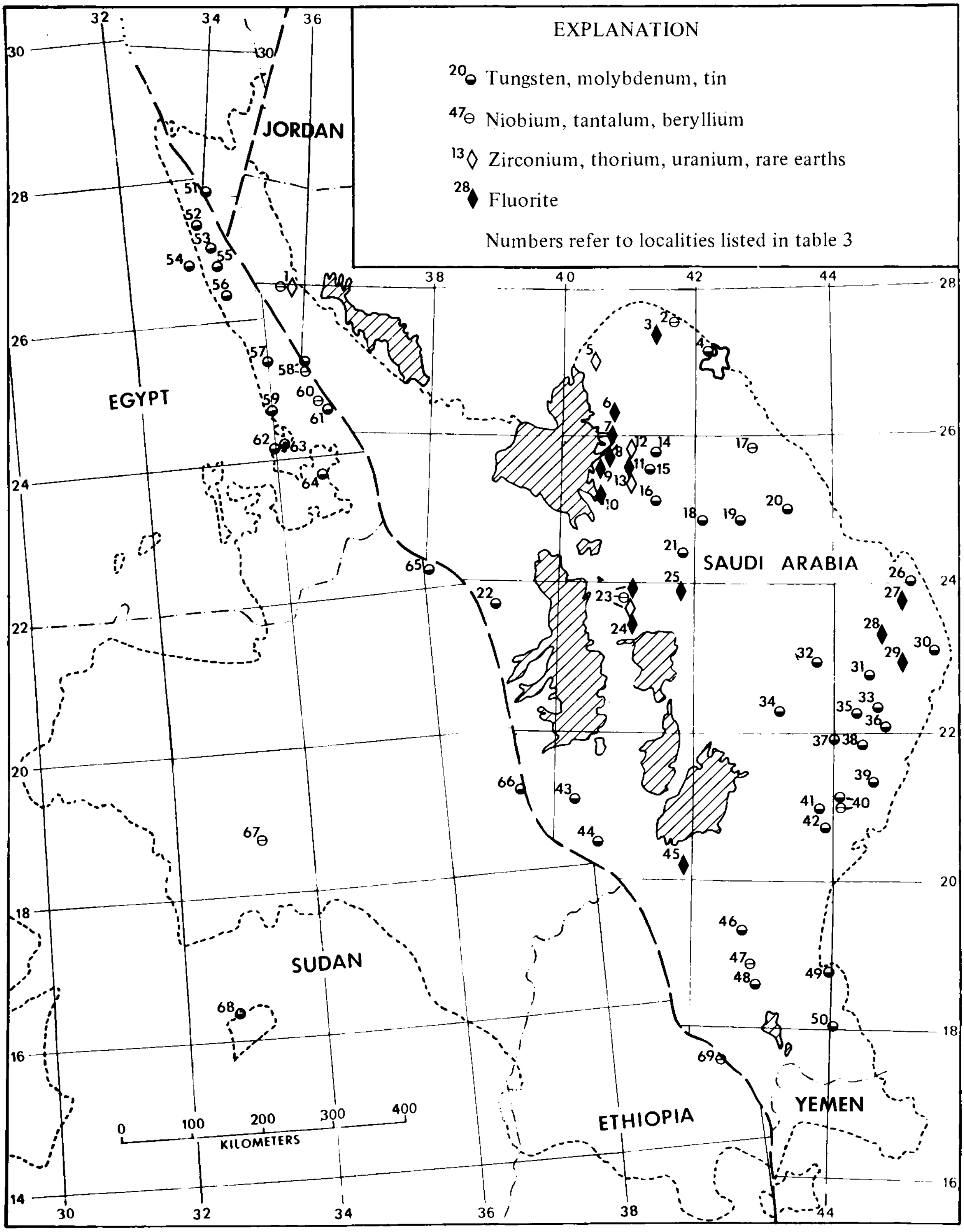

FIG. 6. Mineral occurrences and geochemical anomalies associated with young granitic plutons in the Arabian-Nubian Shield.

TABLE 3. NAMES, DESCRIPTIONS AND REFERENCES FOR MINERAL OCCURRENCES AND GEOCHEMICAL ANOMALIES SHOWN IN FIG. 6

Locality number	Locality name	Description	References
1	Al-Ghurayyah	Prospect; granite with Zr, Nb–Ta, U	Lalande, 1977; Shepherd, 1966
2	Ha'il area	Occurrence; Nb, Th, rare earth elements in veins and granite	Matzko and Naqvi, 1978
3	Jabal Aja	Occurrence; quartz-fluorite vein in granite	Present study
4	Jabal Selma	Geochemical anomaly; W, Mo in wadi sediments	Mytton, 1970
5	Baydā'Nathīl area	Occurrence; elpidite (Na–Zr-silicate) in granite	Present study
6	Zarghat–Hanakiyah–Nuqrah area	Occurrence; fluorite	Kemp, 1977
7	-do-	-do-	-do-
8	-do-	-do-	-do-
9	-do-	-do-	-do-
10	-do-	-do-	-do-
11	-do-	-do-	-do-
12	Jabal Awja	Occurrence; Th-bearing zircon in pegmatites	Delfour, 1977
13	Jabal at Tuwalah–Jabal ar Rabuth	-do-	-do-
14	Al-Hayitiyah	Occurrence; scheelite in quartz vein	MODS no 539, 540[1]
15	Wadi Shaela	Occurrence; scheelite in veins	MODS no. 562, 566
16	Jabal Subhah	Occurrence; scheelite in veins	MODS no. 219; Le Chapelain, 1971
17	Wadi Maraghān	Geochemical anomaly; Be in Wadi sediment	Mytton, 1970
18	El-Koom	Occurrence; wolframite and scheelite in quartz veins in granodiorite	Ankary, 1965
19	Jabal Sha'bā	Geochemical anomaly; W in heavy mineral concentrates of wadi sediment	Mytton, 1970
20	Jabal Minya	-do-	-do-
21	Wadi Al-Furdukhiyah	Occurrence; scheelite in heavy mineral concentrates of wadi sediment	MODS no. 389, 390; Duhamel, 1971
22	Jabal Subh area	Occurrence; scheelite in heavy mineral concentrates of wadi sediment	Goldsmith, 1971
23	Jabal Sayid	Occurrence; Nb, U, fluorite, rare earth elements in granite	Aguttes and Duhamel, 1971; Shepherd, 1965
24	Jabal Hadb Daheen	Occurrence; fluorite-bearing quartz vein	Kemp, 1977
25	Jabal Al-Jayasir	Occurrence; fluorite with limestone, rhyolite and granite	-do-
26	Southern Jabal Khuff quadrangle	Occurrences; cassiterite in quartz veins and scheelite in marble near granite	Eijkelboom and others, 1971
27	Hajlan	Occurrence; fluorite with quartz in rhyolite	Kemp, 1977
28	Sabhah	Occurrence; fluorite in granite	-do-
29	Jabal Hawshat ibn Huwayl	Occurrence; fluorite-bearing veins in granite	-do-
30	South-western Ayn Qunay quadrangle	Occurrence and geochemical anomaly; scheelite in quartz vein in granite; W in heavy mineral concentrate of wadi sediment	Overstreet *et al.*, 1972
31	Uyaijah ring structure	Occurrence; scheelite in contact metamorphic zone and molybdenite in quartz veins in granite	Dodge, 1973; Dodge and Helaby, 1974

TABLE 3 (CONTINUED)

Locality number	Locality name	Description	References
32	Jabal Kirsh	Occurrence; disseminated molybdenite in granite	Letalenet *et al.*, 1972
33	Jabal Ahmera	Occurrence; molybdenite in pegmatite in microgranite	Leca, 1970
34	Ad Duwayh	Geochemical anomaly; W in heavy mineral concentrate from mined area	Whitlow, 1966b
35	Jabal ash Shumrah	Geochemical anomaly; W in heavy mineral concentrate	-do-
36	Jabal Sāhah	Geochemical anomaly; W and Sn in wadi sediment and heavy mineral concentrates associated with granite	-do-
37	South of Athīrayn	Occurrence; molybdenite in quartz pegmatite and granite	-do-
38	West of Jabal ash Shawnah	Geochemical anomaly; W and Mo in heavy mineral concentrates	-do-
39	Jabal Khida	Geochemical anomaly; W, Sn, and Mo in heavy mineral concentrates associated with granite	-do-
40	S.W. of Jabal Tarban	Geochemical anomaly; Sn, W, and Mo in wadi sediment and heavy mineral concentrates; occurrence; beryl in pegmatite dike	-do-
41	Dahlat Shahāb	Geochemical anomaly; W in sample from mine waste	Whitlow, 1966b
42	West of Bi'r Zā'in	Occurrence; scheelite in contact metamorphic zone	D. L. Schmidt, personal comm., 1978
43	At-Tā'if area	Geochemical anomaly and occurrence; W in heavy mineral concentrates and scheelite in heavy mineral concentrates and small veins	Goldsmith and Kouther, 1966; Kouther, 1966
44	Jabal Afaf area	Geochemical anomaly and occurrence; W and scheelite in heavy mineral concentrates of wadi sediments	Goldsmith, 1971
45	Ablah Hill	Deposit; fluorite-bearing pipe associated with granite	Allcott, 1970; Kemp, 1977
46	Khadrah quadrangle	Occurrence; scheelite in heavy mineral concentrates of wadi sediment; associated with granite	Mytton and Ankary, 1966
47	Bi'r Karath	Occurrence; beryl-bearing pegmatite in granite	Coleman, 1973a
48	Wadi As-Salile area	Occurrence and geochemical anomaly; scheelite and W in heavy mineral concentrates and in contact metamorphic zone of granite	Abuannaja, 1970
49	Jabal Al-Mutbig	Occurrence; scheelite in shear zone	MODS no. 671; van Daalhoff, 1974
50	Area near Jabal Ghern	Occurrence and geochemical anomaly; Sn and Nb in granite and wadi sediment; cassiterite in heavy mineral concentrates of sediment	Greenwood, in prep.; present study
51	Wadi Dib	Occurrence; W–Sn deposit	Said, 1962
52	Abu Marwa	-do-	-do-
53	Um disi, Gattar	-do-	-do-
54	Abu Hammad	Occurrence; wolframite in quartz veins in granite	El-Ramly *et al.*, 1970

TABLE 3 (CONTINUED)

Locality number	Locality name	Description	References
55	Abu Kharif, El Dob	-do-	-do-
56	Maghrabiya	-do-	-do-
57	Umm Bissila	-do-	-do-
58	Abu Dabbab, Nuweibi, Igla	Prospects; columbite–tantalite, cassiterite and wolframite with fluorite, topaz and mica in quartz veins and greisenized zones of granite	-do-
59	El Mueilha	Prospect; cassiterite and wolframite in quartz veins near granite	-do-
60	Nugrus, Zabara, Sikait	Occurrence; beryl deposit	Said, 1962
61	Um Harba	Occurrence; Sn–W deposit	-do-
62	Um Selim	-do-	-do-
63	Homr Akarem	Prospect; stockwork of molybdenite-bearing quartz veins in granite	Shalaby, 1974
64	Zargat Naam	Occurrence; wolframite in quartz veins in granite	El-Ramly *et al.*, 1970
65	Gash Amer	-do-	-do-
66	Khor Arbent	Occurrence; W	Whiteman, 1971
67	Rahaba	Occurrence; beryl in pegmatites	Vail, 1971
68	Sabaloka	Occurrence; cassiterite and wolframite in quartz stockwork near contact of microgranite	Whiteman, 1971
69	Shilicki	Occurrence; beryl in pegmatite	Jelenc, 1966

[1]MODS is the Mineral Occurrence Documentation System used in Saudi Arabia for the recording of all mineralized outcrops, ore bodies and districts (Delfour, 1974).

meters long. The granite adjacent to the veins is altered and locally contains anomalous amounts of Mo. The highest Mo values occur in two zones in an area 3 km long by 1 km wide; each zone contains a weighted average of 80 ppm Mo, far below the grade of ore from Mo deposits such as the Henderson mine in Colorado, U.S.A. The Henderson ore body has reserves of 303 million tonnes at an average grade of 0.49 percent MoS_2 based on a 0.2% MoS_2 cut off (Wallace *et al.*, 1978).

Undoubtedly the most important mineral deposit found thus far in association with the younger granitic rocks is the Al-Ghurayyah radioactive granite in the north-western part of the Arabian Shield. The deposit consists of a small stock of riebeckite-aegirine alkali granite about 900 m in diameter that has resources of Zr, Nb–Ta, U and other metals contained in irregularly distributed accessory minerals including zircon, columbite–tantalite, uraninite, monazite and others (Lalande, 1977). The granite is leucocratic and porphyritic and consists commonly of euhedral phenocrysts of alkali-feldspar and quartz in a fine- to medium-grained groundmass. Grain size is variable from fine to coarse and the percentage of groundmass is variable from nil to 40%. Semi-quantitative analyses indicate highly anomalous contents of Nb, Ta, Ce, La, U, Th, Y, Zr, Sn, F, and Zn. Some samples also contain anomalous amounts of Ti, Cr, Co, Mo, W, Pb, Sr, and Li. Quantitative analyses of drill core indicate that the Nb–Ta ratio is approximately 10; Nb ranges from 2780 to 3040 ppm and Ta from 230 to 300 ppm.

Possible reserves of the order of 411 million tonnes, containing 0.75% Zr, 0.25% Nb–Ta, 0.0115% U, 0.105% Y, 0.25% rare earths and 0.02% Sn have been outlined. The economic potential of this deposit is currently being assessed.

In general, minerals and metals associated with the younger granites may be separated into two suites; one mainly of Nb, Zr, Th and fluorite that has a close spatial relationship with alkaline to peralkaline granites, and another of W, Mo and Sn that is associated mainly with calc-alkaline granites or granodiorites. Examples of the first suite include the Al-Ghurayyah radioactive granite and the Zarghat–Hanakiyah–Nuqrah area (nos. 1, 6–13; Fig. 6), where occurrences of fluorite and Zr–Th are associated with alkali amphibole/pyroxene-bearing granites. Examples of the second suite are El-Koom (no. 18; Fig. 6), where wolframite-bearing quartz veins occur in a granodiorite stock; the Uyaijah ring structure, where scheelite and molybdenite are associated with an intrusive complex consisting of calc-alkaline granite and granodiorite; the At-Ta'if area (no. 43; Fig. 6), where scheelite occurrences and W anomalies apparently are related to a large calc-alkaline granitic complex; and the Wadi As-Salile area (no. 48; Fig. 6) where scheelite is associated with a calc-alkaline granite.

Certain areas of the Arabian Shield may be more favorable than others for the occurrence of mineral deposits associated with the younger granites. Criteria for evaluating different areas of the shield are: (1) the distribution of occurrences and anomalies of minerals of interest as shown in Fig. 6; (2) the distribution and abundance of younger granites including both calc-alkaline as well as alkaline to peralkaline types; (3) the occurrence of favorable host rocks and/or structures; and (4) the level of emplacement of the younger granites represented by the present level of erosion.

For evaluation, the shield is arbitrarily divided into five areas as follows: (1) north-western north of lat. 24° and west of long. 40°; north-eastern north of lat. 24° and east of long. 40°; (3) west-central between lats. 20 and 24° and west of long. 42°; (4) east-central between lats. 20 and 24° and east of long. 42°; and (5) southern south of lat. 20°.

Reconnaissance geologic and geochemical studies in the north-western shield area, thus far, have resulted in the discovery of only one deposit, the Al-Ghurayyah radioactive granite. Younger granites of both alkaline-peralkaline and calc-alkaline types are present and are very abundant in the northern part of this area. Further exploration of these granites would seem warranted, because the Eastern Desert of Egypt, which is adjacent to this area in the palinspastic map of the Arabian–Nubian Shield shown in Fig. 6, has numerous occurrences of W, Mo, Sn and other metals associated with younger granites.

The north-eastern shield area has numerous occurrences and anomalies associated with younger granites, but no economic deposits have been discovered. Favorable factors include the great abundance of younger granites of both alkaline-peralkaline and calc-alkaline types, exposures of the upper parts of many granite bodies as indicated by the presence of cogenetic (?) volcanic rocks, and the presence of abundant favorable sedimentary host rocks, some of which are carbonates. The area is one of the most favorable of the shield for the occurrence of mineral deposits in association with the younger granites, and the authors are currently carrying out reconnaissance mapping and geochemical sampling of these granites.

Occurrences and anomalies are few in the west-central shield area and include scheelite occurrences associated with calc-alkaline (?) granites and Nb-fluorite-U occurrences associated with alkaline-peralkaline granites. In general, older rocks and a deeper crustal level of the Arabian Shield are exposed in this area, and younger granites are less common than in other parts of the shield. Furthermore, the area of exposure of Precambrian rocks is limited because of an extensive cover of younger basalts, alluvium and sedimentary rocks. The area appears to have a low potential for the discovery of mineral deposits associated with younger granites.

The east-central shield area has many occurrences and anomalies especially in W and Mo, and to a lesser extent, of Sn. The area has many features in common with the north-eastern shield, including a great abundance of younger granites, exposures of upper levels of granite intrusions, and younger sedimentary sequences that have favorable host rocks. However, calc-alkaline granites predominate over alkaline-peralkaline types, whereas in the north-eastern area alkaline-peralkaline granites are apparently more abundant. The potential for the discovery of mineral deposits associated with the younger granites seems to be at least as high for this area as in the north-eastern shield.

Occurrences and anomalies associated with younger granites in the southern shield area are relatively few, although this is perhaps the most thoroughly studied area of the shield. In general, older rocks and deeper crustal levels are exposed in this area, and younger granites are abundant only in the central and eastern parts. Because the potential for granite-related deposits is generally low, and the area has been studied adequately, further exploration of the younger granites would likely be unproductive.

REFERENCES

ABUANNAJA, A. S. 1970. General geology of Wadi as Salile area, Asir quadrangle, Saudi Arabia. *Unpubl. M.S. thesis.* South Dakota School of Mines and Technology, U.S.A.

AGUTTES, J. 1971. Geology and mineral exploration of the Jabal Ash Sheba quadrangle. *Bur. Rech. Geolog. Minieres Open-File Rept.* 71-JED-6.

AGUTTES, J., and DUHAMEL, M. 1971. Geology and mineral exploration of the Jabal Sayid quadrangle, photomosaic 111 east. *Bur. Rech. Geolog. Minieres Open-File Rept.* 71-JED-4.

ALLCOTT, G. H. 1970. Diamond drilling at the Ablah ancient mine. *U.S. Geol. Survey Saudi Arabian Proj. Rept.* 114.

ALMOND, D. C. 1977. The Sabaloka igneous complex, Sudan. *Phil. Trans. R. Soc. Lond.* A287, 595–633.

ALMOND, D. C., HALLORAN, D. O., AHMED, F., CURTIS, P., MCCORMAC, M., and VAIL, J. R. 1977. Concentrations of younger granite ring complexes and of small Cainozoic volcanic field in the Bayuda Desert, Sudan. 20 *Ann. Rep. Res. Inst. Afr. Geol.* University of Leeds, 20, 61–65.

AL-SHANTI, A. M. 1974. Al Jl'Lani layered basic intrusion, ad Dawadimi district, Kingdom of Saudi Arabia. *Saudi Arabian Dir. Gen. Mineral Resources Bull.* 12, 45 p.

ANKARY, A. O. 1965. The occurrence of tungsten in the southwestern portion of the Wadi ar Rimah quadrangle, Saudi Arabia. *U.S. Geol. Survey Saudi Arabian Proj. Technical Letter* 11.

BAILEY, D. K., and SCHAIRER, J. F. 1966. The system Na_2O–Al_2O_3–Fe_2O_3–SiO_2 at 1 atmosphere, and the petrogenesis of alkaline rocks. *J. Petrology* 7, 114–170.

CARMICHAEL, I. S. E., TURNER, F. J., and VERHOOGEN, J. 1974. *Igneous Petrology.* McGraw-Hill, New York, 739 p.

COLEMAN, R. G. 1973a. Reconnaissance geology of the Khaybar quadrangle, Kingdom of Saudi Arabia. *Saudi Arabian Dir. Gen. Mineral Resources Geologic Map* GM-4.

COLEMAN, R. G. 1973b. Reconnaissance geology of the Khamis Mushayt Quadrangle, Kingdom of Saudi Arabia. *Saudi Arabian Dir. Gen. Mineral Resources Geologic Map* GM-5.

COLEMAN, R. G., BROWN, G. F., and KEITH, T. E. C. 1972. Layered gabbros in southwest Saudi Arabia. *U.S. Geol. Survey Prof. Paper* 900-D, D143–D150.

COLEMAN, R. G., GHENT, E. D., and FLECK, R. J. 1977. The Jabal Shay'i' gabbro in southwest Saudi Arabia, with a section on geophysical studies by Griscom, A. *Saudi Arabian Dir. Gen. Mineral Resources Bull. 17,* 46 p.

CONRAUX, J. 1969. Report on the mineral resources and geology of the Umm ad Dammar-Jabal Rokham area. *Bur. Rech. Geolog. Minieres Open-File Rept.* SG-JED-66A9.

COOPER, J. A., STACEY, J. S., STOESER, D. B., and FLECK, R. J. 1979. An evaluation of the zircon method of isotopic dating in the Southern Arabian craton. *Contrib. Mineral. Petrol.* (in press)

DELFOUR, J. 1974. Mineral occurrence documentation system—M.O.D.S.—revised input manual. *Bur. Rech. Geolog. Minieres Open-File Rept.* 75-JED-1.

DELFOUR, J. 1977. Geology of the Nuqrah quadrangle, sheet 25E, Kingdom of Saudi Arabia. *Saudi Arabian Dir. Gen. Mineral Resources Geologic Map* GM-28.

DODGE, F. C. W. 1973. Geology and evaluation of tungsten anomalies in Bahairan–Abu Khurg area, southeastern part of the Uyaijah ring structure, Kingdom of Saudi Arabia. *U.S. Geol. Survey Saudi Arabian Proj. Rept.* 163, 32 p.

DODGE, F. C. W. 1979. The Uyijah ring structure, Kingdom of Saudi Arabia. *U.S. Geol. Survey Proj. Paper* 774-E, 17 p.

EL-RAMLY, M. F., BUDANOV, V. I., ARMANIOUS, L. K., and DERENIUK, W. E. 1969a. A petrological study on the central part of Gabal Abu Kurg ring complex, southeastern desert of Egypt. *Geol. Surv. Egypt Paper* 51, 53 p.

EL-RAMLY, M. F., BUDANOV, V. I., ARMANIOUS, L. K., and DERENIUK, N. E. 1969b. The three ring complexes of gabal Elkahfa, gabal Nigrub El Fogani and gabal El Naga, southeastern desert of Egypt. *Geol. Surv. Egypt Paper* 52, 39 p.

EL-RAMLY, M. F., IVANOV, S. S., and KOCHIN, G. G. 1970. Tin-tungsten mineralization in the eastern desert of Egypt, pp. 43–52 in *Studies on Some Mineral Deposits of Egypt.* Geological Survey of Egypt, Cairo.

FLECK, R. J. 1979. Rubidium-strontium geochronology and plate tectonic evolution of the southern part of the Arabian Shield. *U.S. Geol. Survey Saudi Arabian Proj. Rept.* 245.

FLECK, R. J., COLEMAN, R. G., CORNWALL, H. R., GREENWOOD, W. R., HADLEY, D. G., PRINZ, W. C., RATTE, J. C., and SCHMIDT, D. L. 1976. Potassium argon geochronology of the Arabian Shield, Kingdom of Saudi Arabia. *Geol. Soc. Am. Bull.* 87, 9–21.

FLECK, R. J., GREENWOOD, W. R., HADLEY, D. G., ANDERSON, R. E., and SCHMIDT, D. L. 1978. Age and evolution of the southern part of the Arabian Shield. *Precambrian Res.* 6, A21–A22.

FRISCH, W., and AL-SHANTI, A. 1977. Ophiolite belts and the collision of island arcs in the Arabian Shield. *Tectonophysics* 43, 293–306.

GARSON, M. S., and SHALABY, I. M. 1976. Precambrian-Lower Paleozoic plate tectonics and metallogenesis in the Red Sea region. *Geol. Assoc. Can. Spec. Paper* 14, 573–596.

GOLDSMITH, R. 1971. Mineral resources of the southern Hijaz quadrangle, Kingdom of Saudi Arabia. *Saudi Arabian Dir. Gen. Mineral Resources Bull.* 5, 62 p.

GOLDSMITH, R., and KOUTHER, J. H. 1966. Notes of field trips to the At-Ta'if–Bilad Zahran area, Saudi Arabia, June 7–August 1, 1964, and August 22–29, 1964. *U.S. Geol. Survey Saudi Arabian Proj. Technical Letter* 47.

GREENWOOD, W. R., and BROWN, G. F. 1973. Petrology and chemical analysis of selected plutonic rocks from the Arabian Shield, Kingdom of Saudi Arabia. *Saudi Arabian Dir. Gen. Mineral Resources Bull.* 9, 9 p.

GREENWOOD, W. R., HADLEY, D. G., ANDERSON, R. E., FLECK, R. J., and SCHMIDT, D. L. 1976. Late Proterozoic cratonization in southwestern Saudi Arabia. *Phil. Trans. R. Soc. Lond.* A280, 517–527.

GREENWOOD, W. R. Geology of the An Nimas quadrangle, sheet 19/42 C, Kingdom of Saudi Arabia. *Saudi Arabian Dir. Gen. Mineral Resources Geological Map* GM-37 (in press).

GREENWOOD, W. R. Geology of the Wadi Wassat quadrangle, sheet 18/44 C, Kingdom of Saudi Arabia. *Saudi Arabian Dir. Gen. Mineral Resources Geological Map* (in prep.).

HADLEY, D. G. 1974. Geology of the Wayban quadrangle, northwestern Hijaz, Kingdom of Saudi Arabia. *Saudi Arabian Dir. Gen. Mineral Resources Geologic Map* GM-7.

HARRIS, N. B. W. 1978. Geology of the northern halves of the Wadi as Surr and al Muwaylih quadrangles (27/35 A & B), northwest Hijaz, Kingdom of Saudi Arabia. *Saudi Arabian Dir. Gen. Mineral Resources Open-File Rept.* 608.

JACOBSON, R. R. E., MACLEOD, W. N., and BLACK, R. 1958. Ring-complexes in the younger granite province of northern Nigeria. *Geol. Soc. Lond. Memoir* 1, 77 p.

JACKAMAN, B. 1972. Genetic and environmental factors controlling the formation of the massive sulphide deposits of Wadi Bida and Wadi Wassat, Saudi Arabia. *Saudi Arabian Dir. Gen. Mineral Resources Tech. Record* TR-1972-1.

JELENC, D. A. 1966. *Mineral Occurrences of Ethiopia.* Ministry of Mines, Ethiopia, 720 p.

KANAAN, F. M. 1979. The geology, petrology, and geochemistry of the granitic rock of Jabal Al Hawshah and vicinity, Jabal Al Hawshah quadrangle. *Saudi Arabian Dir. Gen. Mineral Resources Bull.* (in press)

KEMP, J. 1977. Fluorite occurrences—a review, Kingdom of Saudi Arabia. *Saudi Arabian Dir. Gen. Mineral Resources Technical Record* TR-1977-16.

KENNEDY, W. Q. 1964. The structural differentiation of Africa in the Pan-African (±500 m.y.) tectonic episode. 8 *Ann. Rep. Res. Inst. Afr. Geol.* University of Leeds, p. 48–49.

KOUTHER, J. H. 1966. Preliminary geologic report on the At-Ta'if area, Saudi Arabia, and an approach to the search for tungsten. *U.S. Geol. Survey Saudi Arabian Proj. Technical Letter* 46.

LALANDE, P. G. 1977. Final report on preliminary geological and geophysical investigations of the Gurayyah radioactive granite, Kingdom of Saudi Arabia. *Saudi Arabian Dir. Gen. Mineral Resources Open-File Rept.* 619.

LECA, X. 1970. Mineral resources and geology of the Jabal Sahah quadrangle, photomosaic sheet 132 east. *Bur. Rech. Geolog. Minieres Open-File Rept.* 70-JED-7.

LENZ, H., BENDER, F., BESANG, C., HARRE, W., KREUZER, H., MULLER, P., WENDT, I., and GERMANY, F. R. 1972. The age of early tectonic events in the zone of the Jordon geosuture, based on radiometric data. *Int. Geol. Congr.* XXIV, Sec. 3, 371–379.

LETALENET, J., BOIS, J., and PFLAUM, J. 1972. Geology and mineral exploration of the Ad Darah quadrangle, photomosaic 119 east. *Bur. Rech. Geolog. Minieres Open-File Rept.* 72-JED-18.

LETALENET, J., and BOUNNY, I. 1977. Geology and mineral exploration of the Jabal As Siham quadrangle 23/42 C. *Bur. Rech. Geolog. Minieres Open-File Rept.* 77-JED-5.

MACDONALD, R., and BAILEY, D. K. 1973. The chemistry of peralkaline over-saturated obsidians. *U.S. Geol. Survey Prof. Paper* 440-N-1, N1–N37.

MARTIN, C., ROBERTS, R. J., and STOESER, D. B. 1978. Titaniferous magnetite in the layered intrusive complex at Lakathah, Kingdom of Saudi Arabia. *U.S. Geol. Survey Saudi Arabian Proj. Rept.* 238.

MATZKO, J. J., and NAQVI, M. I. 1978. A summary of niobium and rare earth localities from Ha'il and other areas in western Saudi Arabia. *U.S. Geol. Survey Saudi Arabian Proj. Rept.* 221.

MINERAL RESOURCES ACTIVITIES, 1390–1395 A.H. (1970–1975 A.D.), 1976. *Saudi Arabian Dir. Gen. Mineral Resources Report.* 70 p.

MYTTON, J. W. 1970. Reconnaissance for mineral deposits in the Precambrian rocks of the Wadi ar Rimah quadrangle, Kingdom of Saudi Arabia. *U.S. Geol. Survey Saudi Arabian Proj. Rept.* 121.

NASSEEF, A. O., and GASS, I. G. 1977. Granitic and metamorphic rocks of the Taif area, western Saudi Arabia. *Geol. Soc. Am. Bull.* 88, 1721–1730.

NEARY, C. R., GASS, I. G., and CAVANAGH, B. J. 1976. Granitic association of northeastern Sudan. *Geol. Soc. Am. Bull.* 87, 1501–1512.

NEBERT, K. 1970. Geology of western al Quwayiyah region, Saudi Arabia. *Neus Jahrbuch fuer Geologie und Palaeontologie,* Abhandlungen 135, 150–170.

NOBLE, D. C. 1968. Systematic variation of major elements in comendite and pantellerite glasses. *Earth Planet Sci. Lett.* 4, 167–172.

NOBLE, D. C., HAFFTY, J., and HEDGE, C. E. 1969. Strontium and magnesium contents of some natural peralkaline silicic glasses and their petrogenetic significance. *Am. J. Sci.* 267, 598–608.

OVERSTREET, W. C., WHITLOW, J. W., and ANKARY, A. O. 1972. Reconnaissance geology of the Precambrian rocks in the Ayn Qunay quadrangle, Kingdom of Saudi Arabia. *U.S. Geol. Survey Saudi Arabian Proj. Rept.* 125.

PETOT, J. 1976. Geology and mineral exploration of the Jabal Radwa quadrangle 24/38A. *Bur. Rech. Geolog. Minieres Open-File Rept.* 76-JED-7.

RADAIN, A. 1978. Peralkaline granite in the western part of the Arabian Shield. *I.A.G. Res. Series 4,* 92–93.

RATTE, J. C. 1974. Geology of the Jabal Sawdah quadrangle sheet 18/42 C, Kingdom of Saudi Arabia. *Saudi Arabian Dir. Gen. Mineral Resources Geologic Map* GM-16.

SAID, R. 1962. *The Geology of Egypt.* Elsevier, Amsterdam, 377 p.

SCHMIDT, D. L. Geology of the Wadi al Miyah quadrangle sheet 20/42 B, Kingdom of Saudi Arabia. *Saudi Arabian Dir. Gen. Mineral Resources Geologic Map* (in prep.).

SCHMIDT, D. L., HADLEY, D. G., and STOESER, D. B. 1979. Late Proterozoic crustal history of the Arabian Shield, southern Najd province, Saudi Arabia. *Inst. App. Geol. (Jeddah) Bull.* 3, vol. 2, 41–58

SCHURMANN, H. M. E. 1966. *The Pre-cambrian Along the Gulf of Suez and the Northern Part of the Red Sea.* Leiden, E. J. Brill.

SHALABY, I. 1974. Molybdenum mineralization at Homr Akarem, in Mineral Deposits in Egypt. *Geological Survey of Egypt and Mining Authority Paper* 61, p. 41–45, Cairo, Egypt.

SHEPHERD, J. H. 1965. Exploration for radioactive materials in the Kingdom of Saudi Arabia. *Saudi Arabian Dir. Gen. Mineral Resources Rept.* 12.

SHEPHARD, J. H. 1966. Exploration for radioactive minerals in the Kingdom of Saudi Arabia; Al Ghrayyat. *Saudi Arabian Dir. Gen. Mineral Resources Unpubl. Rept.*

SORENSEN, H. 1974. Classification and nomenclature of plutonic rocks. pp. 557–576 in *The Alkaline Rocks* (ed. SORENSEN, H.). John Wiley, New York.

STRECKEISEN, A. 1975. To each plutonic rock its proper name. *Earth Sc. Rev.* 12, 1–33.

TAYLOR, H. P., JR. 1978. Oxygen and hydrogen isotope studies of plutonic rocks. *Earth Planet. Sci. Lett.* 38, 177–210.

THEOBALD, P. K., and ALLCOTT, G. H. 1973. Tungsten anomalies in the Uyaijah ring structure, Kushaymiyah igneous complex, Kingdom of Saudi Arabia; section A, Geology and geochemistry of the Uyaijah ring structure. *U.S. Geol. Survey Saudi Arabian Proj. Rept.* 160.

VAIL, J. R. 1971. Geological reconnaissance in part of Berber district, Northern Province, Sudan. *Mineral Resources Bull.* 18. Sudan Ministry Industr.

VAIL, J. R. 1976. Location and geochronology of igneous ring-complexes and related rocks in north-east Africa. *Geol. Jahrbuch.* Reihe B, no. 20, 97–114.

VAN DAALHOFF, H. 1974. Mineral locality map of the Arabian Shield. *Saudi Arabian Dir. Gen. Mineral Resources Geologic Map* GM-15.

VILLEMUR, J. R., ALABOUVETTE, B., MOTTI, E., and RENAUD, C. Reconnaissance of the sedimentary strata at the eastern edge of the Arabian Shield. *Bur. Rech. Geolog. Minieres Open-File Rept.* (in press).

WALLACE, S. R., MACKENZIE, W. B., BLAIR, R. G., and MUNCASTER, N. K. 1978. Geology of the Urad and Henderson molybdenite deposits, Clear Creek County, Colorado, with a section on a comparison of these deposits with those at Climax, Colorado. *Econ. Geology* 73, 325–368.

WHITEMAN, A. J. 1971. *The Geology of the Sudan Republic.* Clarendon Press, Oxford, 290 p.

WHITLOW, J. W. 1966a. A mineral reconnaissance of the Al Kushaymiyah quadrangle, Kingdom of Saudi Arabia. *U.S. Geol. Survey Saudi Arabian Proj. Technical Letter* 77.

WHITLOW, J. W. 1966b. Areas in the southern Najd quadrangle, Saudi Arabia, recommended for mineral investigation. *U.S. Geol. Survey Saudi Arabian Proj. Technical Letter* 79.

WRIGHT, J. B. 1969. A simple alkalinity ratio and its application to questions of non-orogenic granite genesis. *Geol. Magazine* 106, 370–384.

الصخـــــور الترسبية البروتيروزووية و أحواض الدرع العربية وتطورها

د.ج. هادلى و د.ل. شميدت

الخلاصـــــة

تتكوّن الصخور الترسبية البروتيروزوويّة للدرع العربية من ثلاثة أطوار قرارية ، يضم (الطور (الأقدم) مجموعات البيش والباحة وجدّة التى تتكون من مجموعة غير ناضجة مكوّنة أساسا من جَرْوَق متحول دقيق التحبّب وشِسْت چرافيتى وصوّان ورخام وكمية قليلة من مُدمّلكات متعددة المكوّنات وحجر غرين متحول. وتتكون الصخور الفتاتية للطور"أ" من مواد بركانية فقط ولاتحتوى على بسيس جوْفى (سحيقىّ) أو سيالى. وتميز صخور حجر الرمل المتحول و الدملكات المتعددة المكونات و الجروق المتحول العليظ التحبب ووفرة من الرخام (استروماتوليتى فى بعض الأماكن).

الطور الثانى "٢" الذى يضم مجموعات عبلة وحلبان ومردما. وتكثر المكونات الجوفية (السحيقية) والبركانية فى المجموعة الفتاتية ، كما تغلب كسارات فلسبار البوتاس البسيسية فى حلبان ومردما.

وتكون مجموعتا شامار و الجوبيلة الطور "٣". والصخور الترسبية لهذا الطور أرضية الأصل ، فتاتية ، دقيقة الى غليظة التحبب ، ومدملكات جلاميد وحجر جيْر استروماتوليتى ودولوميت . وتضم الأطوار الثلاثة وفرة من الصخور البركانية الثورانية.

وباستبعاد الأحواض الترسبية المحتوية على صخور الطور"٣" ، فان الأحواض الترسبية تتجه عموما للشمال خصوصا فى الأجزاء الوسطى والجنوبية للدرع. وفى الجزء الأوسط والشمالى من الدرع تقطع الأحواض و البنيات المتجهة شمالا فجائيا بواسطة مسارات ترسبية شمالية غربية متوازية تكونت بواسطة حركات بنائية أخدودية نتجت عن صدع التواء يسارى .

وتدل الخصائص النسيجية و التركيبية للصخور الترسبية البروتيروزوويّة وكذلك العلاقات المكانية للأحواض القرارية على تغيّر الترسّب من ترسّب محيطى الى ترسّب بحرى ضَحْل وقارى ، كما أنها تدل على تزحزح محاور الأحواض من الغرب الى الشرق . وتوضح المعايير الترسّبية خلال هذه الفترة الزمنية الطويلة الاتجاهات العامة الآتية :-

زيادات فى كل من النضوج التركيبىّ و النسيجى ومحتوى الكربونات وحجم الحبات ونسبة الصخور الترسبية الى الصخور البركانية وبسيس جوْفىّ (سحيقى) حامل فلسبار البوتاس ويمكن تفسير الأسلوب الترسّى لكل طور كدالة للظروف البنائية أثناء التقرار كمايلى:

	البيئة القرارية	البيئة الجيولوجية/البنائية
طور "١"	ماء بحرى عميق (الفليش)	قوس الجزر المحيطة / اندساس
طور "٢"	ماء بحرى متوسط الضحولة (سيف كربونات القنديد (الدّبس))	قوس محيطى/تقارب وتزايد قارى
طور "٣"	بحرى، ضحْل / قارى	قارى/تصادم/ترسخ

SEDIMENTARY ROCKS AND BASINS OF THE ARABIAN SHIELD AND THEIR EVOLUTION

DONALD G. HADLEY and DWIGHT L. SCHMIDT
U.S. Geological Survey, Jeddah, Saudi Arabia

Abstract—Proterozoic sedimentary rocks of the Arabian Shield consist of three depositional phases. Phase I (the oldest) includes the Baish, Bahah, and Jiddah Groups, which consist of an immature assemblage dominated by fine-grained meta-graywacke, graphitic schist, chert, marble, and subordinate polymictic conglomerate and meta-siltstone. Clastic rocks of Phase I are composed solely of volcanic material and do not contain plutonic or sialic detritus. Meta-sandstone, polymictic conglomerate, coarse-grained meta-graywacke, and abundant marble (stromatolitic in places) characterize Phase II, the Ablah, Halaban, and Murdama Groups. Plutonic and volcanic components are abundant in the clastic suite; K-feldspar detrital fragments are common in the Halaban and Murdama. The Shammar and Jubaylah Groups form Phase III. Sedimentary rocks of this phase are fine- to coarse-grained terrigenous clastic rocks, boulder conglomerate, and stromatolitic limestone and dolomite. All phases include abundant eruptive volcanic rocks.

Excluding those containing Phase III rocks, sedimentary basins generally trend North, especially in the central and southern parts of the shield. In the central and northern part of the shield, North-trending basins and structures are abruptly truncated by parallel N.W.-trending sedimentary corridors (Jubaylah basins) formed by sinistral wrench-fault graben tectonics.

Textural and compositional characteristics of the Proterozoic sedimentary rocks together with spatial relations of the depositional basins document a change from oceanic to shallow marine and continental sedimentation with time and a shift in the basin axes from west to east. Sedimentary parameters during this lengthy time span show the following general trends: increases in compositional and textural maturity, carbonate content, grain size, the ratio of sedimentary rocks to volcanic rocks, and plutonic and K-feldspar-bearing detritus. The sedimentary style of each phase was a function of tectonic conditions during deposition.

INTRODUCTION

Early Work

Reconnaissance geologic mapping and mineral resource studies of the Arabian Shield began in the early 1950's culminating in geologic map coverage of the Arabian Shield at 1:500,000-scale (Bramkamp and Ramirez, 1958; Bramkamp *et al.*, 1963 a,b; Brown and Jackson, 1958, 1959; Brown *et al.*, 1963a,b,c; and Jackson *et al.*, 1963) and the Arabian Peninsula at 1:2,000,000-scale (U.S. Geological Survey–Arabian American Oil Co., 1963). Based on this early work several reports were published that summarized the basic geology, age relations, and geomorphology of the shield (Brown and Jackson, 1960; Aldrich and Brown, 1960; and Brown, 1960). Several other studies were conducted during this period under the auspices of the Ministry of Petroleum and Mineral Resources along the Red Sea coastal plain and in Precambrian rocks along the western margin of the shield (Richter-Bernburg and Schott, 1954; Karpoff, 1957).

The scope of these early maps and reports was such that only brief treatment could be given to specific geologic aspects of the shield and discussion of the sedimentary rocks was confined to very general terms only.

Middle Period Studies

Detailed geologic studies of the Arabian Shield began in the early sixties by personnel of the Directorate General of Mineral Resources (DGMR), U.S. Geological Survey (USGS), Bureau de Recherches Geologiques et Minieres (BRGM), and the Japanese Geological Mission (JGM). The work included reconnaissance geologic mapping at 1:100,000-scale of selected areas containing known and potential mineral deposits, detailed mineral assessment, geochemical prospecting, and geophysical studies of ancient mines, mineral belts, and sedimentary and volcanic formations showing considerable mineral potential. Reports on Precambrian sedimentary rocks and formations during this period were few and were restricted primarily to descriptions of sedimentary ore deposits. Notable among these were publications related to the Wadi Sawawin iron ore deposits (Hirayama and Assad, 1967; Hirayama *et al.*, 1967), and copper mineralization and mineral deposits in the Ablah Formation (Earhart, 1968, 1969; Gaskill, 1970).

Recent Investigations and Purpose of This Paper

Beginning in 1969, detailed mapping of the Arabian Shield at 1:100,000-scale began on controlled photomosaic bases, with the principal objective of establishing a geologic framework for all of the Arabian Shield. As a result of this work several papers were published dealing with detailed aspects of regional geology. These included stratigraphic and sedimentologic reports related to defined formations (Delfour, 1970; Hadley, 1973, 1974b) and the first regional stratigraphic and tectonic synthesis of the Shield

(Schmidt *et al.*, 1973). During this period, other summary papers dealt briefly with the sedimentary geology of the shield (Brown and Coleman, 1972; Greenwood *et al.*, 1973, 1975), but to date there has been no overall synthesis or summary of the sedimentary rocks of the Arabian craton.

The purpose of this paper, therefore, is to describe the sedimentary rocks of the Arabian Shield and to define the nature of the depositional environments and tectonic conditions under which they accumulated.

STRATIGRAPHIC FRAMEWORK

Previous Syntheses

Brown and Jackson (1960) were the first to present a stratigraphic synthesis of the Arabian Shield (Table 1). They recognized a three-fold stratigraphy based on major unconformities and plutonic–orogenic episodes. In their review three sequences of rocks comprise the oldest stratigraphic order, which they considered to be older than 1,000 Ma. These included a gneiss unit, the Hali schist, and also the Baish greenstone and Lith complex, considered to be of equivalent age. Schists of various kinds, slate, marble, quartzite, and metavolcanic rocks are the dominant lithologies of this period.

The second stratigraphic order of rocks ranges between 1,000 Ma and 700–750 Ma and includes the Halaban andesite and the Murdama Formation. Metavolcanic rocks dominated by andesite characterize the Halaban whereas the Murdama is described by them as being chiefly sedimentary, including pelites, quartzite, and conglomerate. They describe no marble and do not note the presence of sialic detritus in the Murdama.

Characterized by a basal unconformity, the final grouping includes two sequences, the Fatima-Ablah formations and Shammar rhyolite, ranging in age from about 700 Ma to about 530 Ma. The Fatima and Ablah, considered by Brown and Jackson (1960, p. 73) to be correlative formations, are described as sedimentary units consisting of fine- to coarse-grained clastics, conglomerate, and stromatolitic limestone. Rhyolitic ash-flow tuff and related pyroclastic beds and subordinate dacite and andesite are the main rock types described for the Shammar rhyolite.

Following an early phase of detailed 1 : 100,000-scale geologic mapping in the early 1970's, Schmidt *et al.* (1973) re-examined the stratigraphy of the shield and recognized eight groups as well as an older gneiss unit; these comprised six major lithostratigraphic sequences (Table 1), separated by erosional and angular unconformities. In contrast to the earlier interpretation, which recognized three tectonic episodes, Schmidt *et al.* (1973) concluded that the six lithostratigraphic sequences were each marked by periods of tectonism. Moreover, their 1973 synthesis defined or incorporated three additional units, namely, the Bahah Group, the Jiddah Group (equivalent to the Jiddah greenstone, U.S. Geological Survey–Arabian American Oil Company, 1963; Schmidt *et al.*, 1973, p. 7), and the Jubaylah Group (Delfour, 1970; Hadley, 1973, 1974b), not discussed previously in a regional synthesis.

Roberts *et al.* (1975, p. 3) modified the earlier stratigraphic synthesis and devised a framework consisting of three phases and four rock assemblages (Table 1). The phases, termed early, middle, and late, are defined on the basis of rock assemblages and tectonic episodes, but the stratigraphic units generally follow the usage of Schmidt *et al.* (1973, p. 3) and, for older rocks in the southern part of the shield, the framework of Greenwood *et al.* (1975, p. 5).

In a paper presented before the Royal Society of London, Greenwood *et al.* (1976, p. 519) re-evaluated the stratigraphy and tectonic framework of the southern part of the shield (Table 1) and defined a basic stratigraphic framework on the basis of three episodes. The episodes are separated by unconformities and each is culminated by an orogenic event that suggests four episodes rather than three. Use of the Hali Group and the older Khamis Mushayt gneiss of Schmidt *et al.* (1973) was abandoned; and the Ablah formation was elevated to group status and depicted as being older than the Halaban and younger than the Jiddah Groups rather than being equivalent to the Murdama Group (Schmidt *et al.* 1973, p. 3) or younger than the Murdama (Brown and Jackson, 1960, p. 76).

For the central and northern parts of the shield, Delfour (1976, p. 4) presents a complex stratigraphy. It consists of three units older than 1000–1200 Ma, namely, the Rharaba Complex, the Hali Group, and old basement, succeeded by five groups (Table 1). In addition to the oldest plutonic event, igneous cycles mark the end of each stratigraphic sequence except for the youngest (Jibalah = Jubaylah).

Correlation of the stratigraphic units as used by Delfour (1976, p. 4) with the earlier syntheses is relatively simple, with the exception of the Urd Group, because the same basic units are used by all the investigators. The Halaban Group is redefined as the Hulayfah Group. Correlation of the Urd Group and the Rharaba Complex with units older than the Halaban is not clear. The Abt Formation of the Urd Group, being dominantly sedimentary, is best correlated with the Bahah Group. Based on composition, the Ar-Ridayniyah

Table 1.--*Chronology of stratigraphic syntheses of the Arabian Shield*

Brown and Jackson (1960)	Schmidt and others (1973)	Roberts and others (1975)		Greenwood and others (1976)		Delfour (1976)		This paper	
Shammar rhyolite	Jubaylah group	Late Phase	Jubaylah group	Third Episode	Murdama group		Jibalah group	Phase III	Jubaylah group
Fatima and Ablah formations	Shammar group	Late Phase	Shammar group	Third Episode			Shammar group	Phase III	Shammar group
							Murdama group		
Murdama formation	Murdama group-Ablah formation	Middle Phase	Murdama group	Second Episode	Halaban group	Hulayfah group	Nuqrah formation	Phase II	Murdama group
Halaban andesite	Halaban group Jiddah group	Middle Phase	Halaban group	Second Episode		Hulayfah group	Afna formation	Phase II	Halaban group
Baish greenstone and Lith complex		Middle Phase	Ablah group	Second Episode	Ablah group	Urd group	Abt formation	Phase II	Ablah group
	Bahah group	Middle Phase	Jiddah group			Urd group	Ar Ridayniyah formation Ophiolitic complex		
	Baish group	Middle Phase	Bahah group Baish group	First Episode	Jiddah group			Phase I	Jiddah group
Hali schist	Hali group	Early Phase	Sequence uncertain	First Episode	Bahah group		Rharaba complex Hali group	Phase I	Bahah group
Gneiss	Khamis Mushayt gneiss	Early Phase		First Episode	Baish group		Old basement	Phase I	Baish group

Formation and Ophiolitic Complex would appear to be, wholly or in part, equivalent to the Baish Group. Correlation of the Jiddah Group with Delfour's stratigraphy is likewise not clear; nor is there any obvious correlative unit to the Rharaba Complex, although this is not a sedimentary or volcanic sequence.

Present Interpretation

The stratigraphic framework envisaged for the shield in this paper (Table 1) is a modification of Roberts *et al.* (1975, p. 3) and Greenwood *et al.* (1976, p. 519). It is based primarily on sedimentologic parameters and considerations, a series of stratigraphic units (phases) being viewed in terms of their sedimentologic continuity. As will be shown in the last section of this paper, the general sedimentologic cohesiveness of the phases is a function of the sedimentary environments in which the rocks were deposited, which in turn is controlled by tectonic conditions existing during each phase.

SEDIMENTARY ROCKS AND BASINS

Distribution

The distribution of the three phases of sedimentary rocks and the groups in which they occur is shown in Fig. 1. This is a generalized geologic map of the shield that has been modified substantially from Greenwood *et al.* (1974) according to the stratigraphic framework presented in this paper. Groups (e.g., Bahah, Halaban, Murdama) rather than individual sedimentary units are plotted because of the scale, and also because the sedimentary rocks are generally distributed unevenly throughout each group and their proportion to volcanic rocks varies widely within each group.

Phase II rocks are clearly the most abundant in the shield. Phase I rocks dominate the southern part whereas Phase III rocks are most abundant in the central and northern parts and are subordinate to Phase II rocks. The Phase III Jubaylah Group rocks are bounded exclusively by the Najd faults (Brown and Jackson, 1960, p. 76; Brown, 1970, p. 79; Delfour, 1970, p. 16).

General Lithologic Discussion

Sedimentary rock types of the three depositional phases include five major lithologic classes—conglomerates, graywackes, non-graywacke clastic rocks, argillaceous rocks and chert, and carbonates—which are divided into 12 main rock types (Table 2). Conglomerates are found in every group. Graywacke is common to all groups except those in Phase III; chert and slate are found mainly in Phase I rocks. Marble or limestone is present in all groups but the Shammar.

Conglomerates

Outcrop Description

Basal and intraformational are the two basic types of conglomerates of the shield. They can be classified according to clast size and apparent degree of water sorting (Table 3). The distinction between boulder and pebble conglomerate is based on clast diameter (Pettijohn, 1975, p. 30). Conglomerates containing abundant clasts larger than 256 mm are classified as boulder conglomerates and those containing clasts averaging 4–64 mm in size are classified as pebble conglomerates. Conglomerates classified herein as transported contain clasts that show some degree of transport; the clasts are mostly sub-rounded to well rounded and are surrounded by finer grained material of similar texture. Non-transported boulder conglomerate contains angular clasts and matrix material and, in rare instances, interbedded stratified material. Non-transported pebble conglomerate is of the flat-pebble and chip-pebble type; the pebbles are angular, represent broken up portions of thin beds, and show no significant transport (rounding of the clasts). The non-transported terminology does not necessarily mean there has been no transport but rather that transport has been minimal.

Basal conglomerates are found at the bases of the Ablah, Halaban, Murdama, and Jubaylah Groups. A thin pebble conglomerate occurs at or near the base of the Shammar Group in the Sahl al Matran quadrangle (Hadley, 1973, p. 6), but its significance is uncertain. Nevertheless, this conglomerate is believed to represent a major unconformity between Phase II and III, due to its regional extent (Delfour, 1977, p. 13) and to the abrupt metamorphic and structural differences between Phase II and III (Hadley, 1973; Schmidt *et al.*, 1973). Other than the Shammar conglomerate, all of the basal conglomerates are of the transported boulder type. These conglomerates represent major unconformities in the geologic record of the shield.

Intraformational conglomerates occur in all groups of all three phases. Examples of all the transported and non-transported boulder and pebble conglomerate types shown in Table 3 can be found among the intraformational conglomerates. Table 4 lists the main sedimentological parameters for the shield conglomerates according to the classification scheme in Table 3.

All conglomerates of the shield contain immature and metastable clast assemblages. Some are orthomictic in composition but contain either meta-stable sedimentary fragments (Table 4, Bahah and Ablah), volcanic fragments (Baish, Halaban and Jubaylah), or orthomictic granophyre clasts, as in the Jubaylah boulder conglomerate in the Qal'at as Sawrah quadrangle (Hadley, 1975b, p. 20). The

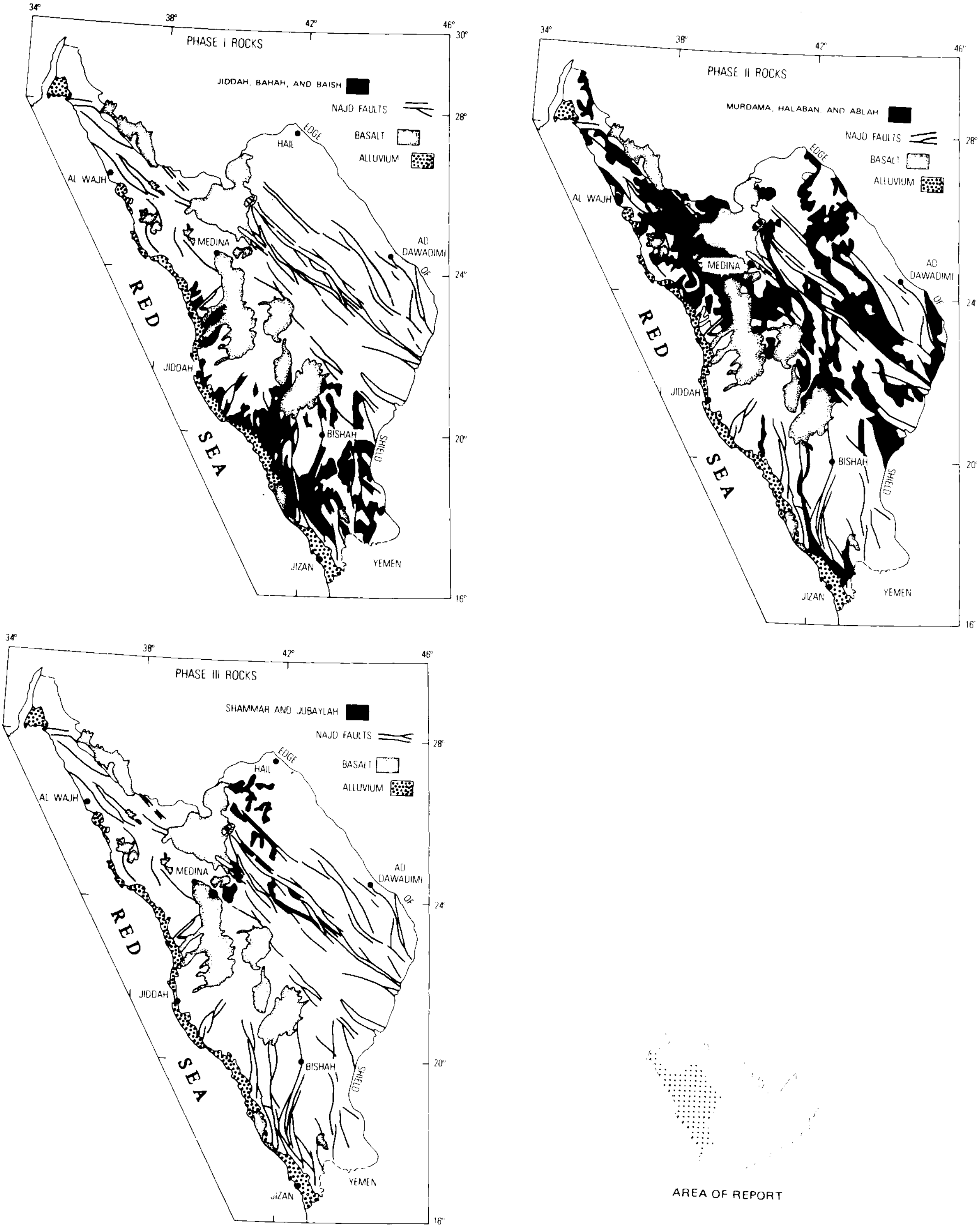

FIG. 1. Maps showing distribution of Phase I, II, III sedimentary and volcanic groups of the Arabian Shield.

Table 2.--*Sedimentary rock classes and types and their distribution in the eight stratigraphic groups of the Arabian Shield*

Class	Rock Type	PHASE I			PHASE II			PHASE III	
		Baish	Bahah	Jiddah	Ablah	Halaban	Murdama	Shammar	Jubaylah
Carbonate rocks	Limestone and dolomite								●
	Marble	●	●	●	●	●	●		
Argillaceous rocks and chert	Mudstone		●		●				
	Chert	●	●	●		●			●
	Shale							●	●
	Slate/argil-lite	●	●	●	●	●	●		
Nongraywacke clastic rocks	Siltstone	●	●	●	●	●	●	●	●
	Quartzite		●						
	Sandstone			●	●	●	●	●	●
Graywacke	Graywacke	●	●	●	●	●	●		
Conglomerates	Pebble conglomerate		●		●		●	●	●
	Boulder conglomerate	●		●	●	●	●		●

Table 3.--*Types of conglomerates of the Arabian Shield and their conditions of deposition*

	DEGREE OF TRANSPORT AND CONDITIONS OF DEPOSITION	
	TRANSPORTED	SHORT-TRANSPORTED
Boulder	Fluvial, Alluvial Fan, and Marine	Submarine Slump
Group	Jubaylah Shammar Murdama Halaban Ablah	Halaban Jiddah Baish
Pebble	Fluvial, Alluvial Fan, and Marine	Tidal Flat
Group	Jubaylah Shammar Murdama Ablah	Ablah Jiddah Bahah

Table 4.--*Sedimentary characteristics of Arabian Shield conglomerates*

Sedimentary characteristics	GROUP AND CONGLOMERATE TYPE										
	BAISH	BAHAH	JIDDAH	ABLAH		HALABAN		MURDAMA	SHAMMAR	JUBAYLAH	
	[1] B/ST[2]	[5] P/ST	B/T[7]	B/T	P/ST	B/T	B/ST	B/T	B/T	B/T	P/T
Color	Green Gray	Gray	Green Gray	Red Green Gray	Reddish	Greenish Gray	Green	Reddish brown	Reddish brown	Reddish brown	Reddish brown
Sorting	Very poor	Poor	Poor	Poor	Poor	Poor	Very Poor	Poor	Poor	Poor	Poor to moderate
Basal relief	NI[3]	NA[6]	NI	1-3m	NA	NI	NI	5m		15m	
Clasts: Maximum size	40cm	10cm	1m	1m	10cm	50cm	50cm	1m	5cm	1m	10cm
Clasts: Shape	Irregular	Tabular	Irregular	Subcircular	Flat to tabular	Irregular	Irregular	Subcircular	Irregular	Subcircular to circular	Subcircular to circular
Clasts: Rounding	Subangular to subrounded	Angular to subangular	Angular to subangular	Subangular to rounded	Angular	Subrounded to rounded	Angular to subangular	Subrounded to rounded	Angular to subrounded	Subrounded to rounded	Subangular to subrounded.
Clasts: Composition	Oligomictic (volcanic)	Oligomictic (siltstone)	Polymictic	Polymictic	Oligomictic siltstone and shale	Polymictic	Oligomictic (volcanic)	Polymictic	Polymictic	Polymictic and oligomictic	Polymictic
Clasts: Granitic	None	None	None	None	None	Sparse to common	None	Common	Common	Abundant	Abundant
Graded bedding	Sparse	Common	Common	Common	Common	Common	NP	NI	Common	NP	Common
Cross-bedding	NP[4]	Rare	Rare	Common	Common	NP	NP	NI	NP	NP	Minor
Inter-beds: Thickness	3-10cm	2-8cm	5-20cm	3-15cm	3-15cm	5-15cm	NP	NP	5-10cm	NP	2-10cm
Inter-beds: Uniformity	Lenticular	Lenticular	Lenticular	Lenticular	Tabular	Lenticular	NP	NP	Tabular	NP	Lenticular
Cement	Mica and calcite	Mica and silica	Mica and silica	Calcite	Silica and calcite	Silica and calcite	Mica and calcite	Silica and calcite	Silica and calcite	Calcite	Calcite

1. Boulder conglomerate; 2. Short-transported; 3. No information; 4. Not present; 5. Pebble conglomerate; 6. Not applicable; 7. Transported.

non-transported boulder conglomerates (Baish and Halaban, Table 3) are chaotic rubble masses. Granitic clasts in the conglomerates do not appear before deposition of the Halaban and they are not particularly abundant even then. They first appear in quantity in the basal Murdama conglomerate, excellent exposures of which can be seen 25 km N.E. of Bishah. Granitic clasts remain common to abundant throughout the younger groups.

Graywacke

Outcrop Description

Walker and Pettijohn (1971, p. 2127) conclude that graywacke is a product of and genetically related to mafic and intermediate volcanism. Graywacke of the Arabian Shield is no exception. It is found in all of the groups except the two youngest ones (Table 2), and each group is characterized by some basaltic or andesitic flow rocks.

Graywacke in each of these groups is intimately interbedded with the lavas. In most groups it comprises thousands of meters. Volumetrically, graywacke is thickest in the Baish, Jiddah, and Halaban Groups. Accurate figures regarding graywacke thicknesses are not available but it is estimated to comprise 30–40% of the Halaban, which, in the Bi'r Juqjuq area, is computed to have a minimum thickness of 19,500 m.

Graywacke forms monotonously uniform units in all groups. Many of the classic graywacke sedimentary structures are to be found, but common structures associated with turbidities, such as flute casts, ball-and-pillow structure, and various other kinds of sole marks are not present. Bedding ranges from 2–30 cm in thickness and is strikingly uniform or tabular. Graded beds ranging from coarse-grained to very fine-grained are present in most exposures, with some beds containing pebbly bases. Other internal features of the beds are millimeter-scale laminations, ripple drift, climbing ripples, and small-scale crossbeds. Exposures containing ripple-marked bedding plane surfaces may be seen in some instances, but they are not common.

Various shades of gray, green, red, and purple are the main graywacke colors. Gray and green are predominant in Phase I rocks, whereas red and purple are common to abundant in Phase II rocks.

Volcanic rocks, conglomerate, chert, slate, and marble are common rock types interbedded with the graywacke sequences.

Petrography

Modal analyses for some typical graywackes of the shield are shown in Table 5. Plagioclase and volcanic rocks fragments dominate most graywacke samples, followed by quartz, magnetite, mica, hematite, epidote, sphene, matrix or cement, and minor accessory minerals. The order of abundance of the petrographic constituents other than plagioclase and rock fragments may vary substantially from sample to sample. For example, in some cases the matrix may be almost as abundant as the principal framework constituents. Potassium feldspar may or may not be present in groups commonly containing potassium feldspar (Halaban and Murdama). No graywacke older than the Halaban contains potassium feldspar. Where present, it may constitute as much as 6% of some samples.

Framework components in a typical graywacke are surrounded by finely comminuted quartz, feldspar, and mica or by the cement materials, quartz (clear, polycrystalline, microcrystalline, and rarely chalcedony), calcite, and hematite. Sorting is fair to good and framework grains range from subangular to subrounded.

Non-Graywacke Clastic Rocks

Non-graywacke clastic rocks include quartzite, sandstone, siltstone, and mudstone. One or more of these rock types is found in all groups. The sandstones follow the classification of Pettijohn (1957, p. 291). They include detrital rocks with less than 15% argillaceous matrix and sandstones in which rock fragments may (protoquartzite and subgraywacke) or may not (arkose and subarkose) exceed feldspar or where the quartz content exceeds 95%. The term quartzite is used here as meaning a recrystallized sandstone (Pettijohn, 1957, p. 169) or a recrystallized sandstone containing abundant quartz (Holmes, 1920, p. 194). These lithologies form substantial parts of some groups and exposures, but they never attain the immense thicknesses of graywacke. In terms of total thickness or importance, they rank next to graywacke. Of these rocks types, sandstone and siltstone are the most abundant; they are thickest and form the most continuous outcrops in the Ablah (Bayley, 1972) and Murdama (Schmidt *et al.*, 1973, p. 8). The Hadiyah slate (Brown *et al.*, 1963a), thought to be equivalent to parts of the Murdama Group, is more than 90% sandstone and siltstone. Although less thick relative to the Ablah and Murdama, the Jubaylah Group is composed of 30 to 50% sandstone and siltstone.

The rocks are gray, green, red, maroon, and brown. They consist of beds ranging from a few centimeters in thickness to as much as a meter. Bedding, as a rule, is uniformly tabular and individual beds may be traced without interruption for tens of meters at many outcrops.

Internal and bedding-plane sedimentary structures include millimeter-scale laminations, graded bedding, ripple drift, small- and moderate-scale

Table 5.--*Modal analyses of some Arabian Shield graywackes*

	PHASE I						PHASE II					
	BAISH		BAHAH		JIDDAH		ABLAH		HALABAN		MURDAMA	
Quartz	19.3	24.9	14.7	18.3	9.9	15.3	10.7	17.9	16.0	19.1	35.0	27.5
Potassium feldspar	--	--	--	--	--	--	--	--	4.0	5.6	6.4	5.3
Plagioclase	21.2	17.8	34.6	29.2	24.3	22.0	22.3	20.7	10.0	12.3	14.6	12.1
Rock fragments												
Volcanic	--	--	--	--	23.2	16.7	29.5	27.2	33.5	32.8	7.9	19.6
Plutonic	--	--	--	--	--	--	2.0	--	--	3.1	2.0	4.7
Metamorphic + sedimentary	--	--	--	--	--	--	1.6	--	6.5	5.3	--	1.7
Biotite	2.3	1.6	5.6	3.6	Tr	0.9	0.5	1.2	0.7	--	1.0	0.5
Chlorite	16.7	15.4	11.4	9.4	3.7	4.2	2.3	3.8		0.5	0.5	1.1
Muscovite + sericite	1.6	2.4	3.3	4.6	4.1	1.0	1.6	0.5	0.3	1.0	--	0.4
Phlogopite	--	--	--	--	--	--	--	--	--	--	--	--
Sphene	0.8	1.1	0.4	--	Tr	--	Tr	Tr	--	--	2.1	--
Epidote	3.8	5.3	5.2	4.4	Tr	1.2	0.8	1.2	5.6	0.3	9.3	0.4
Apatite	--	0.3	--	0.2	--	--	--	--	--	--	2.3	Tr
Zircon	--	--	--	--	--	--	--	--	--	--	0.1	Tr
Magnetite	5.1	4.9	6.1	7.2	7.6	3.6	4.8	5.0	--	2.5	Tr	2.4
Hematite	2.6	3.1	0.9	1.7	2.2	1.8	1.6	1.7	1.0	1.0	Tr	0.6
Calcite	1.7	2.5	1.1	1.2	3.2	0.5	0.7	--	3.4	1.0	1.0	0.6
Matrix or cement	24.9	20.8	16.6	20.2	21.8	32.8	21.7	20.8	19.0	15.5	19.2	23.6
Total	100.0	100.1	99.9	100.0	100.0	100.0	100.0	100.0	100.0	100.0	100.4	100.1
No. point counts	723	678	300	566	700	588	416	593	531	620	632	800
Sample number	74281	74274	74563	74540	74515	74507	74455	74456	74735	81302	81448	81396
Percent of plutonic rock fragments	--	--	--	--	--	--	6.0	--	--	7.5	20.2	18.1

cross bedding, graded bedding, massive bedding (in the mudstones), convolute laminations, and ripple marks. These features are indicative of shallow water deposition in an environment signifying current transport. They occur in the groups dominated by sedimentary rocks, such as the Bahah, Ablah, Murdama, and Jubaylah, as opposed to those dominated by volcanic rocks (Baish, Jiddah, Halaban and Shammar; see Table 2).

Petrography

Modal analyses of some representative non-graywacke clastic rocks are shown in Table 6. Quartzite has been mapped only in the Bahah Group in the southern part of the shield. It is medium-grained, moderately well sorted, and contains as much as 69% recrystallized quartz and feldspar and a few percent accessory minerals. The matrix is composed of recrystallized quartz, probably silica cement originally, and about 5% very fine-grained detritus. The detrital grains appear to have been well rounded prior to recrystallization.

The nonquartzitic clastic rocks (mostly immature lithic sandstones) contain variable amounts of feldspar. Arkosic sandstones and siltstones are found in the Ablah through Jubaylah Groups. Plagioclase is the dominant feldspar in Phase II groups, whereas potassium feldspar is a prominent framework constituent of the Phase III clastic rocks (Table 6). Rock fragments are abundant in these rocks in all three phases (Table 6). Sorting ranges from poor to good and detrital fragments range from subangular to rounded; the better sorted rocks contain better rounded framework components. The matrix and cement of these rocks may be over 15%. It comprises quartz, calcite, hematite, sericite, and finely comminuted detrital material.

Petrographically, the mudstones consist of very fine-grained angular quartz, rock fragments, feldspar, and argillaceous material. The argillaceous material in most cases has been recrystallized to fine-grained mica. The fragmental components are generally massive textured, but in some samples laminations are present or the rock is lineated by aligned mica.

Argillaceous Rocks and Chert

Outcrop Description

Argillaceous rocks of the shield include slate, argillite, and shale. Because these are fine-grained rocks, chert is included. Stratigraphic distribution of these rocks is shown in Table 2. Slate and argillite are found in Phases I and II, and are particularly abundant in Phase I rocks. Phase III rocks contain minor amounts of shale. Chert is confined largely to Phase I groups, but is also common in the Jubaylah Group.

The argillaceous rocks are fine-grained, gray, green and black, and are thin- to medium-bedded. Due to shearing, alternating light and dark bands are juxtaposed in some outcrops to produce mottled striped rock. Graphitic material is common to abundant in argillitic rocks of Phase I (Greenwood, 1975a, b, c, d; Hadley, 1975a, c) and when such rocks are rubbed by hand a black sooty appearance results. The slates are highly siliceous in some areas, a good example of which is the graphitic schist unit of the Baish Group in the Wadi Hali quadrangle (Hadley, 1975c).

The stratigraphic thickness of argillitic rocks in the shield was not computed owing to the fact that these rocks are generally interbedded with other sedimentary or volcanic rocks and would have been too difficult and time consuming to separate. The Baish graphitic schist unit is one of the thickest and most continuous argillitic units of the shield, comprising a thickness of 1–3 km or about 15% of the Baish.

Chert in the Phase I rocks is not quantitatively abundant. It is found as tabular and irregular beds in argillite, graywacke, and volcanic sequences. Bedding ranges from 3 to 15 cm, can be traced for several tens of meters in some outcrops, and is devoid of internal structure. It is medium gray to black and reddish gray where ferruginous.

In the Jubaylah Group, primary chert is found as tabular beds as much as 1 m thick and as secondary irregular and lenticular masses and nodules replacing limestone in the lower part of the upper Jubaylah Muraykhah Formation (Hadley, 1974b). Unicellular microfossils, probably blue-green algae, and the coiled microfossil, *Obruchevella*, have been extracted from Jubaylah cert (Cloud *et al.*, in press). *Obruchevella* from the USSR indicates a Lower Cambrian (Lensk) age with a questionable Cambrian Atdaban stage occurrence and possibly Yudomian (Vendian or "Eocambrian"), but pre-Nemakit–Daldin. The Yudomian or Vendian is considered by Soviet geologists to be the terminal time-rock unit of the Proterozoic.

Petrography

Fine-grained material comprising mica, quartz, and feldspar commonly make up more than 50% of the argillitic rocks, followed by 30% or less of very fine-grained but discretely recognizable quartz, mica, opaque minerals, and hematite (Table 7). In addition to massive textures, primary and secondary laminations may be recognized in thin section, but other textural distinctions cannot be made practically.

A mosaic of microcrystalline quartz characterizes the chert in thin section. Alternating fine

Table 6.--*Modal analyses of some Arabian Shield clastic rocks*

	PHASE I		PHASE II					PHASE III			
	BAHAH	JIDDAH	ABLAH		HALABAN	MURDAMA		SHAMMAR		JUBAYLAH	
	Quartzite	Lithic Sandstone	Lithic Sandstone	Lithic Sandstone	Lithic Sandstone	Arkose	Lithic Sandstone	Lithic Sandstone	Lithic Sandstone	Lithic Sandstone	Lithic Sandstone
Quartz	66.3	14.7	18.6	17.2	15.9	35.0	33.9	12.0	20.4	13.2	5.3
Potassium feldspar	--	--	--	--	7.8	10.4	3.4	10.3	7.8	18.1	4.0
Plagioclase	2.3	27.9	20.7	14.3	16.6	14.6	4.0	15.7	21.6	6.2	10.5
Rock fragments											
Volcanic	--	10.8	21.8	18.4	21.6	4.7	29.3	11.5	14.4	3.0	40.1
Plutonic	--	--	4.0	2.5	2.8	1.2	7.8	14.1	14.9	36.2	5.2
Metamorphic + sedimentary	--	--	--	1.6	3.4		2.3	2.4	3.9	1.1	3.0
Biotite	0.2	1.0	0.9	0.9	--	1.5	0.3	1.3	0.7	Tr	3.0
Chlorite	1.7	2.2	4.3	3.0	--	--	1.9	1.5	0.1	--	--
Muscovite + sericite	1.2	1.2	0.4	0.6	--	--	--	0.2	--	1.4	--
Phlogopite	--	--	--	--	--	--	--	--	--	--	--
Sphene	--	0.3	Tr	--	--	--	Tr	--	Tr	--	0.3
Epidote	0.7	2.9	3.0	2.2	0.3	13.8	Tr	--	0.6	Tr	1.3
Apatite	--	0.7	0.2	Tr	--	--	--	--	--	Tr	--
Zircon	--	--	Tr	--	--	--	--	--	Tr	Tr	Tr
Magnetite	1.3	8.7	5.5	3.4	1.7	Tr	0.9	--	2.6	3.5	1.3
Hematite	0.3	4.5	2.2	1.2	Tr	10.7	0.6	--	0.4	Tr	0.3
Calcite	0.4	--	--	0.8	0.7	--	0.8	--	0.3	--	--
Matrix or cement	25.6	25.1	19.5	33.8	29.4	8.5	14.8	31.0	12.6	17.4	26.2
Total	100.0	100.0	100.1	99.1	100.2	100.4	100.0	100.0	100.3	100.2	100.5
No. of point counts	955	497	576	650	477	300	1112	600	631	576	302
Sample number	75377	74491	74450	74445	55007	55636	55641	55295	74295	74742	74035
Percent of plutonic rock fragments	--	--	15.5	11.1	10.1	20.3	19.8	50.4	44.8	89.8	10.8

Table 7.--*Modal analyses of some argillaceous rocks, chert, and marble of the Arabian Shield*

	PHASE I					PHASE II				PHASE III
	B A I S H			B A H A H		A B L A H		HALABAN	MURDAMA	JUBAYLAH
	Marble	Argillite	Chert	Slate	Marble	Marble	Mudstone	Marble	Marble	Limestone
Quartz										
Detrital	6.1	2.3	--	11.2	5.0	7.7	12.2	5.0	6.3	10.3
Microcrystalline	--	--	94.6	--	--	--	--	--	--	--
Secondary	--	--	--	7.8	--	--	--	2.5	--	--
Potassium feldspar	--	--	--	--	--	--	--	--	--	1.4
Plagioclase	1.3	--	0.9	3.4	2.7	5.6	6.9	--	8.3	4.6
Biotite	3.4	--	0.7	1.7	1.2	--	2.2	--	3.3	0.8
Chlorite	1.0	--	0.5	3.8	3.9	--	3.6	--	--	--
Muscovite + sericite	2.1	32.7	0.8	10.5	4.9	--	16.7	--	--	--
Phlogopite	--	--	--	--	--	2.3	--	--	--	--
Sphene	--	--	--	--	--	--	--	--	--	--
Epidote	0.1	--	--	1.1	Tr	--	Tr	--	--	Tr
Magnetite	2.4	3.3	2.7	5.6	4.7	3.1	5.2	2.5	0.4	3.3
Hematite	--	--	--	0.7	--	--	0.6	--	2.5	Tr
Carbonate	83.8	--	Tr	0.6	77.5	81.7	Tr	90.0	79.2	78.1
Argillaceous material	--	61.7	--	53.6	--	--	53.2	--	--	--
Total	100.2	100.0	100.2	100.0	99.9	100.4	100.0	100.0	100.0	100.1
No of point counts	700	300	439	425	398	470	300	1200	480	900
Sample number	74120	74433	74380	74284	74242	74149	74458	55048	81112	55555

and coarser grained mosaic bands define bedding laminations in some samples; in others it may be defined by very fine-grained opaque minerals. Some samples are massive and of uniform grain size.

Carbonate Rocks

Outcrop Description

Carbonate rocks are found in all three phases of the shield and in all groups except the Shammar (Table 2). Phase I and II rocks are metamorphosed to the greenschist and amphibolite facies and are therefore described as marble. Limestone and dolomite are found in the Phase III Jubaylah Group.

The marbles are pure, siliceous, dolomitic, and carbonaceous, and display a wide assortment of colors, including several shades of gray, green, pink, blue, brown, buff, red, yellow, and black and white. In some exposures the marble is more or less uniformly color banded. At others shearing has intricately juxtaposed marble bands of several colors producing a variegated rock suitable for building stone. In general, marble associated with groups dominated by volcanic rocks, such as the Baish, Jiddah, and Halaban (Hulayfah) is black, shades of gray or white (Hadley, 1975c, 1976; Delfour, 1977). In contrast, marble in the groups dominated by sedimentary rocks (Bahah, Ablah, and Murdama) exhibits a wide range of color and is therefore more suitable for ornamental purposes.

Marble beds and units of the shield are resistant to erosion and may be traced without break for scores of kilometers. Examples are Bahah, Ablah, and Murdama marble units in the Wadi Yiba, Wadi Hali, Jabal Sawdah, Jabal Aya, Harjab, and Bi'r Juqjuq quadrangles in the southern part of the shield (Bayley, 1972; Cornwall, 1973; Hadley, 1975c, 1976; Prinz, 1975; Ratte and Andreasen, 1974); and Halaban marble in the Sahl al Matran and Nuqrah quadrangles in the northern part of the shield (Delfour, 1977; Hadley, 1973).

The marble is exposed as individual beds and as units containing numerous beds. Individual marble beds, characteristic of volcanic units (Baish, etc.), are 10 to 25 cm thick. Marble units in the volcanic sequences may, however, attain thicknesses of as much as 200 m. Bedding and unit thicknesses of marbles in the sedimentary sequences are 10 cm to 1 m thick and as much as 500 m thick, respectively. Bedding is generally constant in thickness over substantial distances. Tops and bottoms of beds are undulatory in stromatolitic sequences, but otherwise, are relatively straight and parallel. Internal structure is massive or laminated in non-stromatolitic marble, but is wavy laminated in stromatolitic marble.

Jubaylah Group (Phase III) carbonate rocks consist of pure calcarenite and calcilutite, limestone, dolomitic limestone, and dolomite (Delfour, 1967, 1970, 1977; Hadley, 1973, 1974b). The carbonates are buff and gray, consist of beds that range from 5 to 30 cm in thickness, and contain abundant bedding and internal structures, including tabular to lenticular millimeter-scale laminations, lenticular anastomosing calcilutite and dolomite, ripple drift, undulose stromatolitic laminations, laterally linked stromatolitic hemispheres, and mud cracks.

Petrography

Shield marbles and limestone consist of fine- to medium-grained mosaics of calcite averaging over 75%, and a balance of detrital quartz and feldspar, microcrystalline quartz, opaque minerals, hematite, and metamorphic biotite and phlogopite. Laminations are defined by minute layers of detrital and opaque minerals.

SEDIMENTARY TRENDS

Stratigraphic Thicknesses and Ratios

Measured and computed thicknesses for shield groups (Table 8) range from 800 m (Jubaylah Group, Hadley, 1974b) to almost 20,000 m (Halaban Group, Hadley, 1976). Calculated and measured thicknesses of sedimentary rocks range from about 200 m (Shammar Group) to 10,000 m (Murdama Group in the Bir Juqjuq quadrangle, Hadley, 1976) and, excluding Phase III, generally fall in the 3000–5000 m range. The group with the thickest section of sedimentary rocks is the Murdama; and Phase II groups appear to contain the thickest sedimentary sections of all the phases.

The second row of Table 8 shows the estimated and computed ranges for the proportion of sedimentary rocks to the total stratigraphic thickness for each group of the shield, and the approximate average percentage of sedimentary rocks in each group. Some groups contain a minimum of 10–30% sedimentary rocks (Baish, Halaban, Shammar), whereas others, depending on the area, are comprised totally of sedimentary rocks (Ablah in the Wadi Hali area, Hadley, 1975c; Jubaylah in the Jabal Umm al Aisah area, Delfour, 1970, 1977). The most significant aspect that emerges from the thickness data is the cyclical nature of the proportion of sedimentary rocks (Fig. 2). There is a high proportion of sedimentary rocks in groups succeeding those dominated by volcanic rocks.

In order to identify trends within the sedimentary rocks related to grain size, the proportion of clastic rocks including siltstone and coarser grained rocks (excluding graywacke) was tabulated (Table 8). Phase I groups contain less than 20% of

Table 8.--*Some sedimentary characteristics for the eight stratigraphic groups of the Arabian Shield*
[The data presented here are mostly approximate but are based on the best available information

	Phase I			Phase II			Phase III	
Sedimentary characteristics	Baish	Bahah	Jiddah	Ablah	Halaban	Murdama	Shammar	Jubaylah
Sedimentary Thickness (in meters)	4,000	3,500	3,000	4,000-6,000	2,500-4,000	4,000-10,000	200-2,000	500-3,000
Sedimentary Rocks (Percent of total section)	15-25[1] (20)[2]	70-85 (80)	30-80 (50)	60-100 (70)	15-30 (25)	70-85 (80)	10-20 (15)	35-100 (75)
Coarse-Grained Nongraywacke Clastic Rocks (Maximum percent)	10	20	10	70	40	75	90	95
Carbonate Rocks (Percent of total sedimentary rocks)	5	5-10	10	10-25[1] (18)[2]	3-15 (9)	10-25 (18)		10-55 (30)

1 - Range
2 - Average

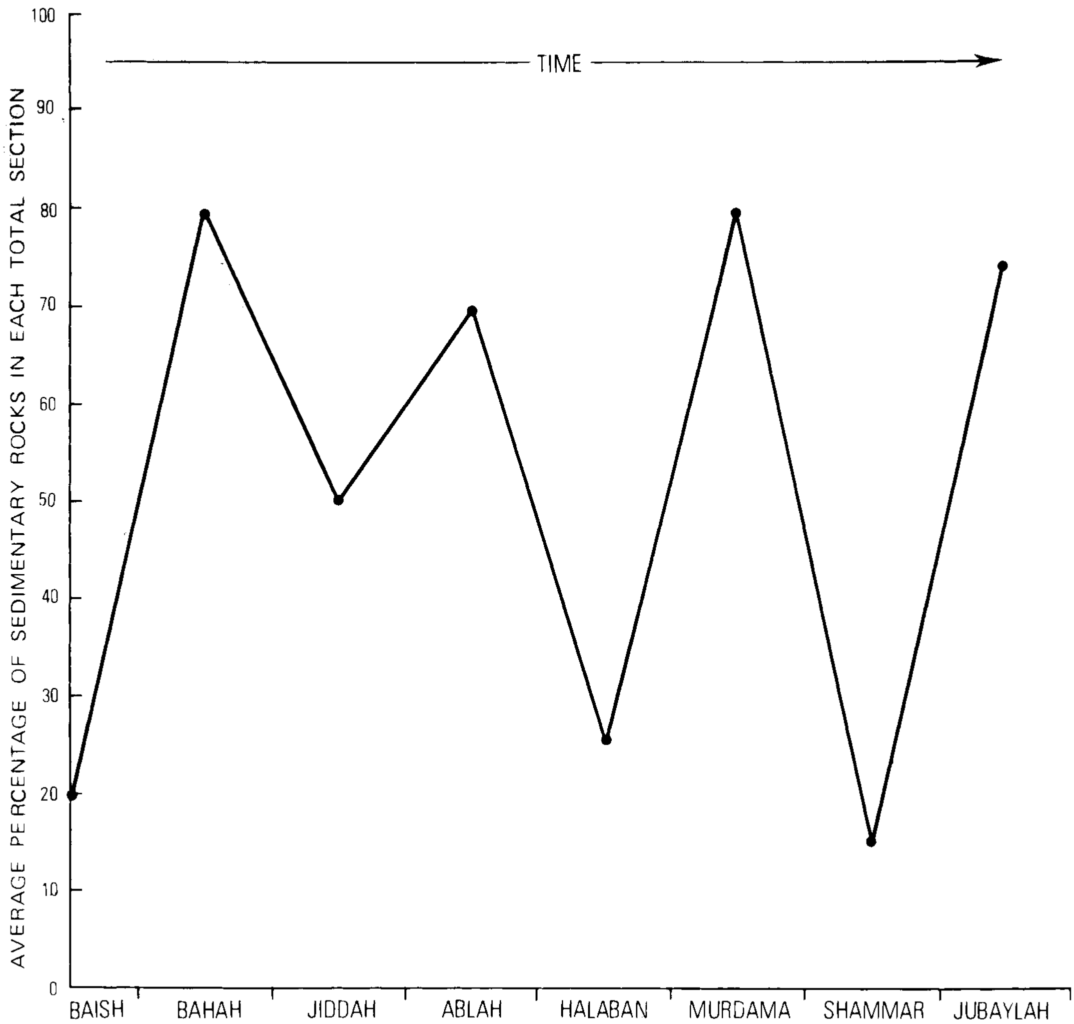

FIG. 2. Average percentage of sedimentary rocks in the total stratigraphic section for each group plotted against time. (Data are mostly approximate but are based on best available information.)

these rocks and the dominantly volcanic Baish and Jiddah Groups contain less than 10%. The proportion of the coarser grained clastic rocks rises abruptly in the Phase II groups. For example, the Ablah and Murdama Groups contain a maximum of 70% and 75% of these rocks, respectively. In contrast, however, the Halaban contains a lower proportion (40%) than its Phase II companions, reflecting a higher proportion of graywacke relative to the Ablah and Murdama. Clastic rocks in the Phase II groups show a further substantial increase, with some measured sections containing as much as 95% (Delfour, 1970, p. 18–19).

A final parameter related to the thickness of sedimentary rocks is the proportion of carbonate rocks to total stratigraphic thickness (Table 8). Phase I groups contain less than 10% carbonate rocks. Phase II groups contain a range of carbonate rocks from 3 to 25% and average 18% for the Ablah and Murdama. The Shammar Group contains no carbonate rocks and is of continental origin. Of all groups, the Jubaylah contains the highest proportion of carbonate rocks (55%, Jabal Nadah, Hadley, 1974).

Petrography

In order to determine whether any petrographic trends existed among the Arabian Shield's sedimentary rocks, modal analyses were made, and published analyses were re-examined for the relative proportions of constituent minerals and type of rock fragments. Judicious selection of the Phase I rocks and in some cases the Phase II rocks was required because of the degree of their metamorphism and tectonism. Samples that were relatively unsheared could be obtained, and these were used for the petrographic analysis. Unmetamorphosed Phase I rocks do not exist, yet recrystallization was not a problem and in most cases textural features were well preserved. Because of the

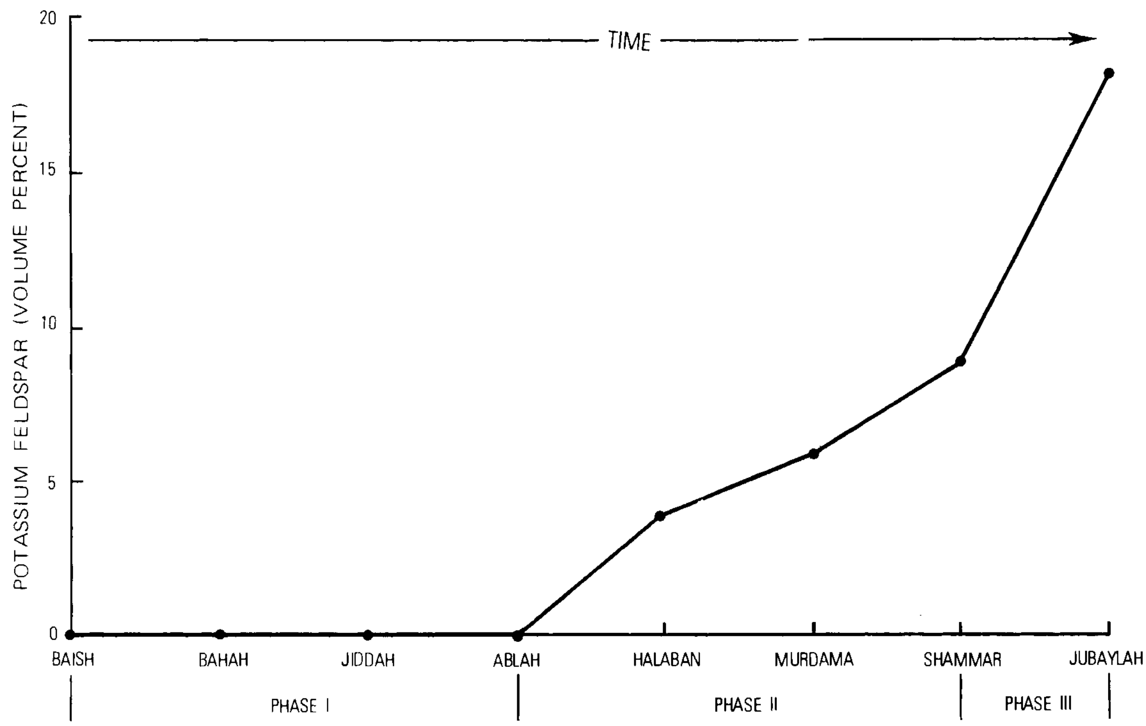

FIG. 3. Potassium feldspar (volume percent) plotted against groups and time.

greenschist grade of metamorphism, Phase I rocks reflect a high mica content (Table 5).

Ten samples of medium- to coarse-grained clastic rocks, including graywacke (especially for Phase I groups), sub-graywacke, arkose, and protoquartzite, were examined for each group. Results of these analyses are summarized in Tables 5 and 6 and Figs. 3 and 4. Potassium feldspar does not appear before the Halaban Group, where it averages 4% but reaches as much as 10%. Following the Halaban, potassium feldspar steadily increases in shield clastic rocks to a maximum average of 18% in the Jubaylah (Fig. 3; Table 6).

Plutonic rock fragments (Tables 5 and 6; Fig. 4)

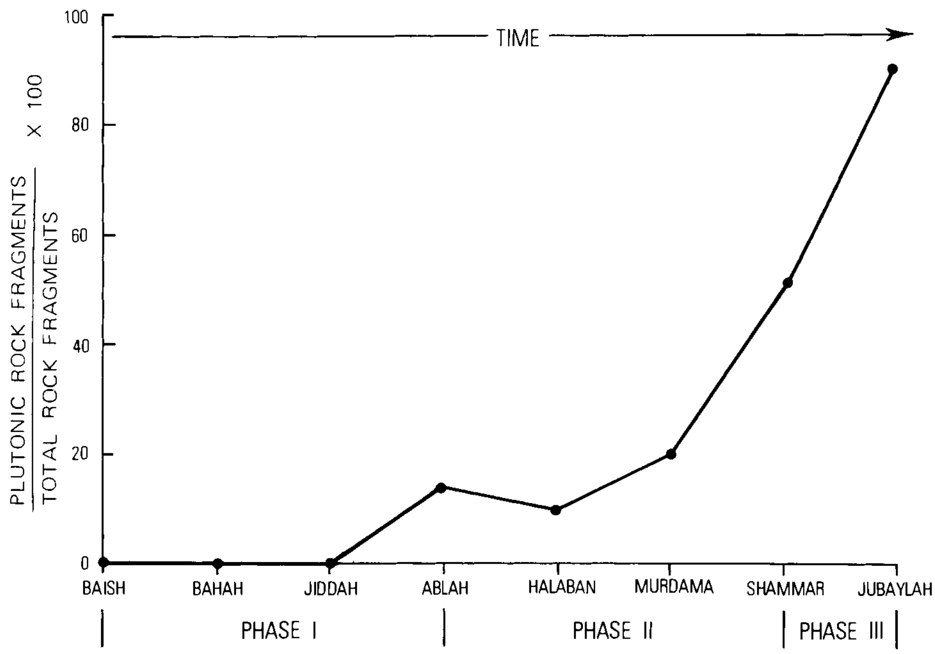

FIG. 4. Maximum percentage of plutonic rock fragments as a function of total rock fragments in clastic rocks of the Arabian Shield plotted against groups and time.

first appear in the Ablah Group (15%), fall to 10% in the Halaban, and then increase steadily to as much as 90% in the Jubaylah Group.

EVOLUTION OF SHIELD SEDIMENTARY ROCKS AND BASINS

General

Past and current studies (this Symposium, for example) have focused for the most part on the plutonic, volcanic, and structural geology of the Arabian–Nubian Shield in an effort to determine its history and evolution. Models proposed for origin of the shield have revolved around volcanic and sedimentary mobile belts surrounding stable cratons in an essentially continental or ensialic regime versus evolution in an oceanic-plate tectonic environment characterized by collision orogeny and subduction (Al-Shanti, 1979). One of the earliest and most significant papers on the Arabian segment was by Brown and Jackson (1960) in which they state "The framework of the shield is granitic". They further concluded that "One or two of these gneissoid belts have no apparent intrusive characteristics with adjoining beds, so may be the oldest exposed rocks". This implies that the oldest rocks, and hence the rocks from which the shield evolved, were granitoid in composition and that the shield's ancestry was ensialic or continental. Shackleton (1976), interpreting the geologic evolution of Pan-African domains across north Africa including the Nubian Shield, concluded that deformation was *in situ*, that the ensialic model is consistent with the evidence, and that there was no evidence for ophiolites, sutures, or collision orogeny.

In a later paper, however, Brown reversed himself and together with Coleman (Brown and Coleman, 1972) concluded that the Arabian craton is segmented by three cryptic sutures and was deformed during the Proterozoic by three orogenies which represented episodes of plate collision. This represented the first proposal involving a plate tectonic model for the Arabian–Nubian Shield. Jackaman (1972), utilizing whole-rock geochemistry from Baish and Jiddah basalt and andesites, postulated an island-arc origin for these rocks. Greenwood *et al.* (1976) inferred that the southern part of the Arabian Shield evolved in a plate tectonic/island-arc environment; an increase in potassium feldspar of the granitic rocks eastward and northeastward suggested to them a N.E. dipping subduction plate. Al-Shanti and Mitchell (1976) proposed a similar model for the eastern part of the shield with an eastward dipping subduction plate.

Virtually no evidence so far, however, has been presented regarding the sedimentary rocks and their bearing on evolution of the shield. Do they have an ensialic affinity or are they oceanic in character? What does the mineralogy of the sedimentary rocks say about their origin, sources of the detritus, and water depth? From a sedimentary standpoint, these and other questions have not been addressed. Thus, this paper has aimed to: 1) summarize descriptively and quantitatively the Phanerozoic–Eocambrian sedimentary geology of the Arabian Shield, and 2) document how the shield evolved, as determined by the record of sedimentation through time.

The sedimentary record indicates that the Arabian Shield changed with time from its inception to cratonization in both a progressive and a cyclical manner. The changes are also marked by well defined boundaries—divisions between the phases—represented by regional unconformities.

Tables 2 and 9 summarize the principal sedimentary factors of the three phases described in this paper. In addition, the volcanic characteristics of the phases are also shown because of the consanguineous association between them and the sedimentary rocks. From this summary documentation, however, one cannot easily devise an unambiguous model for evolution of the shield. Instead, a broad interpretation, slanted toward current plate tectonic concepts is offered here, with the realization that many ambiguities remain and that many questions are unresolved.

Group Summary

In Phase I, the Baish and Jiddah (Tables 2 and 9) consist solely of graywacke, chert, graphitic argillaceous rocks, non-stromatolitic marble, and a general absence of current structures and graded bedding. Thick abundant intraformational conglomerates (Table 3) dominated by ill sorted angular clasts of the same composition as the associated volcanic rocks indicate contemporaneous volcanism and a near-source submarine slump origin for these coarse rocks. A general lack of graded bedding and bedding-plane sedimentary structures in Phase I graywackes indicates distal deposition. The associated volcanic rocks are dominated by basalt (in places showing pillow structure) and andesite, and associated pyroclastic rocks. Collectively, these features indicate deposition in a deep-water marine flysch environment.

The sedimentary and volcanic character of the Bahah Group (Tables 2 and 9) contrasts sharply with the Baish and Jiddah. It is dominated by siltstone, mudstone, quartzite, flat-pebble conglomerate, marble, and argillite, and contains minor amounts of graywacke, chert, and interlayered flow rocks. Sedimentary structures include cross-bedding, ripple marks, mud cracks, flat-pebble chips, graded bedding, and wavy laminated (stromatolitic?) marble. Sialic components such as

Table 9.--*Sedimentary structures recorded in clastic and carbonate rocks of the Arabian Shield and the types and abundances of volcanic rocks found in each group*

	Phase I			Phase II			Phase III	
Sedimentary Structures	Baish	Bahah	Jiddah	Ablah	Halaban	Murdama	Shammar	Jubaylah
Clastic								
Crossbedding	--	C-A	--	C	S	C	S	C
Ripple marks	--	S	--	C	S-C	C-A	S	C
Ripple cross laminations	--	C	--	C-A	S-C	C-A	S-C	C-A
Mud cracks	--	S	--	C	--	C	--	S
Graded bedding	S	C-A	S	A	A	A	C	A
Rain drop imprints	--	--	--	S	S	--	--	--
Carbonate								
Stromatolite hemispheres	--	--	--	--	--	--	--	C-A
Stromatolitic algal laminites	--	S	--	C	--	C	--	A
Ripple drift laminations	--	S	--	C	--	C	--	A
Mud cracks	--	--	--	S	--	S	--	C
Volcanic Rocks								
Rhyolite-Dacite	S	--	S	S-C	C-A	C	A	--
Andesite	C	S	A	S-C	A	C	S	C
Basalt	A	--	C	--	S	--	--	--

A - Abundant; C - Common; S - Sparse; --Not recorded potassium feldspar and plutonic rock fragments have not been identified petrographically (Tables 5 and 6; Figs. 3 and 4). The types of sedimentary rocks and structures in the Bahah reflect deposition in a marine environment of moderate to shallow water depth.

Of the Phase II groups, the Ablah and Murdama contain basically the same types of sedimentary rocks and structures (Table 9). They are characterized by thick basal boulder conglomerates (recording unconformities), intraformational conglomerates, abundant arkosic and lithic (protoquartzite) sandstone, mudstone, siltstone, and marble, and subordinate amounts of pebble conglomerate and argillitic rocks. Sedimentary structures such as cross-bedding, ripple marks, ripple drift, mud cracks, sparse raindrop imprints, and graded bedding abound in the clastic rocks; in the carbonate rocks, stromatolites, and oolites have been recorded at numerous localities. Together with the sedimentary rock types and structures described above, abundant potassium feldspar and plutonic rock fragments in the Ablah and Murdama identify nearby sialic source rocks and indicate molasse and carbonate shelf sedimentation in a marine environment of moderate to shallow water depth.

In contrast to the Ablah and Murdama Groups, the Halaban is dominantly volcanic but contains a substantial thickness of sedimentary rocks, comprising boulder conglomerate (basal and intraformational), graywacke, siltstone, argillite, and marble. Plutonic rock fragments and potassium feldspar are common to abundant. Volcanic flow rocks and pyroclastic rocks ranging in composition from andesite to rhyolite dominate the group; andesite is abundantly interstratified with the sedimentary rocks and is closely interbedded with, and a contributor to, the Halaban chaotic boulder conglomerates. Sedimentary structures include graded bedding, cross-bedding, ripple marks, mud cracks, and rain drop imprints. The depositional environment is interpreted to be low-energy marine in water of moderate to shallow depth.

Phase III sedimentary and volcanic rocks differ substantially from rocks of the two older phases. Apart from carbonate rocks in the Jubaylah, the Shammar and Jubaylah Groups are dominated by terrigenous clastic rocks. Each consists of basal conglomerates (boulder-sized in the Jubaylah), medium- to coarse-grained arkosic sandstone, and siltstone. The Jubaylah, in addition, contains minor amounts of mudstone, shale, and abundant cherty limestone and dolomite containing chert nodules and interbeds. Potassium feldspar and potassium feldspar-bearing plutonic rock fragments are abundant components of the clastic rocks. Both groups are unmetamorphosed and only moderately deformed; thus, sedimentary structures are excellently preserved. Sedimentary structures consist of moderate-scale cross-bedding, graded bedding, ripple drift, mud cracks, laterally-linked-hemisphere stromatolites, and stromatolitic algal laminites. The volcanic rocks comprise rhyolite, rhyolitic ignimbrite, and andesitic basalt. The sedimentary and volcanic composition and structures of the Shammar and Jubaylah Groups show that they were deposited in a continental—alluvial fan, fluvial, and lacustrine environment; for the carbonate rocks, an intertidal marine or possibly lake bed environment is indicated.

Discussion

Sequential evolution of the sedimentary rocks and basins of the shield is ascribed to three phases (Table 10) schematically depicted in Fig. 5 (Hadley and Schmidt, 1978). Superimposed upon the phases is the cyclical aspect of evolution which documents volcanism followed by sedimentation, repeated four times from the inception of Baish volcanism. However, with time, plutonism (beginning with the post-Jiddah batholiths) became a co-parent with volcanism and assumed an ever increasing role in supplying sedimentary products to the shield (Figs. 3 and 4).

Evolution of the Arabian Shield was initiated by sea-floor volcanism during Baish time in an oceanic environment which continued through Jiddah time (Fig. 5). Sedimentary basins were North-trending and confined to the southern and western parts of the neo-craton. During this phase the Bahah was deposited mainly as moderate- to shallow-water depth back-arc (?) products, probably contemporaneous with volcanism and sedimentation of the Baish and Jiddah Groups. A westward-dipping oceanic plate is envisaged because sedimentary, volcanic, and plutonic rocks of the shield decrease in age toward the east and N.E. (Greenwood and Brown, 1973; Greenwood *et al.*, 1976) and $^{87}Sr/^{86}Sr$ ratios of plutonic rocks show the same trend (Fleck *et al.*, this symposium, vol. 3; Schmidt *et al.*, this symposium, vol. 2; Gass, this symposium, vol. 1). The complex distribution of Phase II rocks (Fig. 5) suggests that the groups of this phase were not deposited in a single linear basin or trough (trench?), but rather that a digitate system of basins or troughs (Frisch and Al-Shanti, 1977) may have existed that were contemporaneous in time. A well defined island arc or series of island arcs emerged late in Baish time and became well established during Jiddah time and continued on through Halaban and Murdama time (Greenwood *et al.*, 1976; Jackaman, 1972; Fleck *et al.*, this symposium, vol. 3; Schmidt *et al.*, this symposium, vol. 2; Dodge *et al.*, this symposium, vol 2).

Table 10.--*Sedimentary depositional environments and corresponding geologic-tectonic environments during evolution of the Arabian Shield*

	DOMINANT SEDIMENTARY ENVIRONMENT	GEOLOGIC/TECTONIC ENVIRONMENT
Phase I	Deep-Water Marine (Flysch)	Oceanic-Island Arc/ Subduction and Collision
Phase II	Moderate to Shallow Marine (Molasse-carbonate shelf)	Island Arc/Continental Accretion and Collision
Phase III	Continental and Shallow Marine (?)	Cratonization

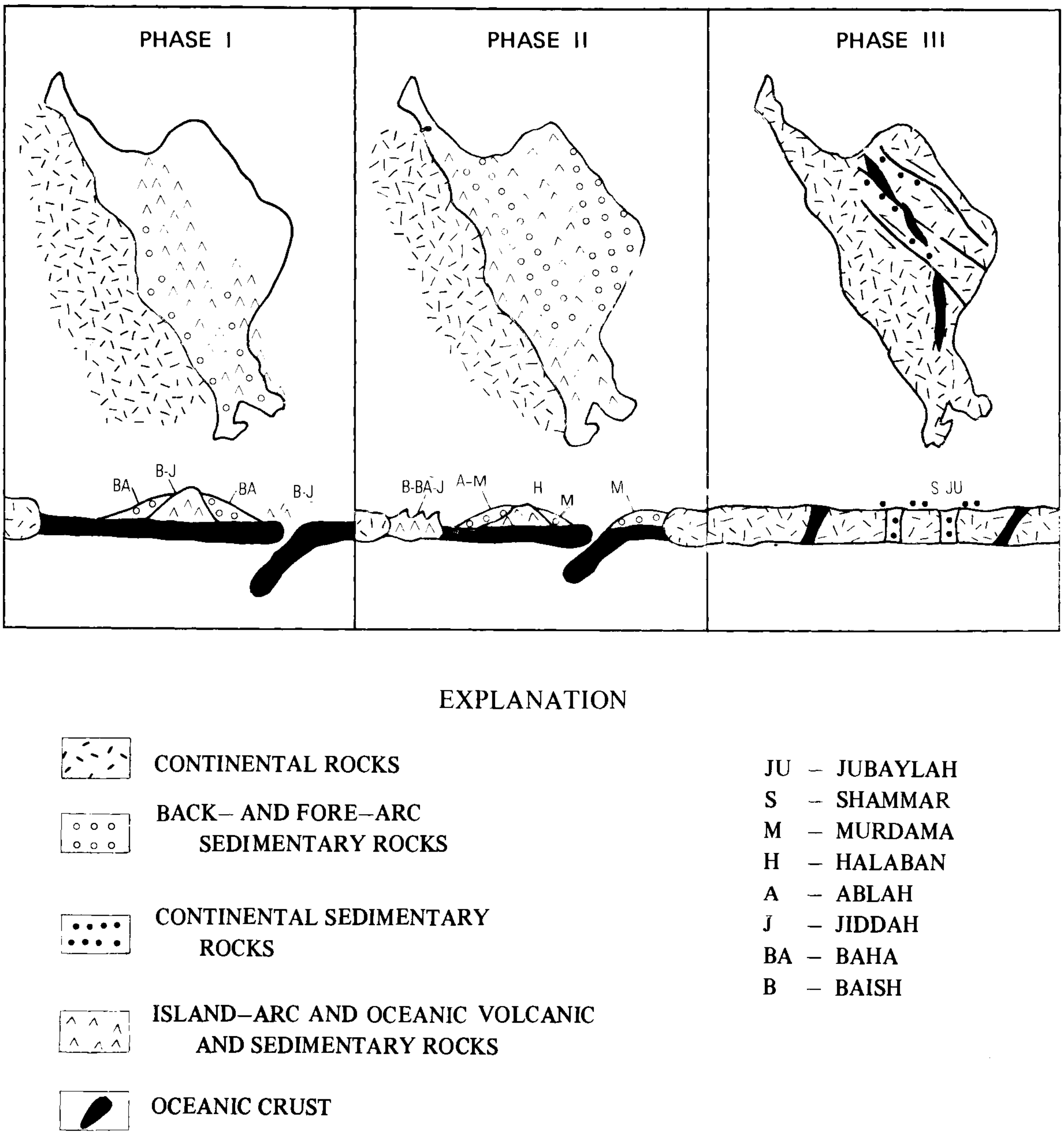

FIG. 5. Schematic diagram showing plate tectonic evolution of the Arabian Shield.

Phase II basins and sedimentary rocks (Fig. 5) are also North-trending, but have an apparent N.E. trend due to subsequent rotation by faulting during Najd time (Schmidt *et al.*, 1973; Moore and Al-Shanti, 1973; Moore and Al-Shanti, this symposium, vol. 2). In general, Phase II basins shifted eastward and northeastward following Phase I time. Sedimentation during Phase II time was influenced by and took place on the flanks of mature island arcs (Halaban) in a marine environment of moderate to shallow water depth. The primitive Phase I oceanic and island-arc products, consumed and intruded (Phase I diorite and trondhjemite batholiths) by late Phase I collision, began to feed plutonic detritus to the island-arc Phase II (Ablah) basins. During early Phase II time, as the adolescent Arabian Shield started to mature, potassium-bearing plutons evolved from Phase I dioritic to trondhjmitic batholiths, and the thick volcanic piles rose sufficiently to the surface to be eroded and subsequently contributed potassium feldspar detritus to the Halaban and Murdama sedimentary basins. A new episode of continental collision during late Phase II and early Phase III time about 640–610 Ma ago (Fleck *et al.*, this symposium, vol. 3; Schmidt *et al.*, this symposium, vol. 2) marked the cessation of Phase II sedimentation and volcanism, terminated oceanic and, for the most part, marine sedimentation, and initiated continental deposition and the development of the Pan-African age Najd fault system (Clifford, 1967; Fleck *et al.*, 1976). The Najd fault system formed during the 640–610 Ma collision event during which the Arabian block was juxtaposed against a pre-Tethyian block in the manner described by Tapponnier and Molnar (1976) for collision of the Asian and Indian plates. Compressional tectonics surrounding the collision swept the old island-arc volcanics and arc- and back-arc sediments together into a complex array of dominantly North-trending fold belts as now observed over most of the shield.

Phase III sedimentation was confined to small local basins (Shammar) and to grabens and half-grabens produced by the Najd faults (Delfour, 1970; Hadley, 1974b) in the northern and northeastern part of the shield. The eastward and northeastward shift of sedimentary basin axes prevalent in Phase I and II is not particularly applicable to Phase III sedimentary rocks because they were not part of the Phase I and II oceanic–island-arc regime.

Phase III sedimentary rocks were deposited unconformably on the deformed Phase I and II rocks in a continental environment. Phase III clastic material was derived primarily from the erosion of Phase I and II rocks, but a substantial portion probably came from the erosion of post-collisional granites in the 620–540 Ma range (Fleck *et al.*, 1976).

ACKNOWLEDGMENTS

The work on which this report is based was financed by the Saudi Arabian Government under a cooperative agreement between the Ministry of Petroleum and Mineral Resources and the U.S. Geological Survey. During the past 7 years many individuals have assisted us with various aspects of the field work and have contributed to our knowledge of the geology of the Arabian Shield, the sedimentary rocks in particular. We would like to acknowledge and thank them for their time and the numerous, enlightening discussions we have held.

First of all, we greatly appreciate the assistance and support of Sheikh Ghazi Sultan, Deputy Minister of the Directorate General of Mineral Resources, and the past Deputy Minister, Dr. Fadil Kabbani. Within the USGS Mission we are deeply indebted to J. J. Norton, Thor H. Kiilsgaard, G. F. Brown, R. G. Coleman, F. C. W. Dodge, R. J. Fleck, W. R. Greenwood, R. O. Jackson, Robert James, R. J. Roberts, Douglas Stoeser, Henry Williams, and R. G. Worl.

Fieldwork in the Kingdom could not have been adequately accomplished without Boyd Shaw and many others in Special Flight Services. To them sincere appreciation is extended for assisting us with aircraft support in the field. Finally, we are deeply grateful to Dr. Ahmed Al-Shanti, Dean of the Institute of Applied Geology, King Abdulaziz University, Jeddah, for convening the symposium on Evolution and Mineralization of the Arabian–Nubian Shield (February, 1978, Jiddah) at which this paper was presented.

REFERENCES

ALDRICH, L. T., and BROWN, G. F. 1960. Distribution of ages in the Arabian segment of the Arabian Shield. *Geol. Soc. Am. Bull.*, 71, 1813.

AL-SHANTI, A. M. S. 1978. Introduction (Abstract). *Precambrian Res.* 6, A, 2; and *Inst. App. Geol.* (Jeddah) *Bull.* 3, vol. 1, (1979).

AL-SHANTI, A. M. S., and MITCHELL, A. H. G. 1976. Late Precambrian subduction and collision in the Al Amar–Idsas region, Arabian Shield, Kingdom of Saudi Arabia. *Tectonophysics*, 30, T41–T47.

BAYLEY, R.W., 1972. Geology of the Wadi Yiba quadrangle, Kingdom of Saudi Arabia. *Saudi Arabian Dir. Gen. Mineral Resources Geologic Map GM*-1, scale 1:100,000.

BRAMKAMP, R. A., LAYNE, Jr., N. M., HOLM, D. A., and BROWN, G. F. 1963a. Geologic map of the Wadi as Sirhan quadrangle, Kingdom of Saudi Arabia. *U.S. Geol. Survey Misc. Geol. Inv. Map I-206A*, scale 1:500,000.

BRAMKAMP, R. A., and RAMIREZ, L. F. 1958. Geologic map of the northern Tuwayq quadrangle, Kingdom of Saudi Arabia. *U.S. Geol. Survey Misc. Geol. Inv. Map* 1-207*A*, scale 1:500,000.

BRAMKAMP, R. A., RAMIREZ, L. F., BROWN, G. F., and POCOCK, A. E. 1963b. Geologic map of the Wadi ar Rimah quadrangle, Kingdom of Saudi Arabia. *U.S. Geol. Survey Misc. Geol. Inv. Map* 1-206*A*, scale 1:500,000.

BROWN, G. F. 1960. Geomorphology of western and central Saudi Arabia. *Int. Geol. Cong.* XXI, 9, 69–77.

BROWN, G. F. 1970. Eastern margin of the Red Sea and the coastal structures in Saudi Arabia. *Phil. Trans. R. Soc. Lond.*, A267, 75–87.

BROWN, G. F., and COLEMAN, R. G. 1972. The tectonic framework of the Arabian Peninsula. *Int. Geol. Cong.* XXIV, 3, 300–305.

BROWN, G. F. and JACKSON, R. O. 1958. Geologic map of the Tihamat ash Sham quadrangle, Kingdom of Saudi Arabia. *U.S. Geol. Survey Misc. Geol. Inv. Map* 1-216*A*, scale 1:500,000.

BROWN, G. F., and JACKSON, R. O. 1959. Geologic map of the Asir quadrangle, Kingdom of Saudi Arabia. *U.S. Geol. Survey Misc. Geol. Inv. Map* 1-217*A*, scale 1:500,000.

BROWN, G. F., and JACKSON, R. O. 1960. The Arabian Shield. *Int. Geol. Cong.* XXI, 9, 69–77.

BROWN, G. F., JACKSON, R. O., BOGUE, R. G., and ELBERG, Jr., E. L. 1963a. Geologic map of the northwestern Hijaz quadrangle, Kingdom of Saudi Arabia. *U.S. Geol. Survey Misc. Geol. Inv. Map* 1-204*A*, scale 1:500,000.

BROWN, G. F., JACKSON, R. O., BOGUE, R. G., and MACLEAN, W. H., 1963b. Geologic map of the southern Hijaz quadrangle, Kingdom of Saudi Arabia. *U.S. Geol. Survey Misc. Geol. Inv. Map* 1-210*A*, scale 1:500,000.

BROWN, G. F., LAYNE, Jr., N. M., GOUDARZI, G. H., and MACLEAN, W. H. 1963c. Geologic map of the northeastern Hijaz quadrangle, Kingdom of Saudi Arabia. *U.S. Geol. Survey Misc. Geol. Inv. Map* 1-205*A*, scale 1:500,000.

CLIFFORD, T. N. 1967. The Damaran episode in the upper Proterozoic-lower Proterozoic structural history of southern Africa. *Geol. Soc. Am. Sp. Paper*, 92, 100.

CLOUD, P., AWRAMIK, S. M., MORRISON, K., and HADLEY, D. G. 1979. Earliest Phanerozoic or latest Proterozoic fossils from the Arabian Shield, Kingdom of Saudi Arabia. *U.S. Geol. Surv. Saudi Arabian Project Rept.* 260, 39 pp.

CORNWALL, H. R. 1973. Geology of the Wadi Harjab quadrangle, Kingdom of Saudi Arabia. *Saudi Arabian Dir. Gen. Mineral Resources Geol. Map GM*-3, scale 1 : 100,000.

DELFOUR, J. 1967. Report on the mineral resources and geology of the Hulayfah–Musayna'ah region, sheet 78, zone 1 north. *Bur. Rech. Geolog. Minieres Open File Rept.* SG. JED. 66, A, 8, 138 pp.

DELFOUR, J. 1970. Le Group de J'Balah, une nouvelle unite du bouclier arabe (The Jubaylah Group, a new unit of the Arabian Shield). *Bur. Rech. Geolog. Minieres Bull.* (ser. 2) sec. 4, ser. 4, 19-32.

DELFOUR, J. 1976. Comparative study of the mineralization in the Nubian and Arabian Shields, Saudi Arabia. *Saudi Arabian Dir. Gen. Mineral Resources Bull.* 15, 22.

DELFOUR, J. 1977. Geology of the Nuqrah quadrangle (25E), Kingdom of Saudi Arabia. *Saudi Arabian Dir. Gen. Mineral Resources Geol. Map GM*-28, scale 1 : 100,000.

DODGE, F. C. W., FLECK, R. J., HADLEY, D. G., and MILLARD, Jr., H. T. 1978. Geochemistry and $^{87}Sr/^{86}Sr$ ratios of Halaban rocks of the central Arabian Shield (Abstract). *Precambrian Res.*, 6, A, 13; and *Inst. Appl. Geol.* (Jeddah) *Bull.* 3, vol. 2, (1979), 1–17.

EARHART, R. L., 1968. A preliminary investigation of a copper occurrence at Jabal Sarbon, Tihamat ash Sham quadrangle, Kingdom of Saudi Arabia. *U.S. Geol. Survey Saudi Arabian Project Rept.* 102, 11 pp.

EARHART, R. L. 1969. Report on the exploration of the Wadi Yiba copper prospect, Tihamat ash Sham quadrangle, Kingdom of Saudi Arabia. *U.S. Geol. Survey Saudi Arabian Project Rept.* 108, 42 pp.

FLECK, R. J., COLEMAN, R. G., CORNWALL, H. R., GREENWOOD, W. R., HADLEY, D. G., PRINZ, W. C., RATTE, J. C., and SCHMIDT, D. L. 1976. Geochronology of the Arabian Shield, western Saudi Arabia: K–Ar results. *Geol. Soc. Am. Bull.*, 87, 9–21.

FLECK, R. J., GREENWOOD, W. R., HADLEY, D. G., ANDERSON, R. E., and SCHMIDT, D. G., 1978. Age and evolution of the southeastern part of the Arabian Shield (Abstract). *Precambrian Res.* 6, A, 21–22; and *I.A.G. Bull.* 3, vol. 3, in press.

FRISCH, W., and AL-SHANTI, A. 1977. Ophiolite belts and the collision of island arcs in the Arabian Shield. *Tectonophysics*, 43, 293–306.

GASKILL, D. L. 1970. Economic evaluation of a marble deposit and a kyanite deposit northeast of Al Lith, southern Hijaz quadrangle, Kingdom of Saudi Arabia; pt. 1, Marble deposit on Wadi Minash; pt. 2, Kyanite deposit near Wadi Al Arj. *U.S. Geol. Survey Saudi Arabian Project Rept.* 116, 19.

GASS, I. G. 1978. Evolutionary model for the Pan-African crystalline basement (Abstract). *Precambrian Res.* 6, A, 23; and *Inst. App. Geol.* (Jeddah) *Bull.* 3, vol. 1, (1979), 11–20.

GREENWOOD, W. R. 1975a. Geology of the Al Aqiq quadrangle 6 sheet 20/4/41D, Kingdom of Saudi Arabia. *Saudi Arabian Dir. Gen. Mineral Resources Geol. Map GM*-23, scale 1 : 100,000.

GREENWOOD, W. R. 1975b. Geology of the Biljurshi quadrangle, sheet 19/41B, Kingdom of Saudi Arabia. *Saudi Arabian Dir. Gen. Mineral Resources Geol. Map* GM-25, scale 1 : 100,000.

GREENWOOD, W. R. 1975c. Geology of the Jabal Ibrahim quadrangle, sheet 20/41C, Kingdom of Saudi Arabia. *Saudi Arabian Dir. Gen. Mineral Resources Geol. Map* GM-22, scale 1 : 100,000.

GREENWOOD, W. R. 1975d. Geology of the Jabal Shada quadrangle, sheet 19/41A, Kingdom of Saudi Arabia. *Saudi Arabian Dir. Gen. Mineral Resources Geol. Map* GM-20, scale 1 : 100,000.

GREENWOOD, W. R., and BROWN, G. F. 1973. Petrology and chemical analysis of selected plutonic rocks from the Arabian Shield, Kingdom of Saudi Arabia. *Saudi Arabian Dir. Gen. Mineral Resources Bull.* 9, 9 pp.

GREENWOOD, W. R., HADLEY, D. G., ANDERSON, R. E., FLECK, R. J., and SCHMIDT, D. L. 1975. Late Proterozoic cratonization in southwestern Saudi Arabia. *U.S. Geol. Survey Saudi Arabian Project Rept.* 196, 23 pp and *Phil. Trans. R. Soc. Lond.*, A 280 (1976), 517–527.

GREENWOOD, W. R., HADLEY, D. G., ANDERSON, R. E., FLECK, R. J., and SCHMIDT, D. L. 1974. Generalized geologic map of the Arabian Shield, Kingdom of Saudi Arabia. *Saudi Arabian Dir. Gen. Mineral Resources*, Kingdom of Saudi Arabia.

GREENWOOD, W. R., HADLEY, D. G., and SCHMIDT, R. L. 1973. Tectono-stratigraphic subdivision of Precambrian rocks in the southern part of the Arabian Shield. *Geol. Soc. Am. Abst. with Programs*, 5, 643.

HADLEY, D. G. 1973. Geology of the Sahl al Matran quadrangle, northwestern Hijaz, Kingdom of Saudi Arabia. *Saudi Arabian Dir. Gen. Mineral Resources Geol. Map* GM-6, scale 1 : 100,000.

HADLEY, D. G. 1974a. Geologic map of the Wayban quadrangle, Kingdom of Saudi Arabia. *Saudi Arabian Dir. Gen. Mineral Resources Geol. Map* GM-7, scale 1 : 100,000.

HADLEY, D. G. 1974b. The taphrogeosynclinal Jubaylah Group in the Mashhad area, northwestern Hijaz, Kingdom of Saudi Arabia. *Saudi Arabian Dir. Gen. Mineral Resources Bull.* 10, 18 pp.

HADLEY, D. G. 1975a. Geology of the al Qunfudhah quadrangle, sheet 19/41C, Kingdom of Saudi Arabia. *Saudi Arabian Dir. Gen. Mineral Resources Geol. Map* GM-19, scale 1 : 100,000.

HADLEY, D. G. 1975b. Geology of the Qal' at as Sawrah quadrangle, sheet 26/38D, Kingdom of Saudi Arabia. *Saudi Arabian Dir. Gen. Mineral Resources Geol. Map* GM-24, scale 1 : 100,000.

HADLEY, D. G. 1975c. Geology of the Wadi Hali quadrangle, sheet 18/41B, Kingdom of Saudi Arabia. *Saudi Arabian Dir. Gen. Mineral Resources Geol. Map* GM-21, scale 1 : 100,000.

HADLEY, D. G. 1976. Geology of the Bi'r Juqjuq quadrangle, sheet 21/43D, Kingdom of Saudi Arabia. *Saudi Arabian Dir. Gen. Mineral Resources Geol. Map* GM-26, scale 1 : 100,000.

HIRAYAMA, KEN, and ASSAD, M. Q. 1967. Types of iron deposits in Saudi Arabia. *Japanese Geol. Survey Saudi Arabian Mission Open-File Rept.* 30.

HIRAYAMA, KEN, NAKAZAWA, JIRO, KOMARA, KOH-JIRO, HIGASHIMOTO, SADAS, ODINI, YOSHITAKA, ISO, MIYOJI, and KUWAGATA, HISAO, 1967. Report on the iron-ore deposits in the Wadi Sawawin district, northwest Saudi Arabia. *Japanese Geol. Survey Saudi Arabian Mission Open-File Rept.* 115.

HOLMES, ARTHUR, 1920. *The Nomenclature of Petrology, with References to Selected literature.* Thomas Murby and Co., London.

JACKSON, R. O., BOGUE, R. G., BROWN, G. F., and GIERHART, R. D. 1963. Geologic map of the southern Najd quadrangle, Kingdom of Saudi Arabia. *U.S. Geol. Survey Misc. Geol. Inv. Map*, 1-211A, scale 1 :500,000.

JACKAMAN, B. 1972. Genetic and environmental factors controlling the formation of the massive sulfide deposits of Wadi Bidah and Wadi Wassat, Saudi Arabia. *Saudi Arabian Dir. Gen. Mineral Resources Tech. Rec.* TR-1972-1.

KARPOFF, ROMAN, 1957. Esquisse geologique del l'Arabie Seoudite. *Bull. Soc. Geol. de France*, 6 ser., VII, 672–674.

MOORE, J. MCM., and AL-SHANTI, A. M. 1973. The use of stress trajectory analysis in the elucidation of part of the Najd fault system, Saudi Arabia. *Proc. Geologists Assoc.*, 84, 383–403.

MOORE, J. MCM., and AL-SHANTI, A. M. S. 1978. The Najd fault system and associated mineralization (Abstract). *Precambrian Res.* 6, A, 30–31; and *Inst. App. Geol.* (Jeddah) *Bull.* 3, vol. 2, (1979), 17–28.

PETTIJOHN, F. J. 1957. *Sedimentary rocks.* Harper and Row, New York.

PETTIJOHN, F. J. 1975. *Sedimentary rocks.* Harper and Row, New York (3rd Ed.).

PRINZ, W. C. 1975. Reconnaissance geology of the Jabal 'Aya quadrangle, sheet 18/42A, Kingdom of Saudi Arabia. *Saudi Arabian Dir. Gen. Mineral Resources Geol. Map* GM-17, scale 1:100,000.

RATTE, J. C., and ANDREASEN, G. E. 1974. Reconnaissance geology and magnetic intensity map of the Jabal Sawdah quadrangle, Kingdom of Saudi Arabia. *Saudi Arabian Dir. Gen. Mineral Resources Map* GM-16, scale 1:100,000.

RICHTER-BERNBURG, R., and SCHOTT, W. 1954. Geological researches in western Saudi Arabia. *Saudi Arabian Dir. Gen. Mineral Resources Open-File Rept.* 38, 69 pp.

ROBERTS, R. J., GREENWOOD, W. R., WORL, R. G., DODGE, F. C. W., and KIILSGAARD, T. H. 1975. Mineral deposits in western Saudi Arabia. *U.S. Geol. Survey Saudi Arabian Project Rept.* 201, 60 pp.

SCHMIDT, D. L., HADLEY, D. G., GREENWOOD, W. R., GONZALEZ, L., COLEMAN, R. G., and BROWN, G. F. 1973. Stratigraphy and tectonism of the southern part of the Precambrian Shield of Saudi Arabia. *Saudi Arabian Dir. Gen. Mineral Resources Bull.* 8, 13 pp.

SCHMIDT, D. L., HADLEY, D. G., and STOESER, D. B. 1978. Late Proterozoic crustal history in the southern Najd Province, Saudi Arabia (Abstract). *Precambrian Res.* 6, A, 35; and *Inst. App. Geol.* (Jeddah) *Bull.* 3, vol. 2, (1979), 41–58.

SCHACKLETON, R. M. 1976. Pan-African structures. *Phil. Trans. R. Soc. Lond.* A280, 491–497.

TAPPONNIER, P., and MOLNAR, P. 1976. Slip-line field theory and large-scale continental tectonics. *Nature*, 264, 319–324.

U.S. GEOLOGICAL SURVEY-ARABIAN AMERICAN OIL CO. 1963. Geologic map of the Arabian Peninsula, Kingdom of Saudi Arabia. *U.S. Geol. Survey Misc. Geol. Inv. Map* 1-270A, scale 1:2,000,000.

WALKER, R. G., and PETTIJOHN, F. J. 1971. Archean sedimentation. Analysis of the Minnitaki Basin, northwestern Ontario, Canada. *Geol. Soc. Am. Bull.* 82, 2099–2130.

محاولة تنسيب وحدات ماقبل الكمبرى
في العربية السعودية والسودان ومصر

أ. ن. باسهل

الخلاصة

مازالت صخور ماقبل الكمبرى فى العربية السعودية والسودان ومصر موضوعا لعديد من البحوث التفصيلية فى هذه الأقطار الثلاثة. وفى هذا البحث محاولة لتنسيب هذه الصخور. وأساس هذا التنسيب الحقائق التالية : انتماء المنطقة كلها الى حزام تجبّلى واحد، وتساوى أعمار الوحدات المتدخلة والمتخرجة ، وتشابه أحجار أحواضها الرسوبية ، وتقارُن كثافة تمعْدنها.

TENTATIVE CORRELATION OF THE PRECAMBRIAN ROCK UNITS OF SAUDI ARABIA, SUDAN AND EGYPT

A. N. Basahel
King Abdulaziz University, Jeddah, Saudi Arabia

Abstract—The Precambrian rocks of Saudi Arabia, Sudan and Egypt have been the subject of several detailed investigations in the three countries. In this paper, a tentative correlation of these rocks is suggested. The correlation is based on the fact that the whole area belongs to the same orogenic belt; intrusive and extrusive units have the same age; sedimentary basins in the area are lithologically similar; and that mineralization density is comparable throughout the area. The correlation involves six orogenies and five unconformities separating five stratigraphic units.

INTRODUCTION

The study presented herein deals with the Precambrian rock units of Saudi Arabia, Sudan and Egypt, which initially formed one continuous mass, though they have been partly separated since Oligo–Miocene time by the Red Sea rift (see Fig. 1). Petrologists and economic geologists interested in classifying and evaluating the Precambrian mineral deposits in these countries would be aided by more precise knowledge of the Precambrian stratigraphy and the events involved. Yamani and Zaghloul (1974), for example, reported that without a generally acceptable Precambrian rock classification, it is difficult to subdivide the important mineral deposits. The same problem was recognised recently in the third geologic conference held in Sudan in 1976.

Several attempts have been made by geologists in the three countries to classify the Precambrian rock units and to unravel the complicated events involved. In order to accomplish this, a regional synthesis is first required, before a new correlation could be proposed.

THE PRECAMBRIAN ROCK UNITS OF SAUDI ARABIA

Several attempts have been made recently to elucidate the geologic history of the Precambrian rocks in the highlands of western Saudi Arabia and their north-west and south-east extensions along the Red Sea coast. No overall agreement on a rock unit scheme has been reached since the work of Brown and Jackson (1960). Two different stratigraphic schemes for rock units and tectonisms have been established by the geologists of the United States Geological Survey Mission (USGS), and Bureau de Recherches Geologiques et Minieres Mission (BRGM). These are summarized in Table 1.

Delfour (1975, Table 1) presented a rather complex stratigraphy for the central and northern parts of the shield. This can be correlated with the work done by Brown and Jackson (1960), Schmidt *et al.* (1973) and Greenwood *et al.* (1976, Table 1). Since units in all columns are comparable except for the Urd group, this paper will discuss the work of Brown and Jackson (1960), Schmidt *et al.* (1973) and Greenwood *et al.* (1976).

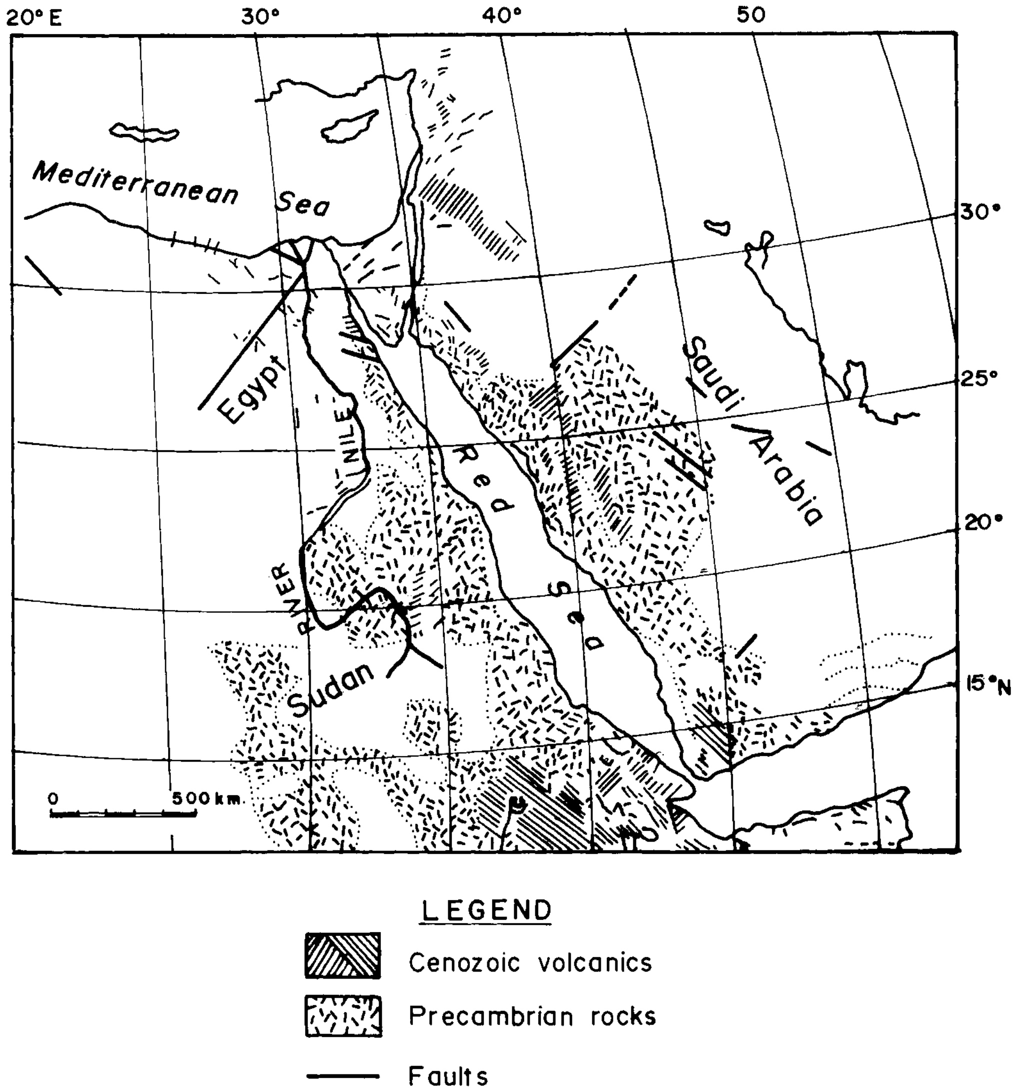

FIG. 1. Distribution of basement rocks in the Red Sea area considered in this paper.

Brown and Jackson (1960) distinguished rock units, from bottom to top, as follows:

1. Older gneiss with injection features and migmatization in some areas.
2. Hali schist including the oldest metasediments and metavolcanics, with dominant greenschist facies and occasional amphibolite facies metamorphism.
3. Baish greenstone and Lith complex, overlying and locally interbedded with Hali schist below. They include meta-diorite, meta-gabbro, amphibolite and subordinate siliceous slate.
4. Batholithic syn-tectonic granodiorite, adamellitic and albite pyroxene granite, with the gneisses at their roots.
5. Halaban andesite in the central and northern reaches of Saudi Arabia, with extrusive phases, subordinate concordant breccia, conglomerate, quartzite, graywacke, marble and phyllite interlayered with andesite and felsite. The latter are mostly in the lower part of the stratigraphic section. Epidiorite, diorite, diabase, gabbro and serpentine in sills and dikes represent the intrusive phase.
6. Murdama Formation composed of slate, phyllite, quartzite, graywacke and conglomerate. These were folded and metamorphosed to sericite and chlorite schist, particularly in the S.E.
7. Calc-alkaline granite series both concordant and discordant, generally outcropping as a mixture of two to three granites bearing gray and salmon to red colors.
8. Fatima and Ablah Formations represent the younger folded and slightly metamorphosed Precambrian sedimentary and volcanic rocks, which occur in an isolated basin above a prominent unconformity.
9. Shammar rhyolites, intrusive granites and

TABLE 1. STRATIGRAPHIC CHART OF THE ARABIAN SHIELD.

	The southern part of the Arabian Shield after USGS					The northern part of the Arabian Shield after BRGM		
Brown and Jackson, 1960	Schmidt *et al.*, 1973	Robert *et al.*, 1975		Greenwood *et al.*, 1976		Delfour, 1975, 1977		
							Group	***Formation***
	Jubaylah Group	Late Phase	Jubaylah Group	Third Episode	Murdama Group	Upper Proterozoic	Jibalah	Jifn Umm Al Aisah
Shammar rhyolite	Shammar Group		Shammar Group				Shammar	Malha Muara
Fatima and Ablah Formations	Murdama Group	Middle Phase	Murdama Group				Murdama	Hadiyah Farida Hibshi
Murdama Formation Halaban andesite	Halaban Group		Halaban Group	Second Episode	Halaban Group		Hulayfah	Nuqrah Afna
	Jiddah Group		Ablah Group Jiddah Group		Ablah Group		Urd	Abt Ar Ridaniyah Ophiolitic complex
Baish greenstone with Lith complex	Bahah Group Baish Group		Bahah Group Baish Group ?—?	First Episode	Jiddah Group Bahah Group Baish Group			
Hali schist	Hali Group	Early Phase	Sequence uncertain			Middle Proterozoic and older	Ajal (Hali)	Rharaba complex
Gneiss	Khamis Mushayt gneiss						Older basement	

agglomerates are disconformably overlain by younger tuffs, dacite, and andesite.

10. Late alkaline granite representing the youngest intrusive granite and syenite cropping out in plugs, small stocks and ring dikes with a wide age span.

This stratigraphic sequence is summarized in Table 2 (column 1). Two major unconformities are identified—below the Halaban andesite, and below the Fatima and Ablah Formations.

Schmidt *et al.* (1973) and Greenwood *et al.* (1976) have dealt with the stratigraphy and tectonism of the southern part of the Precambrian shield of Saudi Arabia. The latter reported six major lithostratigraphic units separated by angular unconformities, and four tectonic episodes. In addition, the Najd faulting cuts younger Precambrian to early Cambrian units. The six stratigraphic units proposed are summarized in Table 1.

The classification of Greenwood *et al.* (1976), though provisional, places much emphasis on the orogenic history in terms of the cratonization of the southern part of the Arabian Shield. Nevertheless, by comparing the work of Schmidt *et al.* (1973), and Greenwood *et al.* (1976) with that of Brown and Jackson (1960) some differences of opinion are found. These are summarized as follows:

1. The Baish Group is suggested by Greenwood *et al.* (1976) to be the first main volcano-sedimentary unit, deposited in a juvenile oceanic island arc, an inference that is supported chemically. The crust upon which the Baish Group rested has not been determined. Rocks initially thought to be older craton (Hali Group and Khamis' Mushayt gneiss; Brown and Jackson, 1960; Schmidt *et al.*, 1973) have been included by Greenwood *et al.* (1976) as highly metamorphosed equivalents in the Baish Group.

2. The Bahah Group is suggested by Schmidt *et al.* (1973) as a new group to include the metasediments above the Baish greenstone. The authors first describe its basal contact with the Baish (p. 6) as "a disconformable relationship, although in most places the contact relations are obscured by shearing." Then they state (p. 12) that the "contact is probably conformable, although the possibility of intertonguing relations between these two pairs of groups cannot be ruled out." These interpretations are conflicting.

3. The Jiddah Group is a second group newly proposed by Schmidt *et al.* (1973). Though it was then recorded only in two 30-minute quadrangles out of twelve, it is now widely mapped through the southern shield. It is said to include mainly meta-andesite and meta-dacite agglomerate, lava flows, pillow lava, bedded tuff and welded ash-tuff. Sedimentary rocks include abundant conglomerate containing dacite, basalt, and andesite clasts and fine-grained volcanoclastic rocks locally interbedded with chert and marble. This unit is mapped in fault contact with rocks of the Baish and Bahah Groups. The Jeddah Group represents, as suggested by Greenwood *et al.* (1976), the end process of common island-arc environments in which the first episode commenced with basalt to basaltic andesite volcanism and associated sediments; and was terminated by the Aqiq orogeny. However, Schmidt *et al.* (1973) state (p. 7) that "Jiddah andesite and lower Halaban rocks above may have been in part synchronous".

4. The name Ablah Group was proposed by Greenwood *et al.* (1976); it was unconformably deposited on the Jiddah, Baish and Bahah Groups and on diorite. It is said to consist of a basal clastic unit, a middle unit of andesite to rhyodacite and pyroclastic rocks, and an upper clastic unit of conglomerate, graywacke with clasts of the underlying diorite and volcanic rocks, and locally thick stromatolitic carbonate beds.

5. The Murdama Group is extended to include the Murdama Formation of Brown and Jackson (1960) which is extensively exposed in the central and northern parts of the shield, as well as the calc-alkaline intrusive granite and the Fatima and Ablah Formations.

6. Brown and Jackson (1960) recognized two principal unconformities; one below the Halaban Andesite and the second below the Fatima and Ablah Formations, whereas Schmidt *et al.* (1973) distinguished four angular unconformities occurring below Baish, Jiddah, Murdama and the Shammar Groups respectively. These are thought to indicate four Precambrian tectonic episodes designated as the Asir tectonism below, followed successively by the Tihamah, Hijaz and Bishah orogenies. However, Greenwood *et al.* (1976) proposed three unconformities, occurring below the Ablah, Halaban and Murdama Groups respectively, which indicate four orogenic events during the Hijaz tectonic cycle. These orogenies are Aqiq below, followed by Ranyah, Yafikh and Bishah.

7. With regard to the emplacement of the plutonic rocks, Schmidt *et al.* (1973) recognized no plutonism during the Tihamah orogeny, whereas Brown and Jackson (1960) assigned the syn-tectonic batholithic granodiorite having radiometric age of about 1000 Ma, to the earliest orogeny. Schmidt *et al.* (1973) reported the occurrence of granodiorite, quartz diorite, and gabbro to granite related to the Hijaz orogeny and in the Halaban Group. These fall in an age range of 665 to 1000 Ma. They further reported younger granite to granodiorite intrusives in the other three late tectonic episodes (Bishah, Shammar and Najd faulting) with absolute ages ranging from 570 to

520 Ma. However, Greenwood *et al.* (1976) assigned the first dioritic series, having a radiometric age of 960 Ma, to the Aqiq orogeny, the second dioritic series having a radiometric age of 800 Ma. They further reported injection gneiss with an absolute age of 785 Ma during the Ranyah orogeny, and quartz monzonite with absolute ages ranging from 650 to 600 Ma during the Yafikh orogeny.

PRECAMBRIAN ROCK UNITS OF EGYPT

Basement rocks occupy about one tenth of the land surface of Egypt, forming extensive mountain masses in the Eastern Desert, the southern part of Sinai and small isolated outcrops to the south of the Western Desert. The mountain masses of the Eastern Desert begin at about 28°40′N and extend southward, increasing in width from a few kilometers to about 400 km along the frontier of Sudan.

Over the past 40 years, many attempts have been made to establish a satisfactory classification for the basement complex of Egypt. Hume (1935) classified these rocks into four main divisions arranged from base to top as follows:

1. Protarchaean, including the fundamental gneisses and the crystalline schists.
2. Metarchaean, including the Barramyia serpentinite and associated carbonate and schistose sediments with diorite and porphyritic sills.
3. Eparchaean, including dacites, andesites and porphyrites intruding the serpentinites, together with slates, siliceous schists and conglomerates with fragments of earlier granites and andesites.
4. Late Precambrian or Gatterian, including diorite fringed by gabbro, biotite to hornblende granites, granodiorites, acid granites with red to pink pegmatites and finally felsite and porphyry to doleritic dikes.

Schurmann (1953, 1955) adopted Hume's classification and nomenclature with the addition of a new subdivision, namely, the "Shaitian" after the granite of Wadi Shait, central Eastern Desert. This represents a period of plutonic activity occurring before the Eparchaean sedimentation.

Amin (1955) subdivided the basement rocks of the central Eastern Desert as follows

Gatterian	Volcanic dikes Purple slate series Granites Gabbros
Metarchaean-Eparchaean Metamorphites	Epidiorite complex Serpentinite and related rocks Metavolcanics Green schists and related rocks Old metasediments

Akaad and El-Ramly (1960) suggested a classification for the basement rocks in the central Eastern Desert, accompanied by a geological map (scale 1:250,000). They combined the gabbros and epidiorites in one group and considered it younger than the metasediments, metavolcanics and serpentinite but older than the gray granites and granodiorites. This is summarized in Table 2 (column 6).

Schurmann (1961) published a geologic map for the basement rocks in the Red Sea area and considered them as belonging to the youngest consolidation rim (about 600 Ma) of the old African cratonic shield. He further reported that they formed either one or two geosynclines; one developed in Saudi Arabia and the other is represented by different rock types in the central Eastern Desert.

El-Shazly (1964) suggested a different picture for the geochronology of the basement in Egypt, taking into consideration previous work, available radiometric age determinations and field data from the neighbouring countries. He accordingly subdivided the basement in Egypt into three major structural stages as follows:

I. Geosynclinal main orogenic stage
- I.1. Geosynclinal sediments.
- I.2. Geosynclinal volcanics.
- I.3. Synorogenic plutonites (grey granite-granodiorite).
- I.4. Emerging geosynclinal volcanics (Dokhan type).

—Major unconformity—

II. Post-geosynclinal and late orogenic stage
- II.1. Post-geosynclinal sediments and associated volcanics (Hammamat).
- II.2. Late plutonics and associated pegmatites (Gatterian) with aplites, felsites and quartz veins.
- II.3. Post-orogenic plutonites. (Aswan type)
- II.4. Post-orogenic volcanics.

III. Foreland volcanic stage (Upper Cretaceus-Tertiary)
- III.1. Alkaline volcanics with subordinate plutonites.
- III.2. Basic volcanics (Qatrani type).

El-Ramly (1972) published a new geologic map for the basement of the central Eastern Desert and South-Western Desert of Egypt (scale 1:1,000,000). A summary of his proposed basement rocks is given in column 7 of Table 2.

With regard to the emplacement of the plutonic rocks, Hashad *et al.* (1972) and Meneisy (1976) carried out radiometric age determinations on the

TABLE 2. CORRELATION CHART OF THE PRECAMBRIAN ARABIAN–AFRICAN SHIELD ROCKS.

1	2	3	4	5	6	7	8
Arabian Shield Brown and Jackson, 1960	Southern part of the Arabian Shield Schmidt *et al.*, 1973	Southern part of the Arabian Shield Greenwood *et al.*, 1976	North Red Sea Hills, Sudan Lotfi and Kabesh, 1964	Northern Red Sea Hills Ruxton, 1956	Basement Rocks, Eastern Desert, Egypt Akaad and El-Ramly, 1960	Eastern S. Western Desert of Egypt El-Ramly, 1972	Author's Classification
Peralkaline granite and syenite Shammar rhyolite	*Najd faulting* Jubaylah Group granite–syenite Shammar Group (Late Precambrian to Paleozic)	*Najd faulting* Murdama Group	*Faulting* Alkaline granite Intrusive granite diorite, syenite *Mild orogeny*	Dikes of Ruxton Red granite(?) Injection metasomatic granite	Post granite dikes Younger-gatterian granite Hammamat series with Igla Formation (third sed. group)	Alkaline granite and syenite Younger granites Red pink granite Gabbro (?) Post Hammamat felsite Hammamat younger sediments	Alkaline granite Young granite (Calc? alkaline) Volc. rhyolite and and felsite Young sediments
			Acid and intermediate volcanics	Acid volcanics Silty mudstone–conglomerate *Uplift and erosion*			
Fatima and Ablah Formations Calc-alkaline granite	*Bishah orogeny* Murdama Group sediments with granite and granodiorite + syenite	*Bishah orogeny* Murdama Group sediments with granite and quartz monzonite	Awat series Mudstone–graywacke conglomerate				
Murdama Formation Halaban andesite volcanics and metasediments with intrusive gabbro epidiorite, serpentine	*Hijaz orogeny* Halaban Group with intrusive granite, granodiorite, gabbro and serpentine Jiddah group metasediments and meta volcanics	? *Yafikh orogeny* Halaban Group with quartz monzonite *Ranyah orogeny* Ablah Group with injection gneiss and second dioritic series	? Dikes of Ruxton gabbro –troctolite serpentinite	Basic intrusives	Volcanic sheets and flows of Dokhan type	Dokhan volcanics	Basic dikes and flows, old un-metamorphic volcanic and gabbro

TABLE 2. (*CONTINUED*)

Granodiorite (syn-tectonic)	*Tihamah orogeny*	*Aqiq orogeny*	Batholithic granite	*Large scale folding*	*Second orogeny* Grey granites	*Syn- to late tectonic Shaitian grey granite complex*	Old grey granite, granodiorite, metasediments, with major volcanics
	Bahah Group Metasediments	Jiddah Group	Metasediments L.S. quartzite, conglomerate slates	Metasediments			
Baish greenstone, with Lith complex of meta-diorite, meta-gabbro, amphibolite and slate	Baish Group	Bahah Group Baish Group	Metavolcanics	Intermediate to basic volcanics	Gabbros–diorites epidiorite	Meta-gabbro, diorite, epidiorite	Meta-gabbro, epidiorite, serpentinite
		With first dioritic series	*Unconformity and orogeny* ?~~?~~	*Uplift and erosion* ?~~?~~	Serpentinite, talc carbonate and metavolcanics	Serpentinite talc carbonate	
	Asir tectonism		Schists, slate, conglo. volc. intercalation	Basic dike swarms	Schists–mudstone–greywacke	Geosynclinal Shadli Group of meta-volcanics	Geosynclinal sediments with metavolcanics
				Folding and regional metamorphism	(Second sedimentary group)	Geosynclinal metasediments	
	Hali Group ~~?~~?~~		*Unconformity and orogeny* ?~~?~~		*Unconf. and orogeny*		
Gneiss	*Inferred tectonism* Khamis Mushayt gneiss		Para and ortho gneisses	Schist, slate, gneiss and granite pegmatite	Granite, volc. and gneisses of Migef, Mitiq Feiran and Hafafit (First sed. group)	Gneiss and migmatites	Tectonized gneiss

pink "Gatterian" granites from Igla El-Ahmar, central Eastern Desert which gave radiometric ages ranging from 621 to 660 Ma, suggesting a late Precambrian intrusive event. Further, Meneisy (1976) reported radiometric ages ranging from 575 to 600 Ma for the Aswan granite. Moreover, Gindy (1972) considered the abundance in the exposure of the true gneisses in southern Egypt as related to comparatively deeper conditions affecting older members of the country rocks. However, El-Dogdog (1976), dealing with the geology of Umm Bakra area, Eastern Desert, pointed out that younger basement rocks generally outcrop progressively northward.

THE PRECAMBRIAN ROCK UNITS OF SUDAN

The basement complex of Sudan includes igneous, metamorphic and metasedimentary rocks, stratigraphically overlain by horizontal to sub-horizontal Paleozoic, Mesozoic or younger sediments. In Sudan, the basement rocks are much more extensive than in Egypt, and cover nearly 50% of the total surface area.

Many workers have tried to classify the basement in Sudan, including Ruxton (1956), Kabesh (1962) and Kabesh and Lotfi (1962). The most comprehensive classification is that of Lotfi and Kabesh (1964), based on studies of the field relations in several localities of Sudan; the classification is summarized in column 4 of Table 2.

The oldest basement rocks are now represented by ortho- and para-gneisses succeeded unconformably by graywackes, slates, calc-sediments with volcanic intercalations of folded and metamorphosed andesites and dacites. These are followed unconformably by a recorded geosynclinal series composed of graywackes and slates with andesite, tuff and basaltic rocks, with local conglomerate, amphibolite, chlorite schist, limestone and quartzite. The latter are also folded, sheared and faulted. Batholithic granite emplacement then took place. This generally occurred in elongated outcrops parallel to the structural axes of the folded sediments and in places the batholiths show gneissic structure. In addition, basic and intermediate dikes of doleritic and andesitic composition cut these rocks. Afterwards, intrusion of basic magma took place. This is represented by gabbro, norite, troctolite, epidiorite and serpentinite. A third geosynclinal phase then followed. This is characterized by interbedded mudstone, sandstone, graywacke with rhyolites, dacites and andesites, which rest unconformably on the older rocks.

The above rock types are generally cut by granite, syenite, diorite and porphyrite. The granites are widely distributed and form conspicuous features extending for tens of kilometers. Then follow alkaline riebeckite granite, and finally scattered minor basic to acidic volcanic dikes.

ARABIAN PRECAMBRIAN ROCK UNITS CORRELATED WITH THE AFRICAN UNITS

The proposed correlation of the rock units of the Precambrian is given in Table 2. This table indicates agreement on the general chronological sequence of events in the three countries. Five tectonic episodes are found to exist in the Precambrian sections, as follows:

1. The oldest inferred tectonism of the Khamis Mushayt gneiss is to be found in both the Sudan and Egyptian literature.
2. The Asir tectonism, which involved the Hali Group of Brown and Jackson (1960) and Schmidt *et al.* (1973) in Saudi Arabia is also recognized in Sudan and Egypt. This orogeny affects the old geosynclinal metasediment and metavolcanics.
3. The orogeny correlative with the Tihamah orogeny of Schmidt *et al.* (1973) and Aqiq orogeny of Greenwood *et al.* (1976) is encountered in the three countries. It involved different sedimentary clastics, mafic volcanics and the emplacement of plutonic intrusives of varied composition ranging from granite to granodiorite to gabbro in the three countries.
4. There is also evidence of the Hijaz orogeny in Sudan and Egypt. It was accompanied by voluminous andesitic volcanism occurring in dikes, sheets, flows and occasional later gabbroic intrusions, not associated with distinct metamorphism.
5. The Bishah orogeny was rather mild, in places. It is represented by gentle folding and faulting in both Saudi Arabia and Sudan and was accompanied by acid and intermediate volcanism. In Egypt, it possibly took place after the deposition of the Hammamat younger sediments.

PRECAMBRIAN ARABIAN–AFRICAN CLASSIFICATION

Concerning the chronological sequence of the major rock units of the Precambrian Era in the Arabian–African Shield, the author proposes the following general classification (see also Table 2, column 8). This classification is summarized (from top to bottom) as follows:

—Tectonism
Post-granite dikes
Alkaline granites
Young calc-alkaline granites
Felsite and rhyolites

—Orogeny and unconformity—
Third geosynclinal sediments.

—Orogeny and unconformity—
Basic dikes and flows
Old granite, granodiorite and gabbros

—Orogeny and unconformity—
Second geosynclinal sediments
Metasediments and minor metavolcanics
Meta-gabbro, epidiorite and serpentines

—Orogeny and unconformity—
Metasediments
Metavolcanics
First geosynclinal sediments

—Orogeny and unconformity—
Old gneisses

This is a tentative correlation which should be refined and elaborated to unravel the stratigraphic and tectonic history of the area. The Arabian and the Nubian Shields are parts of one orogeny, and their geological and stratigraphic sequence may be easily correlated. This is based on: (1) the whole area is part of the same orogenic belt, which is recognized in the Nubian and Arabian Shields; (2) the related intrusive and extrusive units in the different parts of the shield are of one origin and have the same age; (3) there are frequent lithological similarities of the forms of the sedimentary basins. (4) a comparable density of mineralization.

REFERENCES

AKAAD, K., and EL-RAMLY, E. 1960. The geological history and classification of the basement rocks of the Eastern Desert of Egypt. *Geol. Surv. Egypt Paper* 9, 24 p.

AMIN, M. 1955. Some regional features of the Precambrian in Central Eastern Desert. *Bull. Inst. Desert Egypt* 5, 193.

BROWN, G. F., and JACKSON, R. O. 1960. Arabian Shield. *Int. Geol. Congr.* XXI, Pt. 9, 69–77.

DELFOUR, J. 1975. Comparative study of mineralization in the Nubian and Arabian Shield. *Saudi Arabian Dir. Gen. Mineral Resources Bull.* 15, 22 p.

DELFOUR, J. 1977. Geology of the Nuqrah quadrangle, 25E, Kingdom of Saudi Arabia. *Saudi Arabian Dir. Gen. Mineral Resources Geologic Map* GM-28, scale 1:250,000.

EL-DOGDOG, A. A. 1976. Geology of Umm Bakra area, Eastern Desert. *Unpubl. M.Sc. thesis.* Cairo University, Egypt.

EL-RAMLY, M. F. 1972. A new geological map for the basement rocks in the Eastern and South-Western Deserts of Egypt. *Annal. Geol. Surv. Egypt* Vol. II.

EL-SHAZLY, M. E. 1964. On the classification of Precambrian and other rocks of magmatic affiliation in Egypt, U.A.R. *Int. Geol. Congr.* XXII, Sec. 10.

GINDY, A. R. 1972. Toward a kinematic classification of the Egyptian basement. *Annal Geol. Surv. Egypt*, Vol. II, p. 47.

GREENWOOD, W. R., HADLEY, D. G., ANDERSON, R. E., FLECK, R. J., and SCHMIDT, D. L. 1976. Late Proterozoic cratonization in southwestern Saudi Arabia. *Phil. Trans. R. Soc. Lond.* A280, 517–527.

HASHAD, A. H., SAYYAH, T. A., EL-KHOLY, S. B., and YOUSEF, A. 1972. Rb/Sr Isotopic age determination on some Precambrian Egyptian granites. *Egypt J. Geol.* 16, 269–281.

HUME, V. E. 1935. *Geology of Egypt*, Vol. II, Part 2, Geol. Surv. Egypt.

KABESH, M. L. 1962. The geology of Muhammed Qol sheet. *Geol. Surv. Sudan Mem.* 3, 1–61.

KABESH, M. L., and LOTFI, M. 1962. On the basement complex of the Red Sea Hills, Sudan. *Bull. Instit. Desert d'Egypt* XII, 1–29.

LOTFI, M., and KABESH, M. L. 1964. On a new classification of the basement rock of the Red Sea Hills, Sudan. *Bull. Soc. Geogr. Egypt* 37, 93–99.

MENEISY, Y. 1976. Contribution to the petrology and geochronology of Igla area, Eastern Desert. *Unpubl. M.Sc. thesis.* Ain Shams Univ, Egypt.

ROBERTS, R. J., GREENWOOD, W. R., WORL, R. G., DODGE, F. C. W., and KIILSGAARD, T. H. 1975. Mineral deposits in western Saudi Arabia. *U.S. Geol. Survey Saudi Arabian Proj. Rept.* 201, 60 p.

RUXTON, B. P. 1956. Major rock groups of the northern Red Sea Hills, Sudan. *Geol. Magazine* 93, 314–330.

SCHMIDT, D. L., HADLEY, D. G., GREENWOOD, W. R., GONZALEZ, L., COLEMAN, R. G., and BROWN, G. F. 1973. Stratigraphy and tectonism of the southern part of the Precambrian of Saudi Arabia. *Saudi Arabian Dir. Gen. Mineral Resources Bull* 8, 13 p.

SCHURMANN, H. M. 1953. The Precambrian history of the Gulf of Suez area. *Int. Geol. Congr.* XIX, Sec. 1, 115.

SCHURMANN, H. M. 1955. Precambrian history of the Gulf of Suez area. *Bull. Soc. Geogr. Egypt* 45, 179.

SCHURMANN, H. M. 1961. The Riphean of the Red Sea area. *Sartrychur Geologiska Foreningens for Hand-tingar,* Bd. 83, H. 2 p. 103.

SCHURMANN, H. M. 1966. *Precambrian along the Gulf of Suez and Northern Part of the Red Sea*, Leiden, E. J. Brill, 404 p.

YAMANI, M., and ZAGHLOUL, Z. 1974. A tentative genetic and age classification of the mineral deposits of Saudi Arabia. A paper presented to the conference of *Mining and Mineral Deposits*, Jeddah, Saudi Arabia.

قرارات الذهب المصاحبة لنطاق صدع جبل إشماس ـ وداى تثليث

ر.ج. وورل

الخلاصة

يوجد كثير من مناجم الذهب القديمة وعروق الكوارتز على طول نطاق صدع جبل إشماس ـ وادى تثليث . وهو نطاق ضخم من التصدع والهصر والتغيّر ضارب الى الشمال فى الجزء الجنوبى الشرقى من الدرع على امتداد خط الطول ٢٥َ ٤٣° شرقا بين خطى العرض ١٨° و ٥١َ ٢١° شمالا . يشيع السّربنتينيت على هيئة كتل بنائية أو متدخلات مهصورة على طول النطاق ، وعلى هيئة أجساد متوافقة فيما يليه . وتوجد دلائل لفترات عديدة من التصدع والهصر أقدم من تصدع نجد الرئيسى الضارب نحو الشمال الغربى .

يوجد نطاق التصدع ومعظم مناجم الذهب داخل حزام حجر أخضر من صخور طباقية بركانية وفتاتية بركانية . هذا وإن حزاما متّصلا من صخور چنيسية يوازى نطاق التصدع وحزام الحجر الأخضر غربا ، كما يوجد حزام متقطع من الصخور الچنيسية شرقا . والصخور الخضراء الطباقية عبارة عن صخور بركانية متحولة أنديزيتية الى داسيتية تتخللها مترسبات فتاتية بركانية وفتاتية .

وتغلب الصخور الكتلية البركانية والرسوبية الغليظة التفتت فى الأجزاء الجنوبية وأقصى الشمال من الحزام ، بينما تغلب الصخور الرسوبية الدقيقة والمتوسطة التحبب والصخور الفتاتية البركانية (الأحدث جزئيا) فى أجزائه الوسطى . وتوجد قرارات الذهب فى أربعة مراكز تمعدن عند تقاطع نطاق الصدع مع الصدوع الممتدة نحو الغرب والشمال الغربى أو مع الأسارير (المسالك) المغنطيسية . ويمكن أن يعزى أصل الذهب الى متدخلات الكوارتز مونزونيت(الجرانيت الأحمر) فى قرارتين، كمايعزى إلى أجساد چابرو فى قرارتين ، غير أن الذهب غالبا مايوجد فى عروق الكوارتز الأقليمية أو قريبا منها . ومن المحتمل تكوّن القرارات أثناء حادث تجبّل يافيخ (٦٥٠ مليون عام) حيث صاحب الذهب المتحرك قطور متدّخلات الكوارتز مونزونيت والچابرو والمحاليل التىكوّنت عروق الكوارتز الناتجة من تحوّل حزام الحجر الأخضر تحوّلا إقليميا .

GOLD DEPOSITS ASSOCIATED WITH THE JABAL ISHMAS–WADI TATHLITH FAULT ZONE*

RONALD G. WORL

U.S. Geological Survey, Jeddah, Saudi Arabia

Abstract—In the south-eastern Arabian Shield, ancient gold mines and quartz veins are numerous along the Jabal Ishmas–Wadi Tathlith fault zone, a major North–South zone of faulting, shearing, and alteration that extends along long. 43° 30′ E between lat. 18° N and 21° 30′ N, a distance of about 390 km. Serpentinite is common as tectonic blocks or sheared intrusive bodies within the zone, and as conformable bodies adjacent to it. Several periods of faulting and shearing older than that of the major N.W.-trending Najd faulting are evident.

The fault zone and most of the gold mines are within a belt of layered metavolcanic and meta-volcaniclastic rocks that is situated between a continuous belt of gneissic rocks to the west and a discontinuous belt of gneissic

*Publication authorized by the Director, U.S. Geological Survey.

rocks to the east. Layered rocks are slightly to highly metamorphosed andesitic to dacitic volcanic rocks intercalated with volcaniclastic sediments. Massive volcanic rocks and coarse clastic sedimentary rocks predominate in the southern and very northern parts of the belt, and medium- to fine-grained sedimentary rocks and volcaniclastic rocks, in part younger than others in the belt, predominate in the central portions.

Ancient gold mines in the belt can be divided into five geographic groups, each of which contains deposits that are typical of that group and that are probably genetically related. These deposits are hydrothermal in nature and are in or next to quartz veins, quartz-breccia zones, or quartz-stringer zones. A few of the deposits are spatially related to felsic dikes or small bodies of gabbro, but most are in quartz veins of regional systems. A few of the deposits in the gold belt have some economic potential, but the majority are too small and isolated to be economic. The nature and distribution of the hydrothermal deposits suggests that an unevaluated potential for gold exists in other types of environments in the gold belt.

INTRODUCTION

The Jabal Ishmas–Wadi Tathlith fault zone is a major North-trending structure in the south-eastern part of the Precambrian shield of Saudi Arabia (Fig. 1). The fault zone lies in a belt of metavolcanic and metasedimentary greenstone that is 300 km long and 20 to 30 km wide. This volcanic–sedimentary belt, now composed of greenschist-facies rocks, is bounded on the west by a continuous and parallel zone of gneiss domes, diorite batholiths, and gabbro to granite plutons. To the east the greenstone belt is partly covered unconformably by Paleozoic sedimentary rocks, but the presence of gneiss and plutonic rocks in areas between the greenstone belt and the Paleozoic cover rocks suggests a parallel belt of gneiss and batholithic rocks to the east also.

Numerous ancient gold mines have been found within the greenstone belt and most are within fault zones that are probably second- or third-order structures related to the major Jabal Ishmas–Wadi Tathlith fault zone. The locations of gold deposits (Fig. 2) define the Jabal Ishmas–Wadi Tathlith gold belt. Numerous mineral belts have been recognized in western Saudi Arabia (Greenwood *et al.*, 1974); most are aligned along tectonic zones that trend North, N.W. and N.E. Many of the belts of gold and silver deposits are related to the second and third episodes of the Hijaz tectonic cycle (Table 1). A mineral belt including deposits of both metallic and non-metallic minerals that lie along the Al Amar fault, a major North-trending structure in the east-central part of the Arabian Shield (Fig. 1), has been delineated by Moore (1976). The Al-Amar fault, a very distinctive lineament, is in a greenstone belt, and separates a series of schistose graywacke sedimentary rocks from felsic to intermediate volcanic rocks.

LITHOLOGIES

Rocks comprising the southern Arabian Shield resulted from volcanic and sedimentary deposition accompanied by tectonism, metamorphism, and plutonism from about 1050 to 550 Ma ago. "The volcanism was predominantly intermediate in composition; however, a shift from early tholeiitic to later calc-alkalic rocks and an increase in potassium content is observed from oldest to the youngest deposits. The plutonic rocks show a parallel shift from early calcic to later calc-alkalic rocks, and an increase in potassium content that perhaps parallels a progressive increase in thickness of [a] neocraton" (Greenwood *et al.*, 1975, p. 16). The stratigraphy, orogenic events, and plutonic rocks in the southern shield are listed in Table 1.

Layered rocks in the gold belt (Fig. 2) comprise three map units, namely, a southern andesite–graywacke assemblage, a northern andesite–graywacke assemblage, and a metasedimentary assemblage. The southern andesite-graywacke assemblage includes rocks assigned to the Jiddah Group (Greenwood, 1979b), the Bayni Oshir Volcanic and Harban Groups (Warden, unpub. data), and the Baish, Jiddah, and Halaban Groups (Overstreet, 1978), as well as rocks of four unnamed metavolcanic and metasedimentary units of Simmons (unpub. data), and of two unassigned metavolcanic and metasedimentary units of Stoeser (unpub. data). The northern andesite–graywacke assemblage (Fig. 2B) includes rocks assigned to the Baish, Bahah, and Halaban Groups (Overstreet, 1978), the Halaban Group (Schmidt, unpub. data; Gonzalez, 1974; and Hadley, 1976), and rocks of two unassigned metavolcanic and metasedimentary units of Greene (unpub. data). The metasedimentary assemblage (Fig. 2B) includes rocks assigned to the Murdama Group (Overstreet, 1978; Schmidt, unpub. data; and Hadley, 1976). The metasedimentary assemblage as exposed in the Tathlith 1° quadrangle 19/43 (Fig. 1) is similar in lithology, degree and type of deformation, and intrusive relationships to the Ablah Group in the Khadrah quadrangle directly to the west, as described by Greenwood (1979a).

The interrelationships of the layered rocks within the gold belt have not been adequately delineated, in part because of the disparity in the detail of geologic mapping from quadrangle to quadrangle by various investigators, and in part because of stratigraphic complexities and lateral facies changes in the middle part of the map area. In general, massive volcanic rocks and coarse

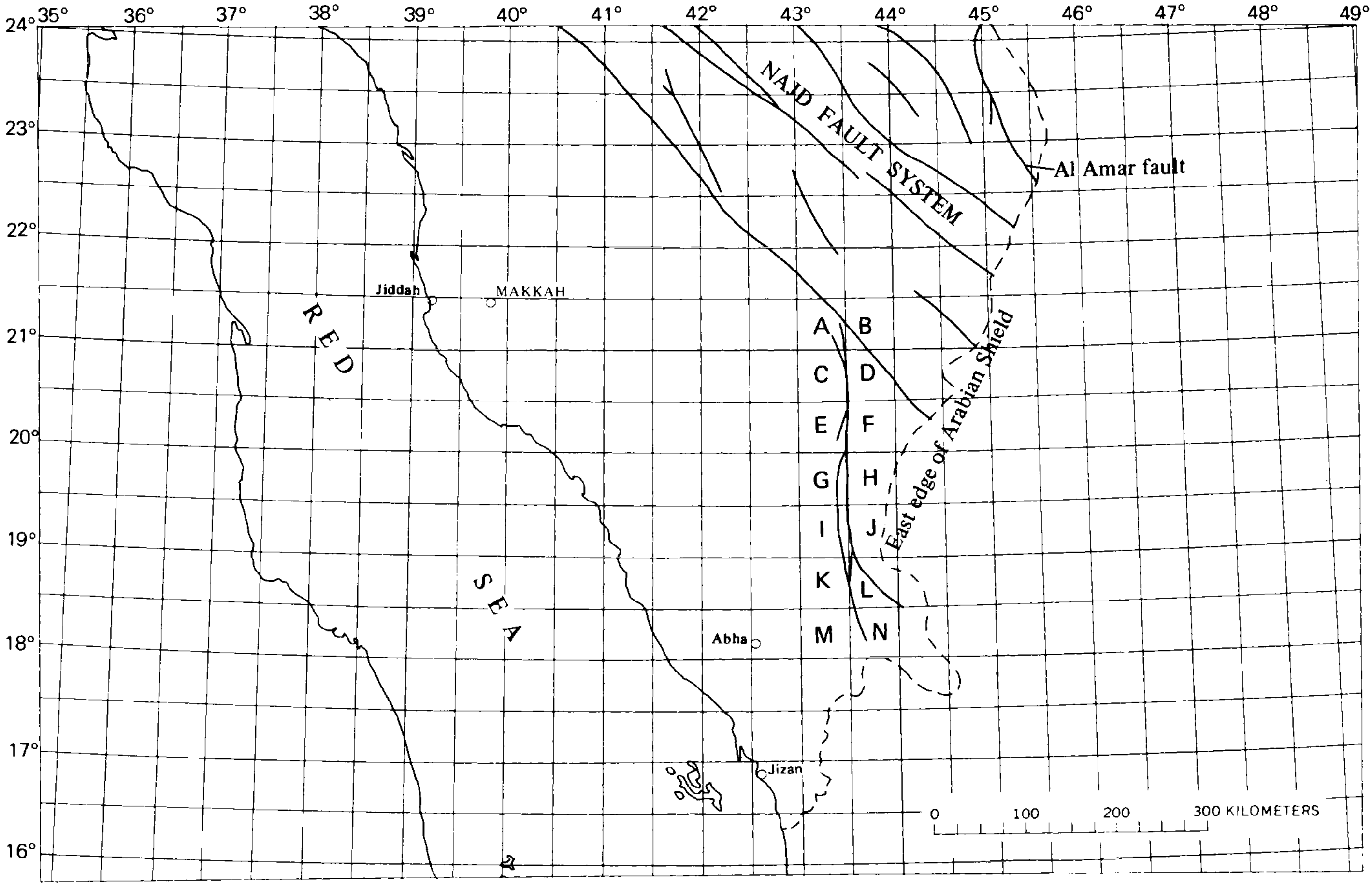

FIG. 1. Index map showing location of the Jabal Ishmas–Wadi Tathlith gold belt and location of the individual 1:100,000 scale geologic quadrangle maps covering the area.

Quadrangle			Reference
A. Jabal Dalfa	21/43C		R. C. Greene (unpub. data)
B. Bir Juqjuq	21/43D		Hadley(1976)
C. Jabal Ishmas	20/43A		Gonzalez (1974)
D. Jabal Yafik	20/43B		D. L. Schmidt (unpub. data)
E. Jabal Al-Qarah	20/43C		D. L. Schmidt (unpub. data)
F. South of Jabal Yafik	20/43D		NOT MAPPED
G. Al-Hashir	19/43A	Tathlith 1° quadrangle	Overstreet (1978)
H. Wadi Haraman	19/43B	Tathlith 1° quadrangle	Overstreet (1978)
I. Duthur As-Salam	19/43C	Tathlith 1° quadrangle	Overstreet (1978)
J. Hamdan	19/43D	Tathlith 1° quadrangle	Overstreet (1978)
K. Madha	18/43A		G. C. Simmons (unpub. data)
L. Markas	18/43B		A. J. Warden (unpub. data)
M. Wadi Tarib	18/43C		D. B. Stoeser (unpub. data)
N. Wadi Malahah	18/43D		Greenwood (1979b)

sedimentary rocks dominate in the southern and very northern parts of the belt, whereas finer grained pyroclastic volcanic rocks and sedimentary rocks dominate in the middle. On the basis of reconnaissance study, rocks shown as the southern andesite–graywacke assemblage seem to grade laterally northward into and intertongue with rocks shown as the northern andesite–graywacke assemblage (Fig. 2). However, intrusive relationships and degree of deformation suggest that the northern adesite–graywacke assemblage is younger; that it is a lithofacies but not the time equivalent of the southern andesite–graywacke assemblage.

The nature of the layered rocks throughout the belt suggests two major volcanic sources, or two

TABLE 1. STRATIGRAPHY, OROGENIC EVENTS, AND PLUTONIC ROCKS IN THE SOUTHERN PART OF THE ARABIAN SHIELD [MODIFIED FROM GREENWOOD *et al.*, 1975]

Units	Orogenic events	Plutonic rocks
	Najd: left lateral wrench faulting, northwesterly trends, latest Proterozoic-earliest Cambrian	
Murdama group	Bishah: northerly trends	Granite and quartz monzonite (570–550 Ma)
—— UNCONFORMITY ——		
Halaban group	Yafikh: northerly trends	Quartz monzonite (650–600 Ma)
UNCONFORMITY?		
Ablah group	Ranyah: northerly and northeasterly trends, transverse shears	Injection gneiss (785 Ma) Second dioritic series(800 Ma)
—— UNCONFORMITY ——		
Jiddah, Bahah, and Baish groups	Aqiq: northerly trends	First dioritic series (960 Ma)

volcanic piles. One, the source of the southern andesite–graywacke assemblage, is centered in the southern or south-eastern part of the map area; the second, the source of the northern andesite–graywacke assemblage, is centered off the northern edge of the map area. Each probably was an extensive series of small centers that fed flows and pyroclastics to the very southern and very northern parts of the map area. Most of the map area from 18° 30′ N to 21° 00′ N is characterized by finer grained pyroclastics and clastic material, and marine precipitates. The sources for these rocks are believed to have been the developing volcanic piles to the north or south, as well as small local sources. Rocks of the northern andesite–graywacke assemblage (Fig. 2) lose their distinct volcanic character, become finer grained, and contain more limestone toward the south. Rocks of the southern andesite–graywacke assemblage show similar but less marked changes toward the north.

Part of the exposed gneissic terrain (Fig. 2) may represent an older basement upon which the layered metavolcanic and metasedimentary units were deposited (Overstreet, 1978). There is little evidence, however, to support this concept. At several locations the gneiss consists of highly metamorphosed rocks of the southern andesite–graywacke assemblage mixed with lit-par-lit intrusives and migmatites in gneiss domes. A quartz-biotite schist unit intercalated with quartz-rich metasedimentary rock exposed in the vicinity of the Hajr mine (18° 55′ N, 43° 40′ E) may be segments of an older basement. This sequence is overlain by rocks of the southern andesite–graywacke assemblage and is intruded by diorite.

Intrusive rocks emplaced during the Yafikh orogenic event (Table 1) are gabbro, granodiorite, and granite and are principally calc-alkaline. Rocks of these types compose most of the larger batholiths and ring-shaped intrusives and many of the smaller circular plutons. Dikes, sills, and irregular bodies of similar petrology are common.

Intrusive rocks emplaced during the Bishah orogenic event (Table 1) range from gabbros to granites, many of which show modal and chemical characteristics of alkalic rocks. Sub-circular homogeneous to zoned plutons and dikes, sills, and layered complexes are the normal modes of occurrence for this group of rocks. Dikes and sheets in country rocks around intrusives are common. These alkalic rocks are generally fresh and undeformed, except along major faults.

JABAL ISHMAS–WADI TATHLITH FAULT ZONE

The Jabal Ishmas–Wadi Tathlith fault system is a major North-trending zone of faulting, shearing, and alteration composed of several individual fault zones 0.5 to 5 km in width. Each fault is marked by numerous parallel and near-vertical fault planes, breccia zones, alteration zones, and, locally, quartz veins. The system has undergone several generations of movement, the latest being rejuvenation during the period of Najd faulting. The very northern segment includes the Ishmas west, Ishmas east, and Nabitah faults of Gonzalez (1974),

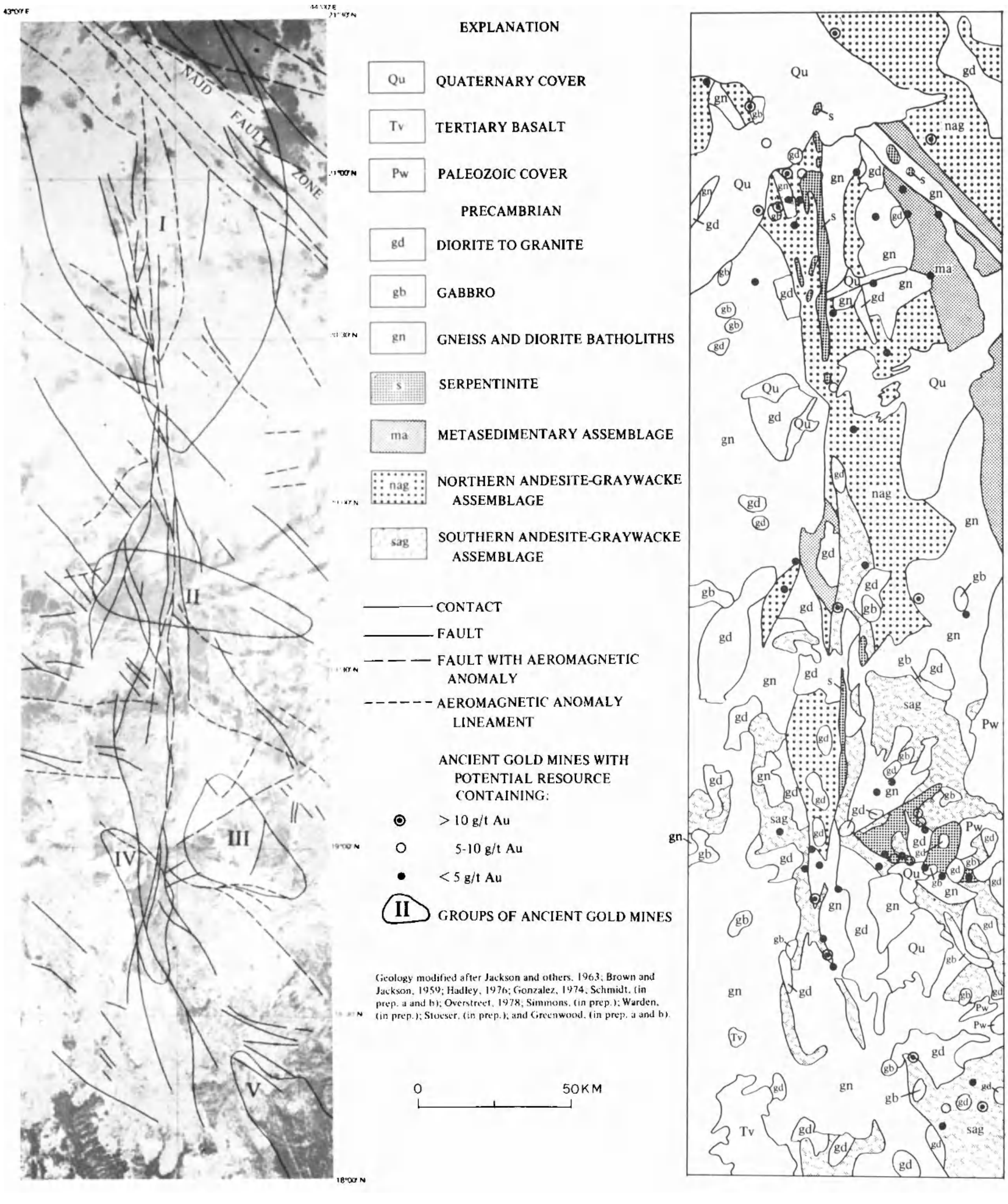

FIG. 2. A (left). Map showing locations of the Jabal Ishmas–Wadi Tathlith fault zone and of groups of ancient gold mines. B (right). Map showing distribution of rock units and of ancient gold mines.

all of which terminate to the north against major N.W.-trending Najd faults. The degree of crushing, shearing, and folding is much greater in rocks of the southern andesite–graywacke assemblage and gneissic rocks than in rocks of the northern andesite–graywacke and metasedimentary assemblages. The Jabal Ishmas–Wadi Tathlith fault zone probably developed originally during one of the older orogenic events, possibly the Aqiq (Table 1), and was reactivated during subsequent orogenic events.

The fracture system has localized emplacement of mafic to ultramafic magmas at several locations. Serpentinite bodies are common along the zone from lat. 18° 45′ N northward, but are not present south of this line. Talc, carbonate, and carbonate-rich alteration zones are also common along the segment north of lat. 18° 45′ N. Serpentinite bodies along the main fault zone are highly sheared and deformed and form tectonic breccias, suggesting tectonic transport of relatively cool, rigid serpentinite. The southern exposures of serpentinite are sheet-like, generally concordant bodies and larger masses of indeterminate shape. The Jabal Ishmas–Wadi Tathlith fault zone and greenstone belt is considered by Frisch and Al-Shanti (1977) to be part of the Hulayfah–Hamdah ophiolite belt, which cuts the Arabian Shield in a north–south direction. Schmidt *et al.* (1978) consider this zone to be a suture zone, the Nabitah suture, which was possibly a westward-dipping subduction zone for an island arc system of Jiddah age (Table 1). If these ideas are correct, the Jabal Ishmas–Wadi Tathlith fault zone (Nabitah suture) would be the remnant of an intraoceanic plate boundary.

Najd faults are part of a major N.W.-trending left-lateral system that is characteristic of the northern part of the shield area (Brown, 1972). Najd faults are present only in the northeastern part of the gold belt (Fig. 2), although faults of indeterminate age, also with a N.W. trend, occur throughout the belt. Numerous quartz veins and mafic dikes of N.E. and east trend in the northern half of the belt are probably second- and third-order Najd-system faults (Hadley, 1976).

The Jabal Ishmas–Wadi Tathlith fault zone north of lat. 19° is readily traceable on the total intensity aeromagnetic maps of Andreasen and Petty (1973, 1974), as are the Najd-system faults. South of lat. 19° the zone is not reflected in the aeromagnetic data; however, a N.W.-trending fault that bifurcates to the southeast at this point is well delineated and probably represents the major deep-seated fault system. The lack of serpentinite, talc-carbonate, and ultramafic bodies along the South-trending segment of the zone, and their presence along the S.E.-trending segment, also supports this concept.

GOLD DEPOSITS

The ancient gold mines along the Jabal Ishmas–Wadi Tathlith fault zone are all within or close to greenstone sequences composed of greenschist-facies metavolcanic and meta-volcanisclastic rocks. No ancient gold mines have been found in rocks of higher metamorphic grade, and gneissic rocks contain only two small gold localities, although quartz veins are common in both terrains. The gold deposits are mostly within or adjacent to quartz veins, quartz-rich breccia zones, or zones of quartz stringers; thus genetically gold is intimately related to quartz. The quartz veins are banded, vuggy, open fracture fillings along second- or third-order faults of the Jabal Ishmas–Wadi Tathlith fault zone. The main faults contain only minor stringer zones and boudinaged veins. Deposits range from single, banded and brecciated veins, approximately 1 m in width and 50 m in length, to sheared and altered zones containing several quartz lenses, pods, breccias, and stringer zones in an area as much as 600 m in length and 80 m in width. Only a small percentage of the quartz veins exposed in the belt contain gold; most are barren of native precious metals and sulfides.

Gold occurs as discrete scattered flakes within quartz, as fine films along fractures in quartz, as flakes in small irregular vugs, and as small specks next to or within chlorite, pyrite, or chalcopyrite. Gold is also present in the weathered selvage zones of veins within stringers, pods, and masses of hematite or limonite. The nature of the gold in unweathered selvage zones is not known.

The deposits can be placed into five geographic groups, each of which contains deposits of a similar type (Fig. 2A). Group I takes up most of the northern part of the belt and contains approximately half of the known deposits within the belt. The veins of group I are at the intersection of major faults of the Najd system with the Jabal Ishmas–Wadi Tathlith fault zone, and a few of the gold-bearing veins may be in third-order faults of the Najd system. However, most of the gold-bearing veins are cut by Najd faults and by barren quartz veins along Najd faults, and thus predate Najd faulting.

The occurrences are in quartz and quartz-rich breccia veins that trend N.E. and slightly west of north that are cut by later N.- and N.W.-trending barren quartz veins. Calcite and chalcedonic quartz are common vein minerals and sulfides are minor constituents. In three of the deposits quartz veins are intimately associated with felsic dikes, but most are part of regional vein systems and show no relationship to intrusive igneous activity. Ancient placer workings are common in the large wadis and flats surrounding several of the deposits in this group (Schmidt *et al.*, unpub. data).

Group II deposits include the two that have the highest potential for future development (Worl, in press). One deposit is in a large lens of altered and sheared quartz porphyry that contains abundant pods and stringers of quartz; the other is in major regional quartz veins that cut gabbro and greenstone. The rest of the deposits in this group are in short, discontinuous veins and pods in and around gabbro bodies. This group of deposits is aligned East–West across the trend of the main fault zone, and is at the intersection of the Jabal Ishmas–Wadi Tathlith fault zone with a N.W.-trending system of faults, which may have localized the deposits.

Group III deposits (Fig. 2) are associated with felsic dikes, and most are beneath flat-lying bodies of serpentinite. Many gold-bearing zones are along a veined and altered contact between an overlying serpentinite and an underlying hornblende schist, and some lie along or extend out from felsic dikes several tens of meters below this contact. Sulfides of lead, zinc, and iron occur locally. The felsic dikes are related to a granodiorite to quartz monzonite igneous event dated by U–Pb methods on zircon at 660 ± 12 Ma (Cooper *et al.*, 1979).

Deposits in group IV are small discontinuous pods and veins of quartz in faults, or scattered within or next to gabbro masses. Only a small percentage of the quartz veins contain native gold or sulfide minerals. All of these deposits are in second- or third-order faults of the Jabal Ishmas–Wadi Tathlith fault zone rather than along main fault segments.

Deposits of group V are in shear zones in quartz veins, quartz pods, and stockworks of quartz stringers that show no spatial relationship to intrusive igneous rocks. Copper, zinc, and iron sulfides are common and locally abundant constituents of the gold deposits, and pyrite is common throughout the shear zones. Two of the deposits are in zones that at present are exploration targets for massive sulfide deposits of copper and zinc.

DISCUSSION

The Jabal Ishmas–Wadi Tathlith gold belt coincides with a major North-South fault system and a belt of metavolcanic and metasedimentary rocks. The gold-bearing quartz veins are largely confined to metavolcanic and metasedimentary rocks of greenschist facies and are spatially related to the main fault system. Such an association is typical of gold deposits of this type in other Precambrian shield areas of the world (Anhaeusser, 1976, p. 30; Goodwin and Ridler, 1977, p. 154). The genesis of the gold in the Jabal Ishmas–Wadi Tathlith gold belt was probably intimately tied to the tectonic and metamorphic history of the belt.

The gold deposits are spatially related to the fault system. Although none of the deposits occurs in major fractures, the fault system was probably a controlling factor in localizing deposition. Movement along the fault system developed the tensional (dilational) second- and third-order fractures that were the loci of deposition of gold and quartz from hydrothermal solutions. The active fault system may have also been a major factor in the localizing of intrusive activity, a possible mechanism for mobilization and transportation of some of the gold.

Known deposits in the gold belt are classified as hydrothermal and epigenetic, but possibly other, mainly syngenetic types, are present. The fact that all the deposits are hydrothermal and occur within zones of metavolcanic and metasedimentary rocks belonging to the greenschist facies is an important exploration guide. The ultimate source of the gold that was transported and deposited in the hydrothermal systems is also important. It has been suggested that the conditions of middle or upper greenschist facies of regional metamorphism constitute and optimum thermal zone wherein gold tends to concentrate preferentially (Anhaeusser, 1976, p. 32). According to this concept, gold from various sources would tend to migrate to the regime of greenschist metamorphism and to be concentrated and deposited there; thus the source of the gold may have been outside the present boundaries of the greenschist belts. Possible sources might be zones of higher metamorphic grade such as anatectic zones, gneiss domes, and mobile tectonic belts. Perhaps, however, the gold was derived from source beds within the rocks that were themselves undergoing greenschist facies metamorphism. Such gold deposits would have stratigraphic relationships similar to those of the gold-bearing deposits in the Abitibi orogenic belt in the Canadian Shield (Goodwin and Ridler, 1977, p. 155). The gold in the quartz veins in those deposits is thought to have been slightly remobilized from relatively local source beds. Possible types of source rocks are numerous: massive sulfide bodies, volcanic ironstones, quartzitic clastic rocks, and porphyritic subvolcanic intrusives and flows of felsic composition. All these rocks are present in the Jabal Ishmas–Wadi Tathlith gold belt, but are untested as probable sources of the gold.

Each of the five geographic groups of deposits in the gold belt (Fig. 2) contains deposits that are typical of that group and probably related genetically. Intergroup comparison of the characteristics of the gold deposits suggests that there are many significant differences in the genesis and ages of deposits among the groups. Some deposits in group I are in rocks assigned to the Murdama group (Schmidt, unpub. data) and some seem to be related to mafic dikes emplaced in Najd faults and are thus younger than 550 Ma. Deposits in group III can be related to a 660 ± Ma intrusive event, but those in groups II, IV, and V are not dated.

Deposits in group I seem to be largely related to regional metamorphism, although in three of the deposits, including one of the larger ones, the gold was transported by and deposited from hydrothermal solutions of quartz monzonitic to granitic derivation. The source of the gold is unknown. The group II deposits may be the result of remobilization and transportation of gold by any system such as felsic or mafic igneous activity or regional metamorphism that generated heat and fluids. Samples collected from this group have higher concentrations of Fe, Zr, Pb, and Ti as compared to the other groups, and gold shows a positive correlation with Pb. The element concentrations and associations may reflect the association of many of the veins with gabbros in this group. Group III deposits may be the result of gold being transported by and deposited from hydrothermal solutions related to the emplacement of quartz monzonite stocks. The serpentinite may have been an impervious cap that dammed gold-bearing solutions, or it may have acted as a chemical reactant or catalyst that promoted deposition of the gold. The source of the gold for this group could have been the ultramafic bodies, now serpentinite, or the relatively abundant black shales, both of which were in contact with the magma and ore-forming solutions. The greater abundance of Cr and Ni in samples from this group, and the correlation of Au with Fe and Ti reflects the association of gold with magnetite in the altered serpentinite. Gold in group V deposits is probably related to massive sulfide deposits in the area, and the quartz veins are material remobilized along shear zones during regional metamorphism. The great abundance of Pb and Cu in samples from this group, and the positive correlation of gold with the same two elements, support the concept that the gold is associated with the base-metal sulfide deposits. Group IV deposits may have a similar origin, but sulfide-rich beds are not known in that area and the ultimate source of the gold is unknown. The greater abundance of copper in samples from this group suggests an association of gold with base metal sulfides, although there is no obvious correlation of gold with the base metals.

Potential gold resourses in these deposits are limited. A majority of the deposits are estimated to contain less than 50,000 tonnes of ore and 12 are estimated to contain 50,000 to 400,000 tonnes of ore at average grades ranging from 7 g/t to 32 g/t (Worl, in press).

Although only gold quartz vein deposits that are obviously hydrothermal are known from the gold belt, a potential exists for gold in other types of environments. Massive sulfide deposits, volcanic ironstones, quartzitic clastic rocks, and porphyritic subvolcanic intrusives and flows of selsic composition are all present within the belt and are all favorable exploration targets for gold deposits.

ACKNOWLEDGMENTS

The Jabal Ishmas–Wadi Tathlith gold belt was investigated in accordance with an agreement between the U.S. Geological Survey (USGS) and the Ministry of Petroleum and Mineral Resources, Kingdom of Saudi Arabia. The wholehearted support of the Directorate General of Mineral Resources (DGMR) of Saudi Arabia is acknowledged. I also wish to thank my colleagues at the DGMR and USGS Mission for discussions, access to unpublished data, and critical comments on the manuscript.

REFERENCES

ANHAEUSSER, C. R. 1976. Archean metallogeny in South Africa. *Econ. Geology*, 71, 16–43.

ANDREASEN, G. E., and PETTY, A. J. 1973. Total intensity aeromagnetic map of the southern Najd quadrangle and part of the Tuwayq quadrangle, Kingdom of Sauid Arabia. *Saudi Arabian Dir. Gen. Mineral Resources Geol. Map* GM-13, scale 1:100,000.

ANDREASEN, G. E., and PETTY, A. J. 1974. Total intensity aeromagnetic map of the Tihamat Ash Sham quadrangle and part of the Asir quadrangle, Kingdom of Saudi Arabia. *Saudi Arabian Dir. Gen. Mineral Resources Geol. Map* GM-14, scale 1:100,000.

BROWN, G. F. 1972. Tectonic map of the Arabian Peninsula. *Saudi Arabian Dir. Gen. Mineral Resources Arabian Peninsula Map* AP-2, scale 1:4,000,000.

BROWN, G. F., and JACKSON, R. O. 1959. Geologic map of the Asir quadrangle, Kingdom of Saudi Arabia. *U.S. Geol. Survey Misc. Geol. Inv. Map.* I-217A, scale 1:500,000.

COOPER, J. A., STACEY, J. S., STOESER, D. G., and FLECK, R. J. 1979. An evaluation of the zircon method of isotope dating in the southern Arabian Shield. *U.S. Geol. Survey Saudi Arabian Project Rept.* 257, 32 pp.

FRISCH, W., and AL-SHANTI, A. 1977. Ophiolite belts and the collision of island arcs in the Arabian Shield. *Tectonophysics*, 43, 293–306.

GONZALEZ, L. 1974. Geology of the Ishmas quadrangle, Kingdom of Saudi Arabia. *U.S. Geol. Survey Saudi Arabian Project Rept.* 186, 34 pp.

GOODWIN, A. M., and RIDLER, R. H. 1977. The Abitibi orogenic belt. pp. 138–165 in *The Archean: Search For The Beginning* (ed. MCCALL, G. J. H.). Halsted, New York.

GREENWOOD, W. R. 1979a. Geology of the Kradrah quadrangle, sheet 19/42D, Kingdom of Saudi Arabia. *Saudi Arabian Dir. Gen. Mineral Resources Geol. Map* GM-38, scale 1:100,000.

GREENWOOD, W. R. 1979b. Geology of the Malahah quadrangle, sheet 18/43D, Kingdom of Saudi Arabia. *Saudi*

Arabian Dir. Gen. Mineral Resources Geol. Map GM-39, scale 1:100,000.

GREENWOOD, W. R., ROBERTS, R. J. and BAGDADY, Abdulaziz 1974. Mineral belts in western Saudi Arabia. *U.S. Geol. Survey Saudi Arabian Project Rept.* 177, 26 pp.; Arab Conference on Mineral Resources, 2nd 1974, Jiddah, Saudi Arabia, Conf. Doc. Background papers, Misc., 130–151.

GREENWOOD, W. R., HADLEY, D. G., ANDERSON, R. E., FLECK, R. J., and SCHMIDT, D. L. 1975. Later Proterozoic cratonization in southwestern Saudi Arabia. *U.S. Geol. Survey Saudi Arabian Project Rept.* 196, 23 pp.; *Royal Soc. London Phil. Trans. A*, 280, 517–527.

HADLEY, D. G., 1976. Geology of the Bir Juqjuq quadrangle, sheet 21/43D, Kingdom of Saudi Arabia. *Saudi Arabian Dir. Gen. Mineral Resources Geol. Map* GM-26, scale 1:100,000.

JACKSON, R. O., BOGUE, R. G., BROWN, G. F., and GIERHART, R. D. 1963. Geologic map of the southern Najd quadrangle, Kingdom of Saudi Arabia. *U.S. Geol. Survey Misc. Geol. Inv. Map* I-211A, scale 1:500,000.

MOORE, J. M. 1976. A major lineament in the Arabian Shield and its relationship to mineralization. *Mineral. Deposita*, 11, 323–328.

OVERSTREET, W. C. 1978. A geological and geochemical reconnaissance of the Tathlith one-degree quadrangle, sheet 19/43, Kingdom of Saudi Arabia. *U.S. Geol. Survey Saudi Arabian Project rept.* 230, 132 pp.

SCHMIDT, D. L., HADLEY, D. G., and STOESER, D. B. 1978. Latest Proterozoic crustal history in the southern Najd Province, central Saudi Arabia. *U.S. Geol. Survey Saudi Arabian Project rept.* 251, 44 pp.

WORL, R. G. (197!) The Jabal Ishmas–Wadi Tathlith gold belt, Kingdom of Saudi Arabia. *U.S. Geol. Survey Saudi Arabian Project Rept.* (in press)

التشتت الكيميائى الأرضى (الجيوكيميائى) الأولى والثانوى
لعناصر الايتريوم والإيتيربيوم والنيوبيوم واللانثانوم
فى الجرانيت والمترسبات الطمية فى وادى بارود –
الصحراء الشرقية – مصر

م.م. حسان و م.أ. قاعود

الخلاصة

اكتشفت تسلسلات تشتت ثانوية لعناصر الايتريوم والايتيربيوم والنيوبيوم واللانثانوم فى مالئات وادى بارود الطمية حيث تظهر صخور الجرانيت الوردى والرمادى والبيروكسينيت. وتدل دراسة التشتت الأولى على أن الجرانيت الوردى يتميز بمحتويات عالية من الإيتريوم والإيتيربيوم والنيوبيوم واللانثانوم، بينما تختفى هذه العناصر جوهريا فى طرز الصخور الأخرى. وعلى هذا فإن تكون الهالات والتسلسلات الثانوية يرتبط بتجوية صخور الجرانيت الوردى. تشير التحاليل المعدنية والطيفية لأربع كسرات من الجرانيت الوردى المتفتت الى الإغناء النسبى للإيتريوم والنيوبيوم واللانثانوم فى الكسرة – ٢ر٠مم حيث يتركز الفلوريت ويوجد الفرجوسونيت.

وفى هذه الهالات والتسلسلات درس التشتت الثانوى بالتحاليل المعدنية والطيفية وحجم التحبب لأربع عشرة عينة تمثل المترسبات الموضعية النشأة وبعيدتها. هذا ويندر الفرجوسونيت بينما يتركز الفلوريت من ١ الى ٩٪ ومن ٤ر٠ الى ٨٪ فى المترسبات الموضعية النشأة وبعيدتها على التوالى. كما تسود الميكا فى كلا الطرزين من المترسبات. وتتركز العناصر النادرة تركيزا أعلى ما يكون فى الكسرة من –٢ر٠ مم الى +١ر٠ مم.

PRIMARY AND SECONDARY GEOCHEMICAL DISPERSION OF Y, Yb, Nb AND La IN THE GRANITES AND ALLUVIAL SEDIMENTS OF WADI BAROUD, EASTERN DESERT, EGYPT

MAHMOUD M. HASSAAN and MOHAMMED A. KAOUD

Al-Azhar University, Cairo, Egypt
Geological Survey of Egypt, Cairo, Egypt

Abstract—Secondary dispersion trains of Y, Yb, Nb and La were detected in Wadi Baroud alluvial fills where pink and grey granites and pyroxenites outcrop. Study of the primary dispersion indicates that pink granites are distinguished by relatively high contents of Y, Yb, Nb and La, whereas these elements are virtually absent in the other rock types. Consequently, the formation of the secondary halos and trains in the alluvium is related to the weathering of pink granites. Mineralogical and spectral analyses of four fractions of disintegrated pink granites point to the relative enrichment of Y, Nb, and La in the −0.2 mm fraction in which fluorite is concentrated and fergusonite is also present. The secondary dispersion in the dispersion halos and trains is studied by grain size, mineralogical and spectral analyses of 14 samples representing the autochthonous and allochthonous sediments. Fergusonite is rare whereas fluorite varies from 1 to 9 and 0.4 to 8% in the autochthonous and allochthonous sediments respectively. Mica is the predominant mineral in both types of sediments. The rare elements are highly concentrated in the −0.2 to +0.1 fraction.

INTRODUCTION

Safaga district was selected for regional geochemical prospecting for dispersion trains. Three dispersion trains of rare earths were revealed at the basin of Wadi Baround which is situated 35 km west of Safaga port on the Red Sea coast. The rocks which outcrop there are pink biotite granites, grey granitoids (granodiorites) and pyroxenites.

Pink biotite granites are composed of medium-grained potash feldspars (orthoclase and microcline), quartz, biotite and hornblende. Grey granitoids comprise fine-grained plagioclase, oligoclase, quartz, biotite, potash feldspars (orthoclase and rarely microcline) and some sphene and hornblende. Pyroxenites are composed of fine-grained pyroxene and some plagioclases and hornblende. Some granitic rocks are highly altered, and the feldspars are sericitized. Biotite is almost completely altered to chlorite and rarely to muscovite with the liberation of iron oxides along the cleavage planes.

The present work was carried out to study geochemical characteristics of the primary and secondary dispersion of Y, Yb, La and Nb in the rocks and the anomalous alluvial wadi fillings. For this purpose seven rock samples (six pink-grey granitoids and one pyroxenite) as well as 12 bulk samples representing the proluvial-alluvium (allochthonous) and eluvial-deluvium (autochthonous) detrital overburden were collected. The location of the rock samples is shown in Fig. 1.

PRIMARY GEOCHEMICAL DISPERSION

The mean average contents of Y, Yb, La and Nb in the pink granites, grey granitoid and pyroxenites are given in Table 1. From the table it is clear that pink granites are Y-, Yb-, Nb- and La-bearing but grey granitoids and pyroxenites are practically void of these elements. The distribution of elements in the different size fractions of pink granites is shown in Table 2. It shows that Y, Yb

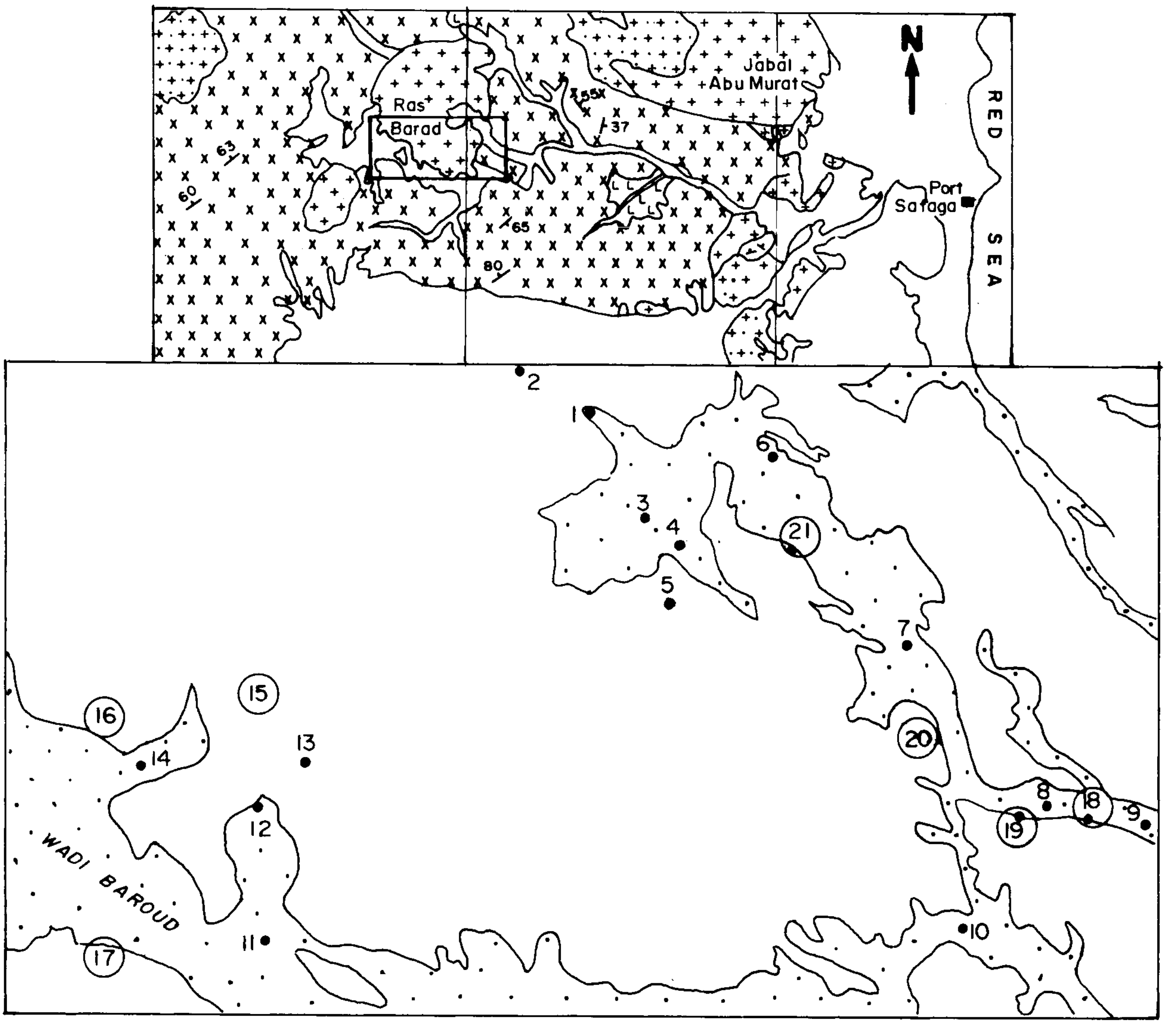

FIG. 1. Key map showing the location of samples.

TABLE 1. AVERAGE Y, Yb, La AND Nb CONTENTS (PPM) OF THE ROCKS OUTCROPPING IN THE WADI BAROUD AREA, EASTERN DESERT.

Rock type	Element			
	Y	Yb	La	Nb
Pink granite (3)*	0.02	0.002	0.022	0.015
Grey granite (3)	0.0015	0.0001	0.009	n.d.
Pyroxenite (1)	n.d.	0.0001	n.d.	n.d.

*Number of samples

TABLE 2. THE MEAN CONTENTS (PPM) OF Y, Yb, La AND Nb IN THE GRAIN SIZE FRACTIONS OF PINK GRANITES.

Fraction	Element			
	Y	Yb	La	Nb
−1 + 0.5 mm	160	15	200	140
−0.5 + 0.2 mm	200	20	180	170
−0.2 + 0.1 mm	200	16	220	150

and Nb are relatively concentrated in the −0.5 + 0.2 mm and −0.2 + 0.1 mm fractions while La is concentrated in the −1 + 0.5 mm and −0.2 + 0.1 mm fractions. The mineralogical examination of these two fractions shows that the −0.5 + 0.2 mm is concentrated in fluorite (10%), hematite (5 − 20%), fergusonite (5%) and monazite (3%). The −0.2 + 0.1 mm fraction is highly concentrated in fluorite (20%), zircon (5%) and relatively concentrated in hematite (7%) and monazite (5%).

SECONDARY GEOCHEMICAL DISPERSION

The detrital overburden in Wadi Baroud basin is represented by allochthonous (mainly proluvial-alluvium) and autochthonous (mainly deluvial–talus) debris. The autochthonous sediments cover the slopes of the basement rocks while the allochthonous sediments form the wadi fillings. The variations curves of the grain size fraction of the allochthonous and autochthonous debris are shown in Fig. 2. The variation curve of the granular composition of allochthonous debris is characterized by three high outputs. The peak output for the −5 + 3 mm and −2 + 1 mm grain-size fractions are those where the frequency percentages are 19.65 and 20.76 respectively. The next high output is that of the −0.5 + 0.2 mm fraction where the frequency equals 15.7%. The variation curve of the mechanical composition of the autochthonous debris shows a high similarity with that of the allochthonous debris. However, the autochthonous debris is distinguished by the relatively low outputs for the coarse grain size fractions and relatively high outputs for the −0.2 mm fraction.

As a rule the coarse grain sizes (more than 1 mm) are the product of physical weathering

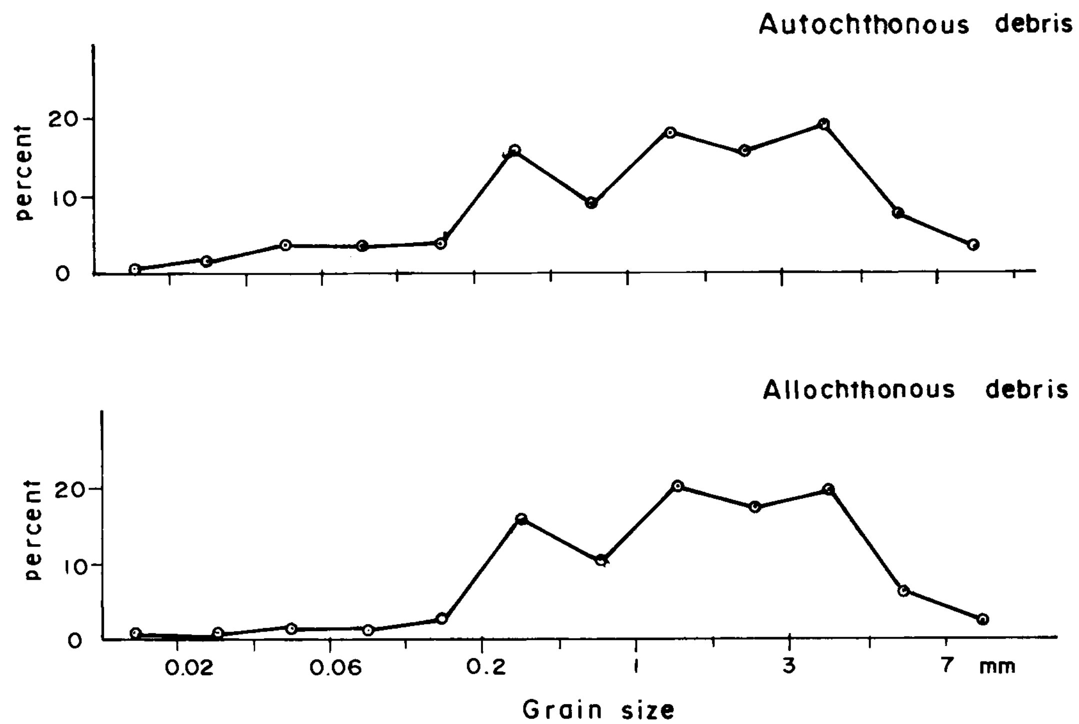

FIG. 2. Mechanical composition of the allochthonous and autochthonous detrital overburden.

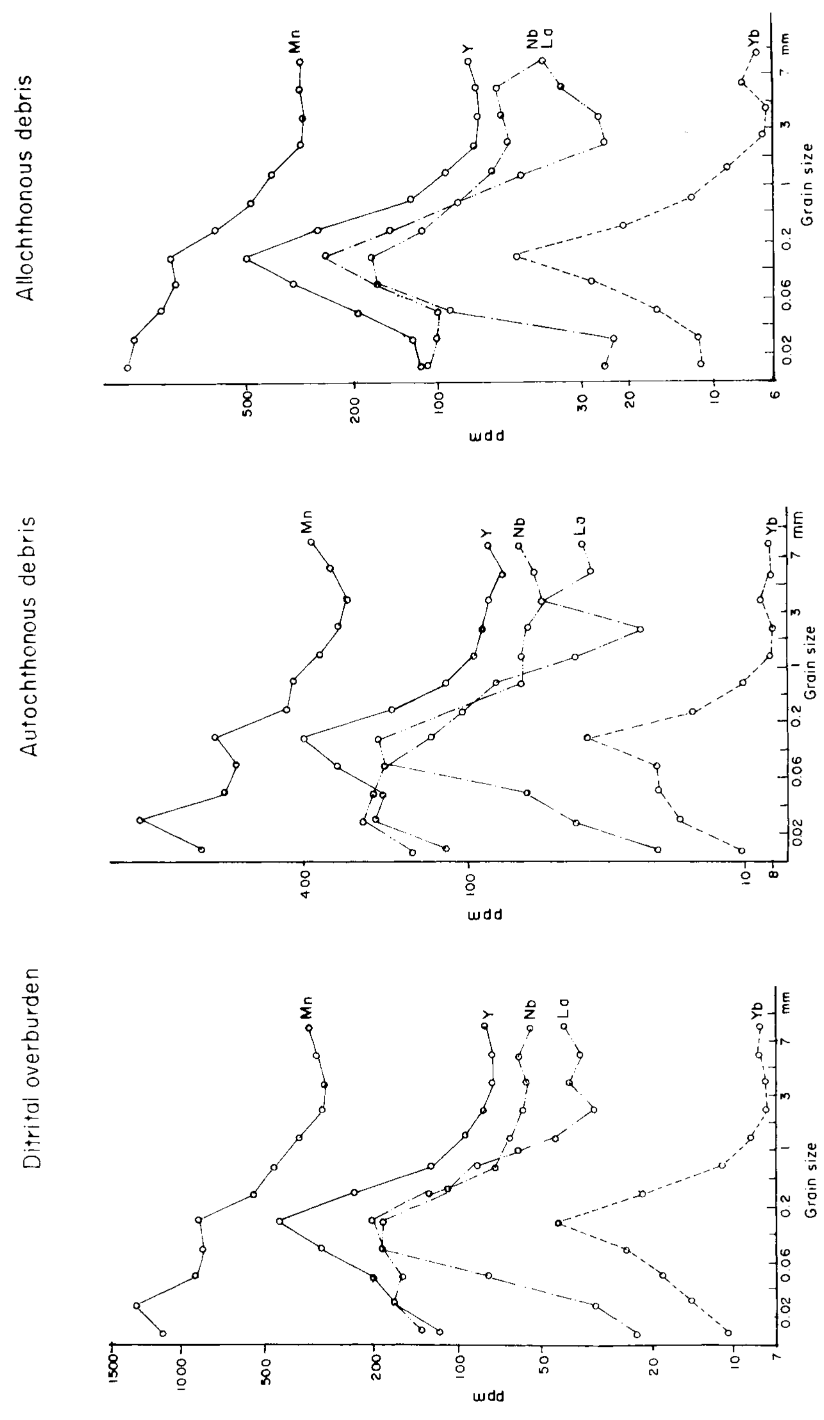

FIG. 3. Variation of Y, Yb, La, and Nb contents as related to the grain size of debris.

composed of stable minerals whereas the −0.5 + 0.2 mm and smaller fractions are mainly the products of chemical weathering. Fractions of larger than 0.5 mm are composed mainly of grains of primary and secondary minerals of the bedrock while the −0.1 m fraction is composed of 60–90% clayey minerals. The −0.5 + 0.01 mm fraction is composed mainly of the hydrous iron and manganese oxides (Kritsok and Kviatkovisky, 1966; Hassaan, 1974). The mineralogical composition of the different grain sizes confirms these rules. The grains larger than 1 mm are mainly composed of orthoclase (50%), quartz (40%), and the rest is albite and mica. In the −1.0 + 0.1 mm fractions, hematite, magnetite, hydrous manganese oxides and fluorite are relatively concentrated in the autochthonous detrital overburden. The allochthonous coarse grain sizes (more than 1 mm) are composed of feldspars (60–79%), quartz (30–40%), biotite and epidote. The grain sizes less than 1.0 mm are enriched in magnetite, hematite, ilmenite and fluorite. Ferugusonite and monazite are rare (0.2 and 0.3% respectively) in the heavy minerals of the grain size fractions between −1.0 + 0.1 mm, while fluorite and hematite are relatively concentrated (0.4–9%, 1–11.5% respectively).

The mean contents of the Y, Yb, La and Nb in the grain sizes of the detrital overburden as well as in the allochthonous and autochthonous types are plotted in Fig. 3. The variation curves of the mean contents of Y, Yb, La and Nb in the autochthonous grain sizes bear close resemblance, where La and Yb as well as Y and Nb curves follow each other. The highest content of Y (400 ppm) and Yb (37 ppm) is present in the −0.2 + 0.1 mm grain size, while La is concentrated (220 ppm) in the −0.2 + 0.063 mm grain size and Nb is concentrated (200 ppm) in the −0.1 + 0.063 mm grain size.

The distribution curves in the various allochthonous grain sizes show that both Nb and Yb as well as Y and La are highly similar to each other. Y, Yb and Nb (500, 50, and 270 ppm respectively) are highly concentrated in the −0.2 + 0.1 mm grain size whereas La (440 ppm) is highly concentrated in the −2.0 + 0.063 mm grain size fractions.

Therefore, the data of this work seem to suggest that Y, Yb, La and Nb are relatively enriched in the pink granites of the Eastern Desert and that they are rare in the grey granitoids and the pyroxenites. The enrichment of Y, Yb, La and Nb in the pink granites is related to fergusonite, monazite and fluorite. Chemical weathering plays a dominant role in the secondary geochemical dispersion of these elements where they are absorbed on the hydrous iron and manganese oxides as well as on the clay minerals. Mechanical weathering plays a remarkable role in the secondary dispersion in the form of fluorite, fergusonite and monazite. Finally, it is suggested that the most effective grain sizes to be analyzed during lithogeochemical prospecting for Y, Yb, La and Nb in the Eastern Desert of Egypt are the −0.5 + 0.063 mm fractions.

REFERENCES

HASSAAN, M. M. 1974. Litokhimetshickie Metodi cvintsovotsinkovikh mestorojdenia v vostotoshnoi Postine, Egipt. *Unpubl. Ph.D. thesis.* Leningrad Mining Institute, Leningrad.

KRITSOK, I. N., and KVIATKOVISKY, E. M. 1966. Raspredeleni metallov V razlitshnikh Klassakh i fraktsiakh dilovialnikh oreolov mestorojdenii vostotshnovo Zabeikelia. *Zap. L.G.I.*, T. 51, B. 2, pp 51–61.

اجتيــــاز جرانيـــت الدرع العربيــــة

ع.ع.نصيف و أ.ج.جـــاس

الخلاصــــة

اقترحت الدراسات السابقة أن النشاط القطرى فى أواخر ماقبل الكمبرى فى الدرع العربية ارتبط بواحد أو أكثر من نطق بينوف القديمة المائلة نحو الشرق. والدراسات التحليلية التمهيدية لصخور جرانيتية عمرها ألف مليون سنة جمعت فى اجتياز شرق – غرب عبر الامتداد تدل على وجود اثنين أو أربعة من نطق الاندساس الأولية الحياة (البروتيرزووية) الشرقية الميل.

ARABIAN SHIELD GRANITE TRAVERSE

A. O. NASSEEF and I. G. GASS

King Abdulaziz University, Jeddah, Saudi Arabia
Open University, Milton Keynes, England

Abstract—Previous studies have suggested that late Precambrian magmatic activity in the Arabian Shield was related to one or more easterly inclined fossil Benioff zones. Preliminary analytical studies of ca. 1000 Ma granitic rocks collected on an East-West cross-strike traverse indicate the presence of two, or possibly four, easterly inclined Proterozoic subduction zones.

INTRODUCTION

Kennedy (1964) proposed the term "Pan African tectono-thermal event" for the processes which affected much of Africa between 650–450 Ma ago but which showed no signs of having involved classic, continental collision, orogenesis. More recently, several proposals explain the evolution of the Pan African in N.E. Africa and the Arabian Shield by the formation and progressive cratonization of Proterozoic intra-oceanic island arcs (Greenwood *et al.*, 1976; Garson and Shalaby, 1976; Greenwood and Brown, 1973; also, Bakor *et al.*, 1976; Neary *et al.*, 1976; Al-Shanti and Mitchell, 1976).

The extensive use of Rb–Sr dating (Garson and Shalaby, 1976; Fleck *et al.*, 1976; Neary *et al.*, 1976), has increased the Pan-African time span to 1100-450 Ma within which, in south-western Saudi Arabia, Greenwood *et al.* (1976) identify three episodes of volcanism and plutonism with attendant sedimentary, tectonic and metamorphic activity. In all episodes the sediments are primarily immature volcanoclastic deposits seemingly related to the emergence of volcanic island arcs. The presence of these arcs is supported by the volcanic rocks which range from older, low-K tholeiitic basalts through basaltic andesites and andesites to dacites and rhyodacites. The plutonic rocks are mainly diorites, granodiorites and granites of calc-alkali affinity. In the Egyptian eastern desert calc-alkali granites are associated with porphyry copper mineralization, whereas Kuroko-type ore bodies occur within the volcanic and volcanoclastic products (Garson and Shalaby 1976).

Greenwood and Brown (1973), on the basis of limited $K_2O : K_2O + Na_2O$ trends and the increasing abundance north-eastwards of more silicic plutonics, postulated the existence of a single north-easterly inclined Proterozoic Benioff zone beneath Arabia. This proposal may have to be modified as some of the ultramafic bodies which extend in zones north-westwards across NE Africa and Arabia have been identified as ophiolites and may represent obducted fragments of Proterozoic oceanic lithosphere (Bakor *et al.*, 1976; Garson and Shalaby 1976; see also Fig. 5 in Bakor *et al.*, 1976).

If the ophiolite identification is correct, then it seems likely that the Arabian Shield could consist of three separate arcs whose boundaries are indicated approximately by the ultramafic (ophiolite) zones. It is seemingly well established that there is a progressive compositional variation of both plutonic and volcanic rocks with depth to an underlying Benioff zone (Dickinson, 1970; Hatherton and Dickinson, 1969; Hutchinson, 1976; Palacious and Oyarzun, 1975). Therefore, the two models for the Arabian Shield could be tested by collecting specimens of similar rock type and age along a traverse normal to the regional north-westerly structural trend which also cuts the three proposed ophiolite zones at near right angles. A preliminary traverse was made early in 1976 and the initial results and provisional and tentative interpretations are presented below.

THE GRANITE TRAVERSE

Greenwood *et al.* (1976) proposed that the cratonization of the Arabian Shield occurred in three major episodes, the dividing dates (based on isotopic dating of associated plutonic rocks) being 550 and 960 Ma. The granite–granodiorites of the oldest episode were identified as being most appropriate for collection. They crop out extensively across the shield, are clearly identified in the 1:2,000,000 Geological Map of Arabia (Brown, 1963) under the symbols 'gg' and 'gn', and are estimated as being ca. 1000 Ma old. Also, by selecting the older granites, the possibility of sampling the products of later within-plate magmatism (Neary *et al.*, 1976) would be avoided.

Field Relations

Fortuitously, the longest, across-strike traverse of the Arabian Shield follows closely the line of the main Jeddah–Riyad highway. Collections were made along this highway, mainly from road cuttings, although excursions to the south were necessary to maintain a reasonably regular sample interval. Regular sampling was possible along the 100 km section between Jeddah and At-Taif (see Fig. 1) as the road rises from the narrow coastal plain and climbs the 2000 m west-facing escarpment to the town of At-Taif. East of At-Taif, the highest point of the traverse, the land surface is an extensive, extremely mature, gently inclined Mesozoic peneplane in which the rock outcrop is sparse and much of the section is covered by recent lavas, blown sands and outwash deposits. Between At Taif and the eastern edge of the basement outcrop, a distance of 600 km, specimens were taken, wherever possible, from road cuts, but mainly from wide separated inselbergs.

In collecting specimens only three basic requirements were adhered to, namely, that

i) the outcrop fell within the older ca. 1000 Ma 'gg' and 'gn' areas as marked on the 1:2,000,000 geological map (Brown, 1963);
ii) specimens were fresh and showed no signs of alteration; and
iii) specimens contained free quartz and had a low color index (ca. 10–15).

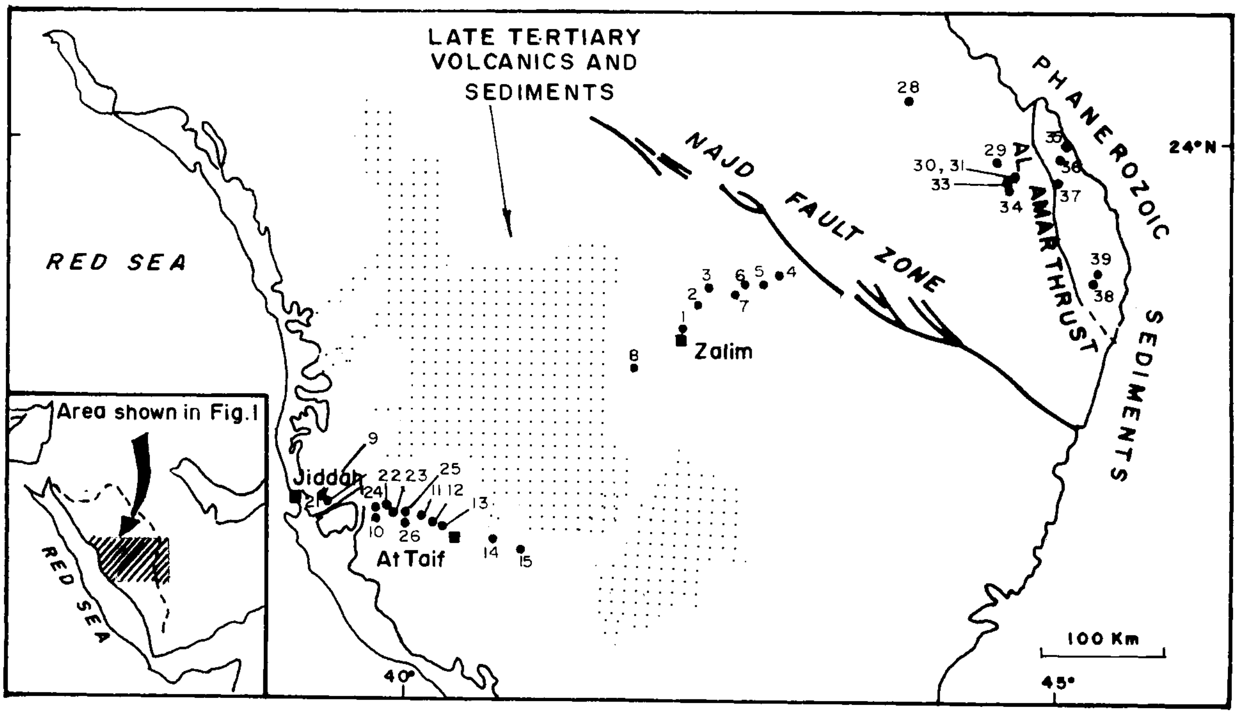

FIG. 1. Specimen location and main structural features along collection traverse.

Petrography

Detailed petrographic descriptions will be presented elsewhere. The results of the modal analyses of the 39 samples selected for chemical analyses are given in Tables 1, 2 and 3, and plotted on a Streckeisen diagram (Fig. 2). The analyses were carried out on stained sections to facilitate point counting. Figure 2 shows that the samples range mainly from quartz diorite through granodiorite to common granites. This variation range can be observed in the two western traverses whereas in the eastern traverse a distinction can be made between samples collected east of Al-Amar fault (mainly quartz diorites) and those west of the fault (common granites). Another feature to be noted is the abundance of quartz diorite and granodiorite among samples of the western traverse, contrary to those of central and eastern traverses which are dominated by the common granites. Common granites completely disappear, however, to the east of Al-Amar fault.

Texturally these granites range from medium-grained, allotriomorphic to mildly porphyritic types. Occasional specimens show well developed fluxion texture and some display incipient gneissosity.

The main rock-forming minerals are quartz, potash feldspars (mainly perthitic) and calcic oligoclase, with minor amounts of micas and am-

TABLE 1. MODAL ANALYSIS OF GRANITIC ROCKS OF THE CENTRAL TRAVERSE.

Sample No.	Quartz	K-feldspar	Plagioclase	Mica	Hornblende	Opaques & accessories	Total
2	26	57	9	7	—	1	100
3	26	55	9	7	1	2	100
4	10	60	12	4	10	4	100
5	35	43	18	3	—	1	100
6	26	56	8	7	1	2	100
7	43	19	26	7	—	2	100
8	33	27	38	1	—	1	100

TABLE 2. MODAL ANALYSIS OF GRANITIC ROCKS OF THE WESTERN TRAVERSE.

Sample No.	Quartz	K-feldspar	Plagioclase	Mica	Hornblende	Opaques & accessories	Total
9	38	31	20	7	2	2	100
10	30	15	45	9	—	1	100
11	10	3	65	17	4	1	100
13	25	12	55	6	1	1	100
14	20	35	28	9	4	4	100
15	22	33	30	8	2	5	100
21	18	22	36	3	15	6	100
22	30	9	44	3	9	5	100
23	24	13	51	4	5	3	100
24	27	11	48	6	6	2	100
25	18	9	53	10	5	5	100
26	23	2	51	6	14	4	100

TABLE 3. MODAL ANALYSIS OF GRANITIC ROCKS OF THE EASTERN TRAVERSE.

Sample No.	Quartz	K-feldspar	Plagioclase	Mica	Hornblende	Opaque & accessories	Total
29	35	38	16	8	—	3	100
30	35	40	13	10	—	2	100
31	30	40	15	12	—	3	100
32	30	48	12	8	—	2	100
33	27	43	16	12	—	2	100
34	26	41	17	13	—	3	100
35	29	3	57	8	—	3	100
36	31	7	49	12	—	1	100
38	13	5	61	—	19	2	100
39	25	18	44	10	—	3	100

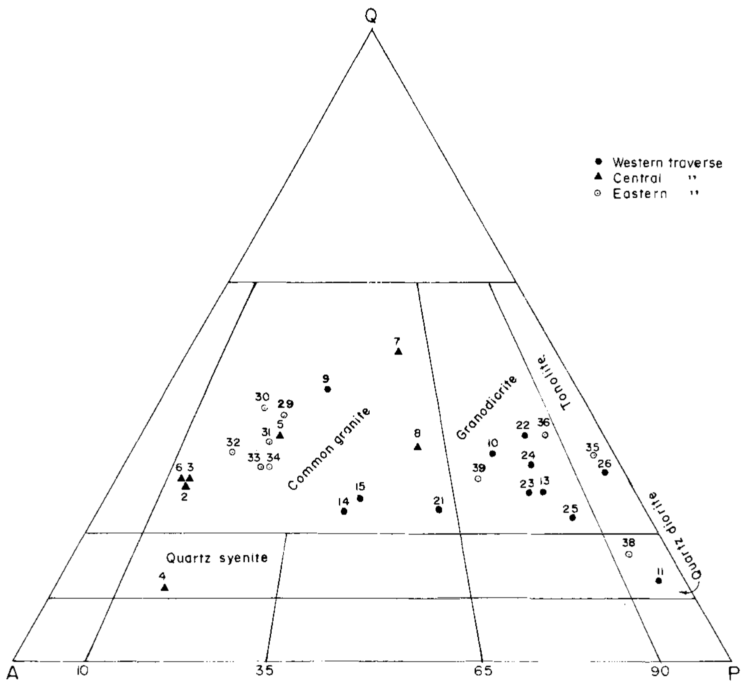

FIG. 2. Streckeisen diagram showing the compositional range of the studied granite rocks.

phiboles; opaque ores, sphene, zircon and apatite are common accessories.

Geochemistry

Thirty nine specimens were chosen for major oxide and selected trace element (Rb, Sr, Nb, Y) analysis. Of these, nine were analysed by INAA methods for rare earth abundances. As with the petrography, the detailed geochemistry will be presented elsewhere, but data relevant to the two models proposed and, in particular, the Nb, K_2O, Sr content and the $K_2O:K_2O+Na_2O$ ratio are discussed briefly.

Pearce and Gale (1977), plotting igneous rocks from known tectonic regimes in the current plate tectonic cycle, have shown that granites overlying island arc or cordillera subduction zones are markedly depleted in Nb (commonly <15 ppm), whereas "hot spot" continental granites are markedly enriched (>100 ppm) in this element. Twenty five of the 39 specimens analysed have Nb contents of less than 15 ppm and those that are higher (up to 39 ppm) are the most fractionated, showing highest Rb/Sr and lowest Zr/Nb ratios.

Several workers (Dickinson, 1970; Hatherton and Dickinson, 1969; Hutchinson, 1976; Palacious and Oyarzun, 1975) have demonstrated, using different oxides and elements, the systematic geochemical variation of igneous rocks with depth to an underlying Benioff zone. Although the tendency is for K_2O, Rb and Sr to increase with depth to the Benioff zone, this is usually applicable only for rocks which have a similar SiO_2 content. Indeed, any rigorous multiple linear regression analysis, such as the quantitative study of active Indonesian arcs by Hutchinson (1976), necessitates the allocation of correlation coefficients to SiO_2 and the element or oxide under consideration.

The SiO_2 contents of the specimens collected in this study range, for most specimens, between 68 and 75%. However, as silica shows no well defined linear trend along the traverse, the calculation of silica-nomalized oxide or element values would be meaningless. Hence, although K_2O and Sr show vague trends, the most realistic plot is probably $K_2O:K_2O+Na_2O$ (Fig. 3). This ratio, used by Greenwood and Brown (1973), not only identifies the increase in an incompatible element (K) but, in the absence of SiO_2 control, moderates it with an oxide (Na_2O) that should theoretically remain constant, irrespective of generation depth.

DISCUSSION

The purpose of the traverse was to decide whether or not there are compositional trends that may or may not be related to one or more palaeo-Benioff zones. It is directly relevant to note, therefore, that there are two traverse sections, between 25–155 km and 300–440 km, where K_2O values and $K_2O:K_2O+Na_2O$ ratios increase eastwards (see Fig. 3). Sr shows a general easterly decrease over these sections but the trend is

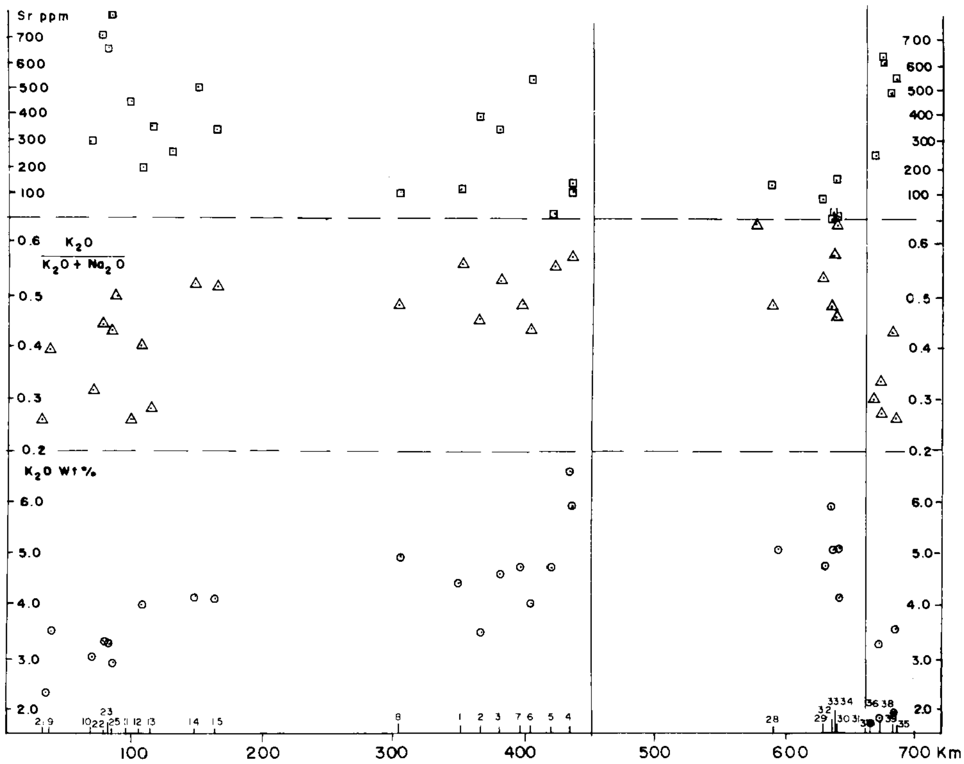

FIG. 3. Sr, $K_2O:K_2O+Na_2O$, and K_2O values plotted against position along traverse (see Fig. 1).

poorly defined (see Fig. 3). This may be attributed to the complex geochemistry of Sr caused by its dual substitution for Ca and K (Turkian and Kulp 1956). Rb, when plotted, showed no systematic variation. At the eastern end of the traverse, between 600–700 km, there are two clusters of K_2O and $K_2O:K_2O+Na_2O$ values, high to the west and low to the east of the Al-Amar thrust. Although no trend can be discerned in either case, the values suggest that the granite rocks to the west of the thrust have a deeper origin than those to the east. This is supported by the rare-earth data which, on chrondrite-normalized plots of the western rocks, show strongly fractionated patterns depleted in heavy rare earths, indicative of eclogite fractionation at depths greater than 100 km (Ringwood, 1974). This proposal is also in keeping with the known structure of the area; Al-Shanti and Mitchell (1976) convincingly identify the Al-Amar thrust as the surface trace of an easterly inclined Proterozoic subduction zone between two "continental" masses.

The absence of analytical data between 440–600 km is entirely due to the lack of granitic outcrops along or near the line of traverse. Granites are the main rock type to the east of the Najd fault and alkali values imply the existence of an underlying, easterly inclined Proterozoic Benioff zone. The termination of the main granite outcrop at the Najd fault zone and the occurrence of granites with the highest alkali values adjacent to it suggest that the zone is a major tectonic feature. The proposals of Brown and Coleman (1972) and of Bakor *et al.* (1976) that this is a faulted suture between once separate continental masses is consistent with the data presented here.

It will be noted from Fig. 3 that K_2O and $K_2O:K_2O+Na_2O$ values increase eastwards from 25–155 km. Any line drawn through these values, when projected eastwards, lies above the values for the 300–440 km section (see Fig. 3). The inference made here is that the two trends represent different subduction zones separated by yet another major tectonic feature. There is, however, no surface trace of this feature, the area being covered by late Tertiary basalts and Quaternary blown sands and outwash deposits. The tentative interpretation for the whole traverse is, therefore, that there are four easterly inclined Proterozoic (ca. 1000 Ma) subduction zones whose position is schematically depicted in Figure 4.

In an excercise of this kind the initial data often generate more caveats than conclusions and, although the tentative nature of the conclusions has been repeatedly emphasized, the caveats are clearer. There is need for far more extensive

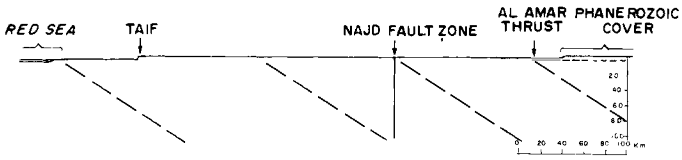

FIG. 4. Suggested position of fossil Benioff zones based on geochemical and structural data.

collections, more analytical data and the critical requirement of precise age control on all specimens analysed.

ACKNOWLEDGMENTS

We thank A. R. Bakor and N. Zohair for assistance and guidance in the field, R. M. Shackleton, A. Al-Shanti and S. A. Drury for useful discussion and P. J. Potts, A. Tindle and H. Ogden for analytical data.

REFERENCES

AL-SHANTI, A. M. S., and MITCHELL, A. H. G. 1976. Late Precambrian subduction and collision in the Al-Amar–Idsas region, Arabian Shield, Kingdom of Saudi Arabia. *Tectonophysics* 31, T41–T47.

BAKOR, A. R., GASS, I. G., and NEARY, C. R. 1976. Jabal Al Wask, Northwest Saudi Arabia: An Eocambrian back-arc ophiolite. *Earth Planet. Sci. Lett.* 30, 1–9.

BROWN, G. F. 1963. U.S. Geological Survey–Arabian American Oil Company (USGS–ARAMCO) Geological map of the Arabian Peninsula (scale 1:2,000,000). *U.S. Geol. Survey Misc. Geol. Inv. Map* 1-270A.

BROWN, G. F., and COLEMAN, R. G. 1972. The tectonic framework of the Arabian Peninsula. *24 Int. Geol. Congr. XXIV*, 1, 300.

DICKINSON, W. R. 1970. Relations of andesites, granites and derived sandstones to arc-trench tectonics. *Geophys. Space Phys. Rev.* 8, 813.

FLECK, R. J., COLEMAN, R. G., CORNWALL, H. R., GREENWOOD, W. R., HADLEY, D. G., PRINZ, W. C., RATTE, J. C., and SCHMIDT, D. L. 1976. Geochronology of the Arabian Shield, Western Saudi Arabia: K–Ar results. *Geol. Soc. Am. Bull.* 87, 9–21.

GARSON, M. S. and SHALABY, I. M. 1976. Precambrian–Lower Palaeozoic plate tectonics and metallogenesis in the Red Sea region. *Geol. Assoc. Canada. Sp. Paper* 14, 573.

GREENWOOD, W. R., and BROWN, G. F. 1973. Petrology and chemical analysis of selected plutonic rocks from the Arabian Shield, Kingdom of Saudi Arabia. *Saudi Arabian Dir. Gen. Mineral Resources Bull.* 9.

GREENWOOD, W. R., HADLEY, D. G., ANDERSON, R. E., FLECK, R. J., and SCHMIDT, D. C. 1976. Late Proterozoic cratonization in southwestern Saudi Arabia. *Phil. Trans. R. Soc. Lond.*, A280, 517–527.

HATHERTON, T. and DICKINSON, W. R. 1969. The relation between andesitic volcanism and seismicity in Indonesia, the lesser Antilles and other island arcs. *J. Geophys. Res.* 74, 5301.

HUTCHINSON, C. S. 1976. Indonesian active volcanic arc: K, Sr, and Rb variation with depth to the Benioff zone. *Geology* 4, 407.

KENNEDY, W. Q. 1964. The structural differentiation of the Pan-African (±500 m.y.) tectonic episode. *Ann. Rep. Inst. Afr. Geol.*, Leeds University, 8, 48.

NEARY, C. R., GASS, I. G., and CAVANAGH, B. 1976. Granitic association of northeastern Sudan. *Geol. Soc. Am. Bull.* 87, 1501.

PALACIOUS, C. M., and OYARZUN, R. M. 1975. Relationship between depth to Benioff zone and K and Sr concentrations in volcanic rocks of Chile. *Geology* 3, 595.

PEARCE, J. A., and GALE, G. H. 1977. Identification of ore deposition environment from trace element geochemistry. *Geol. Soc. Lond. Sp. Publ.* 7, 14–24.

RINGWOOD, A. E. 1974. The petrological evolution of island arc system. *J. Geol. Soc. Lond.* 130, 183.

TURKIAN, K. A., and KULP, J. L. 1956. Geochemistry of Strontium. *Geochim. & Cosmochim. Acta* 10, 245–296.

طباقية الصخور فى منطقة أم سميوكى
الصحراء الشرقية ـ مصر

ن.م. شكرى و م.ص. منصور

الخلاصة

كشف العمل الحالى فى منطقة أم سميوكى على أن المترسبات القديمة الزرق أرضية تتكون أساسا من بلاجيوكلاز الأمفيبوليت ونسب ثانوية من ستات كلوريت ـ أكتينوليت وكلوريت ـ تريموليت ورخام دولوميت .

أما البركانيات الزورق أرضية فتتمايز إلى بركانيات الشيخ شادلى المتحولة وصحبة البرامية الأحدث منها . وبركانيات شادلى القديمة أكبر عمرا من بركانيات الدخان ، تدخلت فيها طرز من الجرانيت مختلفة ،وتتمايز بركانيات شادلى طباقيا الى أربع وحدات متتابعة يزيد سمكها على ١٠ كم ويمكن رسمها فى خريطة . والفيوض الطبقية تكون معظمها تحت الماء ولكن لاتوجد لها فوهات ظاهرة . وتتكون هذه البركانيات من صخور الأنديزيت المتحولة (٥ر٤٢٪) والريوليت (٥ر٣٢٪) والبازلت العادى (٥ر٦٪) وفتاتيات نارية متنوعة .

LITHOSTRATIGRAPHY OF UM SAMUIKI DISTRICT, EASTERN DESERT, EGYPT

N. M. SHUKRI and M. SABER MANSOUR

U.N. Adviser, Economic Committee of Africa, Nairobi, Kenya
Geological Survey of Egypt, Cairo, Egypt

Abstract—The Um Samuiki district (1540 km^2) is covered successively by Precambrian geosynclinal metasediments and Shadli metavolcanic flows that were intruded by serpentinites and meta-gabbros, then by biotite and hornblende syn–tectonic granitoids followed by the late- to post-tectonic muscovite granites. The metasediments (2.5 km thick) are represented mainly by plagioclase amphibolites with minor chlorite–actinolite schists and dolomite marbles. The Shadli metavolcanics, stratigraphically divided into four mappable units exceeding 10 km in thickness, are made up of pillow andesites (42.5%), rhyolites (32.5%), basalts (6.5%) and andesitic–rhyolitic volcanoclastics (mainly pyroclastics).

INTRODUCTION

The Um Samuiki district in the Eastern Desert of Egypt (Fig. 1) covers an area of 1540 km^2 and lies between lat. 24° 40′ and 24° 26′ N and long. 34° 37′ and 35° 00′ E; it forms parts of the Sheikh Shadli topographic sheet (scale 1:100,000). It is rough mountainous country with many peaks rising to over 1200 m, of which Jabal Abu Hamamid (1745 m) is the most prominent. The district is disected by Wadi Huluz with its southern Samiuki and Hilgit tributaries, and the big Wadi Abu Hamamid that gives rise to Wadi El-Sheikh, Wadi El-Maqal and Wadi Marasan.

Ball (1912) published a geological map (scale 1:750,000) showing the district as schists and granites only, and described the Wadi Huluz–Jabal Abu Hamamid and Jabal Hamata area as "crushed volcanics, basalts, felsites, and associated hornblende schists". Barthoux (1922) described some conglomerates from Wadi El-Sheikh as belonging to the Hammamat Series, but volcanic pebbles

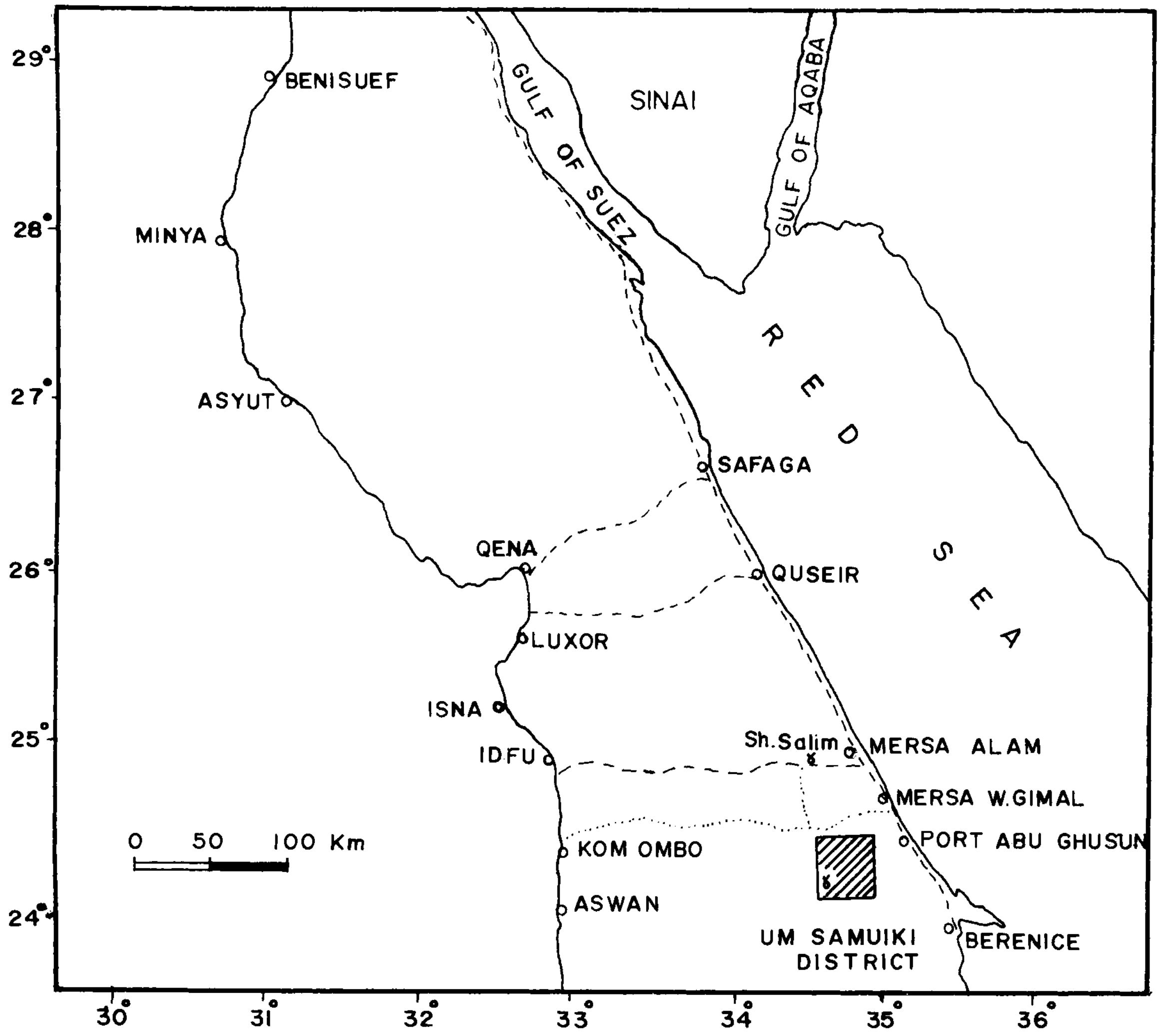

FIG. 1. Location map showing the studied area.

were not described. Hume (1934, 1935) regarded the district as made up of schists and dolerite, basalt, purplish porphyries, rhyolites and tuffs, and ascribed them to the Shadli Series. El-Shazly (1957; El Shazly and Afia, 1958) stated that the Shadli Series is mainly formed of intermediate and basic volcanics, volcanic agglomerates and tuffs. Akaad and El-Ramly (1960) differentiated an unmetamorphosed old volcanic series (Dokhan type) from an older metavolcanic series (Shadli type) of upper Precambrian age. Hunting (1967) stated that the metasediments are related mainly to the greenschist facies and locally pass into the amphibolite facies. In the Abu Hamamid volcanic assemblage, the acid volcanics appear subordinate, the intermediate are most prominent, and basic rocks ubiquitous. Akaad and Noweir (1969) grouped the geosynclinal metasediments and metavolcanics together as the Abu Ziran Group; they deduced that the metasediments were, at least in part, contemporaneous with the metavolcanics. Said (1971) showed the Shadli Series on the geological map of Egypt as "Shadli Geosynclinal Metavolcanics". El-Ramly (1972) mentioned that the metavolcanics are closely associated with the greenschist facies metasediments, interdigitating or alternating with them; he added that the metavolcanics are represented by regionally metamorphosed rhyolites, dacites, andesites, basalts and pyroclastics. Sabet (1972) agreed with El-Ramly's conceptions regarding the nature and composition of the metavolcanics, but considered the grade of regional metamorphism to range between the greenschist and almandine amphibolite facies. Ghanem *et al.* (1973) described the metavolcanic rocks north of lat. 26° 40′ N as essentially metabasic lavas and tuffs; the acid to intermediate varieties and thin related pyroclastics are present as sills interbedded with and intruding the metasediments. Searle *et al.* (1976) divided the Wadi Um Samuiki volcanics into older unmetamorphosed, massive, basic and intermediate lavas with subordinate rhyolites and rhyolitic volcanoclastics, and the younger Hamamid Group of basal basaltic pillow lavas, rhyolites, and beds of breccia, banded tuffs, and cherts.

During the present study, a structural geological map at a scale of 1:40,000 was prepared from the aerial photographs and then reduced to 1:100,000 (Plate I). Following Akaad and El-Ramly (1960) and El-Ramly (1972), the geological sequence of the basement rocks of the district began with the deposition of a geosynclinal sedimentary series, unconformably overlain by a thick pile of cyclic submarine volcanic flows (the Shadli Series) and bedded volcanoclastics. Peridotites and gabbros were injected directly after the main phase of geosynclinal filling. All the above mentioned rocks were subjected to medium-grade regional metamorphism. In the present work, the Shadli Metavolcanics are considered older than the Dokhan Volcanics; they are a major source of the metamorphosed volcanic pebbles recorded in the later Hammamat sediments. Four granite types were then intruded. The oldest was the white, gneissose biotite granite (Abyad granite) followed by the hornblende granite, both of which granitized the meta-gabbros into gneissose diorites, diorites and granodiorites. The pink biotite granite and the muscovite granites were emplaced later. The last phase of igneous activity is represented by various dykes and sills.

STRATIGRAPHY

Geosynclinal Metasediments

These form an elongated belt trending W.N.W.–E.S.E. parallel to the regional foliation and bedding planes. The maximum thickness of the metasediments is about 2.5 km, and the rocks commonly dip 20°–60° southwestwards. They have been slightly affected by regional metamorphism of greenschist and albite–epidote–amphibolite facies; but certain types are metamorphosed to low amphibolite facies. The rocks are well bedded, show characteristic sedimentary features such as graded bedding and repetition bedding, and vary from fissile schists to massive gneissic varieties. A representative section, 1750 m thick, was measured, and is shown in Plate II, the geological units (as in the other columns) are represented as horizontal, though they are really inclined.

The carbonate rocks (originally argillaceous limestones and dolomites) are represented by amphibolites (89.5%), chlorite–actinolite schists and chlorite–tremolite schists (4.7%), and massive or schistose hematitic dolomite marbles (1.3%). The amphibolites are either porphyroblastic (about 63%) with oriented metacrysts; or non-porphyroblastic foliated (26%) or non-foliated (11%) varieties. The arenaceous rocks (originally shaly arkoses) are multicoloured, sometimes laminated, and are represented by a variety of garnetiferous mica–quartz schists.

Shadli Metavolcanics

The Shadli Metavolcanics (> 10 km thick) can be differentiated into four mappable units. Beginning with the youngest, they are the Hamamid Metavolcanics (avg. thickness 2.6 km); Burrad Metavolcanics (>2.8 km thick); Huluz Metavolcanics (>3.5 km thick); and Marasan Metavolcanics (> 1.6 km thick).

The Marasan Metavolcanics, commonly recorded in anticlines, are characterized by the presence of thick felsic rhyolites at the top, and banded rhyolites and tuffs overlying thick amygdaloidal andesites at the base. The rhyolitic flows (49%) and andesitic and basaltic pillow lavas (51%) make up practically the entire succession; tuffs and other rocks occurring in negligible amounts (Plate II).

The Huluz Metavolcanics are characterized by the rhythmic alternation of rhyolites and andesitic and basaltic lava flows interrupted by relatively few volcanoclastic beds and later gabbroid sills. Thick, microcrystalline rhyolite flows (specific for the Huluz unit) occur at the top and similar felsitic flows occur at the base. However, variations within the Huluz unit are sometimes seen, e.g., in the El-Anguria area where only andesitic and basaltic pillow lavas occur; in the Wadi Hilgit section (Plate I) basaltic rocks are absent.

The Burrad Metavolcanics outcrop mainly on both sides of the Hamamid unit as homogeneous, massive, thick, meta-andesitic vesicular pillow lavas, sometimes associated with a few andesitic agglomerates and tuffs. The Hamamid Metavolcanics occur in a syncline which is fault bounded. They are distinguished by the predominance of thick, banded volcanoclastic beds mainly of andesitic nature (40%), andesite flows (32%), rhyolites (18%) and prominent gabbroic intrusions (10%).

In terms of their lithology, the Shadli Metavolcanics are made up of rhyolites (32.5%), andesites (42.5%), basalts (6.5%), and volcanoclastic rocks (15%).

Serpentinite and Meta-gabbro–Diorite Complex

Blackish serpentinite occurs as a 15 m thick sill just under a meta-gabbroid cap in a tributary from Wadi Marasan to the east, within the Shadli flows. Meta-gabbros (epidiorites) are present as intrusive laccoliths and sills in the metasediments and metavolcanics, and bear the imprint of epidote–amphibolite facies metamorphism. The meta-gabbro–diorite complex as well as the Abyad and hornblende granites contain abundant xenoliths of varying sizes showing different degrees of assimilation.

STRUCTURE

The metasediments and metavolcanics lie in a W.N.W.–E.S.E. trending synclinorium flanked by two large anticlinoriums. This is the Jabal Hamamid synclinorium. An angular unconformity separates the metasediments and the overlying Huluz Metavolcanics on the southern limb of the northern anticlinorium, and the pink biotite granite mass along Wadi Huluz is intruded along the unconformity. The Jabal Hamamid synclinorium (Fig. 2) is made up of the Um Samuiki syncline; the Abu Hamamid syncline; the Um Hasidok anticline, all of which trend W.N.W.–E.S.E.; and the Wadi Hilgit Lil Huluz anticline which trends East–West.

The Um Samuiki syncline, about 15 km long, and 5 km wide is formed mainly of Burrad meta-andesites. Dips on the northern flank are 15–20° to the S.W., and those on the south are 40–50° to the N.E. The Abu Hamamid asymmetric syncline is the most prominent. Dips on the southern limb commence at about 40° but become steeper towards the axis; the southern limb is nearly vertical. The syncline is downfaulted between two faults giving rise to a graben-type structure, about 35 km long and 10 km wide. The downthrow of the faults is probably more than 1500 m (Syagaev, 1959). The syncline contains the Hamamid Metavolcanics; it passes southward into a monocline, formed successively of the rocks of Burrad and Huluz units which dip northward at 30–70°, forming the northern limb of the southern anticlinorium.

The Um Hasidok anticline is located east of the Um Samuiki and Abu Hamamid synclines extending from Jabal Hasidok to Jabal Hamata. Its core consists of Marasan flows, while on the flanks and on the pericline are the Huluz metavolcanic rocks. The Wadi Hilgit Lil Huluz anticline is a small horst-anticline block where the Marasan rocks have been raised relative to the younger blocks on either side. Its length along these oldest rocks is 8 km and the width is up to 3 km. Towards the north are the Huluz flows which form a monocline dipping at 30–45° S.W. The following fault systems are present in the area: (1) strike-slip faults trending W.N.W.–E.S.E. parallel to the main folds and showing intense shearing; (2) younger perpendicular faults trending N.E.–S.W.; and (3) N.W.–S.E. faults sometimes swinging to North–South which are more or less parallel to the Red Sea, and seem to be the oldest.

PETROGRAPHY

Geosynclinal Metasediments

The metamorphosed carbonate rocks of these metasediments comprise amphibolite gneisses, chlorite–actinolite schists, chlorite–tremolite schists, and impure marbles. The amphibolites are either porphyroblastic or non-porphyroblastic, the porphyroblasts being plagioclase, hornblende or diopside. The metacrysts often lie at oblique angles to the foliation planes (Fig. 3). Plagioclase metacrysts are saussuritized and hornblende metacrysts are chloritized. Quartz grains up to 5.9 mm long are elongated parallel to the foliation. Amphibolites with hornblende porphyroblasts are widespread. Amphibolites with diopside metacrysts (3.4×3.2 mm diameter with hornblende inclusions) include a marked segregation into dark and light layers. The groundmass of the amphibolites contains zoisite, pistacite, piedmontite, diopside and bluish-green hornblende.

The impure marbles show a dense matrix of dolomite aggregates admixed with hematite and enclosing untwinned plagioclase grains, as well as some granular quartz, muscovite, diopside and chlorite. In some thin sections, muscovite and diopside are absent but a little biotite and tremolite are present.

The metamorphosed arenaceous rocks of the metasediments are: (a) porphyroblastic garnet – sericite – biotite – chlorite – plagioclase – epidote – quartz schists which occur in relatively thick green beds showing oriented crushed quartz and epidote augen (0.4×0.94 mm), with which are associated massive olive-green epidosites (epidote-quartz rocks) that occur as oriented nodules (40×15 cm); (b) laminated almandine – chlorite – sericitite – biotite – orthoclase – plagioclase – quartz schists of dark brown colour in which the lamination is produced by parallel mica folia and magnetite streaks; and (c) porphyroblastic garnet – biotite – muscovite – orthoclase – plagioclase – quartz schists of buff, grey colour, with eye-shaped grains of crushed quartz up to 2.5×0.5 mm in size, orthoclase and plagioclase metacrysts (average 0.7×0.4 mm), almandine garnet up to 2 mm in diameter, epidote, and a few chlorite shreds.

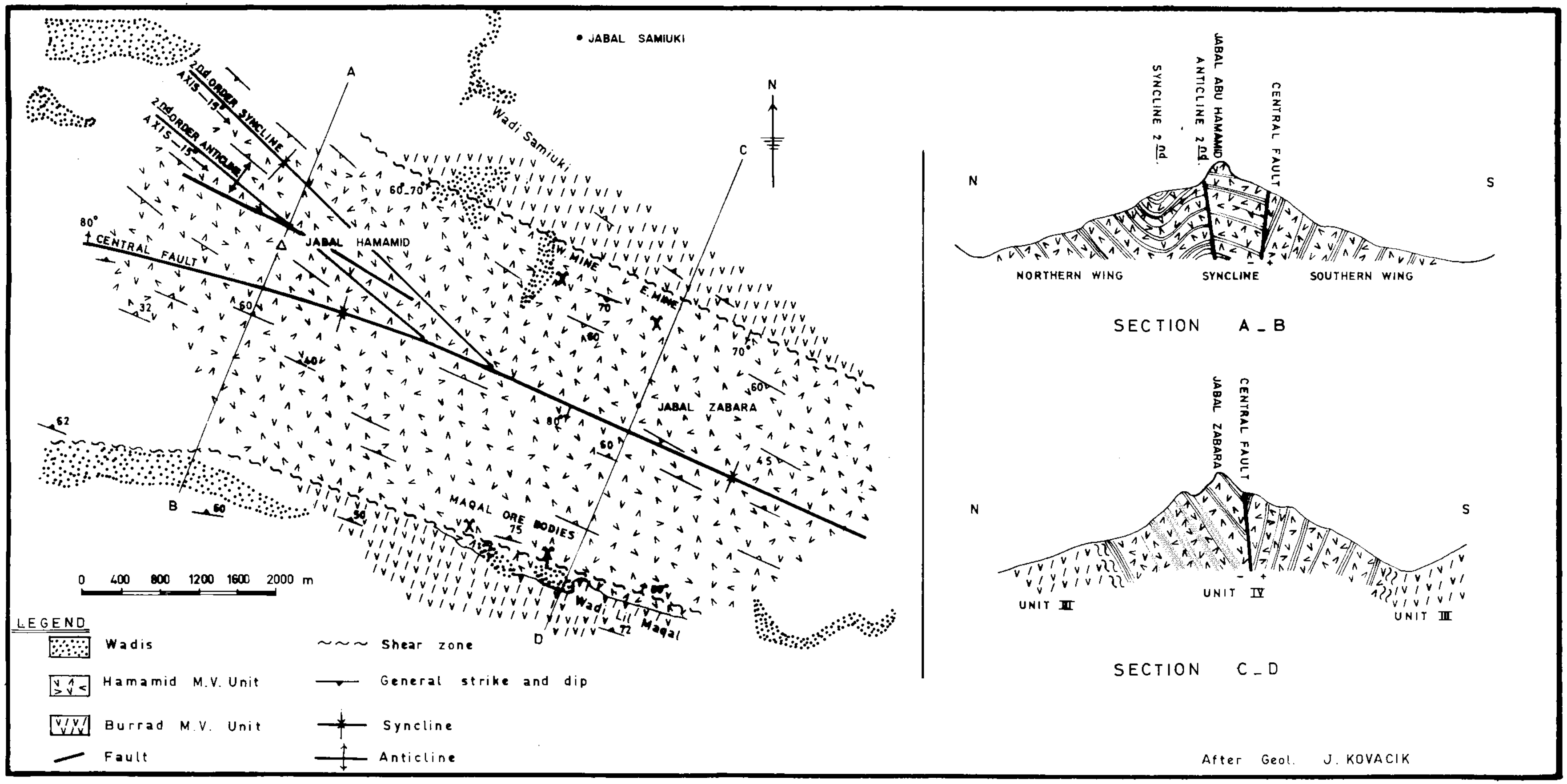

FIG. 2. Structural sketch map of the area.

FIG. 3. Photomicrograph of a porphyroblastic plagioclase amphibolite gneiss illustrating an augen-shaped hornblende metacryst. O.L., × 192.

Shadli Metavolcanics

These rocks comprise regionally metamorphosed porphyritic rhyolites, andesites, basalts and volcanoclastics. They are also altered, intense carbonatization, epidotization sometimes accompanied by chloritization, and silicification being obvious.

Rhyolites

These rocks are porphyritic and can be differentiated according to the texture of the groundmass into microcrystalline, cryptocrystalline, and glassy rhyolites. The microcrystalline rhyolites, confined to the Huluz unit, are characterized by glassy quartz and feldspar phenocrysts, and are foliated or unfoliated. The foliated types consist of oriented, embayed, cracked, crushed phenocrysts of strained quartz, altered sanidine, anorthoclase, and plagioclase which are augen-shaped or subrounded, set in a groundmass of quartz, feldspar crystallites or microlites, and biotite, chlorite, and sericite shreds. The mica shreds are grouped in parallel folia which are contorted and undulate around the phenocrysts (Fig. 4). They are sometimes granophyric, the groundmass being made of quartz and feldspar crystallites or microlites often intimately interwoven either in spherulite-like fashion or in micrographic texture. The glassy rhyolites have devitrified groundmasses sometimes with perlitic cracks.

Andesites

Phenocrysts in the andesites are either altered plagioclase or plagioclase and uralitized pigeonite, sometimes associated with hornblende, set in a vesicular, amygdaloidal, glassy, devitrified, rarely cryptocrystalline groundmass which shows typical hyalopilitic texture (Fig. 5). The groundmass also contains chlorite, epidote, zoisite, and andesine microlites (An_{33} to An_{41}). The groundmass of the Burrad andesites is relatively richer in femic minerals and the feldspar is more calcic.

Basalts

These are normal olivine-free basalts, vesicular or amygdaloidal, and porphyritic, in which the original ophitic, intersertal and intergranular textures are preserved. They can be differentiated into orthopyroxene (hypersthene) basalts and clinopyroxene basalts. The latter are more abundant, are foliated or non-foliated, and the phenocrysts are either plagioclase and pigeonite, or plagioclase set in a glassy groundmass of altered feldspar rods and microlites (An_{52-60}), granular uralitized pigeonite, chlorite, green hornblende, calcite, epidote, zoisite and iron oxides.

Volcanoclastic Rocks

These rocks are made of lithic and crystal fragments in a glassy or devitrified matrix (sometimes amygdaloidal), or cemented by a reddish, ferruginous paste. The lithic fragments and crys-

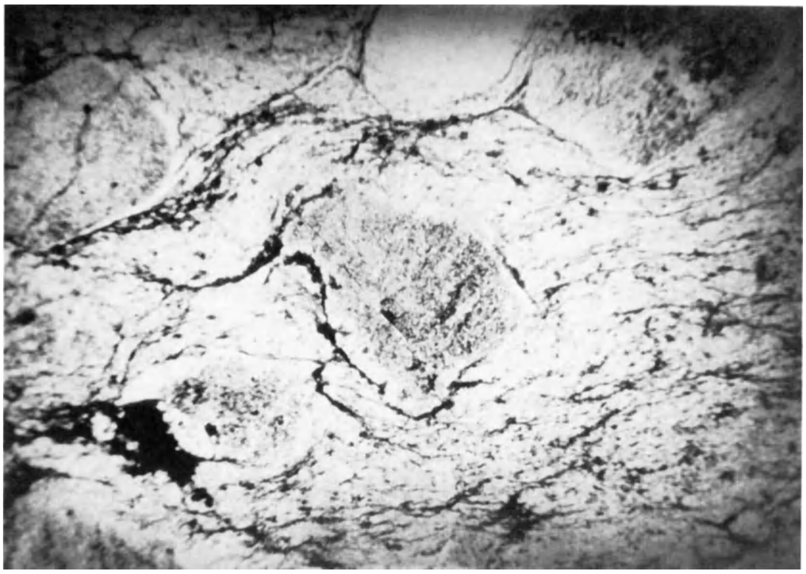

FIG. 4. Photomicrograph of foliated porphyritic microcrystalline rhyolite showing rotation of the metacrysts to lie concordant to flow during metamorphism. The parallel fine biotite flakes sweep round the metacrysts. O.L. × 90.

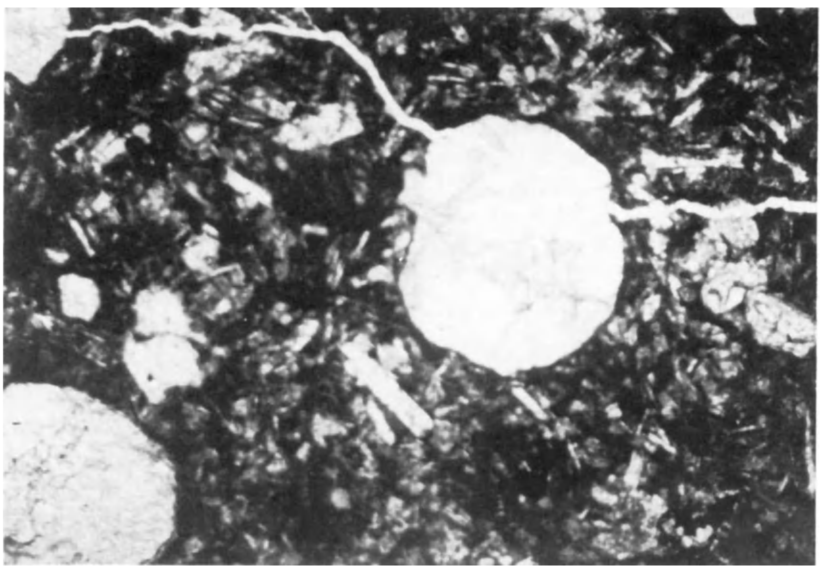

FIG. 5. Photomicrograph of Marasan meta-andesite characterized by condensed, united, subangular amygdales which are flattened and drawn out by the flowing of the lava. O.L., ×75.

tals are subangular and belong to the neighbouring lavas, and occur with minor pieces of reworked quartzose epiclasts and igneous rocks coming from greater depths. They may be scoriacous and show various fluxion phenomena including discontinuous flow lines (Fig. 6), parallel orientation of fragments, lamination and banding. Graded bedding is a common feature of the banded tuffs.

Serpentinites and Meta-gabbro–Diorite Complex

The meta-gabbros retain sub-ophitic, intersertal and poikilitic textures of the parent rocks. They are normally altered and consist of chloritized uralitic hornblende, epidote, zoisite, altered plagioclase, serpentine, iron oxides and sometimes quartz. The fresh rocks show albite-oligoclase,

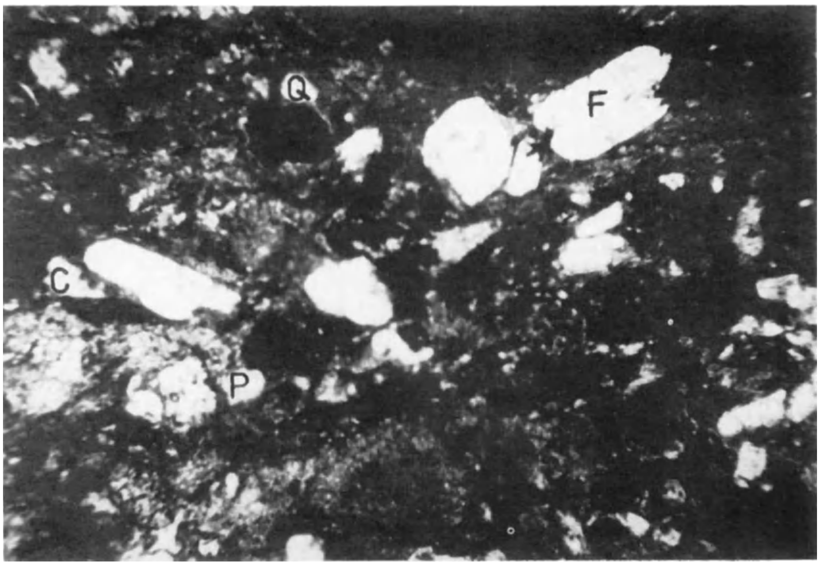

FIG. 6. Photomicrograph of a coarse andesitic vitric crystal lithic tuff consisting of oriented andesitic fragments and crystals of plagioclase (F), quartz (Q), calcite (C), pyroxene (P), set in vitreous matrix representing discontinuous flow. O.L., ×90.

augite relics in chloritized hornblende, and few serpentinized olivine grains. These meta-gabbros show the mineral assemblages diagnostic for the epidote-amphibolite facies of the medium-pressure type of regional metamorphism (Miyashiro, 1973).

The hybrid dioritic rocks are made up of saussuritized plagioclase, schillerized blue-green hornblende, plus interstitial quartz. The granodiorites consist of oligoclase, perthitic orthoclase, strained quartz, hornblende altered to brown biotite with release of magnetite and sphene, calcite, epidote, apatite, and almandine garnet.

The ultrabasic rocks are made of antigorite, crysotile, olivine, enstatite, zoisite and a little hypersthene; the zoisite is mostly after plagioclase. The rock can be regarded as a peridotite with a transition to norite.

CHEMISTRY OF THE SHADLI METAVOLCANICS

Nineteen samples representing the main types of Shadli Metavolcanics were chemically analysed. The results of these analyses are given in Tables 1, 2, and 3. The rocks show affinities with the generalized chemical composition of volcanic rocks given by Turner and Verhoogen (1951), and are compared with the values given by Nockolds (1954).

The rhyolites of the Huluz unit have a wider range of silica and higher content of XaO than those of the Marasan unit (Table 1). The rocks of both units have comparable alkali contents, but those of Huluz are slightly more potassic. The "average" alumina contents in both units are slightly different, those of Huluz being of lower alumina content; this may reflect the relative enrichment of quartz in Huluz rocks in accordance with the petrographic data. Generally, the Huluz rhyolites are of lower oxidation state where the ferrous iron predominates over ferric iron. The Huluz fine rhyolite tuff is more or less similar in composition to the rhyolites, with a slight increase in ferric and titanium oxides at the expense of silica. The average composition of the studied rhyolites is similar to that of the calc-alkalic rhyolites (sample A) of Nockolds (1954) but is distinguished by higher values of TiO_2, FeO, MnO, P_2O_5 and lesser amounts of K_2O. The chalcophile elements have higher values than those recorded by Rankama and Sahama (1950), pointing to the effect of later hydrothermal solutions.

A comparison of the Huluz with the Burrad meta-andesites (Table 2), shows that the former are more siliceous, sodic, and potassic whereas the latter are relatively enriched in ferromagnesian oxides, CaO and Ti. These differences are related to the mineralogical composition, the Huluz meta-andesites being more feldspathic with sodic feldspars, those of the Burrad unit being enriched in femic minerals with relatively higher Mg content and more calcic feldspars. Samples 13 and 14 belonging

TABLE 1. CHEMICAL ANALYSES OF THE META-RHYOLITIC FLOWS

	Huluz Unit								Marasan Unit		Nockolds†, (1954)		
Sample*	1	2	3	4	5	6	7	8	9	10	A	B	C
SiO_2	70.56	71.79	73.82	71.30	71.60	75.48	78.51	68.39	70.12	73.63	73.66	74.57	72.31
TiO_2	0.38	0.71	0.87	0.25	0.55	0.24	0.90	1.34	0.40	0.67	0.22	0.17	0.42
Al_2O_3	15.08	15.84	15.75	15.27	15.51	12.41	11.88	14.83	15.51	14.15	13.45	12.58	10.88
Fe_2O_3	0.89	1.76	1.99	1.16	0.89	0.33	1.37	4.89	2.08	4.22	1.25	1.30	2.98
FeO	6.41	2.68	1.45	7.64	3.08	6.41	2.09	1.92	4.61	2.52	0.75	1.02	2.42
MnO	0.39	0.74	0.84	0.04	0.35	0.60	0.71	0.53	0.61	0.24	0.03	0.05	0.14
MgO	—	traces	traces	traces	traces	traces	traces	traces	traces	traces	0.32	0.11	0.16
CaO	3.19	0.89	1.33	1.12	1.24	1.03	0.71	1.76	0.99	1.32	1.13	0.61	0.68
Na_2O	2.29	2.29	2.16	2.56	1.78	2.24	2.03	1.94	2.15	1.26	2.99	4.13	5.17
K_2O	0.36	1.88	0.72	0.29	1.40	0.43	0.84	0.89	0.82	traces	5.35	4.73	4.42
H_2O^+	0.27	0.32	0.23	0.28	0.26	0.26	0.35	0.52	0.21	0.67	0.78	0.66	0.45
P_2O_5	0.13	0.04	0.11	0.11	0.07	0.11	0.66	0.15	0.46	0.51	0.07	0.07	0.03
Pb	0.04	0.01	0.25	0.01	—	0.01	—	0.01	0.01	0.01	—	—	—
Cu	0.11	0.06	traces	0.04	0.11	0.01	0.09	0.41	0.06	0.03	—	—	—
Zn	0.01	0.22	traces	0.13	0.11	0.08	0.11	0.96	0.11	0.03	—	—	—
Cd	0.02	traces	—	0.04	—	0.02	—	0.01	0.01	—	—	—	—
S	0.06	0.03	0.06	0.04	0.22	0.07	0.05	0.05	0.12	0.09	—	—	—

*Samples 1 to 5: Porphyritic microcrystalline rhyolite; samples 6, 7, 9, 10: porphyritic fine rhyolite; sample 8: fine rhyolitic crystal lithic tuff.
†A: Calc-alkalic rhyolite and rhyolite obsidian; B: alkalic rhyolite and rhyolite obsidian; C: peralkalic rhyolite and rhyolite obsidian.

TABLE 2. CHEMICAL ANALYSES OF THE META-ANDESITES

	Burrad Unit	Huluz Unit			Nockolds (1954)
Sample	11	12	13	14	D
SiO_2*	52.11	55.55	62.83	59.83	54.20
TiO_2	1.40	1.02	0.96	0.90	1.31
Al_2O_3	15.01	15.15	7.57	11.79	17.17
Fe†	8.64	7.56	8.17	8.39	6.71
MnO	0.13	0.19	0.16	0.20	0.15
MgO	5.10	3.83	1.39	2.27	4.36
CaO	9.09	5.83	4.35	6.91	7.92
Na_2O	2.57	4.39	3.06	2.84	3.67
K_2O	0.24	0.45	1.22	0.84	1.11
P_2O_5	0.17	0.16	0.23	0.16	0.28

*The high SiO_2 is due to the relative increase of amygdales filled with quartz.
†Total iron.

TABLE 3. CHEMICAL ANALYSES OF THE META-CLINOPYROXENE BASALTS

	Marasan Unit		Huluz Unit			Nockolds* (1954)	
Sample	15	16	17	18	19	E	F
SiO_2	44.70	46.27	50.26	44.18	49.70	50.83	45.78
TiO_2	0.11	0.85	0.92	0.84	1.06	2.03	2.63
Al_2O_3	9.86	15.92	13.42	10.88	10.42	14.07	14.64
Fe†	8.84	7.74	7.89	9.28	10.34	9.07	9.00
MnO	0.10	0.17	0.13	0.11	1.13	0.18	0.20
MgO	6.02	8.52	4.66	6.53	4.54	6.34	9.39
CaO	11.92	11.05	9.03	15.43	11.42	10.42	10.74
Na_2O	1.88	1.49	2.97	2.31	3.06	2.23	2.63
K_2O	1.02	0.45	1.68	0.84	0.72	0.82	0.95
P_5O_5	0.78	0.10	0.22	0.13	0.54	0.23	0.39

*E: Tholeiitic basalt (and dolerite); F: normal alkalic basalt (and dolerite).
†Total iron.

to the Huluz unit are highly enriched in silica, due to relative increase of amygdales filled with quartz.

CONCLUSIONS

The Shadli Series is made up of repetitive flows of pillow andesite lavas, rhyolites, normal basalts, andesitic–rhyolitic volcanoclastics, and intrusive peridotite and gabbroid rocks. The ultrabasic and basic rocks as well as the host eugeosynclinal formations have undergone regional metamorphism at medium pressures, resulting in greenschist and albite–epidote–amphibolite facies rocks, with the development of amphibolite facies rocks in some instances. The metasediments are represented mainly by plagioclase–amphibolite gneisses (sometimes with diopside metacrysts), minor chlorite–actinolite schists and dolomite marbles. The psammites gave rise to garnetiferous mica–quartz schists, some of which contain orthoclase feldspar. The Shadli Metavolcanics usually preserve their original textures and identity although subjected to alteration and autoclastic phenomena. They may be of submarine origin, as indicated by the pillow lavas and graded bedding. These rocks are stratigraphically differentiated into four mappable units, and correspond to the main geocynclinal volcanics of Precambrian I (El-Shazly, 1964).

Syn-tectonic granitoids (such as the Abyad gneissose biotite granite) and the hornblende granite as well as the diorites, gneissose diorites and granodiorites appear to have originated during the synorogenic stages by transformation of previously existing gabbroid rocks. They were followed by the late- to post-tectonic pink biotite granite, and then by the muscovite granites. The last phase of igneous activity is represented by dykes and sills of early Palaeozoic age (El-Shazly, 1964), some of which belong to a later Cretaceous alkaline generation related to those of Wadi Natash.

REFERENCES

AKAAD, M. K., and EL-RAMLY, M. F. 1960. Geological history and classification of the basement rocks of the Central Eastern Desert of Egypt. *Geol. Surv. Egypt Paper* 9.

AKAAD, M. K., and NOWEIR, A. M. 1969. Lithostratigraphy of the Hammamat–Umm Seleimat district, Eastern Desert, Egypt. *Nature* 223, 284–285.

BALL, J. 1912. The geography and geology of South–Eastern Egypt. *Surv. of Egypt*, pp. 182–183, 273–283, 312–351.

BARTHOUX, J. C. 1922. Chronologie et description des roches ignees du Desert Arabique. *Mem. Inst. d'Egypte* V, Le Cairo, pp. 26–34, 160–162.

EL-RAMLY, M. F. 1972. A new geological map for the basement rocks in the Eastern and Southwestern Deserts of Egypt, scale 1:1,000,000. *Annals Geol. Surv. Egypt* II, 1–18.

EL-SHAZLY, E. M. 1957. Classification of Egyptian mineral deposits. *Egypt. J. Geol.* 1, 1–20.

EL-SHAZLY, E. M. 1964. On the classification of the Precambrian and other rocks of magmatic affiliation in Egypt. *Int. Geol. Congr.* XXII, Sec. 10.

EL-SHAZLY, E. M., and AFIA, M. S. 1958. Geology of Samiuki deposit, Eastern Desert. *Egypt. J. Geol.* 2, 25–42.

GHANEM, M., DARDIR, A. A., FRANCIS, M. H., ZALATA, A. A., and ABU ZEID, K. M. 1973. Basement rocks in Eastern Desert of Egypt north of latitude 26° 40′ N. *Annals Geol. Surv. Egypt* III, 33–38.

HUME, W. F. 1934. *Geology of Egypt.* Vol. II, Part I, Surv. of Egypt, 240–243.

HUME, W. F. 1935. *Geology of Egypt.* Vol. II, Part II, Surv. of Egypt.

HUNTING GEOLOGY AND GEOPHYSICS, 1967. Assessment of the mineral potentials of the Aswan Region, U.A.R. Photogeological Survey.

MIYASHIRO, A. 1973. *Metamorphism and Metamorphic Belts.* John Wiley, New York.

NOCKOLDS, S. R. 1954. Average chemical composition of some igneous rocks. *Geol. Soc. Am. Bull.* 65.

RANKAMA, K., and SAHAMA, TH. G. 1950. *Geochemistry.* University Press, Chicago.

SABET, A. H. 1972. On the stratigraphy of the basement rocks of Egypt. *Annals Geol. Surv. Egypt* II, 79–102.

SAID, R. 1971. Explanatory notes to accompany the Geol. Map of Egypt. *Geol. Surv. Egypt Paper* 56.

SEARLE, D. L., CARTER, G. S., and SHALABY, I. M. 1976. Mineral exploration at Um Samuiki. *Geol. Surv. Egypt.* Unpublished report.

SYAGAEV, N. 1959. Brief characteristics of the geological structure of Samuiki area, Eastern Desert. *Geol. Surv. Egypt.* Unpublished report.

TURNER, F. J., and VERHOOGEN, J. 1951. *Igneous and Metamorphic Petrology.* McGraw Hill, New York.

PLATE 1 AND 2. Lithostratigraphy of Um Samiuki. [In pocket at end of book.]

حزام چنيس فيران – سولاف ، جنوب غربى سيناء ، مصر

س . الجابى و أ . أحمد

الخلاصة

يبلغ عرض حزام چنيس فيران – سولاف من ٥ الى ١٠ كم ويمتد نحو ٤٠ كم فى اتجاه الشمال الغربى . وقد حدث التحول والتَّمَجْمُت خلال التجبُّل الرئيسى (أى الثانى) الذى شكل أساس الصحراء الشرقية وسيناء . وقد اختلفت الچنيسات فى تمجمتها . وقد قمنا هنا بمحاولة لاعادة بناء طبقيتها الصخرية .

ومن الناحية التركيبية فان الچنيسات تكوّن قبوين مزدوجى الغطس (قبو فيران الى الغرب ، وقبو سولاف الى الشرق) يمتدان شمال غرب – جنوب شرق ، وينفصلان بصدع دفع وجناح غربى مقلوب لقبْو ناقص يندفع فوق قبْوسولاف . وممال الطيات نحو الجنوب الغربى .

هذا ويضم قبو فيران متكوّنين : نيديا السمرا الرملىّ – الطينىّ السّفلى ، ومتكون عليات الطينىّ الكلسىّ العلوىّ . والمتكوّن السّفلى يتكون من الچنيسات الچرانيتية يحيطها چنيس بيوتيتى ، وچنيس بيوتيتى–هورنبلندىّ دقيقا التحبّب ويتمايز المتكون العلوى الى عضوين : العضو السفلى يتكون أساسا من چنيسات بيوتيتية–هورنبلنديّة متوسطة التحبب شريطية أو متجانسة . وهذا الأخير يحتوى بقعا من الچرانيتات المجماتيتية والچنيس الكروىّ . والعضو العلوى يتكوّن من چنيسات بيوتيتية – هورنبلنديّة دقيقة التحبّب متداخلة مع أشرطة دقيقة من الچنيس البيوتيتى وأحيانا مع الچارنت أو السلّيمانيت أو الكورديبريت .

أما قبو سولاف فيضم متكونين : السفلى وهو متكون خالى الطينى والكلس–طينىّ ، والعلوى وهو متكون أم تار الرملىّ . والجزء السفلىّ من متكون خالى يتركب من الچنيسات البيوتيتية والچنيسات البيوتيتية الهوربنلنديّة المتوسطة التحبب والتى تظهر محليا على هيئة چنيس أعْيُنىّ ، والجزء العلوى يتركب من چنيسات بيوتيتية دقيقة التحبب متبادلة فى أشرطة مع الچنيسات البيوتيتية الهورنبلدنية . ومتكون أم تار يتكون (من القاعدة الى القمة) من چنيس رملى ، وچرانوليتات كوارتزية فلسپاثية متوسطة التحبب ، مع تداخلات من الچنيس البيوتيتى الدقيق التحبب والچرانوليتات الكوارتزية الفلسپاثية الدقيقة التحبب .

ويكوّن متكوّن الشيخ الجناح الغربىّ من القبو المقلوب . ومن الناحية الطباقية فهو سفلى ، ويتركب من چنيسات بيوتيتية هورنبلندية غليظة التحبب وچنيسات هورنبلندية بيوتيتية متوسطة التحبب .

THE FEIRAN–SOLAF GNEISS BELT, S.W. OF SINAI, EGYPT

SAMIR EL-GABY and ABDEL-MOHSEN A. AHMED

Assiut University, Assiut, Egypt

Abstract—The Feiran–Solaf gneiss belt represents a thick sedimentary succession with minor basic magmatic intercalations that was folded into three anticlines separated by thrust faults and metamorphosed into gneisses and migmatites. The fold axes and thrust faults trend nearly N.W.–S.E.. The gneisses and migmatites are grouped into five formations. The western Feiran anticline comprises two formations: a lower semipelitic Nidia El-Samra Formation, and an upper calcareous-pelitic Aleiyat Formation. The central Solaf anticline also comprises two formations: and a lower pelitic and calcareous-pelitic El-Khali' Formation, and an upper arenaceous Um Tarr Formation. The calcareous-pelitic El-Sheikh Formation forms the western limb of an incomplete and overturned Sheik anticline thrust over the Solaf anticline from the east. The metasomatic changes which the paragneisses have suffered are also considered.

INTRODUCTION

The Feiran–Solaf gneiss belt lies in the southwestern part of Sinai, Egypt, stretching for about 40 km in a N.W.–S.E. direction, with Wadi Feiran and Wadi Solaf meandering in it (Fig. 1). It was delineated in the early reconnaissance surveys carried out by Hume (1906), Barron (1907) and Ball (1916). Schurmann (1966) studied the rocks within and around this gneiss belt and incorporated the results in a publication on the crystalline rocks on both sides of the Gulf of Suez. More recent studies on the Feiran–Solaf gneiss belt are presented by Akaad (1959), Akaad *et al.* (1967a,b) and El-Gaby (1967).

The Wadi Feiran area is an elongated belt of Precambrian gneisses, 36 km long by 5–10 km wide, intruded on both sides by a number of granitic plutons and dissected by a series of dyke swarms (Akaad *et al.*, in press). The intrusive rocks are treated in a separate publication (El-Gaby and Ahmed, in press). Field and microscopic studies suggest that the gneisses of the Feiran–Solaf gneiss belt were originally sediments, with only minor basic magmatic intercalations, that were regionally metamorphosed and variably granitized. Anatexis and metasomatism caused considerable mineralogical and textural alterations in the original rocks. Grouping of several rock types into larger rock units on the basis of assumed original lithology, together with the delineation of certain major structures, has served to establish the lithostratigraphy of the gneiss belt (Table 1).

Detailed mapping revealed the presence of two asymmetrical, doubly plunging anticlines, namely, the Feiran anticline on the west and the Solaf anticline on the east, separated by a synclinal trough and a high-angle thrust fault trending nearly N30°W. In the central eastern part of the gneiss belt, the western limb of an incomplete overturned anticline, the El-Sheikh anticline, is thrust over the Solaf anticline from the east. From the foliation measurements all around the Feiran anticline (Fig. 2), it was found that the axial plane might dip either at 80° to the S.W. or at 88° to the N.E.; the attitude of the minor fold axes favours the northeasterly dip of the axial plane. The Solaf anticline is overfolded in its southern part and overturned in the northern and central parts, where the axial plane dips as much as 56° to the N.E.

The lithology of the original sediments of the Feiran–Solaf gneiss belt and the limited volcanic activity suggest that they belong to a preeugeosynclinal succession. However, the migmatization of this belt was accomplished during the same phase of regional metamorphism as that which affected the eugeosynclinal metasediments and Noweir, 1969) of the Egyptian basement. This phase of regional metamorphism took place 1100–1300 Ma ago (El-Shazly *et al.*, 1973; Siedner *et al.*, 1974).

LITHOSTRATIGRAPHY OF THE GNEISS BELT

Feiran Anticline

The Feiran anticline comprises two formations (Table 1). The lower Nidia El-Samra Formation (I) (about 2000 m thick) was originally formed of semipelites, with minor marly and arenaceous intercalations. The upper Aleiyat Formation (II) (about 3000 m thick) was formed of calcareous shales interbedded with subordinate pelites and minor limestones. The whole succession was subjected to regional metamorphism and migmatization. The contact between the two formations is well marked on the southern flank of the Feiran anticline by a complex zone of intrusive pegmatites (P-1), about 6 km long and 500–700 m wide, in which gneisses from both formations are partly assimilated.

The Nidia El-Samra Formation (I) is differentiated into two members, the boundary between them being locally marked by a discontinuous and disrupted amphibolite band, up to 18 m thick. The lower surface of this amphibolite band is veined by coarse-grained trondjemitic and granodioritic pegmatites whereas the upper surface is devoid of them. The lower Nefuz Granitic Gneiss Member (I-1) is formed largely of leucocratic, medium-grained granitic gneisses with intercalations of minor amphibolite and thin quartzo-feldspathic lenticles and bands. They are also highly dissected by concordant, medium-grained, trondjemitic pegmatite bands, up to 25 cm thick. Locally, the granitic gneisses are thoroughly homogenized and the gneissic structure is hardly perceptible. The abundant amphibolitic intercalations are gradually transformed into hornblende gneisses, particularly along the contacts with pegmatites.

The upper Nidia Gneiss Member (I-2) is represented mainly by a complex of closely folded and intimately intercalated fine-grained biotite- and biotite–hornblende gneisses (2a). Biotite gneisses prevail in the lower part of this complex, enclose garnets, and are dissected by a few granitic pegmatite patches containing tourmaline on the southern banks of Wadi Rummana. A distinct layer of contorted biotite gneiss (2b), up to 400 m wide, is present within the biotite- and biotite–hornblende gneiss complex on the southern limb of Feiran anticline. The whole complex is frequently interbanded with thin para-amphibolite and calc-silicate rocks, 40 m thick in places.

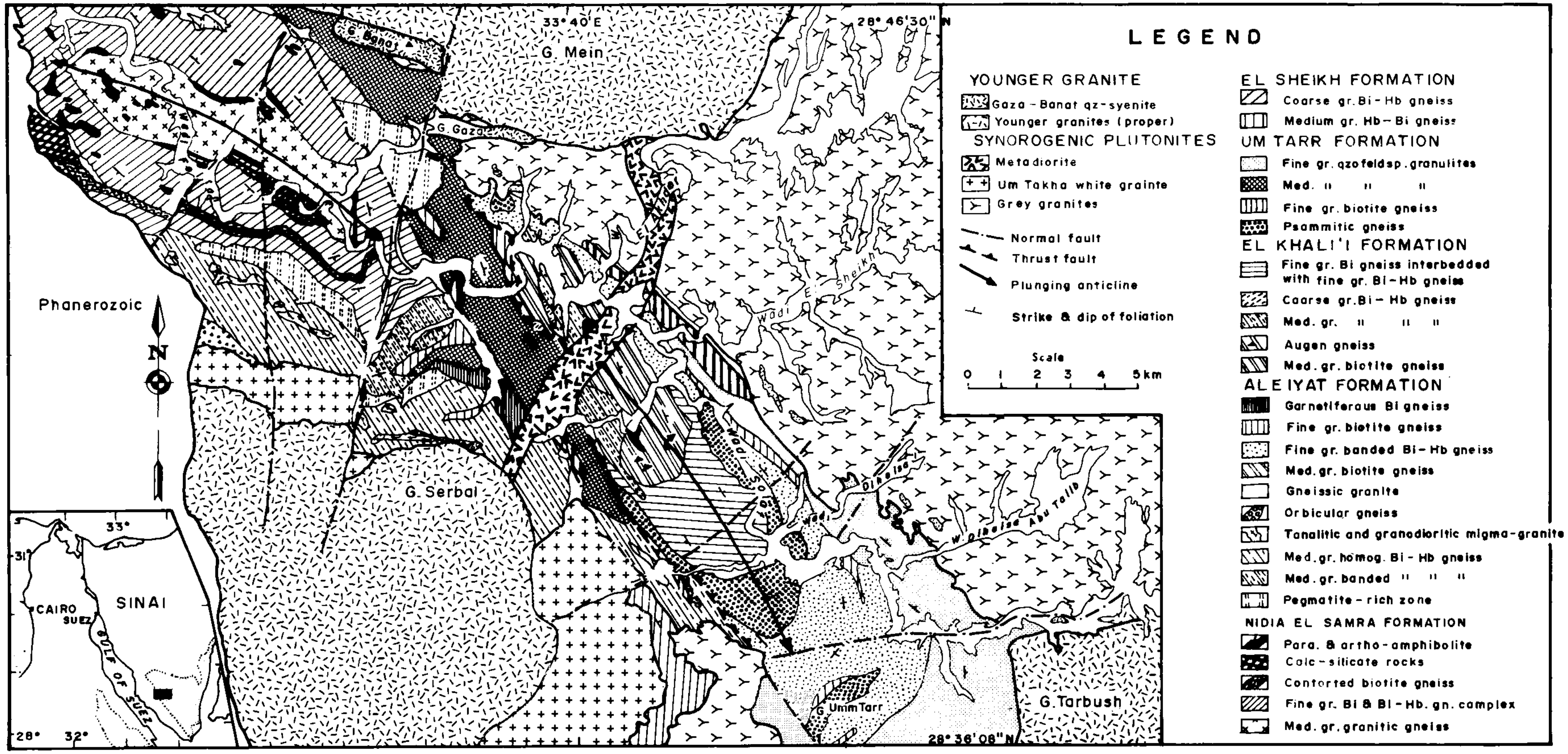

FIG. 1. Geological Map of the Feiran–Solaf district, southwestern part of Sinai, Egypt (after Akaad *et al.*, in press).

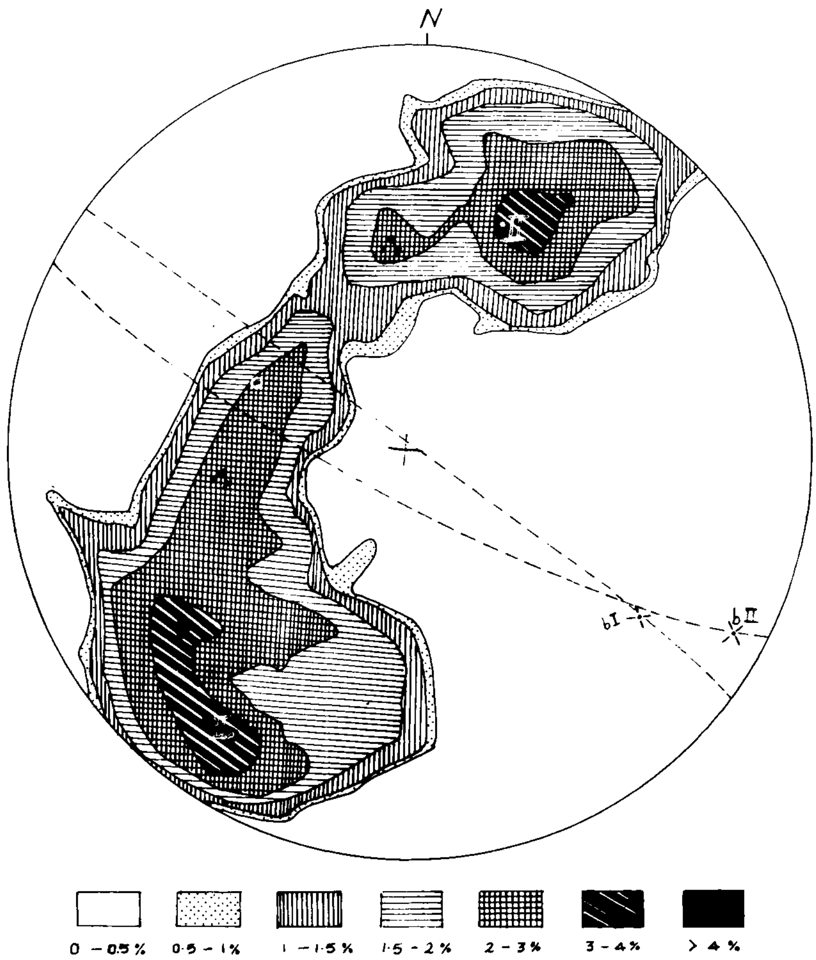

FIG. 2. Contour diagram of 743 foliation readings in the Feiran anticline. The dashed lines represent the traces of the two axial planes obtained from the two maxima present on both limbs; b_I and b_{II} represent the two possible plunge positions of the major fold axis.

The Aleiyat Formation (II) is subdivided into a lower West Aleiyat Gneiss Member (II-3) and an upper East Aleiyat Gneiss Member (II-4), the gneisses of the upper member being less affected by ultrametamorphism. The West Aleiyat Gneiss Member (II-3) consists mainly of medium-grained, banded and homogenized biotite–hornblende gneisses (3a and 3b, respectively). The latter locally grade into conformable patches of coarse-grained tonalitic and granodioritic granites (3c and 3d). They pass into orbicular gneiss (3e) on the southern limb of Feiran anticline. The passage from the homogenized biotite–hornblende gneiss into the granite is rapid, taking place over a short distance as the granite has been mobilized and intruded into still plastic gneisses. The concordant trondjemitic and granodioritic pegmatite swarms traversing the gneisses were never observed dissecting the granites, suggesting that the pegmatites were intruded prior to the emplacement of the granites.

Although the grade of ultrametamorphism increases towards the core of the Feiran anticline, the rocks of the West Aleiyat Gneiss Member (especially in the area north of Jabal Abura) increase in metamorphic grade towards the south, where the homogenized biotite–hornblende gneisses pass into gneissic granite (3f).

The East Aleiyat Gneiss Member (II-4) is essentially a fine-grained, banded biotite–hornblende gneiss (4a). It contains abundant, commonly thin, pelitic and semi-pelitic intercalations and minor limestones. The semi-pelitic intercalations gave rise to fine-grained biotite–plagioclase gneiss (4b)

TABLE 1. LITHOSTRATIGRAPHY OF THE FEIRAN–SOLAF GNEISS BELT.

Formation	Member	Principal rock type(s)
(V) EL-SHEIKH	(V-11) Gufa Gneiss	(11) M.g. Hb–Bi gneiss
	(V-10) Akhdar Gneiss	(10) C.g. Bi–Hb gneiss
(IV) UM TARR	(IV-9) Diheisa Granulite	(9) F.g. quartzofeldspathic granulites
	(Iv-8) Um Gerifat Granulite	(8b) M.g. quartzofeldspathic granulites (8a) F.g. Bi gneiss
	(IV-7) Lebni Gneiss	(7) Psammitic gneiss
(III) EL-KHALI'	(III-6) Um Takha Gneiss	(P-2) Intrusive pegmatites (6) F.g. Bi gneiss, interbanded with Bi–Hb gneiss
	(III-5) Rimm Gneiss	(5d) C.g. Bi–Hb gneiss (5c) M.g. Bi–Hb gneiss (5c) Augen gneiss (5a) M.g. Bi gneiss
(II) ALEIYAT	(II-4) East Aleiyat Gneiss	(4c) Garnetiferous Bi gneiss (4b) F.g. Bi gneiss (4a) F.g. banded Bi–Hb gneiss
	(II-3) West Aleiyat Gneiss	(3h) M.g. Bi gneiss (3g) F.g. Bi gneiss (3f) Gneissic granite (3e) Orbicular gneiss (3d) Granodioritic magma-granite (3c) Tonalitic migma-granite (3b) M.g. homog. Bi–Hb gneiss (3a) M.g. banded Bi–Hb gneiss (P-1) Pegmatite-rich zone
(I) NIDIA EL-SAMRA	(I-2) Nidia Gneiss	(2f) Ortho-amphibolite (2e) Para-amphibolite (2d) Quartzofeldspathic granulite (2c) Calc-silicate rocks (2b) Contorted Bi gneiss (2a) F.g. Bi and Bi–Hb gneiss complex
	(I-1) Nefuz Granitic Gneiss	(1) M.g. granitic Bi gneiss

Bi = biotite; Hb = hornblende; F.g. = fine-grained; M.g. = medium-grained; C.g. = coarse-grained.

and garnetiferous biotite gneiss (4c), whereas the minor pelitic intercalations were altered to cordierite-bearing biotite gneiss (El-Gaby, 1967).

Solaf Anticline

The Solaf anticline comprises two formations. The lower El-Khali' Formation (III) attains a thickness of 1800 m and was formed of an alternation of predominately pelitic and semi-pelitic sediments and less abundant calcareous pelites. The upper Um Tarr Formation (IV) (about 2000 m thick) was formed mainly of arenaceous sediments with minor pelitic intercalations. The clear contact between the two formations is due to the marked colour difference between the leucocratic quartzo-feldspathic rocks of the Um Tarr Formation and the darker coloured, fine-grained biotite- and biotite–hornblende gneisses of the underlying El-Khali' Formation.

The El-Khali' Formation (III) is subdivided into a lower Rimm Gneiss Member (III-5) and an upper Um Takha Gneiss Member (III-6). The lower member consists of medium-grained biotite gneiss (5a) and medium-grained biotite–hornblende gneiss (5c). The former locally develops into augen gneiss (5b) whereas the latter grades into coarse-grained biotite–hornblende gneiss (5d) by the increase in the grade of ultrametamorphism. The medium-grained biotite gneisses are dissected on the western side of Wadi Solaf by intrusive pegmatite masses (P-2) with knife-sharp contacts.

The Um Takha Gneiss Member (III-6) is composed mainly of fine-grained biotite gneiss (6) interbanded with fine-grained biotite–hornblende gneiss. This member includes abundant calc-silicate and para-amphibolite intercalations, up to 25 cm thick. The contact between the medium-grained biotite gneiss (5a) and the overlying Um Takha Gneiss Member is gradational; relict bands and lenses, up to 1 m thick, of fine-grained biotite gneiss are present in it (6).

The meta-arenaceous Um Tarr Formation (IV) is arbitarily subdivided into three members. The grain size of the quartzo-feldspathic rocks increases progressively from fine-grained quartzo-feldspathic granulites (9) of the upper Diheisa Granulite* Member (IV-9) to medium-grained granulites in the middle Um Gerifat Granulite Member (IV-8), and finally into psammitic gneiss (7) in the lower Lebni Gneiss Member (IV-7). The middle member is characterized, however, by the presence of mappable intercalations of fine-grained biotite gneisses (8a). The fine-grained granulites and the enclosed calc–silicate rocks have been thermally metamorphosed along the contacts with the El-Sheigh grey granite intrusion.

The uppermost El-Sheikh Formation (V) is subdivided into a lower Akhdar Gneiss Member (V-10) composed of coarse-grained biotite–hornblende gneiss (10) of calcareous pelitic parentage, and an upper Gufa Gneiss Member (V-11) composed of medium-grained hornblende–biotite gneiss (11) derived from slightly calcareous shales. The succession represents the overturned western limb of the El-Sheikh anticline thrust over the Solaf anticline from the east. The medium-grained hornblende–biotite gneiss (11) encloses abundant, weakly anatectic relics, comprising mainly fine-grained biotite- and hornblende–biotite gneisses, which are usually lacking in the coarse-grained biotite–hornblende gneisses (10).

EVOLUTION OF GNEISS

The Feiran–Solaf gneiss belt is composed largely of migmatites. The migmatites are believed to have contained an appreciable amount of a melt-phase of trondjhemitic to granodioritic composition during their transformation, an inference made from the following observations: (1) the presence of pegmatitic segregation lenses in the gneisses and the infilling of fracture in the solid amphibolites by quartzo-feldspathic materials exuded from the enclosing gneisses; and (2) the increasing degree of idiomorphism of feldspars and the presence of inclusions in the feldspars, with a preferred orientation parallel to original crystal faces of the host minerals. Consequently, the presence of quartzo-feldspathic lenses and streaks (neosomes) in the migmatites is considered to be the outcome of anatexis and not, as suggested by Schurmann (1966), the result of *lit-par-lit* injection of granitic magma.

Metasomatism affected the rocks undergoing anatexis and caused extensive mineralogical changes. It can be seen from Fig. 3, which is based on the modal composition of about 50 gneiss samples (Table 2), that with the increase in the degree of ultrametamorphism, there is a general increase in the feldspar content, accompanied by a corresponding decrease in the content of ferromagnesian minerals; the increase in the content of plagioclase precedes that of potash feldspars. Petrographical investigation showed that hornblende is transformed into biotite at an early stage in the outer zones of relative lower temperatures; biotite dissociates later, during the rising temperature and expanding migmatitic front, and the released potash helps in transforming more hornblende into biotite.

*The term granulite is applied, after Harker (1952), to fine-grained, quartzo-feldspathic rocks of equigranular texture.

TABLE 2. MODAL COMPOSITION (VOLUME PERCENTAGE) OF SOME ROCK TYPES OF THE FEIRAN–SOLAF GNEISS BELT.

Specimen No.	Plag	Qz	Kf	Bi	Hb
Granitic biotite gneiss (I-1) and hornblende–biotite gneiss intercalations					
185	35.6	28.3	26.6	8.2	—
1094	51.7	29.7	4.4	12.6	—
1137	62.0	26.6	0.5	9.5	—
1183	60.5	28.7	—	9.7	0.8
1288	56.2	24.0	6.8	11.0	—
1336	58.3	24.8	1.4	14.2	0.3
1404	54.9	33.3	4.4	6.6	—
1507	26.9	33.5	32.2	6.0	—
1512	40.7	32.9	22.0	4.0	—
Fine-grained biotite gneiss (2a)					
1261	53.3	22.7	—	22.3	—
1362	53.0	25.5	—	20.4	—
1629	42.6	34.2	—	22.2	—
Fine-grained hornblende-biotite gneiss (2a)					
821	32.1	13.1	—	31.5	1.5
1163	55.2	11.6	—	24.4	5.3
1452	50.6	20.6	—	26.1	2.3
Contorted biotite gneiss (2b)					
111	49.8	38.3	7.1	3.9	—
261a	59.1	22.2	9.4	8.0	—
Medium-grained banded biotite–hornblende gneiss (3a)					
82	53.7	13.8	8.8	14.4	8.6
89	60.0	13.4	7.1	11.6	7.1
213	64.1	11.3	0.6	12.6	9.9
246	61.8	11.2	0.2	15.2	10.5
1662	60.8	5.0	0.2	12.1	19.4
1664	62.2	12.9	—	10.6	13.7
Medium-grained homogenized biotite–hornblende gneiss (3b)					
11	54.8	17.6	9.9	7.6	8.9
12a	74.3	1.3	1.2	12.0	7.9
12b	69.0	10.2	0.8	7.4	10.9
12c	62.9	10.1	0.3	10.2	15.2
143	62.4	8.9	1.7	11.7	13.9
227	56.8	19.6	5.3	7.1	10.7
248	59.0	12.4	0.9	13.2	12.6
1590	54.4	9.0	0.2	10.7	24.2
1698	56.6	20.3	4.0	9.3	9.6
1705	67.5	10.3	4.3	5.4	11.6
1706	57.2	16.0	10.4	8.2	6.8
Tonalitic migma-granite (3c)					
143b	73.6	7.5	5.9	4.3	7.7
156b	76.8	11.5	0.6	4.5	5.9
158a	86.0	5.0	1.8	3.8	2.8
1005	85.1	3.2	0.2	2.5	8.6
1048	84.4	5.8	1.7	2.5	5.2
1049	86.0	7.1	1.1	5.5	0.1
Granodioritic migma-granite (3d)					
1695	70.0	9.9	18.6	1.4	—
1696	66.9	22.7	5.1	4.8	—
Gneissic granite (3f)					
1579	59.1	27.5	5.9	7.3	—
1580a	62.8	22.2	5.7	7.7	—
1580b	48.6	16.5	32.8	1.8	—
1582	46.5	29.6	21.4	1.7	—
TABLE 2 (CONTINUED).					
Fine-grained banded biotite–hornblende gneiss (4a)					
58b	44.8	6.7	—	13.0	34.1
294	46.7	21.5	—	13.2	17.1
745	60.5	4.2	—	10.2	23.5
799	55.7	8.1	—	17.7	16.5
Medium-grained biotite gneiss (5a)					
471	66.1	24.2	—	8.6	—
514	70.1	11.9	0.1	16.7	—
537b	57.6	19.6	0.7	20.6	—
1896	65.5	26.0	2.6	5.3	—
Augen gneiss (6b)					
316a	50.0	14.1	24.5	6.8	1.8
316b	53.3	19.8	14.6	7.2	2.3
Medium-grained biotite–hornblende gneiss (5c)					
273	63.4	14.1	0.7	11.3	9.5
303b	56.0	17.9	9.4	6.8	7.6
314	61.8	10.8	4.4	14.3	4.8
319	59.1	13.9	5.0	11.2	8.0
521	59.0	12.9	8.4	12.7	4.4
522	57.0	19.4	1.9	9.9	8.7
1892	62.0	13.5	2.5	12.3	7.5
Fine-grained biotite gneiss (6)					
513	69.4	16.6	0.9	12.6	—
537a	60.0	19.3	—	19.8	—
Coarse-grained biotite–hornblende gneiss (10)					
547	40.7	31.1	4.8	13.8	9.1
1798	48.6	30.0	4.3	10.4	5.9
Medium-grained hornblende–biotite gneiss (11)					
546	58.9	24.6	6.5	6.5	2.2
1797	56.9	24.6	8.4	6.7	2.2

Biotite–Hornblende Gneisses

This group comprises the fine- and medium-grained banded and homogenized biotite–hornblende gneisses as well as the medium-grained gneissic granite and the tonalitic and granodioritic granites. As shown in Fig. 3, the fine-grained biotite–hornblende gneisses are transformed *in situ* into medium-grained banded and/or homogenized biotite–hornblende gneisses and ultimately into medium-grained gneissic granite. Tonalitic and granodioritic granites are considered as the rheomorphosed, highly anatectic members of this progressive series.

Amphibolites follow one of two different trends of evolution depending on their original hornblende to plagioclase ratio. Plagioclase-rich amphibolites are transformed into fine- to medium-grained hornblende–plagioclase gneisses, whereas hornblende-rich amphibolites commonly give rise to coarse-grained appinites.

With increasing grade of metamorphism, the development of gneissic granite and granites is

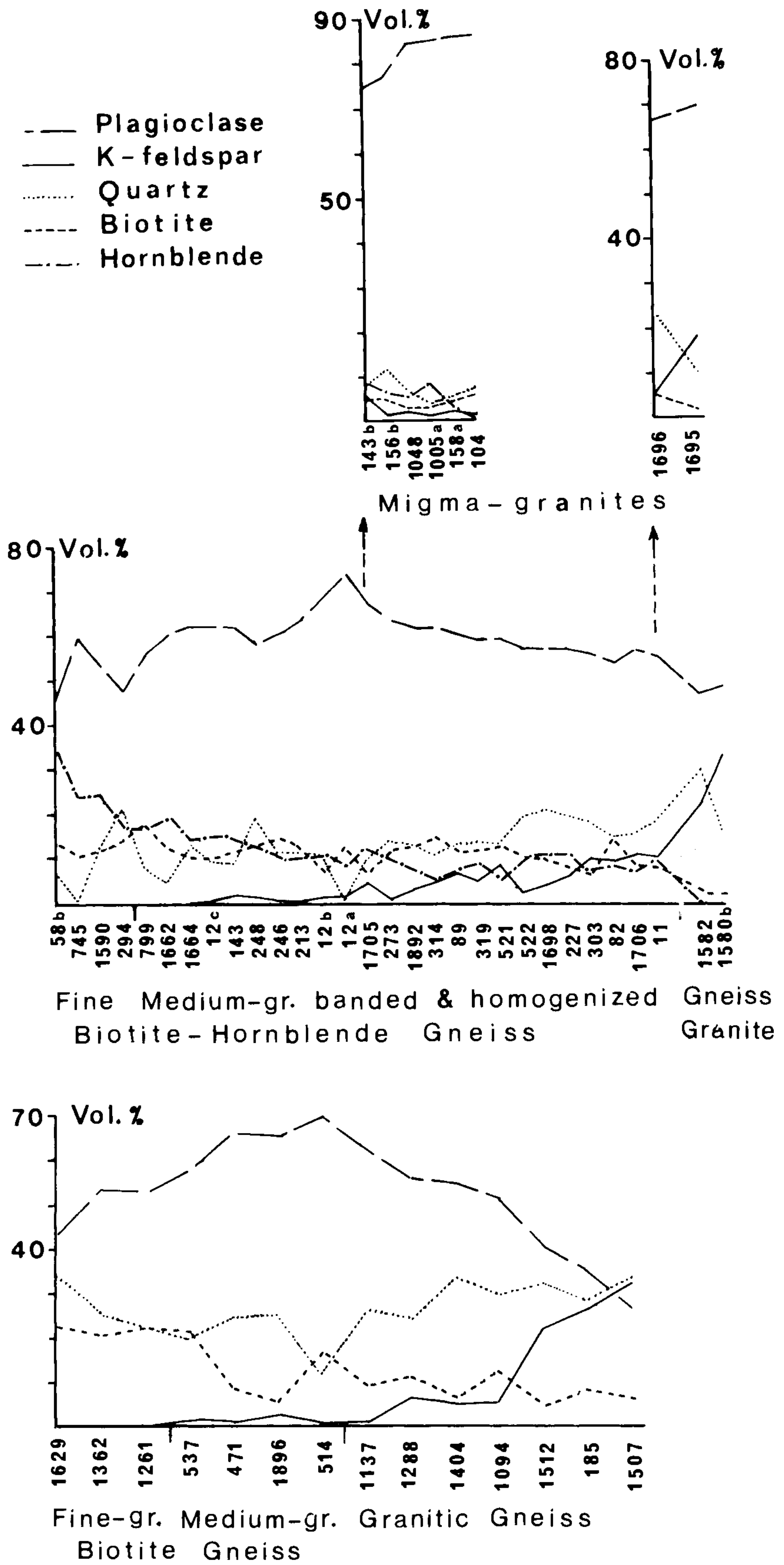

FIG. 3. Generalized variation diagrams of the modal composition of biotite-hornblende and biotite gneisses; anatexis increases to the right.

accompanied by the following features:

(1) gradual and continuous increase in the grain-size of the mineral components;

(2) progressive loss of gneissosity, banding, and homogeneity in the gneisses. The fine-grained gneisses frequently pass directly into the homogenized medium-grained gneiss (diatexite) without passing through the banded (metatexite) stage;

(3) rapid decreases in the amount of hornblende at first, accompanied by a concomitant growth and increase in the amount of biotite; in the more advanced stages, both mafic minerals tend to decrease in amount with the continual increase in the amount of feldspars;

(4) an increase in the degree of idiomorphism of the plagioclase feldspars, the anatexites acquiring more and more hypidiomorphic granular texture. The anorthite content of the plagioclase decreases from the fine-grained gneisses (An_{35-27}) to the medium-grained varieties (An_{30-24}), thereafter remaining almost constant. Most of the plagioclase crystals in the gneissic granite, and to a less extent in the granodioritic granite, possess the lowest anorthite content (An_{23-21}) measured in this series. However, some irregularly zoned large plagioclase crystals possess anorthite-rich cores of about An_{30}, suggesting that the anorthite content was originally higher. Later interaction between the plagioclase metablasts and the abundant intergranular melt-phase caused a thorough reduction of the anorthite content of the plagioclase crystals present (Engel and Engel, 1958); and

(5) the first occurrence of potash feldspar in appreciable amounts in the coarser grained anatectic rocks. It is always later than plagioclase, and corrodes the plagioclase crystals along crystal faces and cracks. However, it is sometimes embayed by myrmekitic plagioclase overgrowths.

The tonalitic and granodioritic granites are thought to represent the mobilized counterparts of the medium-grained biotite–hornblende gneisses and gneissic granites, respectively. The pronounced enrichment of the tonalitic granite in plagioclase and its impoverishment in quartz might have been caused by the filtration of the pore-magma rich in quartz (and usually potash feldspar) during the upwards migration of the granite. As potash feldspar crystallizes later than plagioclase, the tonalitic granite is considered to be a mobilized earlier phase, while the granodioritic granite, containing few porphyritic potash feldspar metacrysts, probably represents a later phase that was rheomorphosed shortly after the beginning of potash feldspar crystallization, or rather after the encroachment of the potash front.

Biotite Gneisses

Biotite gneisses comprise metamorphosed rocks of pelitic and semipelitic parentage. Pelitic and semipelitic rocks responded differently to metamorphism and to the early stages of ultrametamorphism, but both gave rise to almost homogeneous granitic gneisses in the final stages. Granitic gneisses derived from semipelites are, however, typically finer grained and relatively lighter in colour.

Preserved relict rock masses indicate that pelites were metamorphosed into biotite–sillimanite–almandine schists before their transformation into cordierite gneiss by the action of magnesia metasomatism moving ahead of the following feldspathic front (El-Gaby, 1967). During the expansion of the migmatitic front, the growing plagioclase metablasts corroded and drove out the early-formed cordierite. Plagioclase metablastesis culminated in the formation of medium-grained biotite–plagioclase gneiss. The extensive development of plagioclase metablasts required the addition of soda from greater depths, whereas lime could have been provided by the surrounding country rocks. Potash feldspar is later than plagioclase and appears in increasing amounts in the more advanced stages of granitization where it frequently forms perthitic orthoclase augen, 1–2 cm long. The final products observed are granitic gneisses of granodioritic composition containing few potash feldspar metacrysts.

Semipelitic schists did not respond readily to ultrametamorphism and were transformed only to the fine-grained biotite–plagioclase gneisses frequently encountered within the medium-grained biotite–plagioclase gneisses of pelitic parentage. Grain-size and amount and idiomorphism of the plagioclase crystals increase rather slowly in the course of ultrametamorphism. The highest stage attained in the area studied is represented by the medium-grained granitic gneisses of granodioritic composition constituting the Nefuz Granitic Gneiss Member (I-1).

Quartzo-Feldspathic Granulites and Psammitic Gneiss

The quartzo-feldspathic granulites (Harker, 1952) were formed largely by the metamorphism of arenaceous and siliceous sediments and acidic tuffs. Metamorphosed arenaceous sediments are well represented by the rocks of the Um Tarr Formation (IV); they also occur as minor intercalations within other formations. The fine-grained Dihesa Granulites (IV-9), least affected by anatexis, grade downwards by the increase in the grade of ultrametamorphism into medium-grained

Um Gerifat Granulites (IV-8) and then into the psammitic Lebni Gneisses (IV-7). The first imprints of ultrametamorphism in the fine-grained granulites are marked by the slight growth of the plagioclase crystals and by the incipient development of their own crystal faces. The granulites tend, at this stage, to be inequigranular, and approach the "granulitic fabric" in which flattened lenticles of rather coarse quartz alternate with layers of finely crystalline quartz and feldspars. Psammitic gneisses are characterized by coarser grainsize, low mafic content and higher quartz content. Quartz usually occurs as flattened lenticles stretched parallel to the weak foliation or banding.

The highest degree of ultrametamorphism attained by the arenaceous rocks is represented by the mafic-poor, highly homogenized nebulitic gneiss incorporated within granitic gneiss and gneissic granite areas.

CONCLUSIONS

The original sedimentary succession in the Feiran–Solaf belt was regionally metamorphosed and variably granitized. Akaad (1959) mentioned that the highly metasomatic metamorphism affecting the gneiss belt took place in two stages, namely, an early phase of medium-grade regional metamorphism, followed by a highly metasomatic phase. The present authors wish to stress that these two stages belong to one cycle of metamorphism and that no tectonic events have intervened between them. Read (1957) stated that one of the most firmly established facts in metamorphic geology is the close association in the field of highest-grade metamorphic rocks and migmatites. Moreover, the reactions leading to the formation of sillimanite and cordierite at the expense of muscovite and biotite are accompanied by the development of a melt-phase of quartz and alkali feldspars (Winkler, 1974) which should be considered as the initial stage of migmatization.

Akaad *et al.* (1967b) believed that the metasomatism that affected the Feiran–Solaf gneiss belt was predominantly sodic. However, expansion of the area of study has revealed the presence of highly granitized rocks, such as augen gneiss, gneissic granite and granodioritic migma-granite, which bear the imprints of the obviously younger potash metasomatism.

Migmatization and metasomatism had caused large-scale textural and mineralogical changes. The following progressive series are deduced from the field relations and petrographic investigation. The calcareous pelites were metamorphosed into fine-grained biotite–hornblende gneisses which were transformed *in situ* by anatexis and metasomatism into medium-grained banded and/or homogenized biotite–hornblende gneisses and then into medium-grained gneissic granites. Successive mobilizations of the highly anatectic medium-grained gneisses and gneissic granite gave rise to tonalitic and granodioritic migma-granites respectively. Preserved relicts indicate that pelites were metamorphosed into biotite–sillimanite–almandine schists before their transformation by granitization into cordierite gneiss, medium-grained biotite–plagioclase gneiss, augen gneiss and finally into granitic gneiss containing few potash feldspar metacrysts. Semi-pelites usually lagged behind and occur mainly as fine-grained biotite–plagioclase gneisses. Medium-grained granitic gneisses of granodioritic composition represent the most advanced stage of ultrametamorphism attained, but they are distinctly finer grained than the equivalent rocks of pelitic and calcareous pelitic parentage.

Psammitic rocks, least affected by ultrametamorphism, occur as fine-grained quartzo-feldspathic rocks having an equigranular granoblastic texture, the fine-grained biotite granulites. They grade by the increase in grade of metamorphism into medium-grained biotite granulites, then psammitic gneisses and finally into nebulitic gneisses.

ACKNOWLEDGMENT

The authors wish to express their deepest gratitude to Prof. M. K. Akaad for his kind suggestions and discussions.

REFERENCES

AKAAD, M. K. 1959. The migmatitic gneisses of Wadi Feiran, Sinai, Egypt. *Assiut Sci. Techn. Bull.*, 2, 211–237.

AKAAD, M. K., EL-GABY, S., and ABBAS, A. A. 1967a. Geology and petrography of the migmatites around Feiran Oasis, Sinai. *Assiut Sci. Techn. Bull.* 10, 67–87.

AKAAD, M. K., EL-GABY, S., and ABBAS, A. A. 1976b. On the evolution of Feiran migmatites. *U.A.R. (Egypt) J. Geol.* 11, 49–58.

AKAAD, M. K., EL-GABY, S., and AHMED, A. A. Geology of the Feiran–Solaf district, Southwestern Sinai, Egypt. *Annals Geol. Surv. Egypt* (in press).

AKAAD, M. K., and NOWEIR, A. M. 1969. Lithostratigraphy of the Hammamat-Um Seleimat district, Eastern Desert, Egypt. *Nature* 223, 284–285.

BALL, J. 1916. Geography and geology of West Central Sinai. *Geol. Surv. Egypt.*

BARRON, T. 1907. The topography and geology of Western Sinai. *Geol. Surv. Egypt.*

EL-GABY, S. 1967. The mode of formation of cordierite gneisses in migmatitic rocks. *Assiut Sci. Techn. Bull.* 10, 91–106.

EL-GABY, S., and AHMED, A. A. The intrusive rocks in Wadi Feiran district, Southwestern Sinai, Egypt. *Annals Geol. Surv. Egypt* (in press).

EL-SHAZLY, E. M., HASHAD, A. H., SAYYAH, T. A., and

BASSYUNI, F. A. 1973. Geochronology of Abu Swayel area, Southeastern Desert, Egypt. *Egypt. J. Geology* 17, 1–95.

ENGEL, A. E. J., and ENGEL, C. G. 1958. Progressive metamorphism and granitization of the major paragneiss, N.W. Adirondak Mountains, New York. *Geol. Soc. Am. Bull.* 69, 1369–1413.

HARKER, A. 1952. *Metamorphism.* Methuen, London.

HUME, W. F. 1906. The topography and geology of the Peninsula of Sinai. *Geol. Surv. Egypt.*

READ, H. H. 1957. *The Granite Controversy.* Murby, London.

SCHURMANN, H. M. E. 1966. *The Precambrian Along the Gulf of Suez and the Northern Part of the Red Sea.* Brill, Leiden.

SIEDNER, G., SHIMRON, A., and PRINGLE, I. 1974. Age relations in basement rocks of the Sinai Peninsula. *Int. Meet. Geochronology*, Paris.

WINKLER, H. G. F. 1974. *Petrogenesis of Metamorphic Rocks.* Springer-Verlag, New York.

الريوليتات الإجنمبريتيّة بمنطقة واصيف الصحراء الشرقية ، مصر

م.أ. هيكل و م.ح.حجازى و م.م. الرحمانى

الخلاصة

يتضمن البحث وصفا تفصيليا لصخور فريش الإجنمبريت فى منطقة واصيف جنوب غربى سفاجة . ويعتبر التسجيل الرابع للصخور الإجنمبريتيّة فى معقّد الأساس بمصر. وتصاحب الإجنمبريت فى التتابع الطباقى نفسه مجموعة من الصخور البركانية الكلس ـ قلوية (ريوليتات ، ريوداسيتات ، أنديزيتات). ولقد أوضحت الدراسات الكيميائية الصخرية (البتروكيميائية) ـ وتشمل أربعة تحاليل من الإجنمبريت ـ أن الريوليتات الإجنمبريتيّة قد نشأت من قطر كلس ـ قلوى ، وربما كان ذلك بالتبلور الجزئى.

IGNIMBRITIC RHYOLITES IN THE WASSIF AREA, EASTERN DESERT, EGYPT

MOHAMMED A. HEIKAL[1], MOHAMMED H. HIGAZY[1] and MAHMOUD M. EL-RAHMANY[2]

[1]King Abdulaziz University, Jeddah, Kingdom of Saudi Arabia
[2]Al-Azhar University, Cairo, Egypt

Abstract—An ignimbritic sheet in the Wassif area, S.W. of Safaga, is petrographically described. This is the fourth record of ignimbritic rocks in the basement complex of Egypt. In close stratigraphic association with the ignimbrite is an assemblage of calc-alkaline volcanic rocks (rhyolites, rhyodacites and andesites). Petrochemical studies (including four analyses of the ignimbrite) led to the conclusion that the ignimbritic rhyolites are derived from a calc-alkali magma, perhaps by fractional crystallisation.

INTRODUCTION

The occurrence of ignimbritic rocks in the stratigraphic succession of Egypt was noted in the Hammamat series of Wadi Dip–Esh Mallaha area (Schurmann, 1958 p. 121) and from the Shadli Dokhan series in the neighbourhood of Samr El-Abd (Schurmann, 1959, p. 135). More recently, Gindy and Mohammed (1971) have recorded the presence of ignimbritic rocks in the Wadi Nuqara volcanics (S.W. of Safaga) and have described in detail the petrography of the ignimbrites and their lithophysae. This is, however, the first record of ignimbritic rocks in the volcanics and pyroclastics of the Wassif area and probably the fourth recorded occurrence in the Basement Complex of Egypt.

The confusing use of the term "ignimbrite" since its first definition by Marshall (1935) necessitates an explanation of the way in which this term is used in describing Wassif ignimbritic rocks. Recently, Vlodavetz (1966, p. 145) discussed the confusion in the use of the term ignimbrite and suggested the use of the term "ignimbritic" to denote a special type of eruption creating pyroclastic flows, the deposits formed as a result of an ignimbritic type of eruption being termed "ignimbritic deposits" consisting of "ignimbritic rocks". Rittmann (1966) stated that "ignimbrite" is a general term that defines only the mode of eruption and deposition but does not say anything about the chemical or mineralogical composition of the resulting rock. Battey (1966) proposed the use of the term "ignimbritic" as a qualifier to denote the composition of the rock (e.g. ignimbritic rhyolite, ignimbritic dacite, etc.). Battey's usage is followed here, and the term "ignimbritic rhyolite" is used to describe the Wassif ignimbritic rocks.

GEOLOGICAL SETTING

The Wassif volcanics—among which the ignimbritic rhyolites are recorded—form a conspicuous feature in the basement area S.W. of Safaga

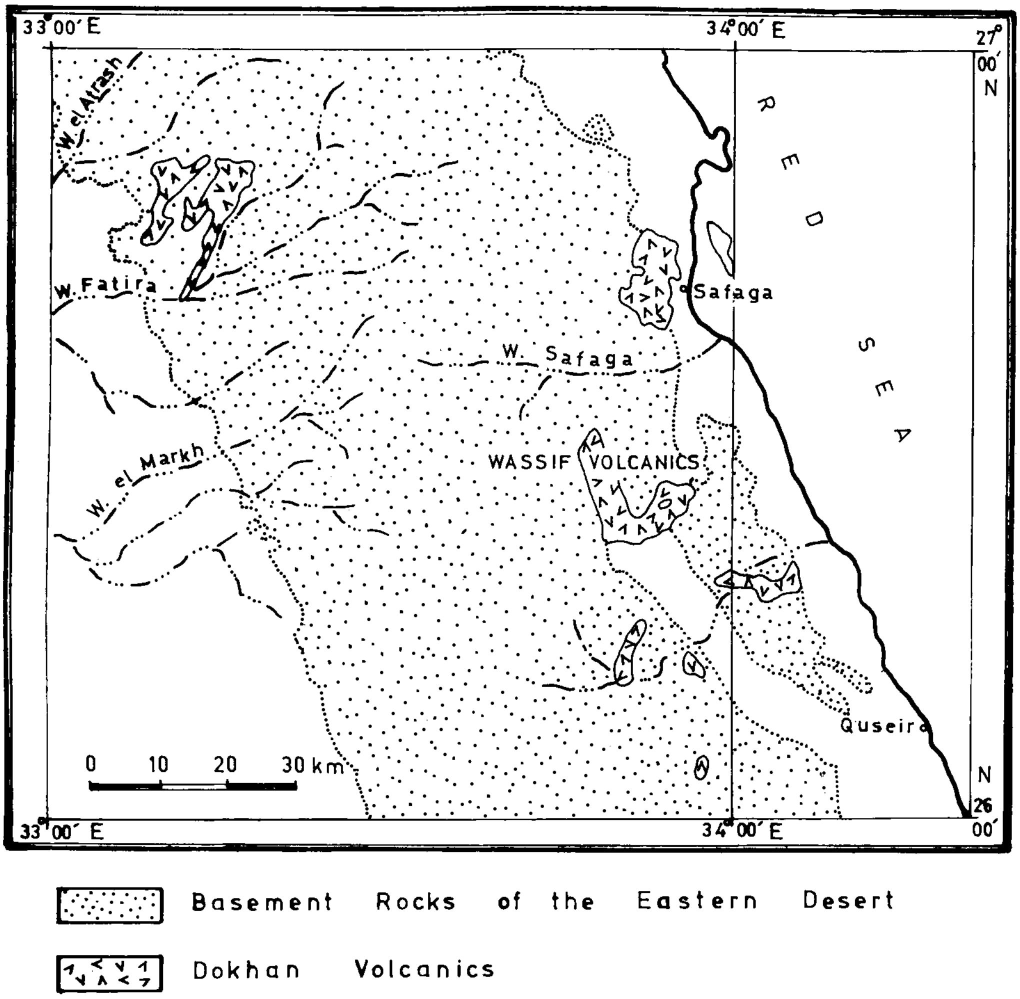

FIG. 1. Distribution of Dokhan volcanics in the vicinity of the Wassif volcanics.

(Fig. 1). These volcanics belong to the "Dokhan Volcanics", the ages of which range between 654 and 665 Ma (El-Shazly *et al.*, 1973).

The Wassif volcanics occur in the form of successive sheets of lavas and pyroclastic rocks. When observed from a distance they exhibit a crude stratification due to variation in colour. The rocks are mainly andesitic and rhyolitic in composition, but original flows of rhyodacites are also present in much smaller amounts. The pyroclastic rocks are lapilli tuffs, vitric crystal tuffs and lithic tuffs.

PETROGRAPHY

The ignimbritic rocks form a thick, lava-like sheet more than 25 m thick, in the Wassif volcanic succession. They are homogeneous in general appearance and massive and brownish black in colour. Close inspection shows that there is a regular orientation of flattened, lenticular particles of glass (fiammé) embedded in a lighter coloured matrix. Such eutaxitic structure is one of the most important and characteristic fabrics of ignimbritic rocks (Zavaritzky, 1955; Schieferdecker, 1959). The main part of the ignimbritic sheet, however, has the lava-like appearance of a quartz porphyry, the result of intense devitrification which has obliterated the shard outlines.

The ignimbritic rocks are chiefly fine-grained rhyolitic tuffs formed mainly of acid volcanic glass. Intratelluric crystals, mostly of quartz, K-feldspar and plagioclase, are present in addition to the lenticular glass shards (fiammé). The orange colour of the groundmass in some rocks is produced by oxidation of the fine fragmental groundmass, in contrast to the included lenticles and crystals.

Under the microscope, the fiammé can be clearly distinguished from the enclosing matrix by their lenticular form and degree of devitrification.

Figure 2 shows the eutaxitic structure in which the fiammé in general lie beside one another in seemingly well ordered distribution. The fiammé are occasionally observed bending around the intratelluric crystals (Fig. 3), indicating their viscous nature when they were deposited. On the other hand, some of these crystals penetrate the fiammé (Fig. 4), the intensity of welding and compaction being indicated by such penetration.

Thin section study of the large fiammé shows that they are frequently composed of two well-defined zones, distinct from each other and from the matrix (Figs. 4 and 5). The outer thin sheath of glass—now devitrified—is distinguished from the inner zone by slight differences in colour and degree of devitrification. The inner zone of the fiammé might have originally represented the central cavities of glass bubbles that were collapsing, their place being subsequently taken by products of late vapour phase crystallization. Some of the fiammé contain more than one cavity filled with crystals of the late vapour phase (Figs. 2 and 4). These fiammé could thus be attributed to collapsed pumice fragments.

The intratelluric crystals of the Wassif ignimbritic rhyolites are mainly K-feldspar, plagioclase and quartz. The ferromagnesian minerals are completely altered and opaque minerals mark their

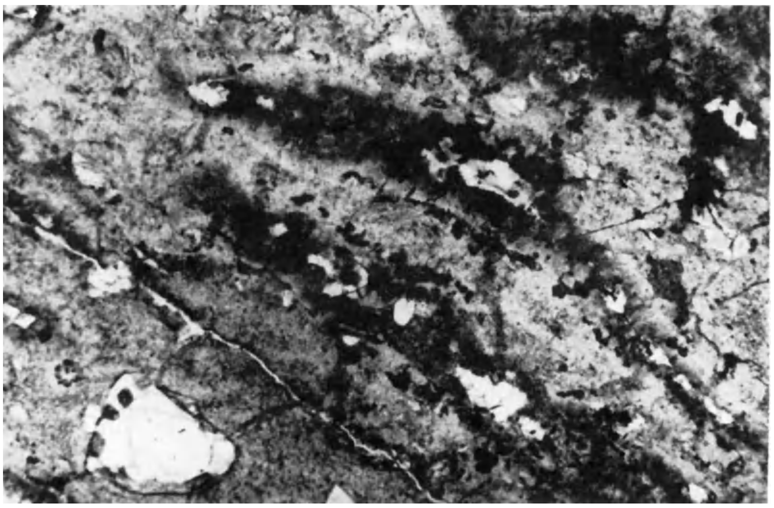

FIG. 2. Wassif ignimbritic rhyolite showing distinctive eutaxitic structure produced by the regular orientation of flattened fiammé (dark areas). P.L. X25.

FIG. 3. Photomicrograph of welded tuff showing evidence of plasticity during welding. One of the fiammé is bending around on an intratelluric crystal with a quartzo-feldspathic intergrowth. P.L. X25.

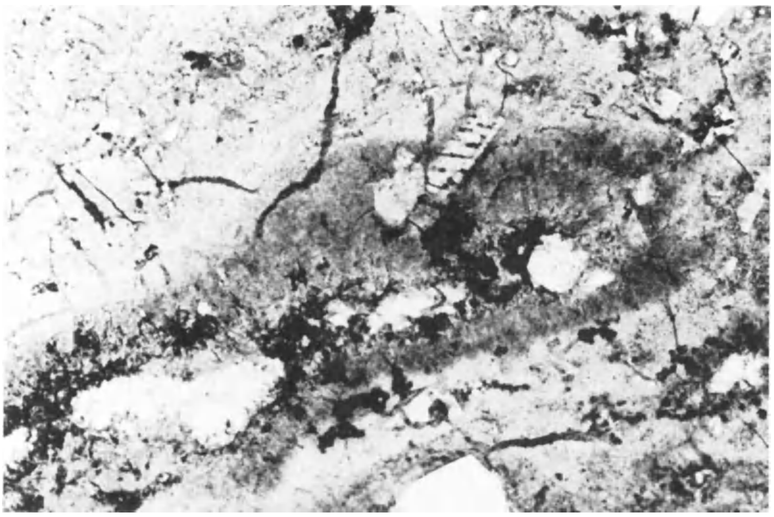

FIG. 4. Photomicrograph of a feldspar crystal penetrating one of the fiammé. P.L. X35.

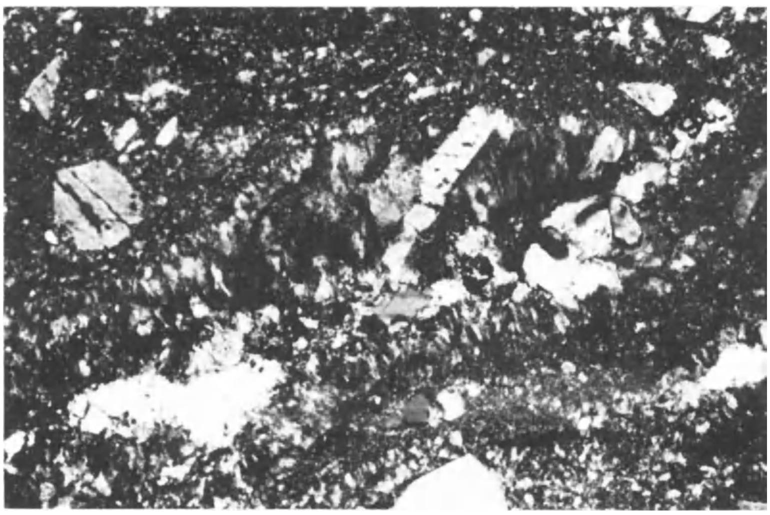

FIG. 5. The same photomicrograph as Fig. 4, showing the composite structure of the fiammé, which is made up of an outer zone of devitrified glass and an inner lighter one of slightly coarser quartzo-feldspathic mosaic. C.N. X35.

outlines. Uncommonly, the intratelluric crystals show signs of intense resorption. Quartz phenocrysts are frequently corroded (Fig. 2), but rarely exhibit faces of the hexagonal bipyramid. Feldspar grains are commonly subhedral; some show one crystal face, the other edges being irregular or fractured. Other feldspar grains are rounded or irregularly embayed. Such observations seem to indicate a high temperature depositional environment (incandescent flows preserve a high temperature for a relatively long time after they come to rest).

WELDING

The Wassif ignimbritic rhyolites differ markedly from each other in structural and textural characteristics as a consequence of different degrees of welding. According to Hatch *et al.* (1972, p. 248), welding of the glass shards and pumice fragments is inevitable, since their temperature may be as high as 900°C, i.e. the temperature of a rhyolitic magma. The loss of heat during transportation is minimal, due to the nature of the dense, particle-charged gas cloud. It has been shown experimentally, however, that the welding temperature of dry pumice is 775° to 900°C, decreasing to 600°C in the presence of water vapour and under loads approximating to those obtaining under natural conditions. Welding is well developed in the central part of the flow at Wassif, where heat is retained as a consequence of the insulation provided by the subjacent and superincumbent rocks. In these strongly welded varieties, the glass fragments have a flattened, even elongated, form and indistinct borders. In the weakly welded ones, the glass shards are angular and sharply delineated from the groundmass. Characteristics of the groundmass also depend on the degree of welding. Ash structures are well preserved in weakly welded varieties, whereas in the strongly welded ones the groundmass is glassy. The latter is mostly recrystallised to microfelsite with a mosaic of ill defined grey areas (under crossed nicols). Rarely, the groundmass has a fluidal structure which apparently is not the result of flowage, but of compression (Aprelkov, 1966). In some of the loosely welded varieties the crystals stand with their long axes at right angles to the lamination of the tuff (Fig. 6), as if they had fallen into it from above, a feature which was described by Pettijohn (1975, p. 307).

DEVITRIFICATION

Devitrification of the Wassif ignimbritic rhyolites can be clearly observed where they are wholly microcrystalline. Sometimes, each component fragment of the rocks behaved as an independent unit where crystallization commenced

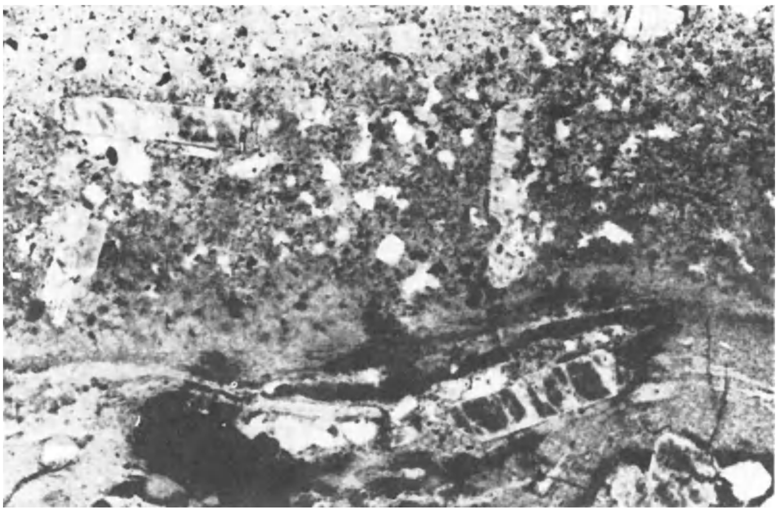

FIG. 6. Loosely welded tuff showing some of the feldspar crystals standing with their long axes at right angle to the lamination of the tuff as if they had fallen into it from above. P.L. X35.

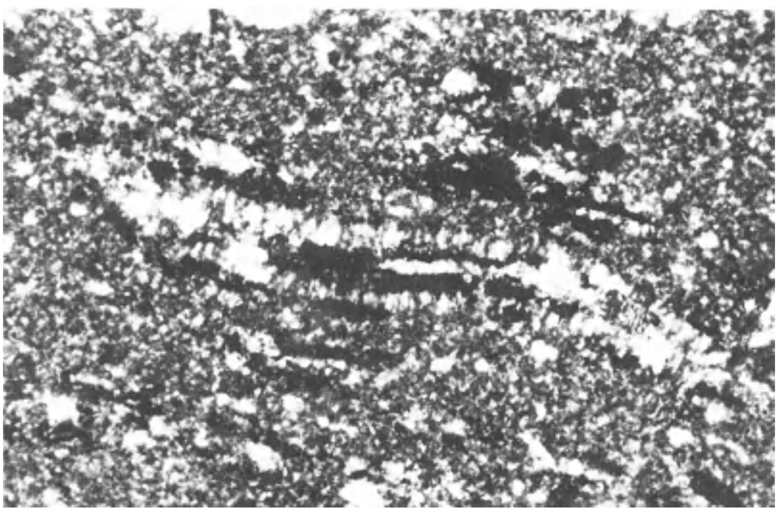

FIG. 7. Devitrified ignimbritic rhyolite. The parallel intergrowth of the replacing crystals (feldspar and cristobalite?) results in the development of axiolitic structure. C.N. X35.

on the margin of the fiammé and continued until the crystals met at a well-defined middle line. The resulting structure is termed axiolitic (Fig. 7). The mineral aggregates within the fiammé cannot be definitely identified by means of the microscope, but many SRD examinations of the devitrified glass shards and pumice fragments of ignimbritic rhyolites from many localities have shown that the products are invariably cristobalite and feldspar (Ross and Smith, 1961, p. 36). This type of devitrification has a minimum effect in modifying shard structure and is apparently due to preservation of volatiles in them (Fedorov, 1966, p. 135). Spherulitic and mosaic devitrification textures are also observed in the fiammé, especially the large ones, and in the groundmass.

CHEMISTRY AND PETROGENESIS

Chemical analysis of the Wassif ignimbritic rhyolites was carried out using the rapid method of Shapiro and Brannock (1962). The results, presented in Table 1, show that the composition of the entire cooling unit varies within a very narrow range. The rocks are classified as rhyolitic on the basis of silica content (70–76%) and total alkalis (7.0–7.6%) (Ewart, 1966). A classification of the ignimbritic rocks according to Churchs' (1975) method is presented in Fig. 8. This shows clearly that the ignimbritic rocks occupy the field designated by Church (1975) for rhyolites.

The normative Q + Ab + Or exceeds 86%. When plotted on the Q–Ab–Or triangle (Fig. 9) of Tuttle and Bowen (1958) the ignimbritic rhyolites lie on the quartz side of the thermal minimum for 1 kb.

Petrochemical studies of the Wassif volcanics

TABLE 1. CHEMICAL ANALYSES OF WASSIF RHYOLITIC IGNIMBRITES (BY WET RAPID SILICATE ANALYSIS).

	1	2	3	4
SiO_2	73.50	73.90	73.60	72.99
TiO_2	0.26	0.27	0.28	0.26
Al_2O_3	13.60	13.44	13.50	13.76
Fe_2O_3	1.50	1.60	1.44	1.45
FeO	0.70	0.73	0.50	0.65
MnO	0.05	0.06	0.07	0.06
MgO	0.26	0.29	0.35	0.38
CaO	1.40	1.43	1.62	1.50
Na_2O	3.66	3.58	3.50	3.55
K_2O	3.80	3.71	3.80	3.70
P_2O_5	0.05	0.05	0.05	0.06
H_2O^+	0.80	0.94	0.95	1.11
Total	99.58	100.00	99.66	99.47
	C.I.P.W. Norm			
Q	34.79	35.87	35.33	34.61
or	22.27	21.71	22.27	22.27
ab	30.94	30.42	29.37	29.89
an	6.12	6.12	7.23	6.68
C	1.22	1.33	1.02	1.43
hy	0.60	0.70	0.90	0.90
mt	1.85	1.85	1.16	1.62
hm	0.16	0.32	0.64	0.32
il	0.46	0.46	0.46	0.46
ap	0.34	0.34	0.34	0.34

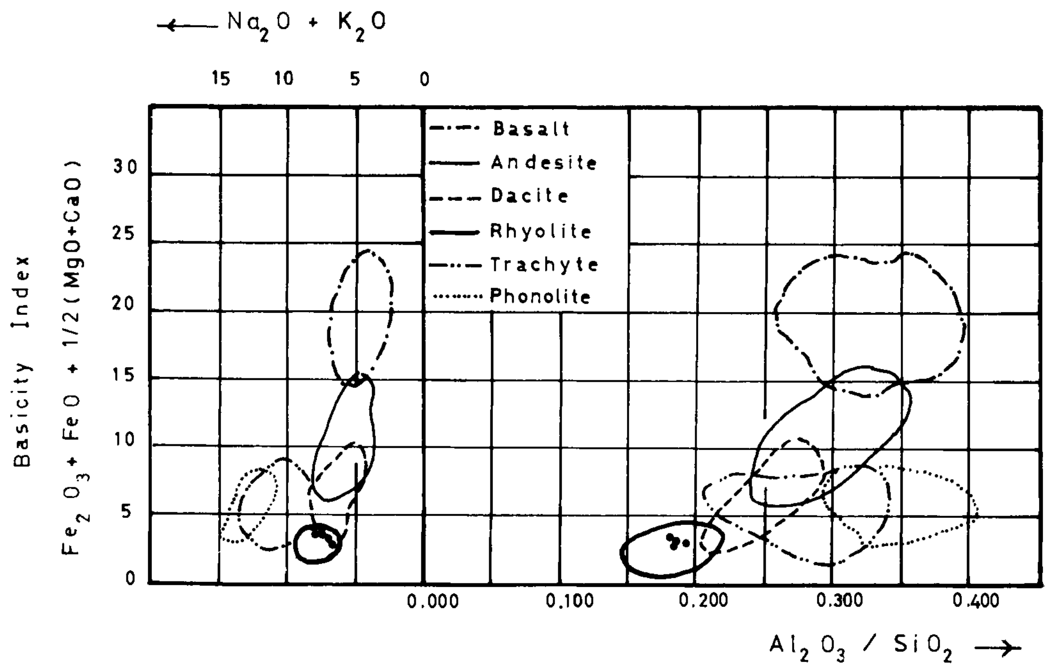

FIG. 8. Compositional classification of the Wassif ignimbritic rhyolites according to the method of Church (1975). Data from Table 1.

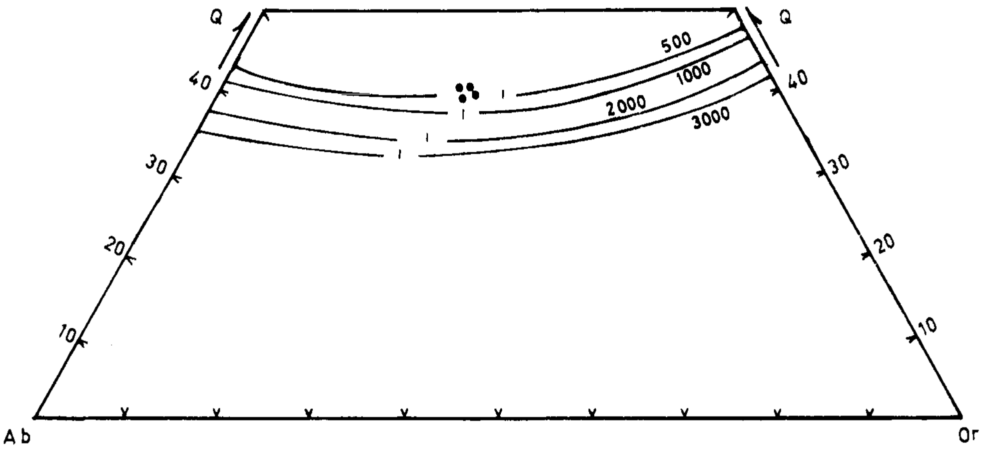

FIG. 9. Normative components of the Wasif ignimbritic rhyolites, plotted on the system Ab–Or–Q (Tuttle and Bowen, 1958). (Data from Table 1). Dashes indicate minima on boundary curves.

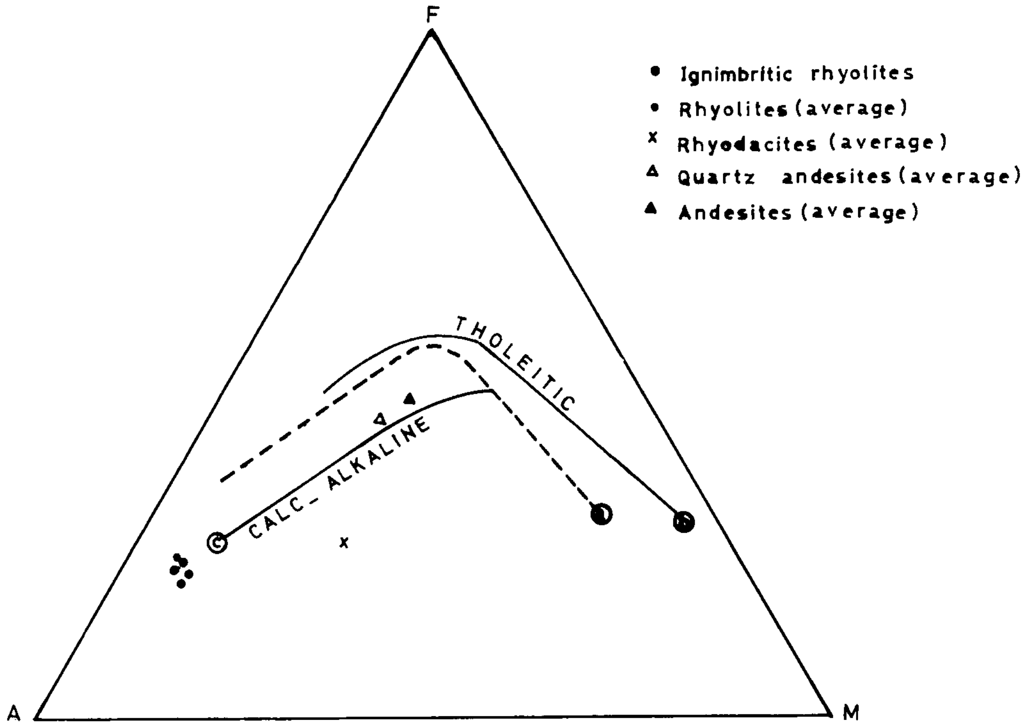

FIG. 10. AFM diagram of Wassif volcanics. (a) line separating tholeiitic (b) and calc-alkaline (c) suites, as generalised by Raschka and Muller (1975) after Irvine and Baragar (1971). A: $Na_2O + K_2O$; F: $FeO + 0.8998Fe_2O_3$; M: Mgo. Data from Tables 1 and 2.

have revealed their calc-alkaline affinity (Heikal *et al.*, 1978). In Table 2 the average chemical analyses of the main volcanic rock-types are given. Figure 10 shows these rocks on the AFM diagram (Irvine and Baragar, 1971). The rocks plot on the line for calc-alkaline suites. A trend of enrichment in alkalis and depletion in Fe and Mg contents from andesites through rhyodacites to rhyolites and ignimbrites is clear. Thus, the petrochemical data indicate that the ignimbrites are genetically related to the associated calc-alkaline suite. The rhyolitic melt which gave rise to the ignimbrites may have been derived from the calc-alkaline magma by fractional crystallisation.

The Wassif ignimbritic rocks are thought to have been formed from a hot, rapidly expanding, turbulent, highly mobile, magmatic gas cloud (nueé ardentê) which carried with it intratelluric crystals and liquid droplets of the expanding magma, as well as rock fragments torn from the walls of the

TABLE 2. AVERAGE CHEMICAL COMPOSITION (%) OF RHYOLITES, RHYODACITES, QUARTZANDESITES AND ANDESITES OF THE WASSIF AREA (HEIKAL *ET AL.*, IN PRESS).

	I	II	III	IV
SiO_2	74.01	65.45	61.50	56.35
TiO_2	0.28	0.41	0.67	0.89
Al_2O_3	13.60	16.10	15.98	18.10
Fe_2O_3	1.21	1.68	3.29	3.67
FeO	1.14	1.73	3.84	4.36
MnO	0.05	0.10	0.14	0.21
MgO	0.37	3.33	3.11	3.66
CaO	1.58	2.90	5.74	6.97
Na_2O	3.51	3.91	3.91	3.62
K_2O	4.01	2.93	1.52	0.91
P_2O_5	0.05	0.08	0.21	0.18
H_2O	0.88	0.85	0.70	0.85
Total	100.69	99.47	100.61	99.77

I. Average composition of six rhyolites.
II. Average composition of two rhyodacites.
III. Average composition of ten quartz andesites.
IV. Average composition of five andesites.

vent (Cook, 1966). The high mobility of ignimbritic rocks results from the relative high density of CO_2 which renders it more efficient than H_2O as a transporting agent for ignimbrite flows (Tazieff, 1970). The comminuted lava fragments are cushioned by hot volcanic gases so effectively that friction is eliminated and therefore the material moves as freely as a liquid.

REFERENCES

APRELKOV, S.E. 1966. Ignimbrites of the Golygin Mountains, Southern Kamchatka. Pp 104–106 in *Tufflavas and Ignimbrites* (ed. COOK, E. G.). Elsevier, New York.

BATTEY, M. H. 1966. Discussion, in VLODAVETZ, V. I., 1966, On the terms ignimbrite and ignimbritic deposits. *Bull. Volc.* 29, 141–145.

CHURCH, B. N. 1975. Quantitative classification and chemical comparison of common volcanic rocks. *Geol. Soc. Am. Bull.* 86, 257–263.

COOK, E. F. 1966. Tufflavas and Ignimbrites (ed. COOK, E. F.). Elsevier, New York.

EL-SHAZLY, E. M., HASHAD, A. H., SAYYAH, T. A., and BASSYUNI, F. A. 1973. Geochronology of Abu Swayel Area, South Eastern Desert, Egypt. *Egypt. J. Geol.* 17, 1–18.

EWART, A. 1966. Review of mineralogy and chemistry of the acidic volcanic rocks of Taupo Volcanic Zone, New Zealand. *Bull. Volc.* 29, 147–171.

FEDOROV, F. O. 1966. Lower Cretaceous ignimbrites of the Upper Amurian Country, Pp 133–137 in *Tufflavas and Ignimbrites* (ed. COOK, E. F.). Elsevier, New York.

GINDY, A. R., and MOHAMMED, M. R. 1971. A Precambrian laminated ignimbrite and its lithophysae in Wadi Nuqara, southwest of Port Safaga, Red Sea Province. *Bull. Fac. Sci. Alexandria Univ.*, XI, 145–177.

HATCH, F. H., WELLS, A. K., and WELLS, M. K. 1972. *Petrology of the Igneous Rocks.* George Allen and Unwin, London.

HEIKAL, M. A., KHAFFAGY, M. B., and EL-RAHMANY, M. Chemistry and differentiation indices of the Wassif volcanics—calc-alkaline suite, Eastern Desert, Egypt. *Bull. Faculty Sci. King Abdulaziz University*, Jeddah, in press.

IRVINE, T. N., and BARAGAR, W. R. A. 1971. A guide to the chemical classification of the common volcanic rocks. *Can. J. Earth Sci.*, 8, 523–548.

MARSHALL, P. 1935. Acid rocks of Taupo-Rotorua volcanic district. *Trans. Proc. Roy. Soc. New Zealand*, 64, 323–326.

PETTIJOHN, F. J. 1975. *Sedimentary Rocks* (3rd Ed.). Harper and Row, New York.

RASCHKA, H., and MÜLLER, P. 1975. Contributions to the geochemistry of volcanic rocks, Afar region, Ethiopia. *Proc. Intern. Symp. Afar Region.* Bad Bergzabern, F.R. Germany 1, 341–351.

RITTMANN, A. 1966. Discussion, in VLODAVETZ, V. I. 1966. On the terms ignimbrite and ignimbritic deposits. *Bull. Volc.* 29, 141–145.

ROSS, C. S., and SMITH, R. L. 1961. Ash-flow tuffs: their origin, geologic relations and identification. *U.S. Geol. Survey Prof. Paper* 366, 81 pp.

SCHIEFERDECKER, A. A. G. 1959. *Geological Nomenclature.* Goringhem, Copenhagen.

SCHURMANN, H. M. E. 1958. Massengesteine aus Agypten, 18. Teil: Die Prekambrischen gneise und schiefer in noreichen Teil der ostilichen Wüste. *Neues Jb. Geol. Paleontol.* Abh. 107, 103–136.

SCHURMANN, H. M. E. 1959. Massengestage aus Agypten, 19. Teil: Prekambrische kristalline schiefer und gneise der ostilichen Wüste 28°30′ und 27°30′ nordl. Breite, *Neues Jb. Geol. Palaontol.* Abh. 108, 137–149.

SHAPIRO, L., and BRANNOCK, W. W. 1962. Rapid analysis of silicate, carbonate, and phosphate rocks. *U.S. Geol. Survey Bull.* 1144-A.

TAZIEFF, H. 1970. Investigations on eruptive gases. *Bull. Volc.* 34, 421–438.

TUTTLE, O.F., and BOWEN, N. L. 1958. Origin of granite in light of experimental studies. *Geol. Soc. Am. Mem.* 74.

VLODAVETZ, V. I. 1966. On the terms ignimbrite and ignimbritic deposits. *Bull. Volc.* 29, 141–145.

ZAVARITZKY, A. N. 1955. *Eruptive Rocks.* Acad. Sci., U.S.S.R.

جيوكيميائية صخور الأپوچرانيت ، أبو دباب ،
وسط الصحراء الشرقية ، مصر

ع.ح. ثابت ، ج. قطب ، م.ح. حتحوت ، م.م. على

الخلاصة

يتكون چرانيت أبو دباب من أربع سحنات : صخور مسكوفيتية دقيقة التحبب وصخور مسكوفيتية متوسطة التحبب وفتاتيات نارية وصخور معدنية التحول. وتُصنّف الصخور المسكوفيتية المتوسطة التحبب الى طُرُز ألبيتية ومتسلسة بينما تحت مجموعات السحنات المعدنية التحول هى: طرز شرائطية وپچماتانية وألبيتية وكوارتز ألبيتية. وقد تم التحليل الكيميائى لعينات ممثلة لكل هذه السّحنات لتقدير محتواها من أكاسيد أساسية وعناصر ضئيلة ، كما عينت صفاتها الكيميائية الصخرية (الپتروكيميائية).

وغالبا ماتشترك السّحنات الأربع فى افتقارها لعناصر: الحديد - المغنسيوم - الكلسيوم - التيتانيوم - الفسفور ، وفى اغتنائها بالعناصر المُجَرْنِتَة (القليّات والسليكا) بمقارنتها بالچرانيتات الفاتحة اللون. وهى تحوى مقاديرّ كبيرةً من البيوتيت والمعادن الثانوية ، ودائما مايسود التنتانوم النيوبيوم فى كل سَحنة بنسب تتراوح بين ٢:١ ، ٤:١ . وفى معظم السحنات يوجد القصدير على هيئة كسّيتريت بكمية تزيد على ١٠٠٠ جزء فى المليون. ويشبه الأپوچرانيت هنا صخورَ الچرانيت القَلِىّ الأپليتية فى صحبة دِترو بالكاربات الشرقية.

وتغيّرُ قِيَم الپوتاسيوم/الصوديوم فى مُكَوِّن الفلسپار هوالخاصية المميزة الأساسية بين السحنات الأربع . وهى قليلة نسبيا فى السحنات الدقيقة التحبب وتزداد تدريجيا فى الصخور المتوسطة التحبب والفتاتيات النارية لتصل الى حدها الأقصى فى پچماتانيات السحنات المعدنية التحول (الأحدث).

GEOCHEMISTRY OF ABU DABBAB APOGRANITE, CENTRAL EASTERN DESERT, EGYPT

A. H. SABET[1], H. KOTB[2], M. M. ALY[1] and A. H. HATHOUT[1]

[1]Geological Survey of Egypt, Cairo, Egypt
[2]Institute of Applied Geology, Jeddah, Saudi Arabia

Abstract—The Abu Dabbab apogranite consists of four main facies, namely, fine-grained and medium-grained muscovite–microcline–quartz–albite apogranite, and porphyroblastic and metasomatic varieties developed in the fissure zones. The medium-grained facies is subdivided into albitic and silicified types, and the metasomatic facies into banded, pegmatoidal, albitic and quartz-albitic types. The four facies vary fundamentally in textural and structural features and in their average contents of the main rock-forming minerals. Representative samples of all facies were chemically analysed for major oxides and minor elements, and their petrochemical characteristics were determined.

Generally, the four facies are deficient in Fe, Mg, Ca, Ti, and P, and have high contents of the granitising elements (i.e. alkalis and silica) as compared with analogous leucocratic granites from other parts of the world. Comparable amounts of biotite and accessory minerals are present in all types. Ta values always predominate over those of Nb within each facies, with ratios varying from 2:1 to 4:1. The Sn contents are almost always over 1000 ppm in most of the facies, Sn being present mainly as cassiterite. The Abu Dabbab apogranite is closely similar to the alkali granite aplitic rocks of the Ditro-association of the Eastern Carpathians.

The variation in the values of K/Na in the feldspar component is the main distinguishing character among the four facies. It is relatively low in the fine-grained facies and increases gradually in the medium-grained and

porphyroblastic rocks, reaching its maximum in the youngest facies, the metasomatic pegmatoids, commonly developed along the fissure zones.

INTRODUCTION

As a result of combined geological, geochemical and geophysical prospecting and exploration work carried out on the late Proterozoic basement rocks in the central Eastern Desert of Egypt, new deposits of tantalum and other associated rare metals connected with apogranites have been discovered at Abu Dabbab, as well as in some other localities (Fig. 1). The term "apogranites" connotes metasomatic rocks formed as a result of intensive post-magmatic alteration of granitoids by high-temperature solutions, causing deep changes in the chemical and mineralogical composition as well as in the structure and texture of the mother granite (Beus *et al.*, 1962). These apogranites seem to be spatially and genetically related to the intrusive complex of the last phase of the Gattarian granites and particularly to the more leucocratic varieties of the concluding sub-phases. Block tectonics and rupture disturbances created favourable circumstances for their intrusion (Sabet *et al.*, 1973).

GEOLOGICAL SETTING

The Abu Dabbab apogranite mass is situated at the periphery of the Mobarak tectonic block in the area of the arched bend of an ultrabasic belt where faults of N.W., sub-meridional and N.E. trends intersect. It outcrops in the form of a truncated cone about 0.06 km^2 in area and 100 to 130 m in height. In plan, the main part of the mass is oval, measuring 290 m by 200 m, and elongated in the N.W. direction, with a narrow off-shoot up to 140 m long and 50–20 m wide on its north-western flank. The shape of the apogranite mass is assumed to be an inclined stock-like body dipping 38°ESE, with its upper part widened owing to the wedge-like projections.

Different varieties of late Proterozoic geosynclinal paraschists, intercalated with metamorphosed tuff–sandstones and tuff–gritstones, occur at the southern and western contacts of the mass. These strike N.E.–S.W. or nearly North–South; talc-carbonate rocks with relicts of serpentinites are

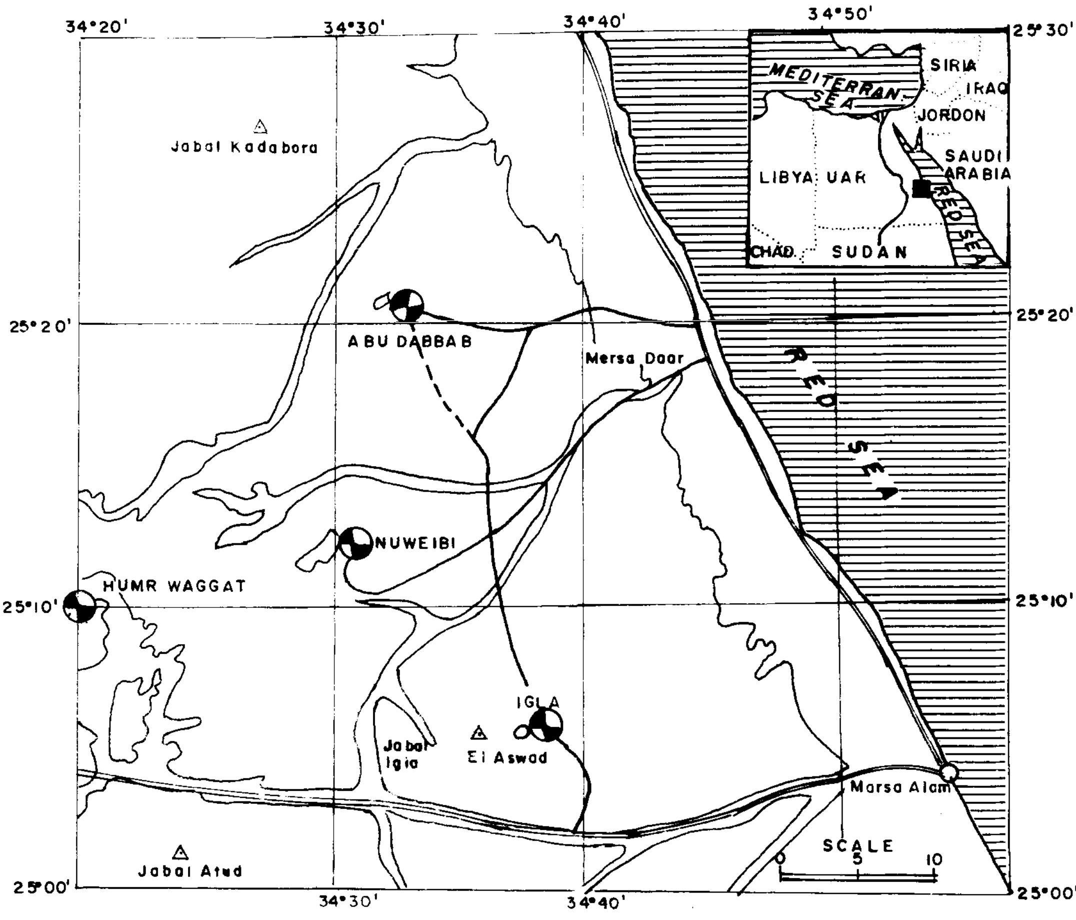

FIG. 1. Map showing occurrences of rare-metal deposits in the Central Eastern Desert region of Egypt. Inset: Location map.

developed at the contact. A laccolith-like body of metamorphosed andesite forms the northern contact, particularly at the junction of the main part of the mass and the off-shoot.

The country rocks are usually greisenized and brecciated over a distance of 1–12 m away from the contact. Quartz-muscovite veins develop along the contact proper as a narrow fringe up to 0.8 m wide. The northern and southwestern contacts are zones of tectonic breccias in which the fragmented material (greisenized meta-andesites or paraschists) makes up 70% and is cemented by quartz-limonite material (up to 30%). A shear zone, 5–12 m wide and 0.5–1.0 m thick, with spots of greisenization and lit-par-lit injections, occurs along the south-western contact. A lens-like body of eruptive breccias occurs at the southern and southwestern contacts where it is traced for 100–150 m along the strike and for 40–60 m along the dip, with a maximum thickness of 20 m. It consists of fragmented material (50–80%) of greisenized meta-rhyolites and tuff–sandstones cemented together with fine-grained muscovite–microcline–quartz–albite apogranites. Thin zones of brecciated rocks with quartz–calcite veins and small lenses (0.5–1.0 m) of metasomatites are also traced along the lower boundary of the mass (Fig. 2).

LITHOLOGY

According to Sabet *et al.* (1976), four groups of rocks can be distinguished within the mass, each group being characterised not only by structural and textural features but also by average contents of albite, microcline, quartz and muscovite. These groups are briefly described below.

Fine-grained muscovite–microcline–quartz–albite apogranites

These form the apical and marginal parts of the mass and represent later facies with respect to the apogranites in the central part of the mass. They are compact, light-grey or greenish-grey rocks composed of muscovite (8–12%), microcline (10–12%), quartz (20–25%) and albite (48–52%).

Medium-grained, muscovite–microcline–quartz–albite apogranites

Two varieties are present, namely, an albitized variety and a silicified variety. Both varieties occur widely and make up the central part of the mass, reaching up to 400 m in thickness.

They are white to light-grey or greenish-grey rocks with the groundmass made up of albite and microcline with dispersed rounded grains of quartz (1.5–2.8 mm across), impregnations of microline (0.8–2.2 mm across) and small amounts of muscovite. The relative proportions of the main rock-forming minerals vary, the average composition being 40–50% albite, 10–20% microcline, 25–40% quartz, and 5–8% muscovite.

Porphyroblastic muscovite–microcline–quartz–albite apogranites

These are found in the core of the mass where they are associated with pegmatitic apogranites. The distinctive feature of this facies, when compared with the rocks of the two upper facies, is their higher content of quartz (up to 45%), present as coarse disseminated porphyroblasts up to 3–5 mm across. In other respects they are almost the same, with 35–45% albite, 10–20% microcline and 2–4% muscovite.

Metasomatic facies of the fissure zones

This facies is younger than the main facies of the apogranites of the mass and is related to the various systems of fractures. Several varieties are present, of which the banded apogranites are the oldest and the pegmatoidal varieties somewhat younger or contemporaneous with the banded apogranites. The two varieties bear signs of later albitization and are cut by the albitites. The greisens are the latest rocks, being developed along the fractures and cutting and displacing the rocks of the fissure facies as well as the quartz–cassiterite and the quartz–microcline veins. The metasomatic varieties of the fissure zones include:

a. banded muscovite–microcline–quartz–albite apogranites;
b. albite and quartz–albite;
c. muscovite–quartz and quartz–muscovite greisens.

Metasomatic zonation of the apogranite mass is seen in the variation in chemical composition of the rocks from the abyssal horizons up to the apical part, and by the distribution of Ta, Nb, Sn and associated indicator elements. The metasomatic facies of the fissure zones play a subordinate role and develop only along the systems of joints intersecting the apogranites of the first three facies (Sabet *et al.*, 1976).

GEOCHEMISTRY

Major Elements

The detailed petrography and mineralogy of the different facies has been given by Sabet *et al.* (1976). To determine the geochemical and petrochemical characteristics of Abu Dabbab apogranites, 36 samples representing the four groups were subjected to complete chemical analysis and their Niggli parameters and normative compositions determined (Table 1); their standard cells are averaged in Table 2.

The component oxides of the different facies of

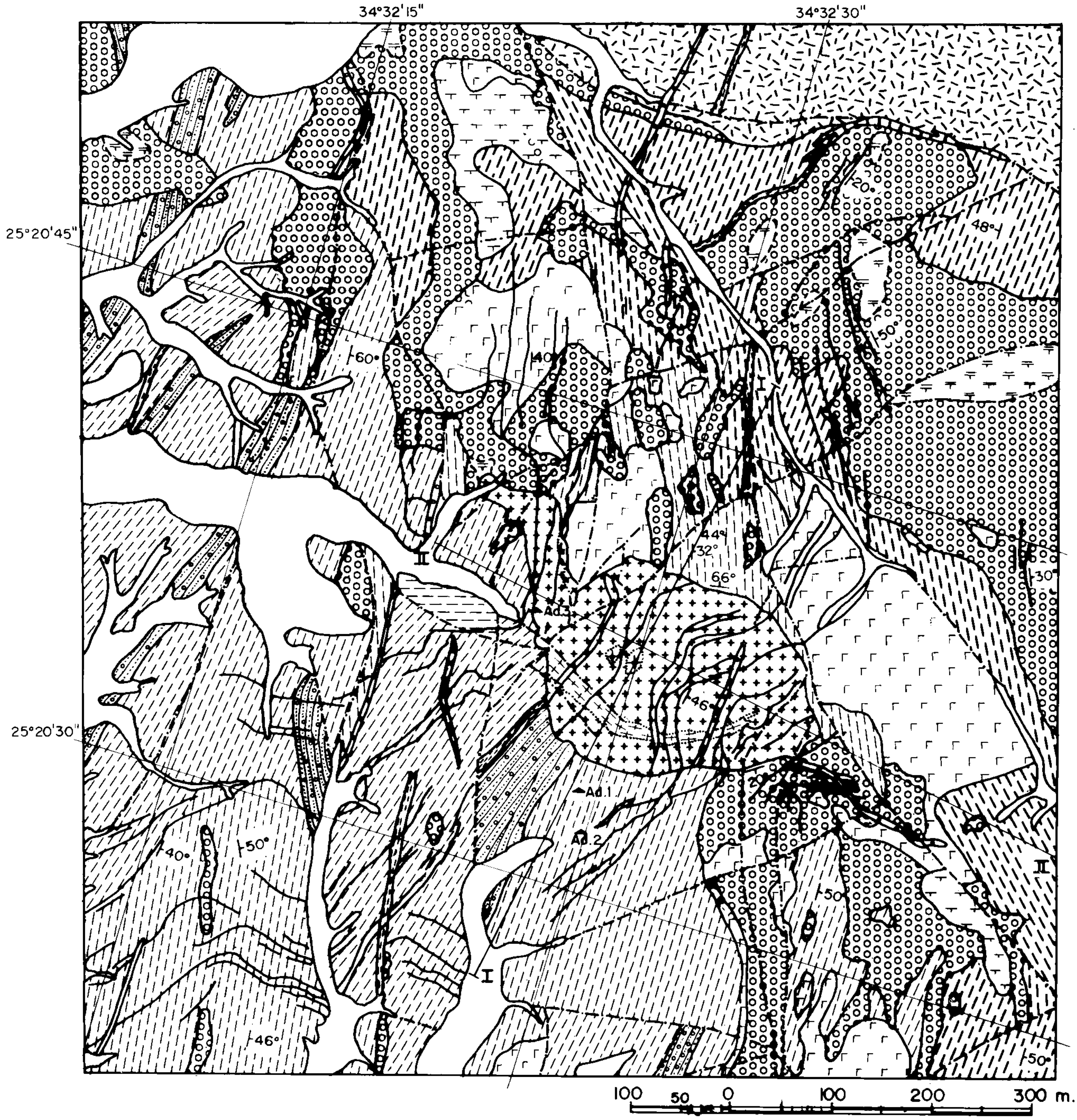

FIG. 2. Geological map of Abu Dabbab. (After Sabet *et al.*, 1976). 1, Wadi deposits: sand rock detritus with rare pebbles. 2, Porphyritic dolerite dykes. 3, Quartz–calcite veins and lenses. 4, Quartz–topaz–fluorite, quartz–cassiterite, quartz–microcline, quartz–amazonite and greisen veins. 5, Fine- and medium-grained muscovite–microcline–quartz–albite apogranite. 6, Fine-grained muscovite–microcline–quartz–albite apogranite. 7, Silicified fine- and medium-grained porphyritic muscovite–microcline–quartz–albite apogranite. 8, Fine- and medium-grained muscovite–microcline–quartz–albite apogranite enriched with albite. 9, Porphyroblastic muscovite–microcline–quartz–albite apogranite. 10, Leucocratic gabbro. 11, Serpentinite. 12, Talc-carbonate rocks. 13, Quartz–biotite orthoschists. 14, Meta-andesite and meta-basalt. 15, Meta-rhyolite. 16, Metamorphosed tuff-sandstone and tuff-gritstone. 17, Quartz–chlorite–biotite paraschists. 18, Tectonic disturbances. 19, Shatter and shear zones. 20, Suggested geological contacts. 21, Geological contacts of apogranite facies. 22, Reliable geological contacts. 23, Adits and their numbers.

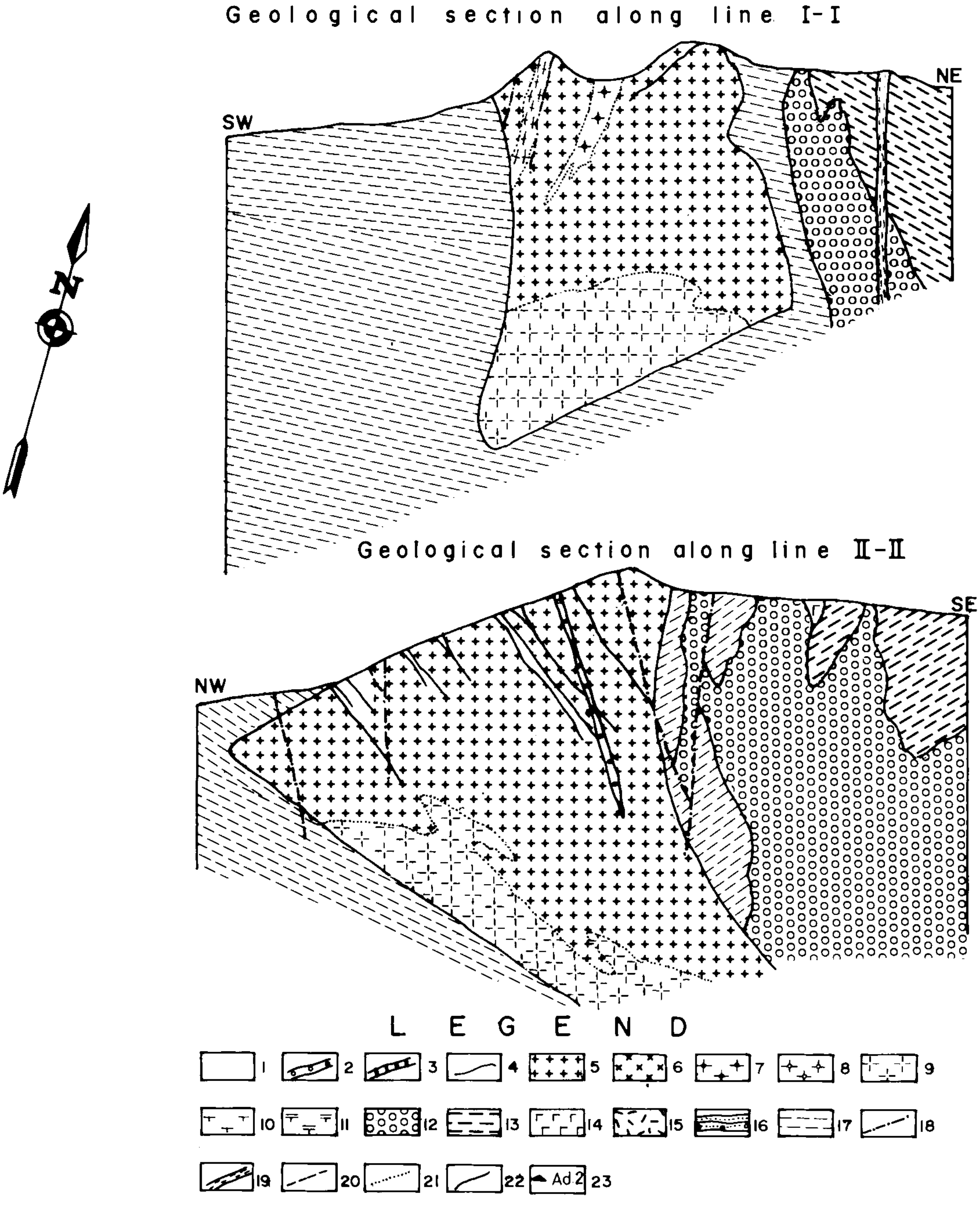

FIG. 2. (*continued*)

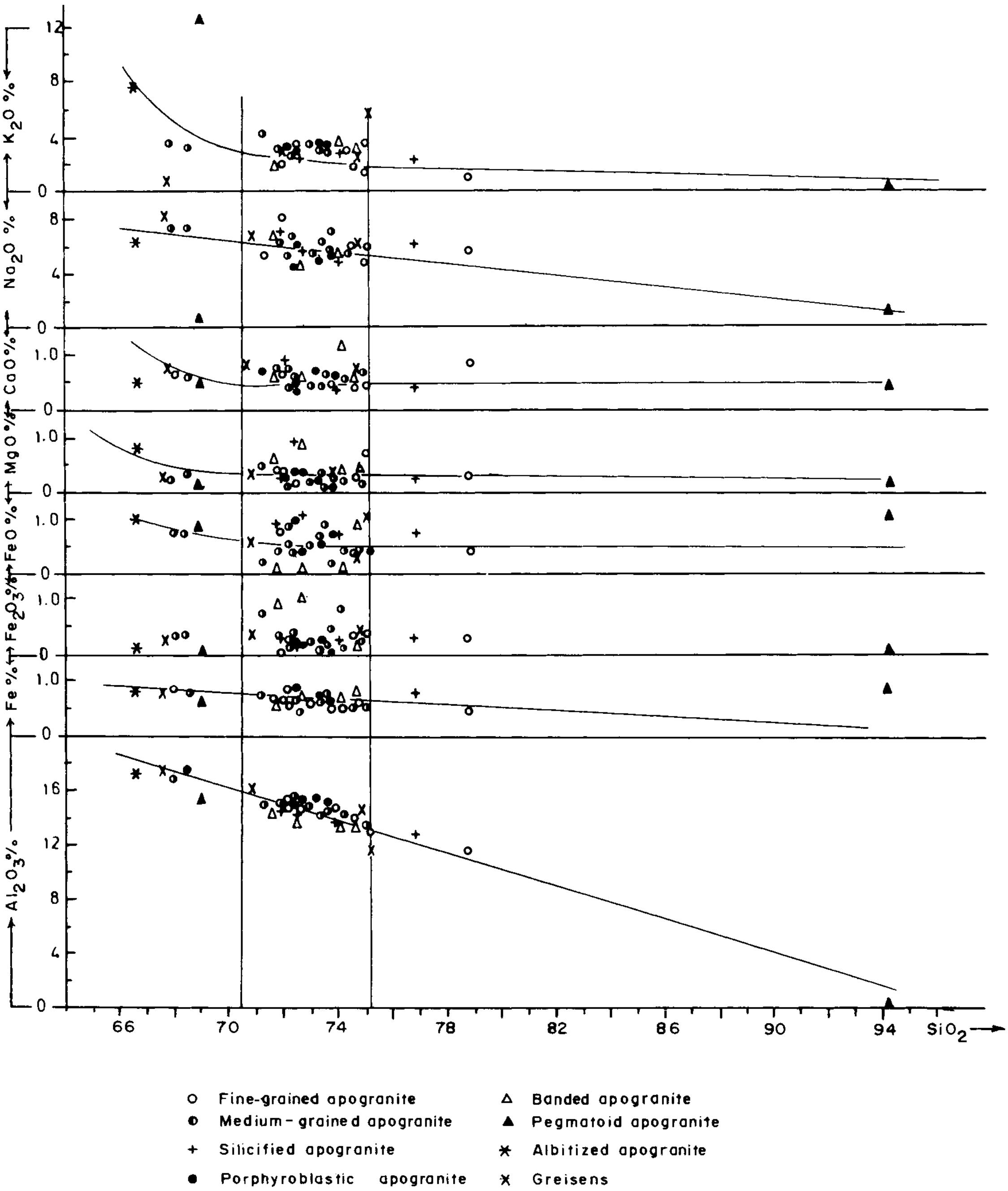

FIG. 3. Variation diagram of component oxides against silica content in the different facies of the Abu Dabbab apogranite.

Abu Dabbab are plotted against their silica content in the variation diagram (Fig. 3). Most of the samples, with the exception of the pegmatoidal facies, fall within the silica range 70.5–75%. The alkaline oxides, alumina, and total Fe contents decrease steadily with increase in silica, while MgO, CaO and K_2O contents show a sharper decrease within the silica region less than 70.5%.

As can be seen from Table 1, the albitized apogranites contain the lowest silica values (66.8%). The non-silicified medium-grained facies, the greisen facies, the silicified medium-grained porphyroblastic facies and the banded apogranites have mean SiO_2 contents of 72.3–73.4%. The fine-grained apogranite has a higher silica content, averaging 75.2%, while the pegmatoid facies contains 69.1% and this increases to 94.3% in its silicified varieties.

Alumina amounts to 17.2% in the albitized facies and decreases to around 15.1% in the medium-

TABLE 1. THE MEAN CHEMICAL COMPOSITION OF THE DIFFERENT FACIES OF ABU DABBAB APOGRANITE.

Type	Fine-gr. Apogranite (4)*	Med.-gr. Apogranite Type a (13)	Med.-gr. Apogranite Type b (4)	Porphyro-blastic Apogranite (4)	Metasomatic facies: Banded Apogranite (4)	Metasomatic facies: Pegmatoidal Apogranite (2)	Metasomatic facies: Albitized (1)	Metasomatic facies: Greisen type (4)
Major oxides (weight percent)								
SiO_2	75.17	72.39	73.92	73.05	73.31	81.66	66.77	72.16
Al_2O_3	13.46	15.07	13.59	15.15	13.84	8.35	17.21	15.04
Fe (total)	0.59	0.65	0.82	0.67	0.74	0.80	0.80	0.79
Fe_2O_3	0.30	0.32	0.21	0.22	0.74	0.02	0.11	0.37
FeO	0.49	0.58	0.88	0.67	0.29	1.02	0.93	0.69
MgO	0.44	0.26	0.42	0.28	0.60	0.17	0.77	0.45
CaO	0.60	0.62	0.55	0.58	0.72	0.56	0.44	0.78
Na_2O	6.68	6.23	5.95	5.21	5.38	0.98	6.20	6.29
K_2O	1.72	3.34	2.74	3.58	3.12	6.60	7.23	3.22
H_2O^+	0.48	0.61	1.17	0.86	1.03	0.40	0.49	0.56
Minor elements (p.p.m.)								
P	70	102	87	83	93	105	100	163
Nb	51	65	62	65	78	14	80	82
Ta	172	277	169	270	187	45	156	251
Ti	400	502	383	350	295	210	300	530
Sn	1723	1500	1837	138	1870	85	65	1188
Mn	1690	1948	1510	950	4843	385	3390	1768
Niggli values								
si	436	392	415	404	404	566	283	371
al	45	47	45	49	45	53	43	45
fm	8	7	10	7	11	8	10	9
c	4	3	3	3	4	4	2	4
alk	43	43	42	41	40	30	45	42
mg	0.45	0.29	0.34	0.34	0.40	0.22	0.49	0.35
k	0.14	0.26	0.23	0.32	0.24	0.60	0.44	0.21
Q%	54.90	51.28	53.42	54.75	54.27	63.14	38.48	50.50
L%	41.81	45.90	43.49	42.09	41.77	30.60	55.08	46.56
M%	3.29	2.81	3.08	3.16	3.96	6.24	6.44	2.93
Normative composition (weight percent)								
or	10.17	19.87	15.91	19.62	17.67	40.00	42.94	19.06
ab	57.85	54.63	54.14	47.31	49.13	8.49	51.31	56.08
an	1.74	2.48	1.99	2.89	2.82	2.72	—	2.62
Mica	2.27	1.95	2.20	2.32	2.28	7.88	2.98	1.44
Q	27.19	20.50	24.80	26.86	26.46	41.02	1.62	19.20
Accessories	0.85	0.90	0.86	0.98	1.61	0.38	1.14	0.93

*No. of samples

TABLE 2. THE AVERAGE STANDARD CELLS OF THE DIFFERENT FACIES OF ABU DABBAB APOGRANITE.

Rock type	Cation/160 oxygen atoms: K	Na	Ca	Mg	Mn	Fe^2	Fe^3	Al	Si	P	O	(OH)
Fine-grained Apogranite	1.87	11.14	0.41	0.57	0.15	0.36	0.21	13.63	64.07	0.01	154.50	5.50
Medium-grained Apogranite												
a. non-silicified type	3.71	10.54	0.57	0.31	0.16	0.42	0.21	15.41	63.00	0.02	152.68	7.32
b. silicified type	3.00	9.87	0.52	0.52	0.15	0.62	—	13.75	63.69	0.02	146.56	13.44
Porphyroblastic Apogranite	3.94	8.71	0.51	0.36	0.10	0.47	0.16	15.40	63.13	0.01	150.14	9.84
Metasomatic Apogranite												
a. Banded type	3.42	8.98	0.67	0.77	0.47	0.21	0.47	14.06	63.40	0.02	148.18	11.82
b. Pegmatoidal type	14.14	0.31	0.54	0.22	0.05	0.70	—	16.14	62.14	0.01	150.50	9.50
c. Albitized type	8.63	4.28	6.45	1.07	0.34	0.73	0.06	13.77	62.80	0.02	153.90	6.10
d. Greisen type	3.55	10.55	0.73	0.57	0.16	0.52	0.26	15.41	62.84	0.03	153.72	6.28

grained, porphyroblastic, greisen and pegmatoidal apogranites. It decreases further to around 13.7% in the fine-grained and silicified medium-grained facies, and reaches a minimum value of 1.4% in the silicified pegmatoidal apogranite.

The different facies of the apogranites are characterised by low average iron contents, generally less than 0.9%. The ferrous iron content always predominates over the ferric iron, except in the banded and the silicified pegmatoidal facies. The average MgO% is always less than 0.5% in the different facies except for the banded apogranite which contains 0.6%. CaO, which predominates over MgO, is less than 0.8%. The fine-grained, medium-grained, banded, albitized and greisen facies show an average Na_2O content around 6.3% which decreases to 5.2% in the porphyroblastic apogranite; the values of Na_2O however, decrease to 1.5% and 0.5% in the pegmatoidal and silicified facies respectively. The pegmatoidal and the albitized facies are characterized by the highest K_2O contents (12.4% and 7.2% respectively), exceeding their Na_2O contents, unlike in the other facies. The K_2O content of the medium-grained, porphyroblastic, banded and greisenised apogranites averages around 3.4% and decreases to 2.7% to 1.7% in the silicified medium- and fine-grained facies; the minimum K_2O content (0.8%) is recorded in the silicified pegmatoidal apogranite.

Minor Elements

Abu Dabbab apogranites are enriched to a greater or lesser extent in tantalum, niobium and tin (Table 1). The average contents of Ta and Nb in granites generally are 4 and 20 ppm respectively (Turekein and Wedepohl, 1961), whereas in the main facies of Abu Dabbab the mean Ta content is around 273 ppm, in the minor facies it ranges from 169 to 251, and decreases in the pegmatoidal facies to around 45 ppm. In all facies the Nb content ranges from 51 to 82 ppm, with only 14 ppm in the pegmatoids. Ta is predominant over Nb in all the facies. In the medium-grained and porphyroblastic facies the ratio of Nb/Ta is 1:4, whereas in the other varieties it varies from 1:2 to 2:7, reflecting less intensive initial accumulation of Nb as compared to Ta. This is in contrast to the apogranite of Stare-Dubrovsk (Lavirnenko and Mishchenko, 1969) and to albitized-greisenized apogranites generally (Beus *et al.*, 1962). Pegmatitization caused impoverishment in both Nb and Ta and local albitization was accompanied by removal of Ta, as shown by Grabezbev (1971).

The medium-grained and the greisenised apogranites contain relatively high values of Ti, around 500 ppm, but this decreases through the other facies to 210 in the pegmatoids and apogranites. The Ti contents are low when compared with figures for similar rocks in other parts of the world (e.g. Nockolds, 1945; Green and Poldervaart, 1958; and Turekein and Wedepohl, 1961) which are almost always over 1000 ppm. This may be due to either the leaching of Ti by metasomatism or its deficiency in the mother rock. The Ti contents show a positive correlation with those of Ta + Nb (Fig. 4), and this is attributed to the close crystallochemical character of Ti to both Nb and Ta (Kuz'menko, 1969).

The fine-grained, banded and silicified facies contain a mean Sn value of around 1800 ppm, decreasing to around 150 ppm in the porphyroblastic and pegmatoidal apogranites, and to minimal values of 65 ppm in the albitized facies. The high values of Sn (over 1000 ppm) are reflected in the presence of cassiterite as a separate mineral. Ti

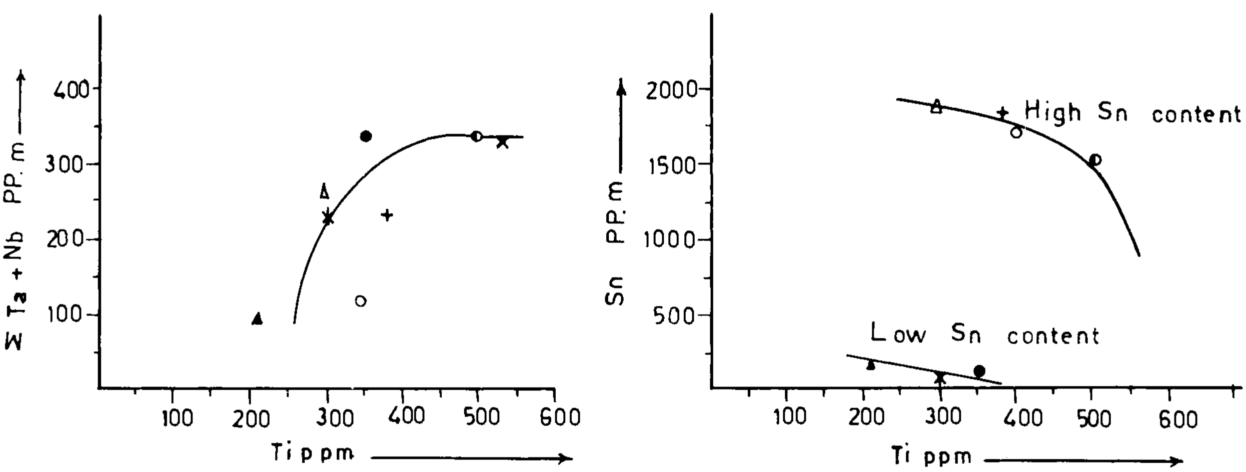

FIG. 4. Correlation diagrams for Ta + Nb against Ti, and Sn against Ti in the different facies of the Abu Dabbab apogranite. (symbols as for Fig. 3).

shows negative correlation with Sn (Fig. 4), suggesting isomorphous replacement due to similarities in the ionic radii, coordination number, electro-negativity and coefficient of ionic substitution (Green, 1959).

The mean values of P are mostly around 85 ppm ± 15, with the exception of the greisen which contains 163 ppm. Such values are low when compared with those of Nockolds (1954) or Gruza and Myzinkov (1970). Thus, the deficiency in P as well as Ti is a geochemical character of the Abu Dabbab apogranites.

The Mn content ranges from 4834 ppm in the banded apogranites to 385 ppm in the pegmatoidal facies. It is noticed that the facies characterized by relatively high Sn contents also contain high Mn values, despite the non-similarity between the two elements with respect to their crystallochemical properties.

Niggli Values

The Niggli values of the Abu Dabbab apogranites (Table 1) are comparable to those of alkali granite of Nockolds (1964) except for their lower *fm* and higher *alk* and *mg* values, the latter indicating that their femic minerals are magnesian-rich. On a QLM diagram (Fig. 5) the Abu Dabbab apogranites are seen to be closer to the alkali-granite aplitic rocks of Ditro-association on the

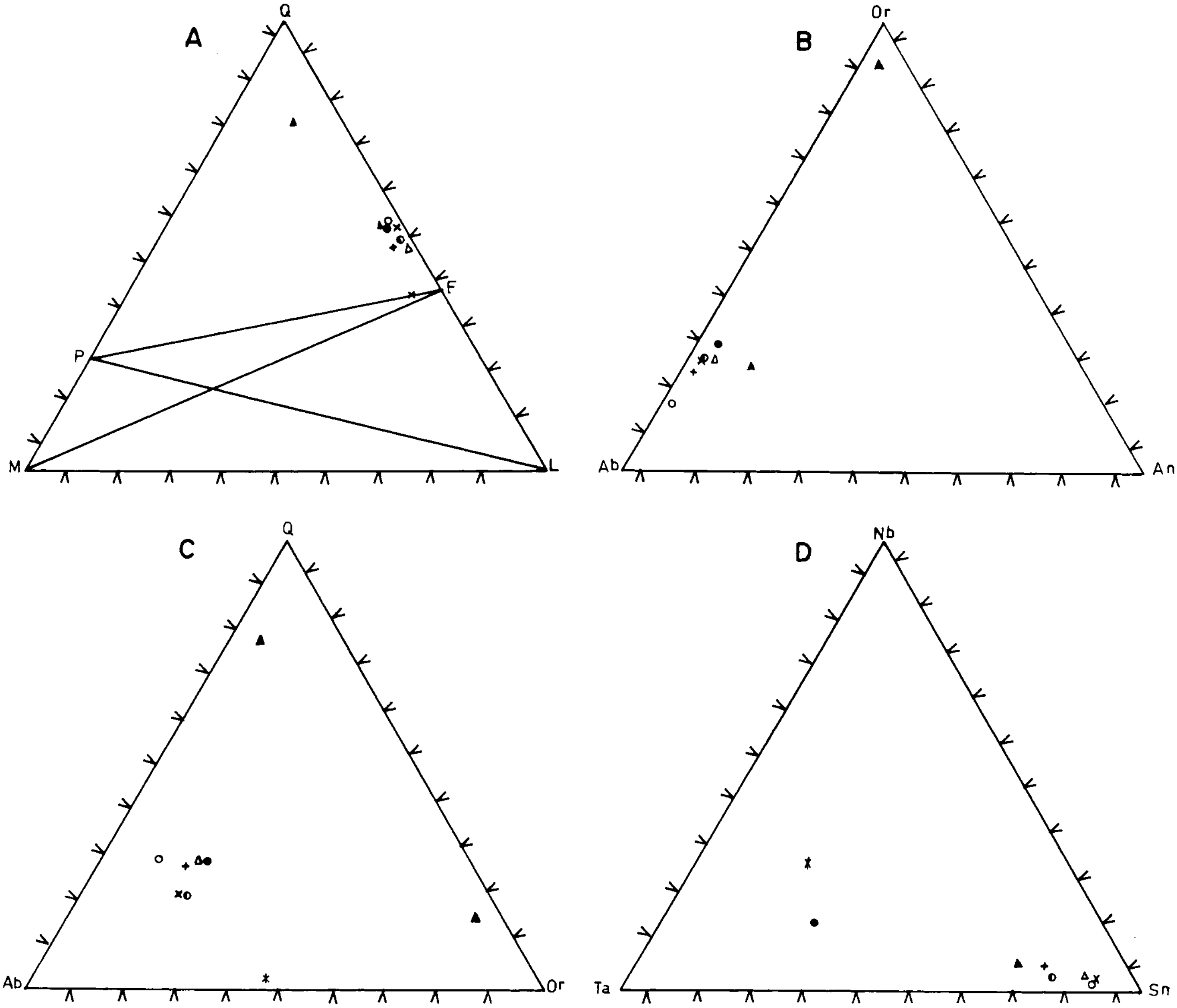

FIG. 5. Triangular diagrams for the different facies of the Abu Dabbab apogranite. A. Q–L–M: B. Or–An–Ab: C. Q–Or–Ab: D. Nb–Ta–Sn.

inner margin of the Eastern Carpathians (Streckeisen, 1960).

An increase in the mean values of *al* and *k* and a decrease in those of *fm*, *c*, *alk* and *mg* is noticed when passing from the fine- to the medium-grained and the porphyroblastic facies. Niggli values of the banded facies are closer to those of the porphyroblastic apogranite. The albitized facies is distinguished by the highest values of K and L and the lowest value of Q. The greisen apogranite is characterized by low Q and higher L values relative to those of the other metasomatic facies. The silicified apogranite is similar to the fine-grained facies in *si* and *al*, to the medium-grained facies in *alk* and *k* and to the porphyroblastic facies in *c* and *mg*. The Niggli values of the pegmatoidal apogranites are also variable.

Normative Composition

As seen from Table 1, the mean mica contents as well as those of the accessories are comparable in the different facies of the Abu Dabbab apogranites. The plagioclase value in the fine-grained, medium-grained and porphyroblastic facies is Ab_{95}, pointing to their albitic character. The medium-grained and the porphyroblastic apogranites are characterized by relatively high microcline content, averaging 19.7% Or, in contrast to the fine-grained facies, with an average of 10.2%. The mean Qz content in the fine-grained and the porphyroblastic apogranites is 27%.

The albitized facies is distinguished by its high microcline content of 42.9%, the microcline+albite content constituting 94% of the rock, and quartz being only 1.6%. In the greisen facies the albite content varies linearly with the content of quartz and inversely with the microcline content. The silicified apogranite is similar in its normative composition to the fine-grained facies, but the former contains a higher amount of microcline and a lower amount of albite.

When plotted on a normative An–Or–Ab diagran (Fig. 5), the Abu Dabbab apogranites, with the exception of the albitized and the pegmatoidal facies, are parallel and close to the Or–Ab side. The area occupied by these facies is bounded by Or_{15-30}, Ab_{70-75}, An_{2-7}. The potassic character of the rocks increases gradually from the silicified types, through the greisen, medium-grained, and banded facies, to the porphyroblastic facies. The feldspars of the pegmatoidal facies are either more calcic or potassic than sodic. The feldspars of the banded facies are non-calcic, the Ab:Or ratio being about 4:3.

The affinities of the albitized and pegmatoidal apogranites in the normative Or–Q–Ab triangle (Fig. 5) also deviate from those of the other facies. Within the same quartz content, both the fine-grained and the greisen facies show comparable Or–Ab ratios. The albitized apogranite is located on the Ab–Or side in both normative composition diagrams because of a lack of quartz. By the increase of the normative quartz in the pegmatoid facies, the alkali feldspar content decreases.

SUMMARY

The petrochemical characteristics of the different facies can be summarized as follows:

a. Deficiency of Fe, Mg and Ca with increase of alkalis and silica is a general character for the different facies compared to other alkali- and leucocratic-granites.
b. The fine-grained facies is characterized by the lowest potassium value and the highest albitic feldspar content.
c. The medium-grained facies show high alumina content resulting in a relatively pronounced feldspathic character with more potassic affinity than those of the fine-grained facies.
d. The feldspars of the porphyroblastic facies are relatively more potassic than those of the fine- and medium-grained facies, with comparable values of Si and Al.
e. The banded and porphyroblastic facies are closely similar. The greisen is comparable to the medium-grained facies. The albitized facies is distinguished by the highest total alkali content and an Na_2O/K_2O ratio of only 0.85.
f. The metasomatic processes that produced the pegmatoidal apogranites varied greatly in nature. Leaching of soda and enrichment of potash gave rise to high microcline and low soda feldspar contents. Elsewhere the reaction resulted in silica-rich pegmatoidal apogranites. Soaking of the country rocks with silica resulted in a decrease of the alkali content and the formation of rocks with high normative quartz.

REFERENCES

BEUS, A. A., SEVEROV, E. A., SITNIN, A. A., and SOBBOTIN, K. D. 1962. Albitized and greisenized granites (apogranites). U.S.S.R. Academy of Sciences, Moscow.

GRABEZHEV, A. I. 1971. Near-fracture albitization in the fine-grained zone of microcline-albite pegmatites in the Urals. *Geokimiya*, 11, 1379–1382.

GREEN, J. 1959. Geochemical tables of the elements for 1959. *Geol. Soc. Am. Bull.*, 79.

GREEN, J., and POLDERVAART, A. 1958. Petrochemical fields and trends. *Geochim. Cosmochim. Acta*, 13, 87–122.

GRUZA, V. V., and MYZINKOV, V. A. 1970. Phosphorus in genetic series of igneous rocks. *Geochim. Intern.*, V, 245–255.

KUZ'MENKO, M. V. 1969. Geochemistry of tantalum and niobium. *Trudy IMGRE Akad. Nauk SSSR.*, No. 3.

LAVRINENKO, I. F., and MISHCHENKO, V. S. 1969. Geochemistry of columbite-bearing granites of Staro-Dubovsk Massive, Azov region. *Geokhimiya*, 7, 867–880.

NOCKOLDS, S. R. 1954. Average chemical composition of some igneous rocks. *Geol. Soc. Am. Bull.* 65, 1007–1032.

SABET, A. H., CHABANENKO, V., and TSOGOEV, V. 1973. Tin-tungsten and rare metal mineralization in the Central Eastern Desert of Egypt, *Annals Geol. Surv. Egypt*, III, 75–86.

SABET, A. A., TSOGOEV, V., SARIN, L. B., AZAZI, S. A., EL-BEDEWI, M. A., and GHOBRIAL, G. A. 1976. Tin-tantalum deposit of Abu Dabbab. *Annals Geol. Surv. Egypt*, VI 93–117.

STRECKEISEN, A. 1960. On the structure and the origin of the nepheline-syenite complex of Ditro, Transylvania, Romania. *Int. Geol. Congr.* XXI, Pt. 13, 228–238.

TUREKIAN, K. K., and WEDEPOHL, K. M. 1961. Distribution of the elements in some major units of the Earth's crust. *Geol. Soc. Am. Bull.* 72, 175–192.

جيولوجية وطباقية صخور حزام التجبل بالصحراء العربية بمصر
بين خطى الغرض ٣٥ ٥٢٥ ، ٣٠ ٥٢٦ شمالا

م.ك. العقاد و ع.م. نويـر

الخلاصـة

إن الخرائط التفصيلية لقطاع هذا البحث (٥٥٠٠ كم٢) تكشف القناع عن أتم تتابع وحدات الصخر فى الحوض المصرى. ولقد طرأ على طباقية الصخر التى تضم وحدات الصخر الرسمية ، إصلاح مستمر وتحسين خلال ١٤ عاما . ونسبت كل وحدات الصخر – وتحوى السحائق (البلوتونيتات) المتنوعة – الى أوضاعها الصحيحة حسب شفرة التسمية الطباقية . ويحوى التتابع الحالى خمس وحدات صخر اعترف بها حديثا .

إن توزع وحدات الصخور وطباقياتها الحجرية ونشأتها المحتملة وتعاقب الأحداث تمثل جميعها الأطوار الرئيسية فى تطور دورة جيولوجية عظمى ، وهى :– الأطوار الزورق أرضية ، والتجبلية ، والتقارية ، والبعد زورق أرضية . وتضم فوق المجموعة بالصحراء العربية كل تحوليات الأساس ، وتنقسم الى ثلاث مجموعات ومتكون فرد واحد. المجموعة المياتية – وقاعدتها غير ظاهرة – تحوى شستات وجنيسات عالية السليسية . وتتدرج هذه المجموعة الى أعلى خلال شست أبو فنانى الانتقالى الى مجموعة أبو زيران الزورق أرضية الحقيقية. إن تناوب الترسب والتبركن فى هذه المنطقة قد أدى إما إلى وجود متكونات منفصلة كالمويلح (اسبليتات وسادية) ومتكون العتود (رواهص مدملكة وجراول) وإما إلى وجودها داخل متكون كعدسة أم همبص من الفتاتيات النارية المتحولة داخل متكون الحمودة . أما مجموعة الربشى فتضم النشاط السحيقى القطرى الأصيل (فوق القاعدى والقاعدى) فى الزورق الأرضى بالصحراء العربية متبوعا بالتسحق الرئيسى للجرانيت الذى حدث فى أثناء طور الخمود من تجبل الصحراء العربية .

أما الرفع بانى القارات ، فقد صحبته بركانيات الدخان الأنديزيتية غير المتحولة ولقد أزاح التآكل المديد معظم هذه الأخيرة ، كما قطع داخل الوحدات الأقدم مكونا مجموعة الحمامات من طراز القنديد (الدبس) . بدأت الصدوع شمال غرب – جنوب شرق فى أخريات ماقبل الكمبرى متحكمة فى كل من فلسيتات مابعد الحمامات والطور الأول من الجرانيتات الأحدث . ولقد تجددت هذه الصدوع على سواء قبل وبعد ترسب حجر الرمل النوبى (الكريتاوى السفلى ؟) الذى يغطى بتخالف جوانب الأساس ، وربما أثرت فى خسف البحر الأحمر أثناء العصر الثالث . ويعد هذا القطاع فريدا فى أن سحائق الجرانيت الحدث تبين علاقات قطع مستعرض تسمح لأول مرة بتقسيمه الى أطوار ثلاثة متميزة ثبت وجودها بالبحث الكيماوى الأرضى (الجيوكيميائى).

GEOLOGY AND LITHOSTRATIGRAPHY OF THE ARABIAN DESERT OROGENIC BELT OF EGYPT BETWEEN LATITUDES 25° 35′ AND 26° 30′ N

M. K. AKAAD and A. M. NOWEIR

Tanta University, Tanta, Egypt

Abstract—Detailed mapping of an area of 5500 km^2 has revealed the most complete succession of rock units in the Egyptian Basement. All rock units, including the various plutonites and volcanites, have now been assigned their appropriate status in accordance with the Code of Stratigraphic Nomenclature. The succession as presented here includes five newly established rock units.

The evolution of the Arabian Desert Orogenic Belt displays geosynclinal, orogenic, epeirogenic, and post-geosynclinal stages. The Arabian Desert Supergroup embraces all the metamorphites of the basement, subdivided into three groups and one individual formation. The Meatiq Group, whose base is not exposed, comprises high-grade siliceous schists and gneisses; it grades upwards through the transitional Abu Fannani Schists into the eugeosynclinal sediments and volcanics of the Abu Ziran Group. The succeeding Rubshi Group comprises ultrabasic and basic magmatic intrusions. It is followed by the Older Granites, emplaced during the waning phase of the Arabian Desert Orogeny.

Epeirogenic uplift was accompanied by the outpouring of andesitic, unmetamorphosed Dokhan Volcanics. Prolonged erosion removed most of the latter and cut into older units, resulting in the molasse-type Hammamat Group. N.W.–S.E. faulting began in the late Precambrian and controlled the emplacement of both the post-Hammamat felsites and Phase I of the Younger Granites. These faults were rejuvenated both before and after the deposition of the Nubia Sandstone (L. Cretaceous?), and probably influenced the Red Sea rifting in Tertiary times. The sector under consideration is unique in that its Younger Granite plutons display cross-cutting relations, permitting, for the first time, their subdivision into three distinct phases.

INTRODUCTION

The basement crystalline rocks of the Eastern (Arabian) Desert of Egypt form a belt about 830 km long trending N.W.–S.E., here named the Arabian Desert Orogenic Belt. The area under consideration represents more than the western half of a sector lying between latitudes 25° 35′ and 26° 30′ N. It is 90 km long and has a maximum width of 77 km (see Plate 1). The basement rocks extend farther north, east and south, but are overlain by Nubia Sandstone on the west. The Qift-Quseir road leading from the Nile Valley to the Red Sea traverses the belt. An area of 5500 km^2 was mapped by the authors and their co-workers on the scale of 1:40,000, critical areas being mapped at 1:20,000.

Field work began in February 1963 on the Hammamat–Um Seleimat district (1145 km^2) and the results, presented briefly (Akaad and Noweir, 1969), revealed the largest and most complete succession of rock units in the Egyptian basement. This succession was larger and more elaborate than, although consistent with, previously known successions (El-Ramly and Akaad, 1960; El-Shazly, 1964). For the first time all metasedimentary, metavolcanic and unmetamorphosed sedimentary rock units were assigned formal names in accordance with the Code of Stratigraphic Nomenclature.

The lithostratigraphy has, since then, undergone continuous amendment, refinement and elaboration throughout the past fifteen years, based on the mapping of new ground. The sequence of rock units in the present map district is presented in Table 1.

LITHOSTRATIGRAPHY

The voluminous systematic description of these units (i.e. definition, nomenclature, lithostratigraphic position, regional set up, content, thickness, distinctive lithology, origin, etc.) necessary for establishing new names is complete, but will be published separately. It is here intended merely to highlight the salient characteristics of the units and their setting, in ascending order.

The ARABIAN DESERT SUPERGROUP, first named and subdivided by Akaad and Noweir (1969), contains the Meatiq Group, the Abu Fannani Schists, the Abu Ziran Group and the Rubshi Group. It thus embraces all metamorphosed rock units in the succession.

MEATIQ GROUP

This is the oldest major lithostratigraphic unit. It occurs at the base of the succession, is exposed in a large domal structure (250 km^2), and includes a large variety of high-grade siliceous gneisses and schists which appear to have originated mainly from acidic tuffs and flows (Akaad and Shazly, 1972, 1977, and in press a, b).

Abu Fannani Schists

The Abu Fannani Schists, first named by Noweir (1968), occur in a nearly circular outcrop, bounding and succeeding the Meatiq Group around the latter's domal structure. The outcrop is about 50 km long by 2.5 km wide and is disrupted by structural features and intrusions (Akaad, Shazly and Noweir, in press). It comprises a bedded sequence of quartz–biotite and quartz–actinolite schists, with minor phyllonites and para-amphibolites. This formation is lithologically transitional between the Meatiq Group and the succeeding Abu Ziran Group.

ABU ZIRAN GROUP

First named by Akaad and Noweir (1969), this includes eight formations, three of which are newly established. They collectively display the alternation of sedimentation (of immature flysch-type sediments) and volcanism, and represent the typical eugeosynclinal filling of the Arabian Desert Geosyncline (or subsidence phase). This association is broadly equivalent to the eugeosynclinal associations of Stille (1936), Kay (1947), Dietz (1963) and Auboin (1965). The group includes both the "Schist-mudstone-graywacke series" and "Metavolcanic series" of El-Ramly and Akaad (1960), equivalent to the "Geosynclinal metasediments" and "Geosynclinal Shadli metavolcanics" respectively in the new basement map (El-Ramly, 1972).

The *Hammuda Formation*, at the base of the group, clearly displays this alternation of sedimentation and volcanism within its four members (Table 1). The new uppermost *Absi Metamudstone Member* comprises an interbedded succession of metamudstones with subordinate metagraywackes and schists (Akaad, Noweir and Kafafi, in press).

The *Muweilih Formation* is the oldest, solely metavolcanic, formation. It is unique in the map district in comprising distinctly pillowed metaspilites, spilitic metadiabase flows, spilitic crystal metatuff and epiclastic-pyroclastic intra-pillowed meta-adinole.

The *Atud Formation* succeeds the above pillowed flows unconformably, and forms a belt 30 km long trending N.N.W.–S.S.E. It comprises a bedded and repeatedly alternating succession of polymictic metaconglomerates and metagraywackes, with minor metamudstones, schists and reworked intraformational metabreccia. It is lithologically similar to the Atud Formation in its type locality east of Jabal Atud, 110 km to the south (Akaad and Essawy, 1965).

The *Atalla Formation* succeeds the Atud Formation and forms a belt, 35 km long, along Wadi Atalla; it continues north-westwards, encircling the Umm Effein granite pluton, west of which it dips beneath the Nubia Sandstone. In the south it consists of siliceous metamudstones with minor metasiltstones, arkosic metagreywacke, intraformational metaconglomerate, and marble (Akaad and Noweir, 1969). These sediments give way northwards to acidic tuffs and flows devoid of epiclastic sediments. Revision of the whole belt showed the intraformational metaconglomerate to be of pyroclastic nature.

The *Um Seleimat Formation*, named by Noweir (1968), covers 600 km^2 in the south-eastern corner of the map district, and continues farther south as far as Wadi El-Miyah, thus forming one of the largest exposures of meta-volcanics in the Egyptian basement. It clearly cuts and encloses xenoliths of the Atalla Formation. The Um Seleimat Formation comprises a distinctly structureless and heterogeneous metamorphosed association of basalts of near-surface intrusive nature, with only minor andesitic basalt, andesite, dacite and tuff.

The *Sukkari Metabasalts* form a triangular outcrop, 80 km^2 in extent, around Wadi El-Saqia, and a second outcrop east of the Saqia serpentinite range. First named the "Saqia formation", these rocks are now equated with other occurrences outside the mapped area (Akaad, Essawy, Shazly and Noweir, in press) and with the Sukkari Metabasalts of Wadi Sukkari, 110 km south (Essawy, 1967).

The formation is made up essentially of metabasalt flows, each up to 20 m thick, with phenocrysts of fresh unaltered augite. These grade into flow-textured, non-porphyritic (fine, through crypto-crystalline to glassy) metabasalts and basaltic tuffs.

The *Eraddia Formation* comprises weakly metamorphosed intermediate metavolcanics, both as thick flows and as intrusive subvolcanics. Tuffs are common, some exposures being mappable at a scale of 1:40,000. The rocks are largely propylitised meta-andesites with their relatively fresh equivalents of oxyhornblende meta-andesites. Amygdaloidal, fine pilotaxitic and coarser microdioritic varieties also occur with quartz metadacite and plagioclase meta-porphyrite. Mineral assemblages suggest a lower greenschist facies. The formation outcrops as a belt, 40 km long, and trending N.N.W., mostly beyond the map district. It eventually passes beneath the Nubia Sandstone.

The *Abu Diwan Formation* has an S-shaped outcrop, 90 km^2 in extent. The northern and central parts of the outcrop consist of slightly metamorphosed, structureless metadiabases, whereas the rocks of the southern part are amphibolites and hornblende schists of high-grade greenschist to low-grade almandine amphibolite facies. The original diabases were intrusive in nature.

RUBSHI GROUP

The serpentinites and metagabbros succeeding the rocks of the Abu Ziran Group constitute the Rubshi Group, named after Jabal El-Rubshi, where both are ideally represented, with the metagabbros intruding the serpentinites.

Barramia Serpentinites. The eugeosynclinal metasedimentary and metavolcanic formations of the Abu Ziran Group are intruded by seven serpentinite bodies, as seen in the Nuweilih, Saneyat, Fannani, Atalla, Rubshi, Kab Amiri and Saqia ranges. The serpentinites are the metamorphosed and altered derivatives of ultrabasic rocks and contain fresh relics of the latter. They consist principally of serpentinites, pyroxenites, peridotite relics, chromitites, talcose and talc-carbonate rocks, and ultramafic orthoschists.

Although the field relations between the in-

TABLE I

		ROCK UNITS	
	SUPERGROUP & GROUP	FORMATION	MEMBER (and remarks)
		Kab Absi Essexite Gabbro	
		Khors Volcanics	
			—(dislodging of contact between Nubia Sandstone and basement)
		Nubia Sandstone	
			— (regional unconformity)
			— — — — — — — — — — — — — — —
		Younger Granites	*Phase III* South Eraddia pluton *Phase II* Gidami, Kab Amiri, Eraddia, Um Effein, Um Had, Um Hombos and Saneyat plutons *Phase I* Abu Qarahish, Sodmein, Kab Absi, Atalla El Murr, Atalla, Atalla gold mine, East Um Effein, Fawakhir and Arak plutons
		Post-Hammamat Felsites	Atalla, Rasafa-Shihimiya, Atshan, Qash, Mahdaf, Kohel, Arak and Zeidun members
			— — — — — — — — — — — — — — —
		Qash Volcanics	
			— — — — — — — — — — — — — — —
	HAMMAMAT GROUP molasse-type sediments	2. Shihimiya Formation	c. Um Hassa Greywacke Member b. Um Had Conglomerate Member
			— — — — — — — — — — (local unconformity)
			a. Rasafa Siltstone Member
		1. Igla Formation	
			— — — — — — — — — (regional unconformity)
		Dokhan Volcanics (unmetamorphosed)	
			— (transforming some Older G nites into cataclastic-mylonitic gneisses of Shaitian ty or Shait Granites)
		Older Granites	Um Shager, Abu Ziran and N & S Eraddia plutons
ARABIAN DESERT SUPERGROUP	RUBSHI GROUP ultrabasic & basic	2. Sid Metagabbros	Hammuda, Khors, Fannani, Sid, Fawakhir, Esh El-Zarga, Eraddia, Saqia, Abu Diwan, Rubshi and Abu ziran complexes
		1. Barramia Serpentinites	Muweilih, Saneyat, Fannani, Atalla, Rubshi, Kab Amiri & Saqia ranges
	ABU ZIRAN GROUP eugeosynclinal filling	8. Abu Diwan Formation	
		7. Eraddia Formation	
		6. Sukkari Metabasalts	
		5. Um Seleimat Formation	
		4. Atalla Formation	
		3. Atud Formation	
			— — — — — — — — — — (local unconformity)
		2. Muweilih Formation	
		1. Hammuda Formation	d. Absi Metamudstone Member c. Khors Schist Member b. Um Hombos Metapyroclastic Lentil a. Um Shager Metagreywacke Member
		Abu Fannani Schists	
	MEATIQ GROUP		Thick succession of high grade siliceous gneisses and schists. Subdivision into units in progress.

TABLE 1(contd.)

Age	Stages of evolution	PRINCIPAL EVENTS
	POST-GEOSYNCLINAL PHASE → major block faulting & uplift, Red Sea rift, platform sedimentation, alkaline volcanicity & plutonism	– Emplacement of alkaline plutonites
		– Explosive volcanism of trachyte lavas, pyroclastics and associated dykes
Lower Cretaceous		– Rejuvenation of old N.W.–S.E. faults
		– Transgressive deposition of quartz-arenites and shales on stable shelf
		– Prolonged quiescence, erosion and peneplanation
		– Uplift and main rejuvenation of old N.W.–S.E. faults
620–590 Ma	EPEIROGENIC PHASE → uplift & andesitic volcanicity, molasse-type sedimentation, regional tilting & granite plutonism	– Emplacement of granite plutons as final epeirogenic manifestation, associated with and followed by various dykes – Granite pluton cutting Phases I and II – Adamellite plutons cutting Phase I, Hammamat Group, Post-Hammamat Felsites and effecting pronounced contact metamorphism – Elongate granodiorite plutons along N.W.–S.E. trends
		– Intrusion of felsites as huge bodies, sheets and dykes along N.W.–S.E. trends
		– Earliest indication of N.W.–S.E. dislocations controlling later emplacement of Post-Hammamat Felsites and Phase I of Younger Granites
		– Eruption of tuffs & intrusion of subvolcanics into folded Hammamat Group
		– Folding & faulting of Hammamat Group & older rock units – second phase folding
		– Deposition of dark greywackes
		– Deposition of conglomerates derived from older units and reworked Igla Formation
		– Uplift in source area
		– Deposition of grey siltstones, minor greywackes and conglomerates
		– Deposition of primary red beds of purple siltstones, greywackes, minor arenites and conglomerates
		– Rapid severe erosion and peneplanation
660–700 Ma		– Epeirogenic uplift accompanied by intrusion and eruption of andesites and porphyries. Subareal eruption of andesitic agglomerates and tuffs
	OROGENIC PHASE → regional tilting, metamorphism & granite plutonism	– Regional fault and thrust movements
900–1000 Ma		– Emplacement of tonalite, grandiorite & monzonite during waning phase of orogeny
		– Emplacement of basic plutonites during orogenic folding and regional metamorphism affecting these and all older rock units
	GEOSYNCLINAL PHASE → flysch-type sedimentation & initial magmatic activity volcanicity & intrusion of ultrabasic & basic magmas	– Recurrent intrusion of concordant ultramafic bodies at different horizons in the Abu Ziran Group, heralding main phase of orogeny
		– Intrusion of diabases
		– Eruption and intrusion of andesites, andesitic tuffs and minor basalts
		– Effusion of basalts and basaltic tuffs
		– Intrusion and eruption of basalts, minor andesites and tuffs
		– Eruption of rhyolite, dacite, porphyries, acidic tuffs and minor interbedded mudstones, siltstones and arkosic greywackes
		– Deposition of alternating conglomerates and greywackes, minor siltstone, mudstone and intraformational breccia
		– Uplift in source area
		– Effusion of pillowed spilites, diabase flows, spilitic crystal tuffs, epiclastic adinole and intrusive andesites
		– Deposition of siliceous tuffaceous mudstones and minor greywacke
		– Deposition of alternating shales and calc-shales, minor siliceous limestone and carbonaceous chert
		– Eruption of lapilli-, lithic-, crystal-tuffs merging into epiclastic sediments
		– Deposition of alternating greywacke, mudstone, minor conglomerate and pelite
1300?? Ma		– Deposition of successive quartz-arenites, calc-pelites and greywackes, transitional to proper turbidite facies
		– Extrusion of acidic tuffs and flows

dividual serpentinite bodies have not indicated any time sequence, they are not thought to be of the same age. Individual serpentinites occur as lensoidal sills or sheets up to 12 km long by about 2 km wide, in conformity with regional trends of host formations. They appear to have originally occupied the hinge zones of incipient regional folds and were clearly tilted together with their hosts. The parent ultrabasic magma was probably of the nature of a cold crystal mush largely of olivine and pyroxene, with minor lubricating liquid; intrusion was immediately followed by serpentinization and later by regional metamorphism (Akaad and Noweir, 1972).

Sid Metagabbros. Eleven intrusive plutonic bodies or complexes occur in the mapped area. These are composed mainly of metagabbros with minor meta-diabases, amphibolites, quartz-diorites, and fresh relics of the parent gabbros. (Similar complexes have previously been referred to in the local literature as "epidiorites", "epidiorite-diorite association", "metagabbro complexes", "metagabbro-diorite complexes" etc.). These metagabbros are here collectively assigned the status of a formation and named the Sid Metagabbros, after Bir El-Sid. The eleven "members" are the Hammuda, Khors, Fannani, Sid, Fawakhir, Esh El-Zarga, Eraddia, Saqia, Abu Diwan, Rubshi and Abu Ziran complexes. Every one of these is intimately associated with or intruded into metavolcanic–serpentinite country rocks. Apart from their unfailing intrusive plutonic nature, their composition, granularity, colour index and even joint systems are markedly heterogenous. These metagabbros, together with all older rock units, have suffered regional metamorphism, as shown by Noweir (1968) and Noweir and Takla (1972).

Older Granites

The mapped area contains twenty granitic masses and plutons, three of which are classified as Older Granites, the other seventeen being Younger Granites. ("Older" Granites are those that are unconformably overlain by sediments of the Hammamat Group, e.g. the Um Shager pluton; "Younger" Granites are those that cut, thermally metamorphosed, or even laterally displace sediments of the Hammamat Group, e.g. the Um Had pluton.)

The Older Granite plutons of Um Shager, Abu Ziran, and N. and E. Eraddia range in composition from tonalite to granodiorite and quartz monzonite. They are medium- to coarse-grained, grey in colour, and commonly foliated, with characteristic spindle-shaped mafic-rich xenoliths. The ages of some Egyptian Older Granites lie between 870 and 1000 Ma (Hashad *et al.*, 1973), which is comparable to ages of 710 to 1000 Ma for older granites from Saudi Arabia (Brown and Jackson, 1960). Fault and thrust movements have converted some of the Older Granites into cataclastic-mylonitic gneisses, as at Wadi Shait (Akaad and Moustafa, 1963) and Jabal El-Maiyit (Akaad and El-Ramly, 1964).

Dokhan Volcanics

These are the oldest unmetamorphosed volcanics in the Egyptian basement and they also constitute the youngest rock unit below the regional unconformity (Table 1). Their type locality is Jabal Dokhan in the northern Eastern Desert, containing the famous Imperial Porphyry or "porfido rosso antico". The most important outcrop of Dokhan Volcanics in the mapped area is that at the mouth of Wadi Atalla. Here, porphyrites, andesites, andesitic basalts, glassy andesitic agglomerates and both massive and banded tuffs are unconformably overlain by sediments of the Hammamat Group.

The importance of the Dokhan Volcanics is twofold. Firstly, they represent an extensive and widespread period of andesitic volcanicity, which marks the start of the epeirogenic uplift following the destruction of the eugeosynclinal depositional trough by the Older Granite plutonism. Secondly, they covered vast tracts of the then newly elevated and probably segmented land surface, and accordingly constitute the main source of the sediments of the succeeding Igla Formation (red beds).

HAMMAMAT GROUP

The type locality of the Hammamat Group (formerly Series), first described by De Roziere well over a century and a half ago, occurs in the area mapped. The Um Had Conglomerate Member includes the classic Breccia Verde d'Egitto of Visconti, the rock type of the group. Except for the Igla Formation (Akaad, 1957), the Hammamat Group was first mapped in detail at the type locality, subdivided into lithostratigraphic units (Table 1) and assigned local names by Akaad and Noweir (1969).

The three largest exposures of the group in the entire basement, collectively covering about 700 km^2, occur in the area. The Wadi Hammamat exposure, covering 400 km^2, embraces the most complete succession of this group (Table 1), and is about 4000 m thick. It is intruded by the Qash Volcanics, the Post-Hammamat Felsites, and the Um Had (Younger Granite) pluton; it rests unconformably on the Dokhan Volcanics and older units. The Wadi Zeidun–Wadi Arak exposure (190 km^2) consists mainly of Igla Formation red beds and forms the southern extension of that of Wadi Hammamat. The stratigraphic sections at El-Shihimiya–Um Hargal and Wadi Atshan are 2200 m and 1150 m thick respectively. The Wadi Kareim exposure covers 130 km^2 in the south-eastern corner of the map, but extends farther east where a section 6–8 km thick of undifferentiated Hammamat sediments was measured.

Small unmappable exposures of the Igla Formation occur north of Jabal Meatiq (Shazly, 1971) and east of the Atalla felsite (Ghanim, 1969).

The Hammamat Group includes a thick succession of unmetamorphosed, wholly clastic, immature to semi-mature sediments of distinct molasse facies. The clastic fragments of the Igla Formation red beds were derived mainly from the Dokhan Volcanics and transported mainly by rivers and torrents to nearby foreland basins and piedmont slopes.

Qash Volcanics

These include a variety of fresh and highly altered basic volcanics and subvolcanics, together with basic pyroclastics and banded tuffs. This association intrudes the folded Igla Formation along the basement–Nubia Sandstone contact at Wadi El Qash in the south-western corner of the map district.

Post-Hammamat Felsites

Although felsites had earlier been known to cut across the Igla Formation (Akaad, 1957; Akaad and El-Ramly, 1958), Noweir (1968) found a Rasafa-Shihimiya felsite cutting both the Igla and Shihimiya Formations of the Hammamat Group, and thus named them the Post-Hammamat Felsites. Field relations with the Younger Granites were uncertain until the Younger Granite pluton of Um Had was found cutting across the Post-Hammamat Felsites (see Shazly, 1971, p. 462).

The map district contains eight "member" masses (Table 1), the following being the main occurrences:–

(a) The *Atalla felsite*, is the largest and longest mass of this unit in the Egyptian basement. It is 28 km long, has a maximum width of 7.2 km, trends N.W.–S.E., and is intruded by five Younger Granite bodies. The mass consists mainly of fine to cryptocrystalline felsites, with minor oligoclase felsite porphyry, spherulitic felsite and rhyodacite.

(b) The *Rasafa-Shihimiya felsite* forms a N.W.–S.E. trending belt, 16 km long and 0.5–2.8 km wide. It cuts the Hammamat sediments and some older units and comprises felsites, felsite breccia, rhyodacite, oligoclase porphyry and andesitic dacite. Minor masses are intruded conformably into the nearby folded sediments of the Hammamat Group.

Younger Granites

The map district contains seventeen Younger Granite plutons which cut the Hammamat Group and are younger than the Post-Hammamat Felsites. These plutons can be assigned to three different phases (Table 1), each phase possessing its own field, petrographic and petrochemical characteristics.

The Younger Granites of the district range from grandiorite through adamellite to granite, and in area from 1 to 125 km^2. They all display sharp contacts, chilled margins and clear magmatic characters.

Phase I embraces nine plutons and masses of moderate relief and elongated in a N.W.–S.E. direction. They are of calc-alkaline, hornblende-biotite granodioritic composition, are rich in xenoliths, variably digested, and show only mild contact effects.

Phase II comprises seven plutons of alkaline character and adamellitic composition, and contains fewer xenoliths which are undigested.

Phase III comprises only one pluton of leucogranite with thick chilled margins of microgranite. It is devoid of xenoliths and dykes.

Plutons of Phases II and III have circular to oval outlines and cut across the regional structures, including those of the Hammamat Group. They form rugged, bold mountainous features and show pronounced contact effects. Meneisy (1976) assigned a late Precambrian age (590–620 Ma) to the Younger Granites.

Khors Volcanics

The Khors Volcanics are a group of plugs and sheets of alkaline trachytic lavas and minor pyroclastics in the south-eastern part of the map district. These cut all basement rock units and are recorded farther south cutting the Nubia Sandstone.

A small plug-like mass of essexite gabbro, intruded into the main outcrop of the Absi Metamudstone Member of the Hammud Formation, is ascribed to the Younger Gabbros of Noweir and Takla (1972) and El-Ramly (1972).

TECTONISM AND EVOLUTION

Regional Metamorphism and Tectonics

Rock units within the Arabian Desert Supergroup have variably suffered regional metamorphism. The siliceous gneisses and schists of the Meatiq Group are partly of almandine amphibolite facies but mainly of the almandine subfacies of the greenschist facies. Zones of regional metamorphism grade outwards to the greenschist facies, e.g. the serpentinites and metagabbros of the Rubshi Group.

The map district appears to be a graben bounded by two major E.-W. faults, namely, the Wadi Zeidun fault north of the southern boundary of the map, and the Wadi Saqia fault in the north-eastern corner of the map. The entire sector is also dissected by step faults trending roughly N.W. to N.N.W., with westerly downthrows in the map district and easterly downthrows in the eastern part of the sector. Owing to the structural setting, therefore, the succession as seen may not represent the complete original sequence.

The earliest indication of the N.N.W. faults is locally marked by the Post-Hammamat Felsites which, together with the subsequent Phase I of the Younger Granites, were emplaced along N.W. to N.N.W. trends. These dislocations could possibly have dated back to the start of the epeirogenic uplift, forming basins in which the Hammamat sediments were deposited. The faults underwent their main rejuvenation prior to the deposition of the Nubia Sandstone; a second rejuvenation led to the dislodgement of the basement–Nubia Sandstone contact. Remnant outliers of the Nubia Sandstone still survive over the elevated basement flanks.

Stages of Evolution

The sequence of events (deduced from the rock units, coupled with associated tectonics and metamorphism) in the geological history of the region are shown in Table 1. The successive stages of evolution of the Arabian Desert Precambrian Orogenic Belt in the Central Eastern Desert of Egypt can thus be seen to be made up of an eugeosynclinal (or subsidence) phase, an orogenic phase, and epeirogenic and post-geosynclinal phases.

During the eugeosynclinal phase, the conventional flysch-type sedimentation alternated with volcanicity, followed by intrusion of both the ultrabasic and basic plutonites, with the latter distinctly cutting the former. The emplacement of the ultrabasics marked the overlap between the subsidence phase and the oncoming orogenic phase, during which regional tilting of the eugeosynclinal filling accompanied by regional metamorphism took place. The Older Granites, formed at lower levels during the culmination of the orogenic phase, subsequently moved into higher levels.

Uplift during the epeirogenic phase was accompanied by the andesitic volcanicity of the Dokhan Volcanics, and this constituted the main source of detritus for the primary red beds of the Igla Formation of the molasse-type Hammamat Group. Second-phase tilting was followed by the Qash Volcanics, Post-Hammamat Felsites and the successive three phases of Younger Granites and associated dykes. The Post-Hammamat Felsites and Phase I of the Younger Granite were elongated along the N.W. to N.N.W. trending fault system.

The post-geosynclinal phase was marked by the rejuvenation of these faults both before and after the platform sedimentation of the Nubia Sandstone, and these faults ultimately influenced the Red Sea rift.

SUMMARY

The stratigraphic succession, as described above, has the following additions and elaborations, as compared with that presented earlier for the Hammamat–Um Seleimat district (Akaad and Noweir, 1969):

1. Of major importance in the present succession is the lithostratigraphic status assigned to (a) the plutonites, whether metamorphosed or not, which include the Barramia Serpentinites, Sid Metagabbros, Older Granites and Younger Granites; (b) the subvolcanic post-Hammamat Felsites; (c) the Dokhan Volcanics. The Qash Volcanics and the Khors Volcanics now constitute basic units readily distinguished in the field, and they are here assigned the status of formations; individual bodies, plutons or complexes are considered as informal members (with a small "m"). Such an arrangement also provides for the components of a composite intrusion or pluton to occupy the status of a bed. Hence, all units throughout the present succession are given local names in accordance with the Code, except for the Older and Younger Granites, and the Post-Hammamat Felsites.
2. The establishment of the Absi Metamudstone Member as the fourth (uppermost) member of the Hammuda Formation.
3. The establishment of three new formations of metavolcanics, viz. the Sukkari Metabasalts, the Eraddia Formation and the Abu Diwan Formation, as the 6th, 7th and 8th formations in the Abu Ziran Group.
4. The Barramia Serpentinites and the Sid Metagabbros constitute the new Rubshi Group within the Arabian Desert Supergroup, which presently embraces all metamorphites.
5. The discovery that the Qash Volcanics intrude the folded Hammamat Group.
6. The Post-Hammamat Felsites are her established as being older than the Younger Granites.

7. The seventeen Younger Granite plutons in the map district uniquely display cross-cutting relations, thus permitting, for the first time, their subdivision into three distinct phases, confirmed by petrographical and chemical work.

8. The distribution, lithostratigraphy and probable origin of rock units, together with the sequence of events, here appear to represent the principal stages of evolution of the Arabian Desert Orogenic Belt, namely, geosynclincal, orogenic, epeirogenic and post-geosynclinal. However, in view of the intense tectonics affecting the present district, it is neither assumed nor implied that the present succession represents the complete original sequence.

REFERENCES

AKAAD, M. K. 1957. Petrography, structure and time relations of the Igla Formation, Eastern Desert. *Egypt. J. Geol.* 1, 93–102.

AKAAD, M. K., and EL-RAMLY, M. F. 1958. Seven new occurrences of the Igla Formation in the Eastern Desert of Egypt. *Geol. Surv. Egypt Paper* 6.

AKAAD, M. K., and EL-RAMLY, M. F. 1964. The cataclastic-mylonitic gneisses north of Jabal El-Maiyit and the origin of the granite of Shaitian type. *Geol. Surv. Egypt Paper* 26.

AKAAD, M. K., and ESSAWY, M. A. 1965. Petrography, origin and sedimentation of the Atud Formation and its bearing on the early part of the geological history of the basement complex of the Eastern Desert of Egypt. *Bull. Sci. Tec. Assiut Univ.* 8, 75–102.

AKAAD, M. K., ESSAWY, M. A., SHAZLY, A. G., and NOWEIR, A. M. The Sukkari metabasalts at Idfu-Marsa Alam and Qift-Qasier districts, Eastern Desert, Egypt. *Bull. Facul. Sci. Alex. Univ.* 18, (in press).

AKAAD, M. K., and MOUSTAFA, G. A. 1963. The Shait Granite: a cataclastic-mylonitic gneiss. *Geol. Surv. Egypt Paper* 19.

AKAAD, M. K., and NOWEIR, A. M. 1969. Lithostratigraphy of the Hammamat-Um Seleimat District, Eastern Desert, Egypt. *Nature*, 223, 284–285.

AKAAD, M. K., and NOWEIR, A. M. 1972. Some aspects of the serpentinites and their associated derivatives along the Qift-Quseir road, Eastern Desert. *Annals Geol. Surv. Egypt* II, 251–270.

AKAAD, M. K., NOWEIR, A. M., and KAFAFI, A. M. Geology, lithostratigraphy and geological history of the area around Jabal El-Rubshi, Eastern Desert, Egypt. *Delta J. Sci.* Vol. II, (in press).

AKAAD, M. K., and SHAZLY, A. G. 1972. Description and petrography of the Meatiq Group, Eastern Desert. *Annals Geol. Surv. Egypt* II, 215–238.

AKAAD, M. K., and SHAZLY, A. G. 1977. Geology and geological history of the Abu Ziran area, Eastern Desert, Egypt. *Delta. J. Sci.* I, 53–69.

AKAAD, M. K., and SHAZLY, A. G. Lithostratigraphy of the Abu Ziran area, Eastern Desert, Egypt. *Ab. 13th Ann. Meeting, Geol. Soc. Egypt* (in press, a).

AKAAD, M. K., and SHAZLY, A. G. On the Meatiq Group, Eastern Desert of Egypt. *Proc. 3rd Conf. Geol. Soc. Africa*, Khartoum (in press, b).

AKAAD, M. K., SHAZLY, A. G., and NOWEIR, A. M. The Abu Fannani Schists and the problem of the gneiss-schist contact in the Qift-Quseir road district, Eastern Desert, Egypt. *Proc. 3rd Conf. Geol. Soc. Africa*, Khartoum, (in press).

AUBOIN, J. 1966. *Geosynclines*. Elsevier, Amsterdam.

BROWN, G. F., and JACKSON, R. C. 1960. The Arabian Shield. *Int. Geol. Congr.* XXI, Pt. 9, 69–77.

DIETZ, R. S. 1963. Collapsing continental rises: an actualistic concept of geosynclines and mountain building. *J. Geology* 71.

EL-RAMLY, M. F. 1972. A new geological map for the basement rocks in the Eastern and south-western Desert of Egypt, scale 1:10,00,000. *Annals Geol. Surv. Egypt* II, 1–18.

EL-RAMLY, M. F., and AKAAD, M. K. 1960. The basement complex in the Central Eastern Desert of Egypt between latitudes 24° 30′ and 25° 40′. *Geol. Surv. Egypt Paper* 8.

EL-SHAZLY, E. M. 1964. On the classification of the Precambrian and other rocks of magmatic affiliation in Egypt. *Int. Geol. Congr.* XXII, Sec. 10.

ESSAWY, M. A. 1967. Geology of the area around Bir Um Khatiga, Eastern Desert. *Unpubl. Ph. D. thesis.* Assiut University, Egypt.

GHANIM, M. 1969. The geology of Wadi Kareim area, Eastern Desert. *Unpubl. Ph. D. thesis.* Cairo University, Egypt.

HASHAD, A. H., SAYYAH, J. A., and EL-KHOLY, 1972. Rb/Sr isotopic age determination of some basement Egyptian granites. *Egypt. J. Geol.* 16, No. 2.

KAY, M. 1947. Geosynclinal nomenclature and the craton. A short statement of Kay's classification of geosynclines with reference to earlier publications. *Am. Assoc. Pet. Geol. Bull.* 31, 1289–1293.

NOWEIR, A. M. 1968. Geology of El-Hammamat-Wadi Um Seleimat area. *Unpubl. Ph. D. thesis.* Assiut University, Egypt.

NOWEIR, A. M., and TAKLA, M. A. 1972. Geology, petrography, ore mineralogy and geochemistry of the synorogenic basic plutonites between Qift-Quseir and Idfu-Marsa Alam road, Eastern Desert of Egypt. *Bull. Desert Inst. Egypt.*

SHAZLY, A. G. 1971. Geology of Abu Ziran area, Eastern Desert, Egypt. *Unpubl. Ph. D. thesis.* Assiut University, Egypt.

STILLE, H. 1936. Wege und Ergebisse der geologisch-tektonische forschung. 25 *Fhr Kaiser Wilhelm Gesell.*, II, 77–97.

PLATE I. Arabia Desert Orogenic Belt of Egypt. [In pocket at end of book.]

رواسب زورق الأرض الحقيقى (مجموعة أبو زيران) فى المنطقة جنوب غربى ميناء سفاجا، الصحراء الشرقية، مصر

س. الجابى و م. حبيب

الخلاصة

تقع منطقة جنوب غربى سفاجا على الحد الشمالى لحوض زورق الأرض الحقيقى للأساس المصرى. ولاتوجد آية صخور فوق قاعدية من الطرزاز الألبى الى الشمال من وادى سفاجا، لكن تسود هناك صخور شديدة الجرنتة (مجموعة سفاجا) وصخور الجرانيت. والى الجنوب من هذا الوادى تسود الرواسب والبركانيات القديمة القليلة التحول (مجموعة أبو زيران) بالاضافة الى بعض الجابرو المتحول والسربنتين.

وتحتوى مجموعة أبو زيران فى هذه المنطقة على كمية كبيرة من الصخور البركانية ممايدل على وجود نشاط بنائى ملحوظ. وتتناول هذه الدراسة العلاقة المكانية بين الترسب والنشاط البركانى خلال هذه الفترة، وكذلك الدور الذى لعبته هذه الأخيرة.

ومجموعة أبو زيران تمثل ثلاثة متكونات هى متكون حمودة (أقدمها) ومتكون مويلح ومتكون أبو مروات. وكلا المتكونين حمودة ومويلح يمثل ظروفا بحرية عميقة بينما تشير نوعية صخور متكون أبو مروات الى بيئة بحرية ضحلة أو قارية.

ومن الناحية البنييية تقع المنطقة على نقطة التحول بين الاتجاه الشمالى الغربى السائد فى الجنوب والاتجاه الشمالى الشرقى السائد فى الشمال. وقد تعرض متكونا حمودة ومويلح وماصاحبهما من سربنتينات الى حركات طى أحدثت مجموعة مائلة غير متماثلة من الأقبية والزوارق تضرب كلها شمال – جنوب بصفة عامة. أما متكون أبو مروات فهو قبو عظيم يقارب مضربه شمال شرق – جنوب غرب.

THE EUGEOSYNCLINAL FILLING OF ABU ZIRAN GROUP IN THE AREA S.W. OF PORT SAFAGA, EASTERN DESERT, EGYPT

SAMIR EL-GABY and MOHAMED E. HABIB

Assiut University, Assiut, Egypt

Abstract—Abu Ziran Group, which embraces the eugeosynclinal filling of the basement complex of Egypt in the area S.W. of Port Safaga, is composed of weakly regionally metamorphosed sediments and volcanics. From oldest to youngest, the Hammuda, Muweilih and Abu Marawat Formations are differentiated in the group. Both the Hammuda and Muweilih Formations had developed under deep marine conditions, whereas the lithological characters of the Abu Marawat Formation imply continental or shallow water environment.

INTRODUCTION

The Abu Ziran Group was proposed by Akaad and Noweir (1969) to include the weakly regionally metamorphosed sediments and volcanics formerly described by El-Ramly and Akaad (1960) as the schist–mudstone–graywacke series and the metavolcanic series, respectively. The metavolcanics comprise subvolcanic masses, the latest phases of which are less affected by regional metamorphism than the meta-gabbros occurring in the vicinity, e.g., at Hamata area (Kamel, 1969). Moreover, meta-gabbro masses incorporate substantial amounts of meta-dolerites which are very similar to those pertaining to the metavolcanics proper. The intimate genetic relationship between the metavolcanics and the ultrabasic rocks is very obvious in the field.

In the area S.W. of Port Safaga, pre-eugeosynclinal sediments and associated magmatic rocks, now present as highly granitized rocks, also prevail in the north-western and northern parts of the map area (Fig. 1) and farther to the south. Thus the present area lies at the boundary between the geanticlinal swell (El-Ramly and Saloum, 1974) to the north, and the eugeosynclinal basin extending to the south. The contact between the eugeosynclinal filling (Abu Ziran Group) and the older rocks (Safaga Group) is occupied either by thrust faults or by magmatic intrusions.

The metasediments and metavolcanics of the Abu Ziran Group are invaded by ultrabasic rocks (serpentinites), meta-gabbroid complexes, syn-orogenic and younger granites and old Dokhan-type volcanics. The country rocks along the contacts of the syn-orogenic granitoid masses are thermally metamorphosed and commonly display wide reaction zones.

The Abu Ziran Group comprises three formations: Hammuda (oldest); Muweilih; and Abu Marawat (youngest). The first two formations are correlated with the Hammuda and Muweilih Formations at their type localities (Akaad and Noweir, 1969) according to their geological and lithological characteristics. However, field mapping carried out by El-Nady (1976) and Khodeir (1976) in the area lying between Hammamat–Um Seleimat district and the area under consideration raised doubt about the validity of the proposed correlation; they consider the Hammuda and Muweilih Formations in the area S.W. of Port Safaga to represent two new formations.

The Hammuda and Muweilih Formations, together with the associated serpentinites, constitute a series of plunging asymmetrical anticlines and synclines whose fold axes trend generally North–South. The Abu Marrawat Formation, on the other hand, forms a major anticline trending N.E.–S.W. The core of this anticline is occupied by the northern occurrence of the Muweilih Formation.

FIELD DESCRIPTION

Hammuda Formation

The Hammuda Formation comprises the following lithostratigraphic units: Abu Qarahish Pebbly Schist Lentil (oldest); Um Hombos Metapyroclastic Lentil; and Khors Schist Member (youngest) (Fig. 1).

The Abu Qarahish Pebbly Schist Lentil occupies the same lithostratigraphic level as the Um Shaghir Metagreywacke Member of Akaad and Noweir (1969). It outcrops in two localities to the east and to the west of Jabal Abu Qarahish which appear to have been once continuous but are now separated by the Abu Qarahish granodiorite intrusion. This lentil was deposited as pebbly mudstones, some of which are of hybrid character, i.e., mixed epiclastic and pyroclatic sediments. The pebbly schists are characterized by a fairly distinct lamination. The pebbles are discoidal in shape, ranging in size from 1×0.5 cm to 30×8 cm, and are stretched parallel to the foliation.

The Um Hombos Metapyroclastic Lentil is represented by a semicircular outcrop, 1.7 km across, of meta-basaltic agglomerates, forming Jabal Um El-Abas and a wedge-like strip of greenschist, 14.0 km long and 1.0 km wide. The agglomerates are pear-shaped bombs, 5 cm across to 150×15 cm, composed of amygdaloidal tholeiitic meta-basalts. The nature and distribution of the volcanic bombs strongly suggest that the meta-basaltic agglomerate outcrop represents originally a volcanic island within the basin of sedimentation. The greenschist strip, on the other hand, was formed originally of rhythmically alternating laminae, 1 mm to 1 cm thick, of crystal and lithic lapilli tuffs, some of which were intermingled with pelitic matter giving rise to tuffites. The strip bounds Jabal Um El-Abas on the south and extends generally in an E.N.E.–W.S.W. direction. It is conformably overlain on the south by the Khors Schist Member, and is invaded on the west by the serpentinite lenses and the Kab Amira granite and on the east by the Waeira Member.

The Khors Schist Member is formed of low-grade laminated schists of hybrid character comprising biotite schists, tuffaceous chlorite–sericite schists and schistose meta-tuff of predominantly dacitic nature. It is represented in the two parts of the present area, both of which appear to have been originally continuous.

The eastern part (6.5 km^2) is exposed along Wadi Saqi as an elongated outcrop measuring about 8 km in a N.N.E.–S.S.W. direction. It is invaded by the bifurcating flank of a concordant phaccolithic serpentinite mass. The western part (5 km^2) is traversed by Wadi Kab Amira, Wadi Kam Um Abas and Wadi Saqi. It forms a lenticular outcrop, up to 8 km along its major dimension, and is 400–750 m thick.

Muweilih Formation

The Muweilih Formation covers an area of about 200 km^2 on the southern side of the map area (Fig. 1) and occupies a large portion of Wadi Saqi. It is present in two localities, the first of which is an outcrop north of Jabal Kab Amira, 16 km long in a N.N.E.–S.S.W. direction, and intruded by the Semna intrusive tonalites, the Bohlog parautochthonous tonalite, and the Kab Amira granite porphyry. The second occurrence is in the south, is conformably underlain by the Hummuda Formation, and is invaded by the Waeira Member, the serpentinites, the Saqi minor intrusive tonalites, and the Saqi granite.

The Muweilih Formation is composed of weakly regionally metamorphosed volcanics comprising mainly greenschists, meta-basalts (meta-spilites) and meta-diabases together with subordinate amounts of spilitic and meta-spilitic pillow lavas, spilitic lava flows and flow breccias, spilitic tuffs, scoriaceous meta-basalts and metadacite tuffs. The greenschists appear to have been largely derived from basalt lava flows and flow breccias and diabases, and to a less extent from basalt tuffs and tuffites. The meta-basalt flows are devoid of pyroclastics and appear in the outcrop as massive uniform dark green hills. They commonly grade imperceptibly into the meta-diabases and are locally transformed along shear zones into greenschists. The spilitic and meta-spilitic pillow lavas are characterized by the peculiar pillow structure. The pillows vary between 10 and 80 cm in length, possess smooth rounded outlines and are usually molded against each other. Their peripheries are partly glassy whereas their central parts are holocrystalline. The spaces between the larger pillows are usually occupied by small rectangular flattended wedges which possibly represent parts of deformed pillows.

The spilitic lava flows and flow breccias occur as thin concordant relict intercalations, 1–1.5 m thick, within the greenschists. The flow breccias are formed of parallel, elongate volcanic fragments (100 × 20 cm), imparting to the rocks a distinct flow banded structure. The fragments are composed of holohyaline to semicrystalline spilite embedded in a scanty matrix of identical composition which, on the contrary, is holocrystalline and displays conspicuous fluidal pattern swirling around the enclosed spilitic fragments. The scoriaceous meta basalt lavas are located on the northern bank of Wadi Saqi near the entrance of Wadi Semna. They are characterized by flow banding. Their upper parts are crowded with extremely vesicular glassy basaltic fragments or scoriae, 1–25 cm long. The spilitic tuffs are recorded at the mouth of Wadi Kab Amira, where they form beds up to 10 m thick, intercalated with the greenschists. The meta-dacitic tuffs are of minor occurrences. They are represented by thinly laminated coarse and fine tuffs.

Abu Marawat Formation

The Abu Marawat Formation is formed of weakly regionally metamorphosed volcanics together with minor metasediments. It includes the following lithostratigraphic units, in descending order of age

(4) Waeira Meta-diabase Member
(3c) Abu Marawat El-Rayam Meta-diabase–Meta-dacite Member
(3b) Abu Kalb Amphibolite–Meta-andesite Tuff Member
(3a) Kab Rushud Basalt Agglomerate Member
(2b) El-Zarga Metasilstone–Meta-arenite Lentil
(2a) Rabbah Meta-dacite Tuffite Lentil
(1b) Wasif Meta-dacite Tuff Member
(1a) Semna Meta-basalt–Metatuff Lentil

The Semna Meta-basalt–Metatuff Lentil forms a lenticular outcrop (18 km^2) in the central western half of the map area (Fig. 1). It is formed of repeated alternations of pyroclastics and lava flows of tholeiitic meta-basalts, meta-basaltic andesite, and meta-andesite. Meta-dacites are represented only by subordinate to minor thin intercalations of coarse lithic and dusty tuffs. The lower part of this lentil consists of an alternation of beds of tuff–breccias, lapilli tuffs and tuffs of overwhelming meta-andesitic and meta-dacitic composition. This sequence is overlain westward by a thick basaltic sheet of tholeiitic composition pear-shaped in plan and constituting Jabal Semna. It is followed upward and northward by another sequence of pyroclastics and lava flows having tholeiitic meta-basaltic and meta-andesitic compositions. This succession is interbedded with three bands of iron ore (Bishara and Habib, 1973).

The Wasif Meta-dacite Tuff Member (22 × 1.6 km) forms an asymmetric anticline with its axis running generally N.E.–S.W. Its southern part is traversed by Wadi Abu Marawat El-Atshan and Wadi Semna. It is formed principally of schistose thick beds of tuffs and tuff-breccias of meta-dacitic composition. The lower part of this member consists generally of the metatuffs passing upwards into the metatuff-breccias. The northern and cen-

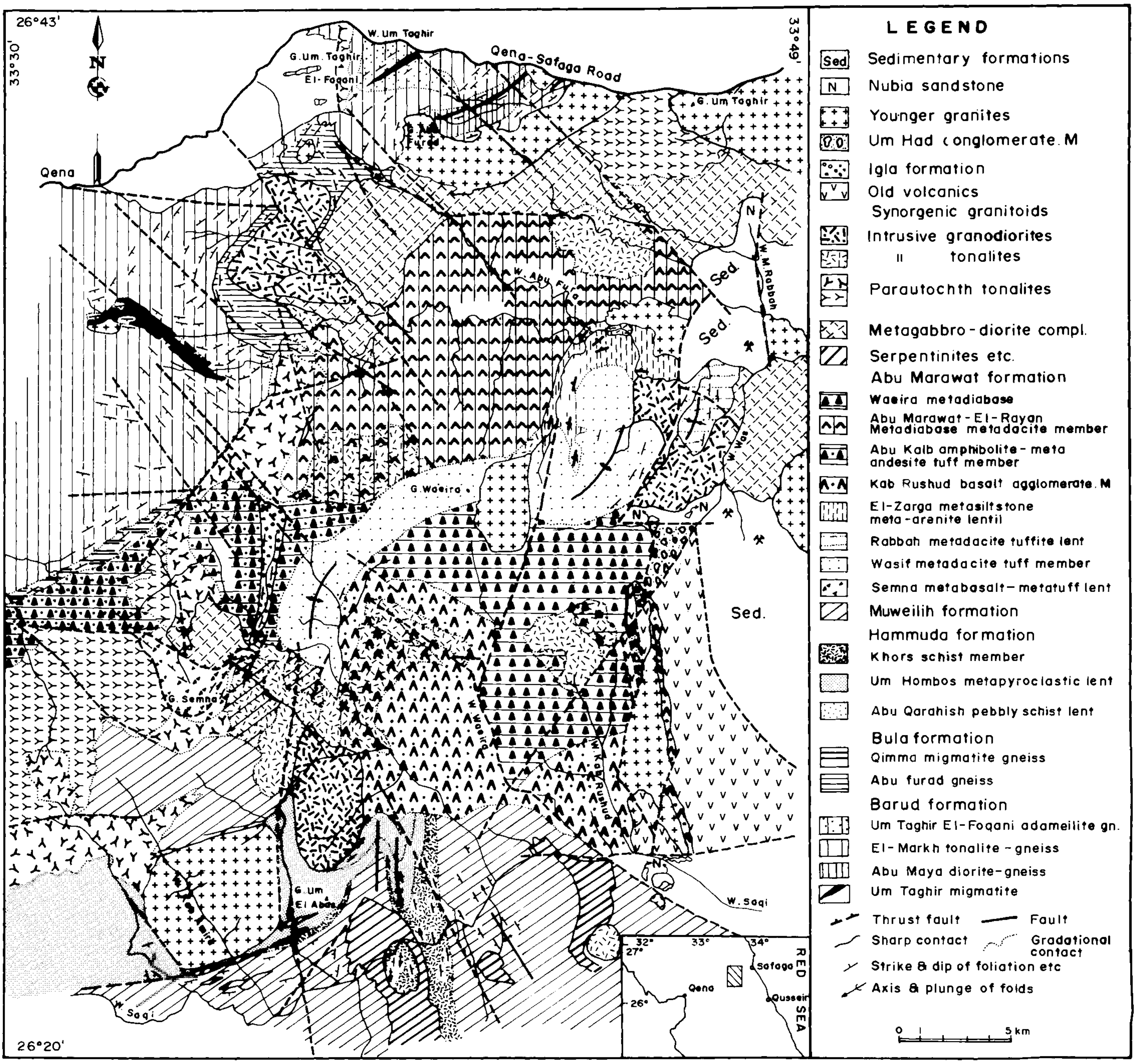

FIG. 1. Geologic map of the area S.W. of Port Safaga, Eastern Desert, Egypt.

tral parts are particularly interbedded with thin intercalations of meta-andesite tuffs, greenschists and saussuritized tholeiitic basalt flow breccias. The metatuffs, particularly the fine varieties, are thinly laminated. Graded bedding or cross-bedding are entirely lacking.

The Rabbah Meta-dacite Tuffite Lentil occupies a minor outcrop (3 km^2) measuring up to 3 km along its major axis. It consists principally of an alternation of beds of metamorphosed tuffs, marls and tuffaceous marls, together with minor bands of highly silicified iron ore, up to 30 cm thick. The beds of the lentil are folded to an asymmetrical syncline whose fold axis plunges at 14° S.W.

The El-Zarga Metasiltstone–Meta-arenite Lentil forms a lenticular outcrop (10 × 1.5 km) lying conformably on the western limb of the Wasif Member. It is formed principally of laminated metamudstones, calcareous metasiltstones, arkosic meta-arenites and pebbly meta-subgreywackes, together with minor proportions of interformational fine polymictic metaconglomerates. Irregular bedding, lamination, current ripple marks and cross-bedding are characteristic features but graded bedding is rare.

The Kab Rushud Basalt Agglomerate Member constitutes a semicircular outcrop (80 km^2) of basalt agglomerates lying conformably on the eastern limb of the Wasif Member. It consists mainly of bombs of saussuritized tholeiitic basalt, embedded in a closely akin groundmass, together with minor proportions of volcanic blocks and lapilli comprising scoriaceous meta-basalts, meta-andesites and meta-dacitic fine crystal tuffs. The volcanic bombs range from semi-globular bodies, 10 cm across, to large ovoidal masses 2 m × 70 cm across; the former usually possess long tails.

The Abu Kalb Amphibolite–Meta-andesite Tuff Member occupies a triangular outcrop (65 km^2) lying conformably on the western limb of the Wasif Member at its southern part. It consists of metatuffs and amphibolites, together with subordinate amounts of lava flows, sills and dykes. The metatuffs are represented by actinolite meta-andesite and meta-dacite. The lava flows, sills and dykes are formed of tholeiitic meta-basalts, meta-basaltic andesites, actinolite meta-andesites, meta-diabases and quartz meta-diabases. The amphibolites constitute the western part of the Abu Kalb Member and may represent originally a diabasic intrusion into the pre-eugeosynclinal Safaga Group.

The Abu Marawat El-Rayan Meta-diabase–Meta-dacite Member forms a semicircular outcrop (120 km^2) lying conformably on the El-Zarga Lentil. It is composed mainly of subequal amounts of meta-diabase and meta-dacite porhyries, together with subordinate varieties of meta-basalts, meta-andesites, amphibolites and basic-granulites. The amphibolites and granulites represent originally diabasic sills injected into the gneisses of the Safaga Group.

The Saeira Meta-diabase Member forms an irregular elongate outcrop (70 km^2) situated in the central southern half of the area studied. It is formed of massive and homogeneous tholeiitic diabases, quartz diabases and dolerites.

Serpentinites and Associated Derivatives

Ultrabasic rocks of Alpine-type do not occur in the Egyptian basement complex to the north of the area under consideration. They occur chiefly near the southern margin of the map area as steeply inclined sheets, lenses and phacoliths running parallel to the regional structure of the enclosing Hammuda and Muweilih Formations. They are formed mainly of talc–carbonates and serpentinite relicts. Ultrabasic parent rocks are entirely lacking.

Meta-gabbro–Diorite Complexes

Meta-gabbro complexes are represented by three masses: (1) Semna saussuritized gabbro–meta-gabbro complex; (2) Wasif meta-gabbro–hybrid diorite complex; and (3) Safaga uralitized gabbro–meta-gabbro–diorite complex. The meta-gabbros are particularly intruded into areas occupied by the metavolcanics, suggesting an intimate genetic relationship. They are in turn invaded by granites; large scale assimilative reactions took place along the contacts with the syn-orogenic granitoids leading to the formation of hybrid diorites.

CONCLUSIONS

From the foregoing description, the sequence of events that resulted in the formation of the Abu Zirhan Group could be outlined as follows: Initial accumulation of sediments (pebbly and tuffaceous mudstones) in an eugeosynclinal basin; interrupted by intermittent explosive basic volcanic eruptions; submarine effusion of basaltic flows; subaerial volcanic eruptions with some epiclastic sedimentation; increased intrusion of gabroic and ultramafic rocks.

Early sedimentation was in deep marine conditions whereas the later sedimentation was in shallow-water continental environment, the change being due either to filling up the basin or to upheaval or gentle folding during the last stages of the basins history.

ACKNOWLEDGMENT

The authors wish to thank the Chairman, Director and colleagues of the Geological Survey of Egypt for the field facilities they kindly provided.

REFERENCES

AKAAD, M. K., and NOWEIR, A. M. 1969. Lithostratigraphy of the Hammamat-Um Seleimat district, Eastern Desert, Egypt. *Nature* 223, 284–285.

BISHARA, W. W., and HABIB, M.E. 1973. The Precambrian banded iron ore of Semna, Eastern Desert, Egypt. *N. Jb. Miner. Abh.* 120, 108–118.

EL-NADY, O. M. 1976. Geology of Jabal El-Rabshy, Eastern Desert, Egypt *Unpubl. M.Sc. thesis.* Assiut University, Egypt.

EL-RAMLY, M. F., and AKAAD, M. K. 1960. The Basement complex in the Central-Eastern Desert of Egypt between lat. 24° 30′ and 25° 40′ N. *Geol. Survey Egypt. Paper* No. 8.

EL-RAMLY, F. M., and SALOUM, G. 1974. The tectonic region of the Eastern Desert of Egypt. *Acta Mineralogica Petrographica* 21, 173–181.

KAMEL, K. E. 1969. Geology of the area around Hamata Talc Mine. *Unpubl. Ph.D. thesis.* Assiut University, Egypt.

KHODEIR, A. A. K. 1976. Geology of Saqi district, Eastern Desert, Egypt. *Unpubl. M.Sc. thesis.* Assiut University, Egypt.

مقارنة بين المعقدات الفوق قاعدية فى بير عمق وحمادة ـ العربية السعودية

م.هـ. رحيلى و أ.ج.واردن

الخلاصة

المعقدات الفوقمافية فى بير عمق وحمادة تموضعت فى بيئات متباينة داخل الدرع العربية السعودية. تضم مجموعة بير عمق المافية ـ الفوقمافية البعيدة النشأة: دونيت متسربين، بيريدوتيت، هارتز برجيت، بيروكسينيت، صخور تراكمية، جابرو، اسبيليت، كيراتوفير. والى حدما يتفق هذا الترتيب طباقيا (استراتجرافيا). وباستثناء معقد جدة فريشية، فالمعتقد وجود كل مكونات معقد أوفيوليت. وهذه الصخور تموضعت فى صور غواش اندفعت فوق بركانيات مردمة التى تحولت محليا قليلا فى سحنة الشست الأخضر. وتتميز أسافل غواشى الدفع العلوى، بالتحول الكربوناتى المخترق، والنمو المحلى للخليط الطينى، والهصر العنيف، والتحول الحرارى المحلى.

وعلى العكس من ذلك، فان فوقمافيات حمادة تميزت بتموضعها فى أثناء طى اقليمى وتحول. وكونت بذلك خوارق لدنة نصف متوافقة فى الصخور الجرانيتية والرسوبية المتحولة والبركانية المتحولة المطيلة التى تحولت فى الشست الأخضر إلى سحنة الأمفيبوليت. ثم تحركت ثانية فى ألباب الطيات المتأخرة المتجهة شمالا، وهصرت بعد ذلك فى اتجاه الشرق. وتتكون الفوقمافيات أساسا من دونيت متسربين وقليل من البيريدوتيت والبيروكسينيت وكثير من عدسات الاسبيليت واضحة التكون من حشود من الجدد تموضعت أثناء تحرك السربنتينيت. فى فوقمافيات حمادة يتدخل بالترتيب: الجابرو، والديوريت، والجرانوديوريت، والجرانيت. كما تتدخل فيها جدد قاعدية الى حمضية. وهذه الفوقمافيات لاتبين الطباقية الزائفة التى تتميز الأوفيوليتات، كما يعوزها كيان خطى مميز. ومع ذلك فيصاحبها مكانيا خط التحام (درز) رئيسى.

COMPARISON OF THE BIR UMQ AND HAMDAH ULTRABASIC COMPLEXES, SAUDI ARABIA

M. H. AL-REHAILI[1] and A. J. WARDEN[2]

[1]Institute of Applied Geology, Jeddah, Saudi Arabia

[2]UNESCO, Institute of Applied Geology, Jeddah, Saudi Arabia

Abstract—The Bir Umq and Hamdah ultramafic complexes were emplaced in contrasted environments within the Saudi Arabian Shield. The allochthonous Bir Umq mafic–ultramafic suite includes serpentinized dunite peridotite, harzburgite, pyroxenite, cumulate rocks, gabbro, spilite and keratophyre, to some extent in that stratigraphic order. Except for a sheeted dyke complex, all the components of an ophiolite complex are thought to be present at Bir Umq. These rocks were emplaced as a series of slices thrust onto Murdama volcanics, locally weakly metamorphosed in the greenschist facies. Penetrative carbonatization, localised development of melange, intensive shearing, and possible localised thermal metamorphism characterise the sole of the overthrust slices.

By contrast, the Hamdah ultramafics were characteristically emplaced during regional folding and metamorphism as plastic, semi-conformable diapirs in ductile metavolcanic, metasedimentary and granitic rocks, metamorphosed in the greenschist to amphibolite facies. They were subsequently remobilised into the cores of later North trending folds and still later East trending shears. The ultramafics consist mainly of serpentinized dunite, minor peridotite and pyroxenite, and contain abundant lenses of spilite, apparently formed from dyke swarms, emplaced while movement of the serpentinite was still in progress. The Hamdah ultramafics are intruded by gabbro, diorite, granodiorite and granite in that order, as well as by basic to acid dykes. They do not show the pseudostratigraphy characteristic of ophiolites, and also lack a characteristic linear form. They are, however, spatially associated with a major suture.

INTRODUCTION

The Bir Umq ultramafic rocks form a N.E.-trending arcuate belt up to 30 km long with a maximum width of 12 km, centred on the village of Bir Umq in the north-central part of the Arabian Shield, 270 km N.N.E. of Jeudah (Fig. 1). Various serpentinized ultramafic and mafic plutonic rocks (of probable ophiolitic affinity), together with associated spilitized greenstones, form three stacked, upthrusted, steeply northward dipping tectonic slices. Chert and a minor keratophyre occurrence are also associated with this assemblage which is in tectonic contact to the south, and inferred stratigraphic contact to the north, with andesitic and acid clastics assigned to the Murdama Group. The Bir Umq ultramafic complex occurs at a high structural and stratigraphic level in the Saudi Arabian Shield.

Intruded in a deeper structural domain, the cluster of ultramafic bodies at Hamdah, located 540 km S.E. of Jeddah, comprises a number of oval to irregularly shaped ultrabasic bodies totalling 180 km^2. They underwent the earliest recognizable deformation, producing North-trending structures in the surrounding rocks; and were emplaced within various metavolcanic and metasedimentary rocks, possibly correlatable with the Hali schist, Jeddah greenstone and Halaban andesite, and various gneisses (Warden, in press). Their mobile style of emplacement constasts with the thrust stacking of rigid, epizonal slices at Bir Umq.

The ophiolitic nature and tectonic mode of emplacement of the Bir Umq rocks was recognized by Aguttes and Duhamel (1971) during the systematic mapping of the area. Few previous data were available for the Hamdah ultramafic rocks although they are outlined on U.S. Geological Survey map 1-217A of the Asir quadrangle, scale 1:500,000, by Brown and Jackson (1959).

GEOLOGY OF BIR UMQ ULTRAMAFIC COMPLEX

Structure

The rocks of the Bir Umq area are broadly divisible into three tectonically emplaced allochthonous slices of ultramafic and associated rocks and autochthonous volcanoclastics (Plate 1), now assigned to the Murdama Group (Delfour, personal communication). The Murdama rocks and enclosed ultramafic belts trend East and E.N.E., dip consistently North at 50–70°, and are slightly arcuate about a northwest axis.

Primary structures include bedding in the Mur-

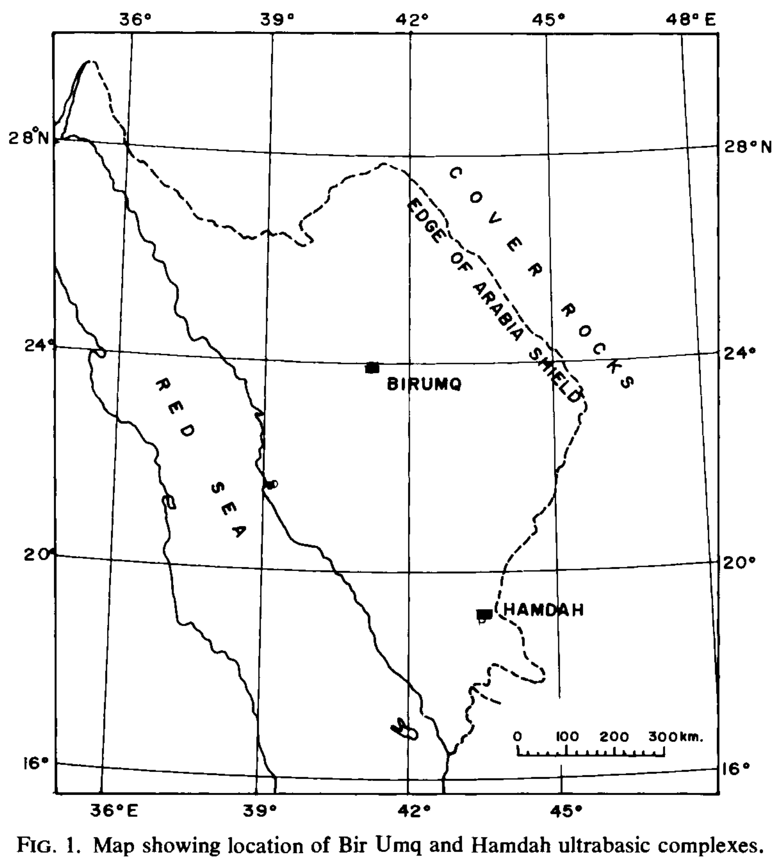

FIG. 1. Map showing location of Bir Umq and Hamdah ultrabasic complexes.

dama rocks and igneous layering in the serpentinized ultrabasic rocks, the latter feature being generally strongly disorientated by flowage.

The most widespread planar structure is a shear foliation in Murdama and ultramafic rocks which is parallel to the thrusts, particularly that at the base of the main (southern) ultramafic belt; the foliation increases in intensity towards this thrust. Penetrative carbonatization, which becomes increasingly developed towards the base of the ultramafic slices, and the presence of tectonic melanges (megabreccias) containing blocks of local and of exotic Murdama rocks within the serpentinite are further evidence of thrusting.

The ultramafic nappes were overthrust southwards and stacked as imbricate slices dipping northwards at about 50–70°, roughly parallel to the lithological layering. Transcurrent N.W.-trending faults of the Najd system bound the mapped area to the west; similar West- to N.W.-trending faults post-dating the thrusting also occur within the area. These, together with a series of North-to N.E.-trending transcurrent faults, progressively offset the southern serpentinized ultrabasic unit north-eastwards and eventually truncate it at the eastern end (Plate 1). They also cause a thickening of the serpentinite in the east. A large zone of massive chert, N.E. of this serpentinite, is extensively sheared and veined by quartz, possibly due to the interaction of the two fault systems.

Allochthonous Ultramafic Suite

This consists of various ultramafic and mafic rock types, greenstone (including metabasalt, Fig. 2), and chert which preserve an ophiolitic pseudostratigraphy as defined by the Penrose Conference (Anon., 1972). Late-stage related differentiated intrusives include trondjemitic veins and a stock of keratophyre emplaced within the southern ultramafic belt.

Ultramafic and mafic plutonic rocks

Serpentinized dunite is the dominant rock type within the three ultrabasic zones. Dark green when fresh, the serpentinite commonly shows vari-coloured alteration to khaki, buff and brown. Rarely relict olivine is preserved. Peridotite and harzburgite were recorded locally in the eastern part of the southern ultramafic unit but lack a distinguishable layered structure and clearly defined boundaries. These features were probably largely obliterated by extensive flowage of the serpentinite and were further dismembered by transcurrent faulting. Locally, however, the primary mineralogy is well preserved (e.g. 75% of olivine and clinopyroxene was preserved in one peridotite specimen). No clear-cut layered gabbro–peridotite zone, similar to that considered to represent the Moho transition zone in other ophiolite complexes, e.g. the Oman (Glennie *et al.*, 1974), could be delineated at the top of the ultrabasic unit. However, discontinuous, rounded to elongate layered bodies up to 200 m long have been found in the eastern part of the southern ultramafic belt (Plate 1). The gabbro is anorthositic and is uralitized and albitized, the interlayered peridotite being serpentinized. These rocks may represent a once more continuous layered gabbro–peridotite unit disrupted by flowage of the ser-

FIG. 2. Valley developed in southern serpentinite belt. On far side locally rodingitized gabbro forms conical hills at upper contact of serpentinite with greenstone beyond. Carbonatized serpentinites near upper contact of thrust may be seen in foreground. Bir Umq area.

pentinite. Farther west, small discontinuous masses of homogeneous, commonly rodingitized, gabbro occur along the upper contact of the serpentinite.

Associated intrusive rocks

Veins and small bodies of trondjemite, too small to be shown on the map, occur in the upper part of the southern ultramafic unit; these probably represent late-stage magmatic residues expressed from the ophiolite. In the west, carbonatized ultramafic rocks within the southern belt are cut by a circular quartz keratophyre intrusion 400 m in diameter, consisting of about 80% of sericitised albite–oligoclase with quartz and traces of chlorite.

Secondary rocks

Widespread but irregular, pervasive carbonatization has occurred within the serpentinite overlying the thrusts, and impregnation by magnesite and dolomite accompanied by silicification and some formation of iron oxides has resulted in partial to complete alteration of the various ultramafic rocks. The middle and upper serpentinite units are almost completely replaced by carbonates.

FIG. 3. Sheared serpentinite near base of southern ultrabasic belt. Kernels of relatively fresh serpentinite survive in a schistose matrix near thrust. East of Bir Umq.

A marked increase in schistosity is generally evident towards the basal thrusts. Approaching these, conjugate shears are formed in the serpentinite and nearer the thrust the shears widen and the schistosity becomes increasingly penetrative, leaving only kernels of fresh serpentinite. Within the thrust zone these disappear and only crinkly, foliated serpentinite schist is left (Fig. 3).

Normally, tectonic melange is confined to the sole of obducting allochthonous slices. At Bir Umq, however, blocks of various rocks ranging from a few to several hundred meters across are embedded mainly within the lower part of the southern serpentinite belt and occur throughout the central section of this unit which is dominated by the development of melange. Megaclasts include spilite, dolerite and gabbro. In a few instances, randomly oriented acicular amphibole cross-cutting the dolerite fabric suggests thermal metamorphism, possibly due to heating at some stage during incorporation within the melange. It is not certain if this metamorphism is of dynamothermal type related to emplacement of the ophiolite (Williams and Smyth, 1973) or of extraneous origin, representing previously metamorphosed material incorporated during obduction. Alternatively, similarity to intrusives within the ultrabasic rocks suggests derivation from tectonically dismembered minor intrusions, possibly metamorphosed by residual heat. Farther east, within the wide part of the southern ultramafic belt, are larger exotics of volcanoclastic rocks measuring up to 400 m across which have, in some instances, been overturned. These are lithologically similar to the Murdama Group from which they were probably plucked during emplacement of the nappe. By contrast, however, some of the megaclasts were probably derived from rocks occurring within the ultramafic slices. Some masses of spilite and dolerite show a semicontinuous linear arrangement and can sometimes be traced into dyke segments. This suggests 'endogenous' derivation from minor intrusions dismembered while still hot and ductile. Melange of this type is developed in the middle ultrabasic belt. Most of the megaclast content can, however, be regarded as true exotics derived from the sole of the obducting slice.

Greenstone

Overlying all three ultramafic belts are predominantly massive but locally schistose fine-grained greenstones. These pass upwards into, and are interbedded with, chert in the northern part of the area. They form one third of the area and comprise the most abundant rock type present within the ophiolite association. Individual greenstone belts are up to 2.2 km thick; like the other rock units they dip consistently northwards.

Pillow structure is well developed in several places, as for example S.W. and N.E. of Bir Umq village and locally along the northern fringe of the northernmost greenstone belt (Fig. 4). Facing evidence indicate that the lavas at these localities are the right way up. These lavas typically consist of sodic plagioclase (An_{5-20}), secondary green tremolite, chlorite, epidote, iron oxide and carbonate. In some cases relict clinopyroxene is preserved. This mineralogical composition and preliminary chemical data indicate a typical spilitic composition. Quench texture with the characteristic development of skeletal iron oxide is well developed. Throughout most of the area however, the greenstones are generally homogeneous and monotonous. Boundaries between individual flows cannot be clearly distinguished, but massive and more schistose zones, possibly representing lava flows and more readily deformed tuffs respectively, can be differentiated. Minor occurrences of pyrite and chalcopyrite with related gossan expression occur near the base of the southern greenstone unit in the east of the area. This is a further similarity to the ophiolite suites of Troodos (Constantinou, 1976) and Oman (Bailey and Coleman, 1975), basalt members of which contain sulphide deposits characteristic of oceanic spreading centers.

Basalt dykes are rare and detailed investigation revealed no sheeted dyke complex at the base of the greenstone unit.

Chert

Beds of chert and jaspilite, 0.5 to 2.0 m thick, occur within the greenstone units. Thick beds of these rocks are present near the top of the northern unit where they form steep ridges up to 500 m wide and several kilometers in length. The chert varies from massive to well laminated and is therefore similar to the chert of more modern ophiolites, e.g. the Hawasina formation in Oman (Glennie *et al.*, 1974). Meso- and micro-folding are well developed within the well laminated type. The cherty rocks are commonly shattered and laced with secondary quartz veins; reddish haematite-stained varieties were also recorded. In the north and N.E. of the area the chert is strongly brecciated. This is thought to reflect shearing near the unexposed contact with overlying Murdama clastics. The chert consists almost entirely of finely granular to cryptocrystalline quartz, a small amount of sericite and a few rhombs of siderite.

Strongly fractured, grey, quartz-veined chert also forms a large mass in the eastern part of the southern serpentinite unit, but the contact relationship could not be delineated there because of poor exposure.

Autochthonous Enclosing Rocks

Murdama Group

The volcano-sedimentary rocks structurally underlying the southernmost ultramafic thrust slice were formerly mapped as units within the Halaban Group (Aguttes and Duhamel, 1968), whereas similar rocks above the contact with the al-

FIG. 4. Pillow lavas at northern edge of northern greenstone belt. Pillows face right way-up; the larger ones range up to 0.7 m in length. Bir Umq area.

lochthonous nappes to the north were assigned to the Murdama Group. However, differences justifying separate formational status were not observed, and both are now regarded as Murdama rocks (Delfour, personal communication).

Interplay of sedimentary and volcanic processes has produced rocks with the characteristics of both reworked volcanic sediments and pyroclastics. Textures are generally sedimentary, with a pyroclastic component directly contributed during deposition. Some predominantly tuffaceous layers are also present. Two compositional facies have been distinguished, namely, greenish, speckled Murdama rocks mainly of andesitic derivation on the east, and vari-coloured, polylithic, fine-grained conglomerates and wackes on the west (Fig. 5). Pronounced shear foliation (S_2) has been superimposed on a weakly developed regional foliation (S_1) in the vicinity of the thrust. Thin marble beds are interbedded with sericite phyllite at the contact of the southern thrust in the central part of the area.

Murdama rocks are commonly well laminated on a scale of a few millimeters to one centimeter and bedded in units ranging from a few decimeters to several meters in thickness. A variety of sedimentary structures, some of which show turbiditic characteristics, are commonly present. Penecontemporaneous erosion and redeposition of siltstone and mudstone while still unconsolidated is evident. Primary sedimentary structures confirm that Murdama rocks are the right way up in the main outcrops. They strike eastwards and dip 40–80° N.

The Murdama sediments are made up of two components. These are (a) andesitic and acid volcanoclastics which were undergoing erosion and rapid deposition at the time of Murdama sedimentation, and which may originally have been derived by reworking of Hulayfah rocks; and (b) directly contributed pyroclastic material in the form of angular andesitic clasts and plagioclase crystals.

GEOLOGY OF HAMDAH ULTRABASIC INTRUSIONS

Structure

Near Hamdah in the south of the Saudi Arabian Shield, two large and several smaller serpentinized ultramafic bodies have been emplaced within a deeper structural level and at an earlier stage of deformation and metamorphism than the Bir Umq rocks (Plate 2). They have, together with many of the surrounding rocks, undergone the main periods of folding in the area. The ultramafic bodies comprise the oldest recognizable plutons within an area consisting of about 70% of intrusive rocks and remnants of layered metamorphic rocks, including metavolcanic and metasedimentary rocks.

The two main ultrabasic plutons are at Hamdah and Dayra. The former is triangular in shape and has a maximum dimension of 12 km; the latter is oval and its maximum length is 16 km. Both bodies have been squeezed into structural conformity with the surrounding metamorphic rocks; their principal axes in plan coincide with the fold trend of these country rocks. Slight inward dips in the marginal zones of the two intrusions suggest that the present outcrops represent low levels in diapirs that once occupied a wider cross-section at higher levels. The smaller intrusions are found at Higera, Sulb, Jabal Harban, and east of Jabal Lahu, all of

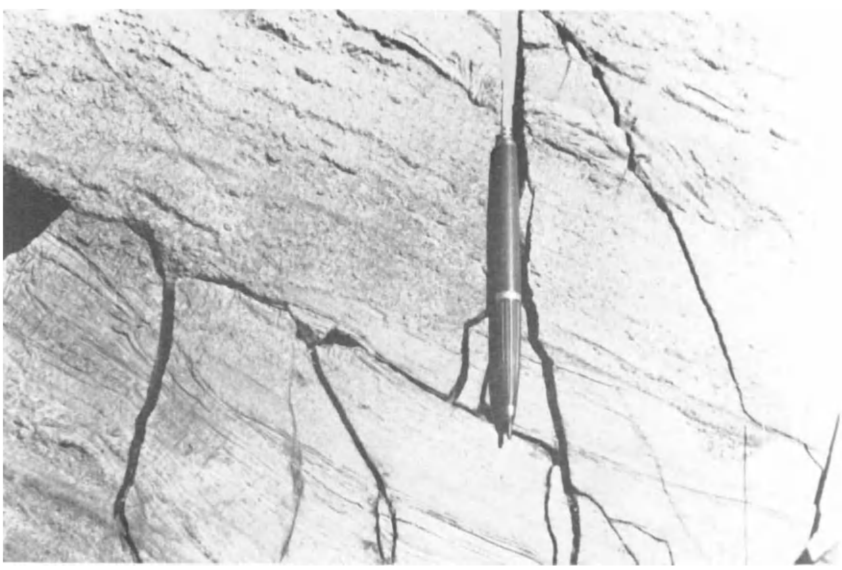

FIG. 5. Polylithic wackes containing mainly acid clasts. Murdama group in southwest of the area below the southern thrust.

which have a more irregular shape. Some of these have been reworked within the cores of folds, e.g. at Jabal Harban, and others into East-trending fault zones e.g. at Garlahu.

The ultramafic intrusions are interpreted as having been emplaced diapirically as cool, viscous, plastic bodies in a hydrated state into a variety of layered rocks that had been already metamorphosed (Warden, in press). Trains of chromite and magnetite crystals, the only primary minerals to survive throughout most of the intrusions, show intricate rheid flow patterns which lack consistency in structural trend. Locally, however, cumulate textures are preserved in pyroxenite and peridotite.

Swarms of dismembered spilitized dolerite dykes are common, particularly within the marginal zone of the larger serpentinized ultramafic bodies. They commonly form aligned lenses from one to several meters long and as much as 2 m wide (Fig. 6), aligned mostly parallel to the margins of the intrusions. Apparently the dolerite was injected into still plastic serpentinite and then stretched and dismembered by continued diapiric movement.

FIG. 6. Stretched metadolerite lens with chilled margin derived from dismembered metadolerite dyke. Near northern margin of Hamdah serpentinite.

In contrast to the plastic structural style described above are the effects of later tectonism on the serpentinized ultramafic rocks. This tectonism probably occurred under reduced lithostatic pressure, and resulted in extensive brittle fracturing. For example, the western part of the Hamdah serpentinite is dislocated by and slightly offset along a N.W.-trending shear, probably an extension of a major suture 12 km to the S.E. A transcurrent fault of similar Najd trend dislocates the Dayra serpentinite and truncates the North-eastern edge of the Sulb serpentinite. Shearing was accompanied by strong silicification (Fig. 7). Extensive breciation, possibly also related to this tectonism, shattered the Sulb serpentinite into blocks up to several hundred metres in diameter and permitted penetration by mainly granodioritic magma.

The country rocks enveloping the serpentinized ultramafic intrusions were distended, compressed and sheared (Fig. 8). Cataclastic and mylonitic textures are common. In some instances, slight rotation of the intrusions is inferred from the presence of steeply plunging minor drag folds. Structures of this type are developed in tremolite schist in the contact zone of an ultrabasic intrusion emplaced within the closure zone of a syncline S.E. of Jabal Lahu.

A North-trending fault which is thought to predate the Najd faulting described earlier truncates the eastern margin of the Hamdah ultramafic intrusions.

It is difficult to establish a direct correlation between the emplacement of the ultramafic intrusions and tectonism within the area. However, as already noted, the N.W.-trending shears cutting the Hamdah intrusion are aligned with a major suture to the S.E., along which granulites are developed and into which is intruded an extensive gabbro sill yet farther to the S.E. Pediment obscures the possible northwesterly continuation of this suture near the ultramafic intrusions, but there are contrasted structural styles on either side of this pediment zone. A genetic relationship may be present between the ultramafic bodies and this feature which is the site of basic magmatism and high heat flow to the S.E. It could represent an intra-continental collisional suture which provided egress for mantle rocks (Sillitoe, pers. comm.).

Ultramafic Intrusions

The primary rock types present, in order of abundance, are serpentinized dunite, serpentinized

FIG. 7. Serpentinite indurated by silification along a N.W.-trending shear zone bounded by light-coloured carbonate-serpentinite breccia. Western part of Hamdah ultrabasic intrusion.

peridotite, extensively uralitized and serpentinized pyroxenite, and less altered pyroxenite. Secondary rock types formed by processes such as shearing, low-grade metamorphism and hydrothermal activity include tremolite–, talc–, carbonate–, and chlorite–tremolite schist, and magnesite. These schists are largely confined to shear zones and to the margins of the intrusions, magnesite being patchily developed within this setting as well as in the serpentinite. Large-scale carbonatization of the ultramafic rocks of the type found at Bir Umq is lacking.

With rare exceptions, the olivine within the dunite has been completely serpentinized; relicts of olivine were, however, recorded in the serpentinite S.E. of Jabul Lahu. As noted, chromite and magnetite are generally the only primary minerals preserved, and the latter gives the ultrabasic bodies strong anomalous expression on the aeromagnetic maps of the area.

Peridotite is similar to the dunite but contains pseudomorphs of clinopyroxene consisting, in some cases, of bastite, and in others of brown carbonate minerals. Some of the peridotite is probably serpentinized harzburgite. Peridotite is more abundant in the Hamdah intrusion than in the others but merges into dunite without showing any well defined structural relationship to it.

The pyroxenite occurs mainly in the marginal zones of the intrusions and probably forms a cumulate phase of the ultramafic rocks. Younger pyroxenite dykes have also been recorded. The largest occurrence of pyroxenite (a lensoid mass, 1 × 2.5 km) is located near, and parallel to, the northern edge of the Hamdah intrusion. Layers of pyroxenite (0.5–3 m thick) alternating with serpentinized dunite also occur in the north-eastern part of this intrusion, and near the eastern and western contacts of the Dayra ultrabasic pluton; and a 250 m thick pyroxenite zone bounds the southern margin of the ultramafic body S.E. of Jabal Lahu. The pyroxenite has generally resisted the plastic deformation which affected the other ultramafic rocks and retains a cumulate fabric, but pyroxene is usually completely replaced by uralitic amphibole, serpentine and opaque minerals.

The younger pyroxenite dykes post-date emplacement of the ultramafic intrusions as they cut both these and the surrounding country rocks. They intrude metamorphic rocks within the Jabal Harban fold, both ultrabasic and sedimentary rocks at Higera, and the northern part of the Hamdah intrusion. They are up to one meter wide and several hundred meters in length. In the Hamdah area, blackening of the serpentinite due to dehydration together with formation of granular secondary olivine was recorded. The dykes consist mainly of fresh clinopyroxene, some orthopyroxene and accessory opaque minerals.

Also grouped with the ultrabasic rocks because of their spatial association and possible genetic relationship are the spilitic dolerite dykes noted earlier. Hot intrusion is inferred from dehydration blackening of the serpentinite up to 30 cm from the dyke margins and marginal chilling of the dismembered lenses. In some instances talc-magnesite rims with asbestos veining indicate reaction

FIG. 8. Pseudoconglomerate formed as a stretched breccia in metasedimentary rocks in the tectonized northern contact zone of the Hamdah serpentinite.

with the enclosing serpentinite. The dolerite locally preserves a relict ophitic texture, the pyroxene being replaced by two generations of amphibole, namely, green hornblende and a blue-green tremolitic variety. Chlorite, granular albite, epidote, opaque minerals and apatite make up the remainder of the rock.

Secondary rocks

These are of much more restricted occurrence than at Bir Umq. Silicification and carbonatization were recorded in the vicinity of shears and fault zones.

Metamorphic effects at the contacts of the ultramafic intrusions vary from negligible (for example, along the slightly cross-cutting, sharply defined western edge of the Hamdah intrusion) to moderate (as in the ultrabasic intrusion S.E. of Jabal Lahu). At Jabal Lahu, phyllite with calcareous interbeds becomes greenish within a few meters of the contact. The formation of green amphibolite, tremolite–chlorite schist, and chlorite–epidote schist indicate metamorphism in the upper greenschist facies with metasomatism near the contact.

Hydrothermal reactions have produced talc- and tremolite-schist in shear zones within the ultramafic intrusions. In places the dolerite lenses of the stretched dyke swarms are sheathed in a layer of chlorite–actinolite schist a few centimeters wide; this represents a reaction zone between the intrusions and the serpentine host rock.

Irregular nodular masses of magnesite are locally common within the ultramafic rocks but large-scale carbonatization is absent. Cross-fibre serpentine asbestos occurs within fractures near the contacts of the ultramafic intrusions, chrysotile being present notably in the N.E. of the Hamdah intrusion, in the layered pyroxenite–dunite zone, and at Higera; it is more abundant than at Bir Umq. Chrysotile is, however, restricted to the narrower veinlets; in the wider ones it has been pseudomorphed by carbonate and steatite.

Country Rocks

The ultramafic intrusions were emplaced within what are now disconnected remnants of layered metamorphosed volcanic and sedimentary rocks. Although they lack stratigraphic continuity, being separated from one another by granodiorite gneiss and plutonic rocks, they are lithologically similar to units with established identity elsewhere in the shield. The eastern ultramafic bodies intrude two units, namely, the Dayra greenstone (consisting of meta-basaltic and meta-andesitic rocks with reworked clastics and minor ultrabasics), and the Harban schist (comprising amphibolite, calc-silicate rock, meta-arkose with pelitic and graphitic schist). These units are correlated with the Jiddah greenstone and the Hali schist respectively. The Bayni Oshir Formation, which is intruded by the Hamdah ultrabasic pluton in the west, consists predominantly of andesitic volcanics and wackes with some basalt, dacitic volcanic rocks, minor phyllite, chert and limestone; it is lithologically similar to the Harban Group (Warden, in press).

The Adaf-Maruwah formation is a distinctive unit. It is less intensely folded than the others, lacks common volcanic lithics, and consists predominantly of arkosic sediments which are better sorted than the other units. It may have been derived from predominantly granitoid terrain, probably post-dates the other units and possibly represents molasse-type sedimentation.

Rubbly layers of serpentinite and pyroxenite sheets (possibly sills) are intercalated with country rocks belonging to the Dayra greenstone and Harban schist. The lack of metamorphic contacts indicates that the former were emplaced in a cold state. It has been suggested that they were deposited contemporaneously with the enclosing rocks as rubble slides from the domes of rising serpentinite diapirs (Neary, pers. comm.); this would account for the lack of metamorphism and increased frequency near the contacts of the ultramafic plutons. However, the rock units described were already present and undergoing folding and metamorphism when the serpentinized ultramafic rocks were intruded into them. This seems to preclude contemporaneous deposition, so their origin remains enigmatic.

The serpentinized ultramafic rocks were intruded at their contacts as well as internally by gabbro, diorite, granodiorite and post-tectonic pink granite in that order, all of which post-date the gneissic granodiorite and diorite which intrude the contact of the Hamdah pluton. These gneissic rocks may comprise a northerly extension of the Malahah batholith recorded to the south by Greenwood (1979).

Magmatism within the Hamdah region is characterized by widespread injection brecciation so that the intrusive rocks mentioned net-vein their predecessors in succession, producing complex agmatitic structures.

The ultramafic intrusions are interpreted as having been emplaced diapirically at a rather deep structural level and in an already hydrated, relatively cold, viscous state (Marmo, 1958) within the layered rocks described; the latter had already been metamorphosed and were undergoing continuing folding. If considered together with some of the surrounding country rocks of the Dayra Greenstone and Bayni Oshir Formations, the assemblage would include many of the lithologies characteristic of an ophiolite suite, such as pillow basalt, spilite, chert, calc-alkaline volcanics and clastics. However, the ultrabasic bodies are clearly intrusive and, moreover, lack the ordered pseudostratigraphy of ophiolite.

CHEMISTRY OF BIR UMQ AND HAMDAH ROCKS

Major element analyses are available for some ultrabasic and associated rocks from both complexes, but these data are inadequate to clearly define trends or differentiate suites.

Some differences are, however, evident when the Saudi Arabian ultramafic rocks are compared with established ophiolites (Coleman, 1977). Serpentinized dunite from the former contains up to 10% less SiO_2 and MgO, and has notably higher Al_2O_3 values and a higher Na_2O content, thus reflecting the spilitic character of the Arabian rocks. The keratophyres from the Saudi Arabian Shield are generally lower in FeO and Fe_2O_3 and CaO, and higher in alkalis, particularly Na_2O, than their counterparts from established ophiolite suites.

DISCUSSION

The Bir Umq complex comprises three imbricate obducted ophiolitic slices over-riding southwards and dipping steeply to the North. Thrusting probably occurred originally at a lower angle and was steepened during regional folding. As the nappes overlie Murdama rocks and the uppermost slice is overlain by similar rocks, the time span of emplacement, due probably to back-arc closure, is relatively short and was accomplished within the depositional period of the Murdama.

Tectonism was accompanied by strong shearing, particularly near the sole of the thrusts, and extensive carbonatization. It has been suggested (Delfour, pers. comm.) that the carbonatization process may be related to litzvenitisation (*in situ* carbonatization on the sea floor), but it is thought more probable that it was due to circulation of hydrothermal solutions within the shear zones, derived perhaps from connate brines in the clastic sediments.

There is generally little evidence of frictional metamorphism near the sole of the thrust zones, of the type found, for example, in the Oman (Glennie *et al.*, 1974); or of thermal metamorphism due to slow obduction over a hot source, of Newfoundland type (Williams and Smyth, 1973). However, meta-dolerite within a restricted central area near the base of the southern ophiolite nappe contains acicular amphibole cross-cutting the original igneous fabric. As previously noted this may be due to thermal metamorphism related to residual magmatic heat in the serpentinized dunite.

The occurrence of megabreccias (or melange) within the serpentinized ultramafic units is atypical, such rocks being normally confined to the sole of obducted nappes, as for example in the Semail nappe in Oman (Glennie *et al.*, 1974).

When a composite stratigraphic section of the Bir Umq ophiolite sequence is correlated with a typical ophiolite such as Troodos (Bakor *et al.*, 1976) remarkably good accordance is evident (Fig. 9A), although allowance must be made for extensive reworking of the Bir Umq rocks. No recognizable primary structure remains in the serpentinite at the base of the middle and uppermost nappes. These units range from one to a few hundred meters in thickness and show strong plastic deformation suggesting 'lubrication smearing' below the overriding thrust slices. As noted earlier, the succession is best preserved near Bir Umq, in

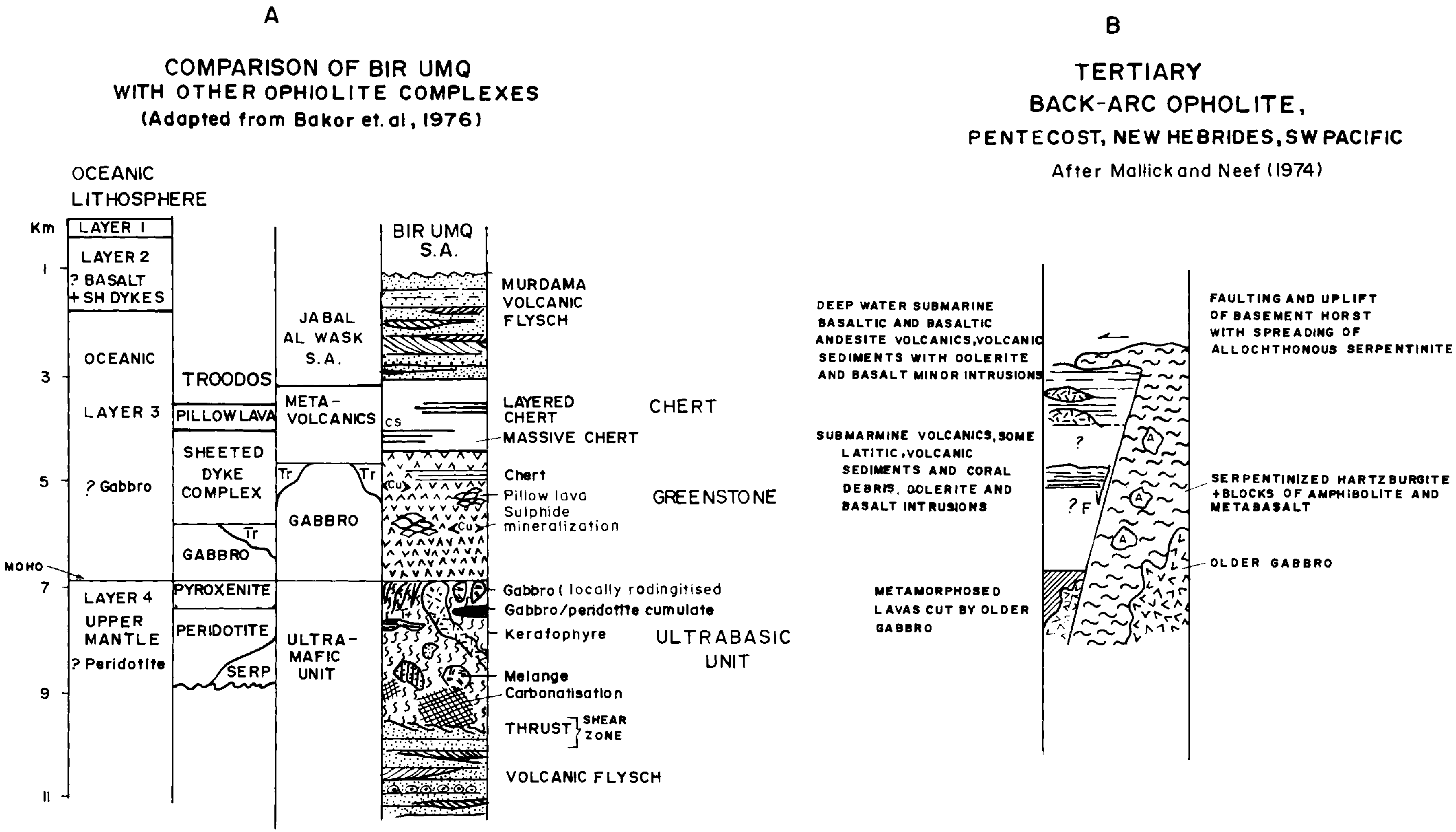

FIG. 9. (A) Comparison of Bir Umq with other ophiolite complex. (Adapted from Bakor *et al.*, 1976). (B) A tertiary ophiolite: synopsis of stratigraphy of Pentecost Island, New Hebrides (After Mallick and Neef, 1974).

the eastern part of the southern ultrabasic unit, where it attains a maximum width of 2.5 km although the thickening of the unit is partly due to offset repetition and flowage related to N.W.- and N.E.-trending transcurrent faults. Serpentinized dunite is the main rock type (some harzburgite containing 50% of relict olivine and pyroxenite is also present), but it lacks a well defined layered structure. Although there is no continuous layered gabbro-peridotite unit overlying the ultramafic rocks, localized zones of gabbro-serpentinized peridotite whose boundaries are unclear occur in the east of the area near the upper contact of the lowest ultrabasic unit. Either this layered unit was incompletely developed, or it was disrupted by subsequent flowage of the serpentinite. Small bodies of locally rodingitized uniform gabbro occur at the top of the lower ultramafic rocks in the central part of this unit. Trondjemite veins representing late-stage ophiolitic differentiates are also found in this area. Keratophyre, usually interlayered in the upper part of the pillow basalt unit in normal ophiolites, is restricted to an annular intrusion within the southern ultrabasic belt at Bir Umq, possibly because the tectonism which produced the melange provided a suitable locale for magmatism.

The most notable difference from a typical ophiolite suite is the absence of a sheeted dyke complex at the base of the greenstone unit. This may be due to rapid spreading (Coleman and Irwin, 1974; Coleman, 1977) though even so some dykes should be present. The basaltic unit, which is up to 2.2 km thick, is mainly represented by greenstone consisting mainly of spilitized tholeiite (Fig. 9A), locally showing well developed pillow structure and minor copper sulphide mineralization. It is interbedded with and passes upwards into chert which is partly well layered and partly massive and recrystallised. As noted, the former closely resembles the abyssal cherts of more modern ophiolites, for example the Hawasina Formation in Oman (Glennie *et al.*, 1974).

On the foregoing evidence it is concluded that, except for the absence of a sheeted dyke complex, the Bir Umq ultrabasic suite fulfils the criteria of an ophiolite. The Jabal Thurwah complex, aligned on the same general strike 170 km west of Bir Umq, contains all the potential components of an ophiolite, including a sheeted dyke complex and well developed gabbro-peridotite layering (M. Nasseef, pers. comm.). However, the Jabal Thurwah ophiolite is more complex and tectonically disturbed than Bir Umq so that the order of some units is as yet unclear.

Modern (Tertiary) ophiolites of a pre-obduction stage from Pentecost Island, New Hebrides (Fig. 9B) provide some clues to the origin of back-arc ophiolites. According to Mallick and Neef (1974), mantle-derived serpentinized ultrabasic rocks, including dunite, harzburgite, lherzolite and wehrlite, were upfaulted along horsts and have commenced allochthonous solifluxional lateral spreading (an alternative mechanism to tectonic obduction) over adjoining downfaulted blocks. Older gabbro is associated with the serpentinite, and amphibolite exotics transported from depth, probably representing metamorphosed ultramafites, may be regarded as a type of melange which also contains blocks of meta-basalt.

Metamorphism related to the emplacement of older gabbro affects both the gabbro and contiguous volcanic rocks and is thought to involve connate water. Silicification and pyritization with traces of Cu and Zn sulphides is also evident but is mainly confined to spilitized mafic lavas and shears. Basalt and mafic andesite which commonly show pillow structure are thought to have been derived from partial melting of oceanic crust (Mallick and Neef, 1974). Some acid rocks with a composition of quartz latite are also present. A deep-water environment is deduced for the lavas and clastics which show the characteristics of flysch. This modern analogue provides valuable evidence of many features and processes observed in ancient counterparts such as Bir Umq. The allochthonous ultramafic and autochthonous volcanic rocks are broadly similar to comparable units at Bir Umq, though the former includes gabbro peridotite layering and layered gabbro. Spilitization is evident in both ophiolites; and comparable secondary processes similar to those at Bir Umq produce silicification and minor sulphide mineralization. While some silicification is evident at Bir Umq, hydrothermal activity differs in the dominance of carbonatization, pointing to the prevalence of carbonated solutions.

A model has been developed (Fig. 10) based on a prototype envisaged by Dewey (1976). Three ophiolite nappes are obducted southwards onto a continental foreland, or back-arc, during closure of a rear-arc basin. As the nappes move into position, melange is incorporated at the base of successive slices and volcanic flysch (similar to allochthonous Murdama at the base of the ophiolite package) is deposited on top of the uppermost slice. This includes turbiditic volcanic sediments reworked from the flank of the craton and directly contributed volcanoclastic material.

Hamdah

This ultrabasic complex is of fundamentally different origin. Unlike Bir Umq, it was not emplaced in an epizonal setting characterised by brittle slice tectonics although it underwent brittle tectonism at a later stage.

The Hamdah plutons were intruded diapirically

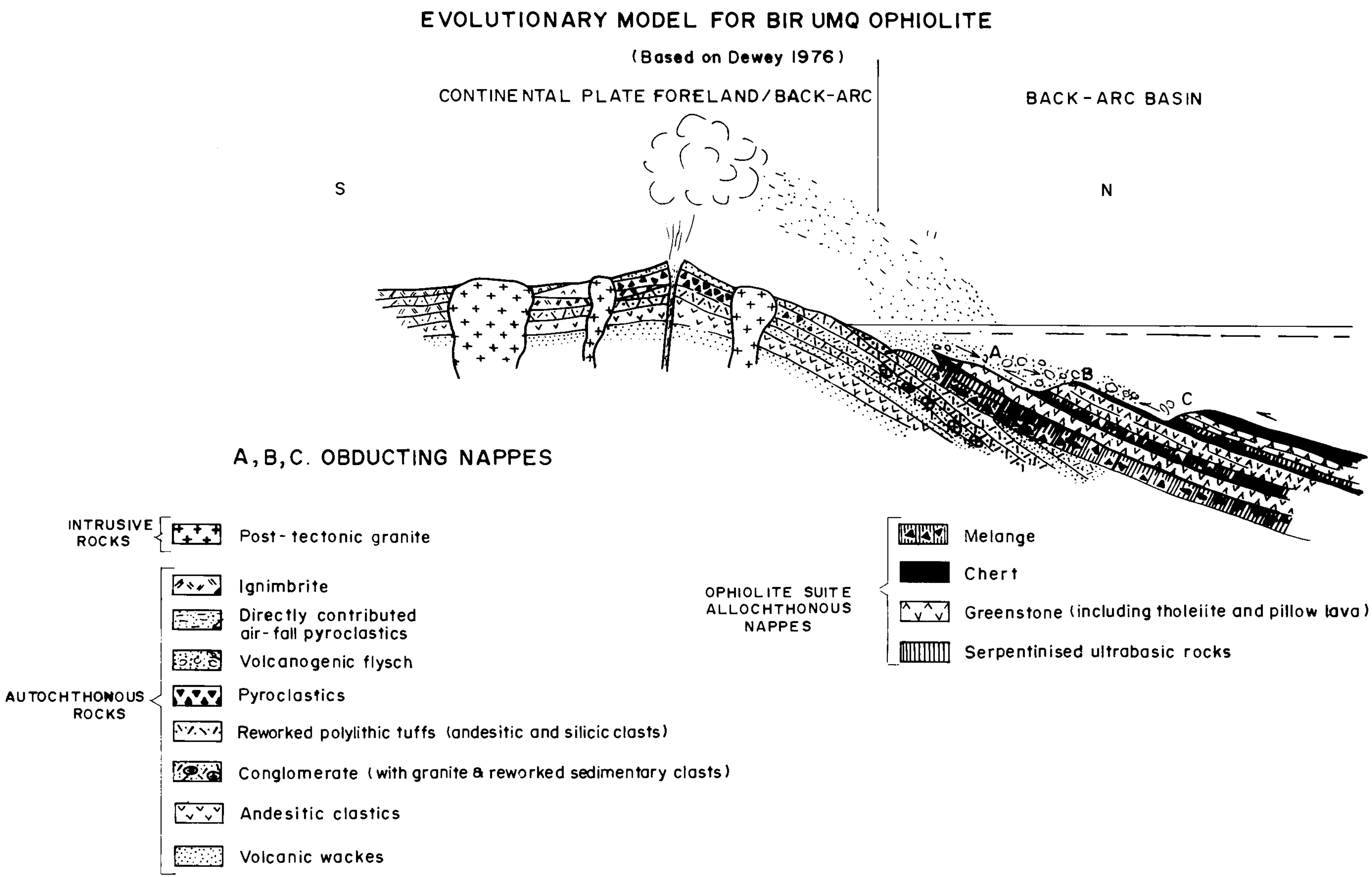

FIG. 10. Evolutionary model for Bir Umq ophiolites, based on Dewey (1976) prototype.

as mainly concordant, cold, viscous, hydrated ultrabasic magma in a relatively deep-seated environment. The intrusions were accommodated by shearing and distension of enveloping rocks. Similar internal deformation is reflected by stretching of marginal dolerite dyke swarms.

Unlike the Bir Umq ophiolite, the Hamdah ultrabasic rocks are intruded by all the other plutonic rocks, ranging from gabbro to post-tectonic granite, and by anatectic gneissic granodiorite representing a late episode of diapirism. Post-ophiolite emplacement magmatism in the case of the Bir Umq ophiolite is restricted to minor intrusions of andesite and dacite, also reflecting a higher structural level expression.

Development of melange is lacking in the Hamdah ultrabasic intrusions, and secondary processes, principally carbonatization, are more restricted than at Bir Umq.

The Hamdah ultramafic suite lacks a well defined pseudostratigraphy. Moreover, it is clearly intrusive into, and therefore not in stratigraphic continuity with, contiguous metamorphosed basalt, andesitic, dacitic and rhyolitic rocks, minor phyllite and chert, some of which might otherwise have been justifiably included within the ophiolitic suite.

There is indirect evidence of a tectonic relationship with a major North-trending suture, possibly of intracontinental collisional origin. The Hamdah ultramafic diapirs may represent mantle material, mobilized during the evolution of this feature.

REFERENCES

AGUTTES, J., and DUHAMEL, M. 1971. Geology and mineral exploration of the Jabal Sayid Quadrangle. *Bur. Rech. Geolog. Minieres Rept.* 71-JED-4.

ANONYMOUS 1972. Penrose field conference on Ophiolites. *Geotimes* 17, 24–25.

BAILEY, E. H., and COLEMAN, R. G. 1975. Mineral deposits in the Semail ophiolite of northern Oman. *Geol. Soc. Am. Abst.* 7 (3), 293.

BAKOR, A. R., GASS, I. G. and NEARY, C. 1976. Jabal Al Wask, northwest Saudi Arabia: an Eocambrian back-arc ophiolite. *Earth Planet. Sci. Lett.*, 30, 1–9.

BROWN, G., and JACKSON, R. O. 1959. Geologic map of the Asir Quadrangle, Kingdom of Saudi Arabia. *Saudi Arabian Dir. Gen. Mineral Resources Map* 1-217A.

COLEMAN, R. G. 1977. *Ophiolites.* Springer-Verlag, New York.

COLEMAN, R. G., and IRWIN, W. P. 1974. Ophiolites and ancient continental margins. Pp 921–931 in *The Geology of Continental Margins* (eds. BURK, C. A., and DRAKE, C. L.). Springer-Verlag, New York.

CONSTANTINOU, G. 1976. Genesis of the conglomerate structure, porosity and collomorphic textures of the massive sulphide ores of Cyprus. *Geol. Assoc. Canada Sp. Paper* 14, 187–210.

DEWEY, J. 1976. Ophiolite obduction. *Tectonophysics* 31, 93–120.

GLENNIE, K. W., BOUEF, M. G. A., HUGHES-CLARKE, M. W., MOODY-STUART, M., PILAAR, W. F. H., and REINHARDT, B. M. 1974. Geology of the Oman mountains. *Verhandelingen van het Koninklijk Nederlands geologische mijnbouwkundig Genootschap*, pt. 31.

GREENWOOD, W. 1979. Geology of the Wadi Malahah Quadrangle, sheet 18/43D, Kingdom of Saudi Arabia. *Saudi Arabian Dir. Gen. Mineral Resources Geol. Map* GM-39, scale 1 : 100,000.

MALLICK, D. K. J., and NEEF, G. 1974. Geology of Pentecost, *New Hebrides Condominium Geol. Surv. Regional Rept.* NN ISSN 077-8443.

MARMO, V. 1958. Serpentinites of Central Sierra Leone. *Bull. Comm. Geol. Finland* 180.

WARDEN, A. J.. Geology of the Markas Quadrangle, Kingdom of Saudi Arabia. *Saudi Arabian Dir. Gen. Mineral Resources Map* (in press).

WILLIAMS, H., and SMYTH, W. R. 1973. Metamorphic aureoles beneath ophiolite suites and alpine peridotites: tectonic implications with west Newfoundland examples. *Am. J. Sci.* 273, 594–621.

PLATE 1 AND 2. Geology of the Hamdah Ultrabasic Intrusions. Interim Geological map of BIR UMK Ultrabasic Complex. [In pocket at end of book.]

الصفات الصخرية لمايحتمل وجوده من الصخور الأفيوليتة
على طول طريق قفط ـ القصير فى الصحراء الشرقية بمصر

ع٠ع٠ نصيف ، ع٠ى٠بكر ، أ٠ح٠ حشاد

الخلاصة

إن السربنتينيتات على طول طريق قفط ـ القصير فى وسط الصحراء الشرقية بمصر يحتمل أن تكون أعضاء من تجمع أفيوليت ماقبل الكمبرى٠ وتتتابع المكونات من صخور فوقمافية فى القاعدة الى صخور جابروية وجدد فريشية فبركانيات قاعدية استوسدت (صارت وسادية) عند القمة ٠

ويتضمن هذا البحث وصف التكوين الصخرى (البتروجرافى) لهذه الصخور٠ إلا أن ثبوت وجود الأفيوليت فى هذا المكان بصفة قاطعة يتطلب توفر بيانات كيميائية صخرية (بتروكيميائية) تعضد الوصف الصخرى ٠

PETROGRAPHY OF POSSIBLE OPHIOLITIC ROCKS ALONG THE QIFT–QUSEIR ROAD, EASTERN DESERT, EGYPT

A. O. NASSEEF[1], A. R. BAKOR[1] and A. H. HASHAD[2]

[1]King Abdulaziz University, Jeddah, Saudi Arabia
[2]Nuclear Materials Corporation, Cairo, Egypt

Abstract—Serpentinites in the central Eastern Desert of Egypt along the Qift–Quseir road are possibly members of a Precambrian ophiolite assemblage. The sequence of components from bottom to top includes ultramafic rocks, gabbroic rocks, sheeted dykes, and basic volcanics which are pillowed at the top.

The petrographic composition of these rocks is described. Petrochemical data are needed to support the petrographic description and, therefore, the suggested ophiolite sequence is yet to be completely verified.

INTRODUCTION

Most of the serpentinites of the Eastern Desert of Egypt have been previously interpreted as either intrusions or extrusions of ultramafic magma associated with mafic volcanism (Hunting, 1967; El-Ramly *et al.*, 1970; Ivanov *et al.*, 1973). Many authors have attempted to identify these serpentinites as members of ophiolite complexes and hence, as segments of oceanic crust (Moores, 1969; Peters, 1969; Reinhardt, 1969; Dickinson, 1971; Church, 1972). They have been considered to be remnants of oceanic crust obducted onto continental crust (Coleman, 1971; Dewey and Bird, 1970; Gass, 1976) or transported in thrust zones associated with subduction zones (Laubscher, 1969; Gass, 1968). Church and Stevens (1971) suggested that some ophiolites may have been emplaced as layered complexes directly over a sialic crust during the development of small intersialic ocean basins. Such an interpretation, in conjunction with other evidence, has been invoked in support of a plate tectonic model for the evolution of the Arabian–Nubian Shield (Brown and Coleman, 1972; Bakor, 1973; Bakor *et al.*, 1976; Greenwood *et al.*, 1975; Garson and Shalaby, 1974).

In this paper, more evidence on the presence of ophiolite sequences in the central Eastern Desert of Egypt will be presented, and a correlation with the ophiolite suites found at Jabal Al-Wask (Bakor, 1973) and other localities currently under investigation in Saudi Arabia will be attempted. The areas visited were El-Fawakhir, El-Ghadier, Um Nar and El-Barramia (Fig. 1). The first of these areas is nearly midway along the Qift–Quseir road and appears to have the most complete development of a possible ophiolite succession; the road passes through an important and major part of the succession between km 86 and km 78 to Qusein.

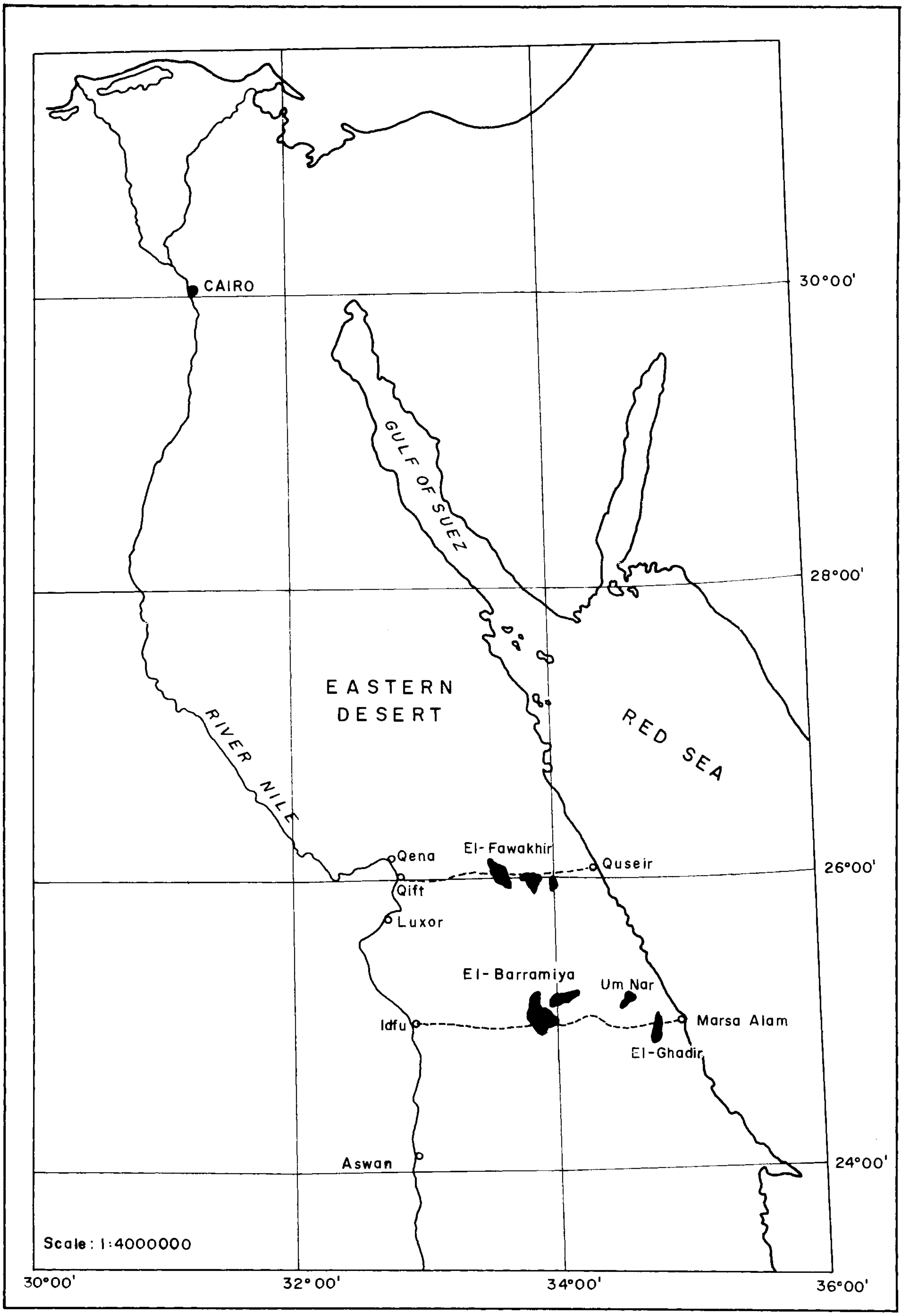

FIG. 1. Location map of the possible ophiolite occurrences in the Eastern Desert of Egypt.

Samples collected from this segment of the sequence were investigated petrographically in thin and polished sections.

GEOLOGY

The area under consideration was mapped by Akaad and Noweir (1972) as an asymmetrical plunging syncline with an inner zone of highly sheared serpentinite intruded by meta-gabbro. The oldest unit in the area is the Khors Schist Member, consisting of an association of semi-pelitic and calcareous pelitic schists with minor bands of marble and graphitic meta-cherts. This member is conformably overlain by the Muweilih Formation consisting of a thick sequence of metamorphosed, soda-rich basic pillow lavas and thick flows of basic lavas together with intermediate intrusive types and tuffaceous varieties. Garson and Shalaby (1974) believe that the sequence as presented is incorrect and that it is overturned.

Although many of the rocks described by Akaad and Noweir (1972) appear to be components of an ophiolite assemblage, these authors have treated them as separate units of serpentinites and gabbros, or included them within the metasediments and metavolcanics.

According to the 1972 G.S.A. Penrose Conference on ophiolites (Gass, 1976), an ophiolite is a distinctive assemblage of mafic and ultramafic rocks. An "idealized" and "complete" assemblage would consist of:

1. Basic volcanics (commonly pillowed).
2. Sheeted basic dyke complex.
3. Gabbros and trondjemites.
4. Layered olivine gabbros.
5. Peridotite* and dunites† with chromites.

Coleman (1977) subdivided the ultramafic unit into cumulate peridotites that are underlain by metamorphic peridotites. If the mafic–ultramafic complex and associated metasediments along the Qift–Quseir road are members of a Precambrian ophiolite assemblage, then the above sequence of units may be expected to exist at this area. It should be noted, however, that although ophiolite assemblages are rarely found complete owing to the complex nature of their emplacement, it is possible to find many of the typical "components" that would help in identifying them as allochthonous oceanic lithosphere. Examples of incomplete successions are found at Jabal Al-Wask and the Bay of Islands, where sheeted dykes are missing, and in the Hary Bay complex, where both sheeted dykes and gabbros are absent.

In the visited area, the following sequence of components is found:

1. Basic volcanics, pillowed at the top.
2. Sheeted dykes.
3. Gabbroic rocks including: Trondjemites; Normal gabbros; Leucogabbros; Pegmatoidal gabbros
4. Ultramafic rocks including: Cumulate peridotites and pyroxenites; Metamorphic peridotites.

This sequence is not present in a continuous order. Repetition of one or more of these units frequently occurs and may represent gravity sliding of segments of the ophiolite sheets into a migrating basin. It is apparent from the description given by Akaad and Noweir (1972), and according to Hussein and Shalaby (personal communication, 1978), that the basic volcanics, when followed farther east, merge into pillowed volcanics towards the top which are clearly exposed near Bir Um Hombos. Still farther east, cherts and limey sediments occur.

PETROGRAPHY

Ultramafic Rocks

Peridotites

These rocks, together with the pyroxenites, represent the ultramafic members of the possible ophiolite assemblage. They were collected a few meters off the Qift–Quseir road at km 85.3. Two varieties were collected, the first of which is a medium-grained peridotite showing occasional development of alternating cumulates, a few millimetres in thickness, of olivines and pyroxenes. The other variety is a massive, fine-grained metamorphic peridotite. The two varieties occur usually in the same outcrop, sometimes as alternating layers 30–40 cm thick. Both rock types are greyish-black in colour, with the olivine cumulates being distinctly lighter, olive green.

In thin section, the metamorphic peridotites consist mainly of secondary minerals of the serpentine group, talc, carbonates and opaques, the primary minerals being almost completely obliterated. Rarely relics of olivine or pyroxene are observed. In the medium-grained peridotite, lizardite occurs as rectangular plates or platelets that are commonly traversed by veinlets of clinochrysotile (Fig. 2). Mesh texture is well developed where lizardite usually forms the core of the mesh and is surrounded by clinochrysotile. Antigorite forms scaly or fine lamellar aggregates exhibiting plumose texture with a radiating habit. Some of the antigorite crystals show a fibrous habit and are colourless to pale beige. Talc forms flakes or patches, and in some cases

---

*harzburgite (sometimes lherzolite).
†commonly serpentinized.

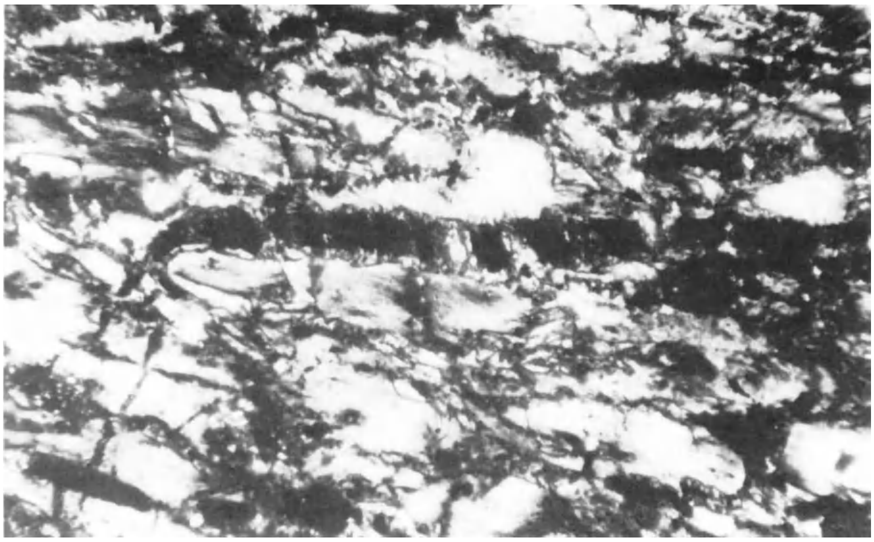

FIG. 2. Coarse plates of lizardite traversed by veinlets of clinochrysotile in fine-grained matrix of lizardite and chrysotile. Crossed nicols, ×140.

fibres; it is associated with the serpentine minerals. Carbonates, probably magnesite or dolomite, form fine- to medium-grained aggregates or discrete grains which may form rims around the serpentine minerals; elsewhere, veinlets of calcite cut the serpentine minerals.

The fine-grained peridotites appear more fine-grained in thin section with the development of large amounts of much scaly antigorite (Fig. 3), otherwise but are mineralogically similar to the medium-grained peridotites.

In polished section, magnetite, titanomagnetite and chromite are the most common ore minerals in the medium-grained variety; ilmenite, pyrite, rutile and goethite being occasionally present. Magnetite is present either as fine-grained, small, anhedral to subhedral globules bordering serpentine (Fig. 4) formed during the alteration of olivine into serpentine; or, with inclusions of arsenopyrite, as euhedral to subhedral crystals, these being primary crystals segregated during the early stages of magmatic crystallization. Some of this magnetite is slightly to moderately martitized along the borders. A few crystals show a dendritic or skeletal growth, and this represents early stages of crystal growth followed by rapid cooling.

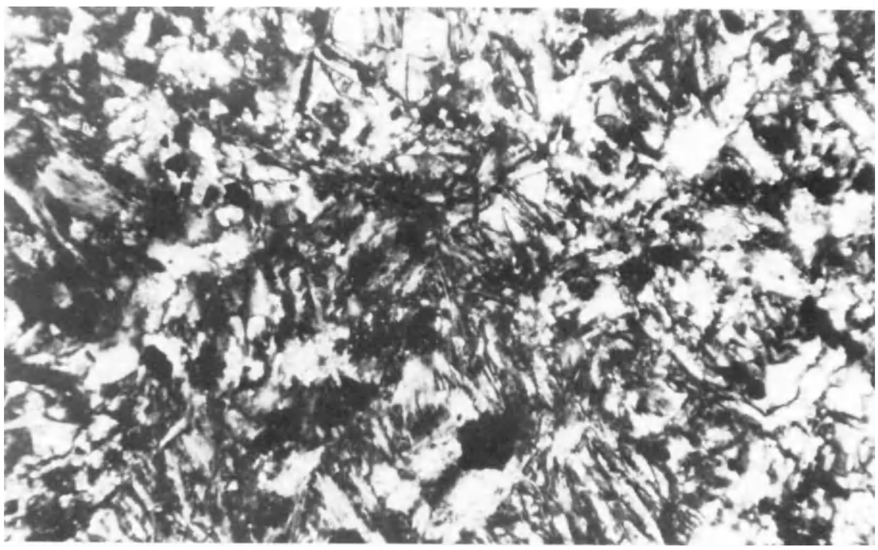

FIG. 3. Bundles of radiating fibres and scales of antigorite. Crossed nicols, ×140.

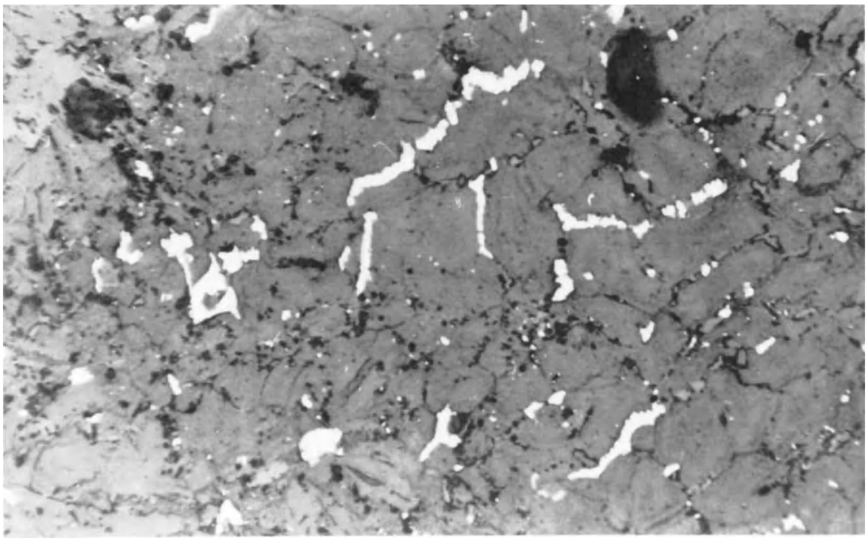

FIG. 4. Fine-grained crystals of magnetite surrounding grains of serpentine. Plane polarized light ×154.

Chromite occurs as discrete single crystals of euhedral to subhedral form, commonly rimmed by an alteration halo of a somewhat more strongly reflecting mineral which is probably a more Fe-rich chrome spinel. The outer rims of chromite may sometimes be converted to magnetite (Fig. 5), a form of alteration also present along the cracks and in the porous parts of the grains. Some grains contain fine inclusions of silicate gangues and fine pyrite blebs. No exsolution texture was observed in the chromites. Small rutile crystals are also found as more or less oriented inclusions in the chromite. In some sections, especially in the fine-grained peridotite, the chromite is relatively more abundant and occurs as disseminated crystals that may form fine cumulate bands (Fig. 6). This could represent the primary layering of the ultramafic rocks.

The titanomagnetite is fine-grained and is anhedral to subhedral. It is randomly disseminated through the rock and partially altered to goethite and pseudo-brookite.

The serpentinites present in this area seem to have been derived from more than one type of ultramafic parent rock. The medium-grained variety is relatively enriched in chromite, and may

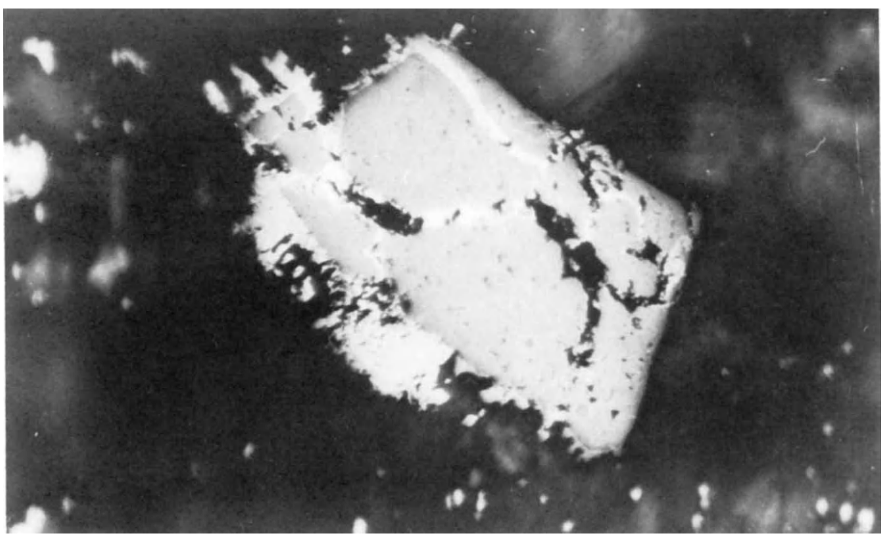

FIG. 5. A grain of chromite showing alteration to partially martitized magnetite along cracks and grain boundaries. Plane polarized light, oil immersion, ×154.

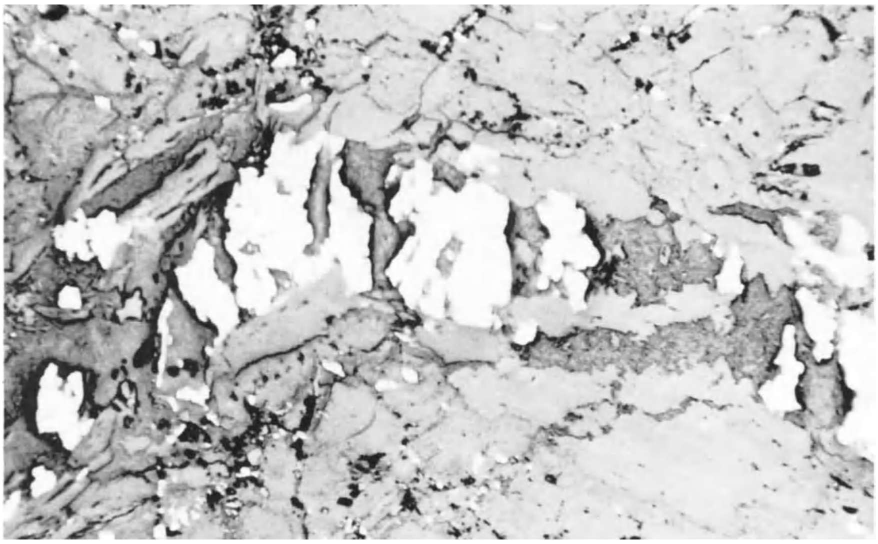

FIG. 6. Subhedral grains of chromite forming a fine cumulate band. Plane polarized light, ×154.

be derived from dunite or olivine-rich peridotite, whereas the fine-grained variety is most probably derived from rocks grading from olivine websterite to harzburgite and/or wehrlite. The extensive alteration of these rocks renders the modal analysis unrealistic and only the presence of relic ortho- or clino-pyroxenes is helpful in inferring the original rock types.

Pyroxenites

These rocks represent the second and less abundant ultramafic member of the ophiolite succession. They are well exposed along the Qift–Quseir road at km 84. The relationship with the serpentinites is not clear. In some places they occur at the base of the serpentinites, with gradational contacts, but they may also extend as narrow bifurcating veins, 10–20 cm wide, into the serpentinite. In other places, they occur as irregular, coarse-grained masses mixed with the serpentinites.

In thin section, these rocks are composed mainly of clinopyroxene and orthopyroxene which occur together in variable proportions; amphibole after clinopyroxene and olivine pseudomorphs are present in minor amounts. Opaque minerals are rare and occur mainly as streaks along the cleavage planes of pyroxenes. The pyroxenites fall generally in the websterite range. Clinopyroxene is the predominant mineral phase, forming about 65% of the rock. It occurs as anhedral to subhedral equant grains ranging in size from less than 1 mm to over 1 cm. Most of the grains are altered along the margins to colourless amphiboles (Fig. 7). Inclusions or lamellar intergrowths of orthopyroxene are common. Cracks are usually filled with iron oxides and/or very fine serpentinous material. Orthopyroxene forms about 15% of the rock. It occurs as subhedral to anhedral, equant to slightly elongated grains, or commonly as exsolution lamellae within the clinopyroxene. The former have well developed amphibolitic reaction rims. Tremolite forms about 15% of the rock and occurs as subhedral, equant grains of about the same dimensions as the clinopyroxene crystals. It is almost colourless and seems to have been developed after pyroxenes. Olivine pseudomorphs form about 5% of the rock, preserving in most cases the original euhedral form of the olivines, but with complete alteration to serpentine minerals.

Gabbroic Rocks

The gabbroic rocks, together with the associated trondjemites, are a common feature of the "mixed zones" of ophiolite succession. They are well exposed between km 84 and km 82 along the Qift–Quseir road. The contacts with the ultramafics are sheared and deformed. Some gabbros contain ultramafic xenoliths and, perhaps for this reason, gabbros were considered by Akaad and Noweir (1972) to be intrusives into the ultramafics. At Jabal Al-Wask in Saudi Arabia, the gabbros show both intrusive and faulted contacts (Bakor, 1973), and in most ophiolite successions, gabbros are separated from the ultramafics by a primary discontinuity (Church, 1972).

In the area studied the gabbros occur as a heterogenous unit which includes pegmatoidal "black and white" gabbros, leuco-gabbros, fine-grained grey gabbros, and tectonically deformed

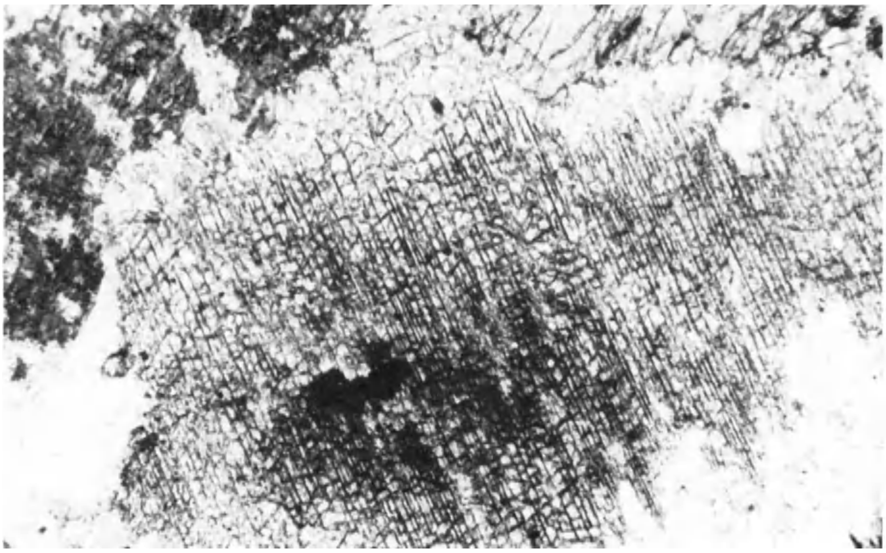

FIG. 7. Remnants of orthopyroxene in clinopyroxene altered at the margins to amphiboles. Plane polarized light, ×140.

gabbros with no regular pattern of distribution. Pegmatoidal and leucogabbros tend, however, to be concentrated near the ultramafic unit and show various types of igneous layering. The different types of gabbros seem to form a composite intrusion.

Normal gabbros

This is the most abundant gabbroic rock and varies in texture from medium- to fine-grained, with a color index between 30 and 50. In thin section, the rock is medium-grained, roughly equigranular, and consists of plagioclase, clinopyroxene and amphibole. Chlorite and clinozoisite are present as alteration products. Opaques, biotite and apatite are accessories.

Plagioclase of composition An_{55-65} occurs as subhedral, equant to tabular crystals, with grain sizes ranging from 1 mm to 1 cm. Saussuritization and sericitization are not uncommon. Relatively fresh grains show pericline and complex albite twinning. Zoning, though not well developed, may be inferred from more intense alteration at the cores of some grains. Clinopyroxene occurs mainly as euhedral to subhedral grains of comparable size to those of the plagioclase. Alteration to hornblende is common, especially along the margins.

The hornblende, which may be primary, is partially to completely altered to chlorite. In one section, much tremolite-actinolite is present as fine acicular needles or as radiating fibers of pale green to neutral colour. Primary red to brown biotite forms irregular flakes intergrown with the other dark constituents. There is a wide development of clinozoisite as discrete grains and as aggregates of crystals (Fig. 8), most probably associated with the saussuritization process. Talc forms patches in some parts of one section.

Only a few more minerals, such as ilmenite and titanomagnetite, are present in polished section but discrete single crystals of pyrite, arsenopyrite and chalocopyrite were identified. Ilmenite tends to form a fine network, with the ilmenite lamellae parallel to the 111 or 100 planes. A myrmekitic intergrowth between ilmenite and the silicate minerals is sometimes observed (Fig. 9). The ilmenite is commonly altered along the periphery to rutile and hematite, where ilmenite lamellae were most probably exsolved from titanomagnetite which was mostly dissolved away. Unexsolved titanomagnetite crystals occurring as cubic, discrete grains disseminated in the rock are rarely observed. Very few fine-grained, subhedral to anhedral crystals of arsenopyrite were also observed. Some sections contain a few euhedral cubes of fine- to medium-grained pyrite, partially to completely altered to goethite. In one section, an anhedral fine chalcopyrite grain was observed associated with a fine-grained sphalerite.

Pegmatoidal gabbros

These rocks occur as coarse-grained to pegmatoid patches and veins of variable dimensions, usually strongly deformed and altered, but sometimes relatively fresh; they seem to be products of recrystallization. Their altered nature is clearly observed in thin section, and only relics of primary plagioclase and clinopyroxene are visible. Amphiboles, most probably secondary, and opaques are also present.

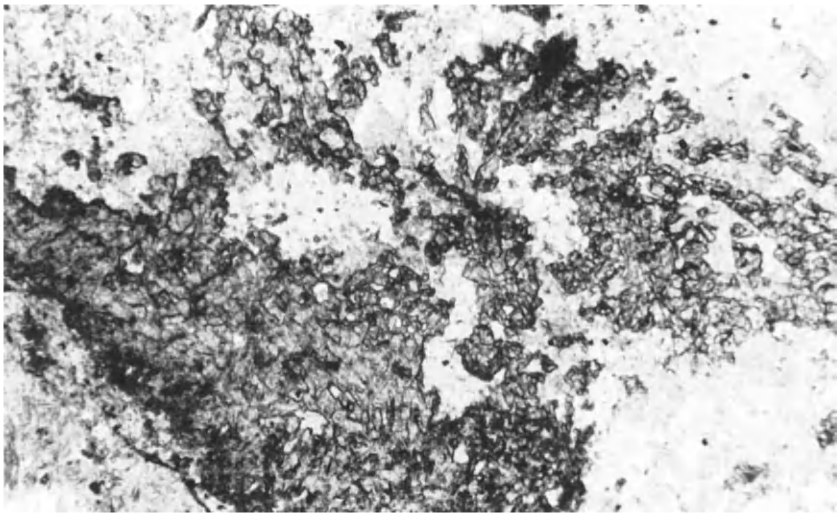

FIG. 8. Saussuritization and wide development of clinozoisite crystals. Plane polarized light, ×140.

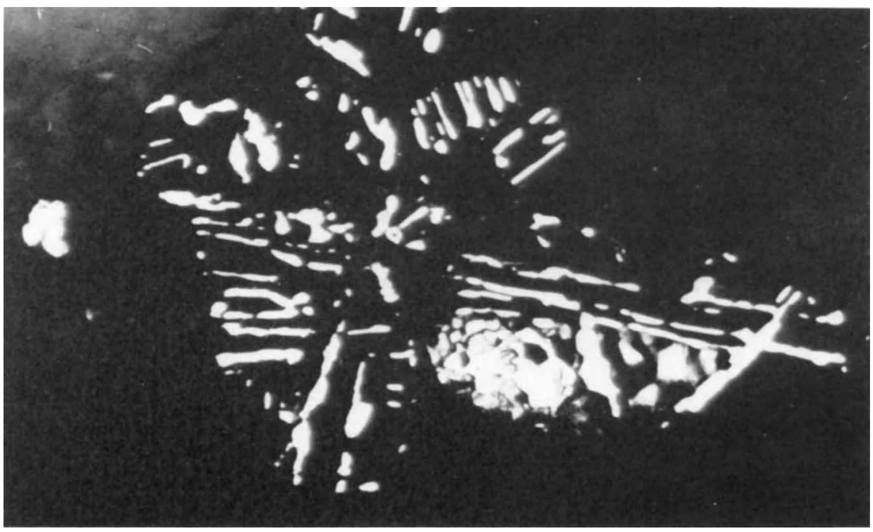

FIG. 9. Fine network of ilmenite crystals altered to rutile and hematite. Plane polarized light, oil immersion, × 154.

Plagioclase forms about 50% of the rock. Saussuritization is complete (Fig. 10) and therefore no estimate of the plagioclase composition could be given. Clinopyroxene together with amphibole constitute about 50% of the rock and both occur as completely chloritized anhedral grains of comparable size to the plagioclase. Tremolite is also very well developed as an alteration product of pyroxenes. Some of the chloritized flakes show signs of deformation (Fig. 11). In one section, calcite is widely developed as discrete, medium- to-coarse-grained subhedral crystals dispersed within the rock and as veinlets about 0.5–2 mm thick. Few patches of talc were also noted in the same section. No polished sections were made for this variety.

Leucogabbros

Leucogabbros occur as patches of variable dimensions. In thin section, the rock is composed mainly of tabular, euhedral to subhedral plagioclase crystals with a compositional range between An_{50}–An_{60}. Complex albite types of twinning predominate. In one thin section, a fine layer of clinopyroxene about 1 mm thick was observed: it may indicate igneous layering. Clinopyroxene and/or amphibole are present in minor amounts.

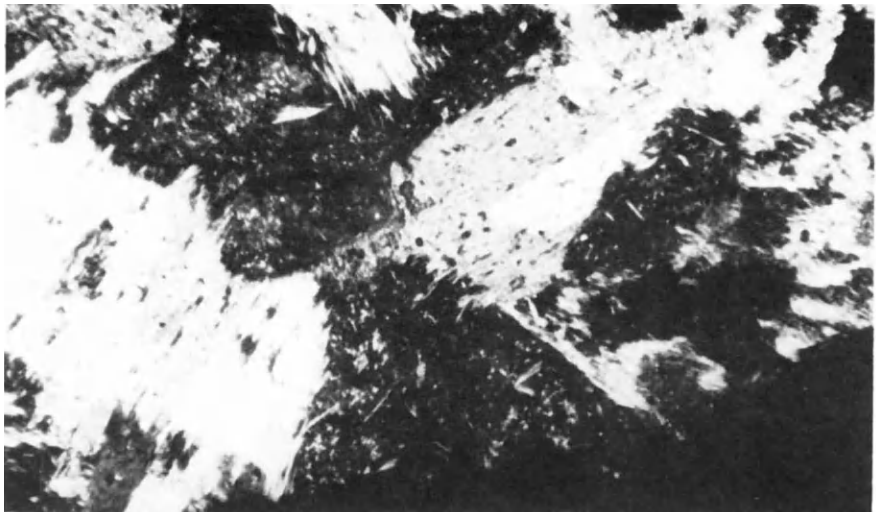

FIG. 10. Saussuritization of plagioclase and complete alteration of clinopyroxene and amphibole to chlorite and tremolite. Crossed nicols, ×140.

FIG. 11. Banding in chloritized amphibole flakes. Crossed nicols, ×140.

Rarely, opaques are present and no polished sections were made for this type. Usually, the rock is less altered compared to the pegmatoidal gabbros.

Trondjemites

Most of the gabbroic units of ophiolite complexes have trondjemites which probably represent late-stage differentiation products derived from gabbroic liquids. Trondjemite occurs in the visited area as irregular masses or dykes within the gabbro unit. It is medium grained and has a pale pinkish colour. In thin section, it shows a hypidiomorphic granular texture. The main constituents are plagioclase, quartz, hornblende and biotite. Potash feldspars and ilmenite are accessories.

Plagioclase makes up about 55% of the rock and is present in two generations, namely, as coarse, euhedral, elongated crystals of approximately 1 cm in length and 2 mm in width, and as fine-grained, equant to slightly elongated euhedral crystals of about 3 mm in diameter. Both types are strongly zoned (Fig. 12). The coarse plagioclase crystals have notable preferred orientation, mocrofaulting, and very well-developed zoning, features which probably indicate a piezocrystalline deformation fabric formed at high temperature (Den Tex, 1969).

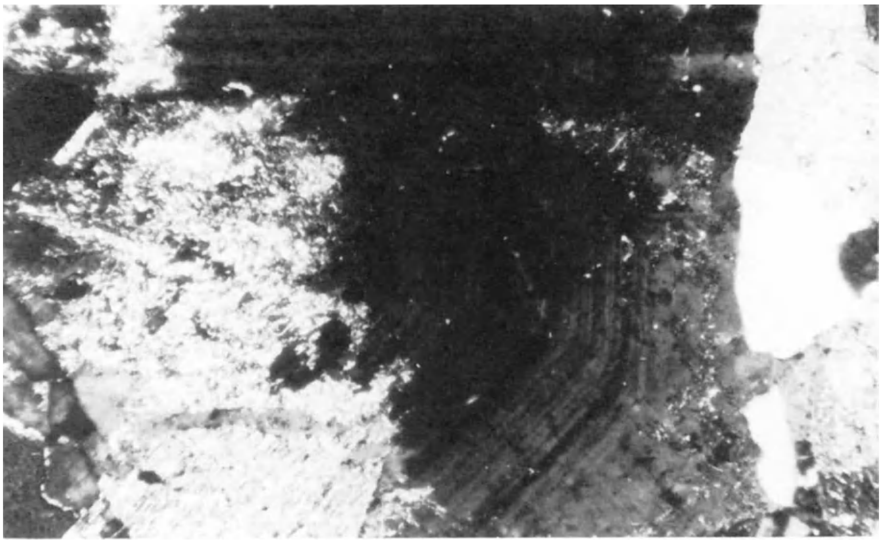

FIG. 12. Zoning in a plagioclase crystal showing complex albite twinning. Crossed nicols, ×140.

Compositionally, the plagioclase ranges between An_{10} and An_{15}.

Quartz is present as fine-grained, intergranular anhedral crystals, making up about 20% of the rock. It is somewhat fractured and deformed. Potash feldspars form less than 5% of the rock and are present as twinned, subhedral, equant grains of orthoclase. Amphibole is present as brown hornblende with relics of pyroxene; it poikilitically encloses altered feldspars and opaques. Alteration of clinopyroxene to hornblende is possible. Biotite is present as fine red flakes, occasionally altered to chlorite. Opaque minerals are mainly ilmenite.

Sheeted Dykes and Basic Volcanics

Following the gabbroic rocks eastward, the basic volcanic unit begins with the appearance of small fragments of a few sheeted dykes (well exposed at close to km 83). These fragments are fine grained, light grey in colour, range between 50 and 70 cm in width, and have characteristic chilled margins. The sheeted dykes do not attain great thickness as a unit; they soon merge farther east into the massive basic volcanics. The contact relations between the gabbro and volcanic rocks are difficult to define and their true relationship is unknown at present. Akaad and Noweir (1972)

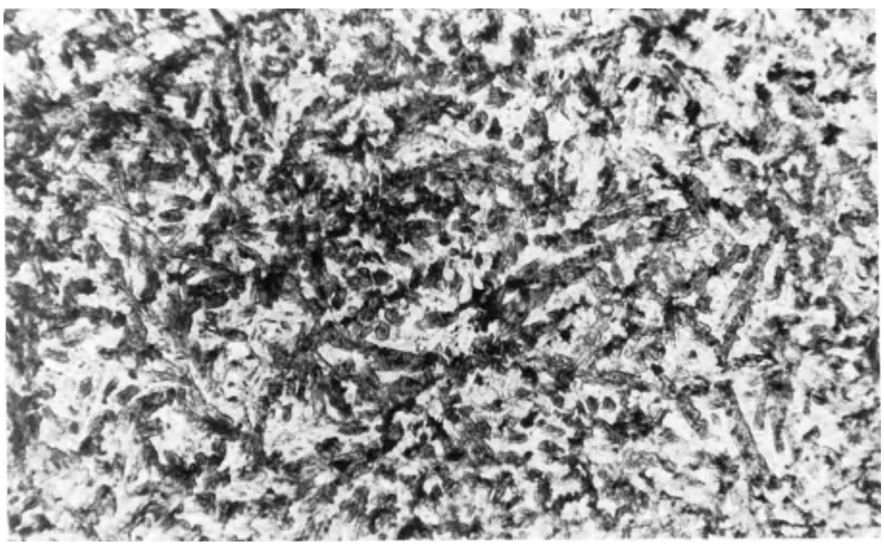

FIG. 13. Intergranular texture in basic volcanic rock. Plane polarized light, ×140.

described the basic volcanics as "consisting predominantly of a thick sequence of metamorphosed soda-rich basic pillow lavas and thick flows of basic lavas together with intermediate intrusive types and tuffaceous varieties". This unit is thus comparable with layer 2 of oceanic crust (Shor and Raitt, 1969).

No significant differences in texture were noted between samples collected from sheeted dykes or from the massive volcanics. In thin section the rocks are fine-grained, with typical intergranular texture (Fig. 13). The constituent minerals are mostly sodic plagioclase, cummingtonite-grunerite, and chlorite; potash feldspar is rarely seen. The accessory minerals include opaques (magnetite), sphene, rutile, and tremolite. The plagioclase occurs as lath-shaped crystals exhibiting lammelar twinning and combined Carlsbad-albite twinning. The laths show few signs of deformation (cracking and slight bending). The crystals are slightly to moderately altered to sericite and are clouded due to the presence of allophane. Cummingtonite occurs as short tabular crystals that are mostly euhedral, with some subhedral grains. It is colourless to pale brown and has a weak pleochroism. Cummingtonite crystals are sometimes arranged in a radial pattern, and the mineral may show partial to complete alteration to chlorite. Few scattered phenocrysts of pre-existing mafic minerals that are now totally altered to

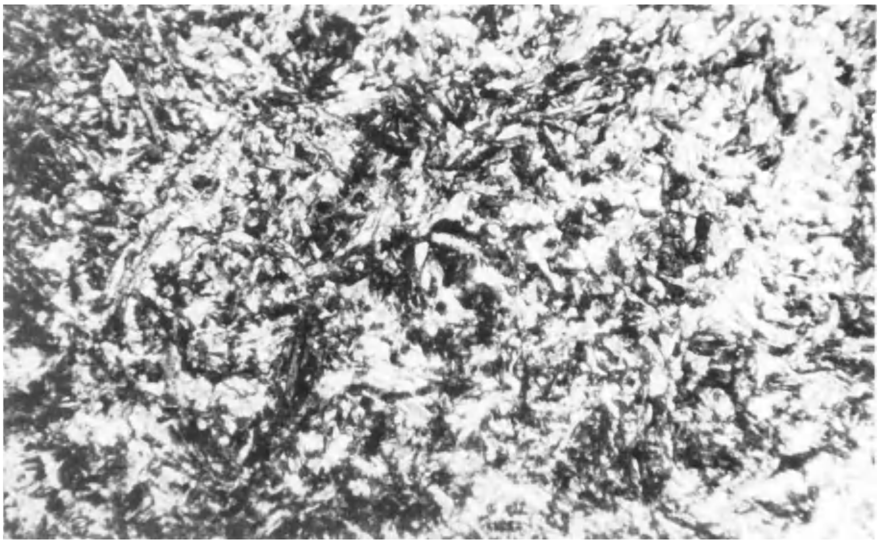

FIG. 14. Intergranular texture of basic volcanic showing flakes of penninite and acicular crystals of tremolite. Crossed nicols, ×140.

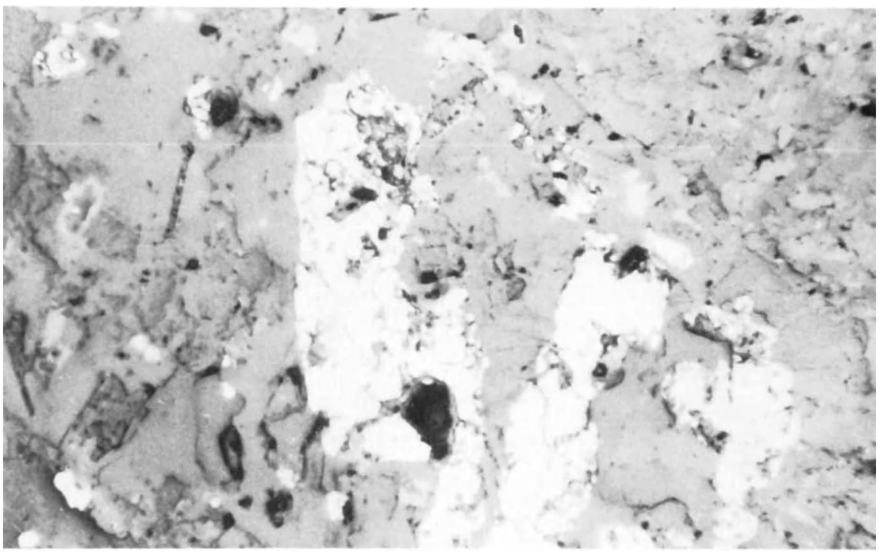

FIG. 15. Colloform banding in pyrite filling cracks and vesicles. Plane polarized light, ×154.

chlorite (penninite) were observed (Fig. 14). Few acicular crystals of tremolite are occasionally present.

In polished section, the opaque minerals are mainly magnetite and pyrite, with subordinate ilmenite. Magnetite is generally in fine- to medium-grained euhedral to subhedral crystals which occur either as disseminated grains or in bundles. Many grains are partially to completely altered to goethite or lepidocrosite, the alteration beginning at the grain boundaries and along cleavage planes and cracks. Other grains are altered to hematite (martitization) along cleavage planes and borders. The grain size is comparable to that of the silicate rock-forming minerals. No exsolution textures were observed.

Pyrite occurs as extremely fine-grained euhedral crystals that are randomly disseminated throughout the rock. Few anhedral, medium-grained pyrite crystals, about 5 times the size of the magnetite, were observed. They are partially altered to goethite and lepidocrosite. There is an occurrence of secondary, colloform and banded pyrite filling vesicles. The pyrites are cryptocrystalline, concentrically banded, and the rims are altered to goethite and lepidocrosite (Fig. 15). Sometimes the alteration is complete and only relics of the colloform banding are observed. A few elongated, prismatic, fine- to medium-grained ilmenite crystals with exsolution blebs of magnetite are observed.

CONCLUSION

Based on a purely descriptive point of view, the presence of an ophiolite assemblage in this area is highly possible. To prove whether the rocks have any characteristics in common with those of an oceanic lithosphere, it remains necessary to have petrochemical data to support the presented petrographic descriptions. Questions concerned with the manner by which these ophiolites were emplaced in their present position need further field studies to be satisfactorily answered.

ACKNOWLEDGMENTS

The authors are grateful to Dr. El-Shazly for the generous facilities he provided in the field and for the useful discussions and observations he made along with Drs. Al-Shanti, Church, Gass, Shackleton, and El-Sharkawy. Dr. El-Mahdy provided valuable assistance throughout this work.

REFERENCES

AKAAD, M. K., and NOWEIR, A. M. 1972. Some aspects of the serpentinites and their associated derivatives along Qift–Quseir road, Eastern Desert, Egypt. *Annals Geol. Surv. Egypt* 2, 251–270.

BAKOR, A. R. 1973. Jabal al Wask: a Precambrian basic and ultrabasic igneous complex in the northern Hijaz of Saudi Arabia. *Unpubl. Ph.D. thesis*. University of Leeds, England.

BAKOR, A. R., GASS, I.G., and NEARLY, C. R. 1976. Jabal al Wask, northwest Saudi Arabia: an Eocambrian back-arc ophiolite. *Earth Planet. Sci. Lett.* 30, 1-9.

BROWN, G. F., and COLEMAN, R. E. 1972. The tectonic framework of the Arabian Peninsula. *Int. Geol. Congr.* XXIV, Sec. 3, 300–305.

CHURCH, W. R. 1972. Ophiolite: its definition, origin as oceanic crust, and mode of emplacement in orogenic belts, with special reference to the Appalachians. *Dept. Energy Mines Res. Canada Spec. Publication* 42, 71–85.

CHURCH, W. R., and STEVENS, R. K. 1971. Early Paleozoic ophiolite complexes of the Newfoundland Appalachians as mantle-oceanic crust sequences. *J. Geophys. Res.* 76, 1460–1466.

COLEMAN, R. G. 1971. Plate tectonic emplacement of upper mantle peridotites along continental edges. *J. Geophys. Res.* 76, 1212–1216.

COLEMAN, R. G. 1977. *Ophiolites*. Springer-Verlag, New York, 229 p.

DEN TEX, E. 1969. Origin of ultramafic rocks, their tectonic setting and history. *Tectonophysics* 7, 457–488.

DEWEY, J. F., and BIRD, J. 1970. Mountain belts and the new global tectonics. *J. Geophys. Res.* 75, 2625–2647.

DICKINSON, W. R. 1971. Plate tectonic models of geosynclines. *Earth Planet. Sci. Lett.* 10, 165–174.

EL-RAMLY, M. F., IVANOV, S. S., and KOCHIN, C. E. 1970. General review of the mineral potentials of Egypt. *Geol. Surv. Egypt Paper*, 3–27.

GARSON, M. S., and SHALABY, I. M. 1974. Precambrian–Lower Paleozoic plate tectonics and metallogenesis in the Red Sea region. pp. 573–596 in *G.A.C.A.M.C. Symp. Metallogeny and plate tectonics*, St. John's, Newfoundland.

GASS, I. G. 1968. Is the Troodos-Massif of Cyprus a fragment of Mesozoic ocean floor? *Nature* 220, 39–42.

GASS, I. G. 1976. Origin and emplacement of ophiolites. *J. Geol. Soc. Lond.* 132, 563–575.

GREENWOOD, W. R., HADLEY, D. G., ANDERSON, R. E., FLECK, R. J., and SCHMIDT, D. L. 1975. Late Proterozoic cratonization in southwestern Saudi Arabia. *U.S. Geol. Survey Saudi Arabian Project. Rept.* 196.

HUNTING GEOLOGY AND GEOPHYSICS LTD. 1967. Assessment of the mineral potential of the Aswan Region, UAR. *Regional Planning of Aswan*, p. 1–138.

IVANOV, T., SHALABY, I. M., and HUSSEIN, A. A. A. 1973. Metallogenic characteristics of South-Eastern Desert of Egypt. *Annals Geol. Surv. Egypt.* 3, 139–166.

LAUBSCHER, H. 1969. Mountain building. *Tectonophysics* 7, 551–563.

MOORES, E. M. 1969. Petrology and structure of the Vourinos ophiolitic complex of Northern Greece. *Geol. Soc. Am. Spec. Paper* 118, 74 p.

PETERS, T. J. 1969. Rocks of the Alpine ophiolitic suite: discussion on the paper "The origin of ultramafic and ultrabasic rocks" by P. J. Wyllie. *Tectonophysics* 7, 507–509.

REINHARDT, B. M. 1969. On the genesis and emplacement of ophiolites in the Oman Mountains Geosyncline. *Sehweitz. Mineral. Petrog.* Mitt 49, 1–30.

SHOR, G. F., JR, and RAITT, R. W. 1969. Explosion seismic refraction studies on the crust and upper mantle in the Pacific and Indian Oceans. Pp. 225–230 in *The Earth's Crust and Upper Mantle. Geophys. Monograph* 13.